Head Tracked Multi User Autostereoscopic 3D Display Investigations

Ph.D. Thesis

Rajwinder Singh Brar

Imaging and Displays Research Group

Faculty of Technology

De Montfort University

2012

Abstract

The research covered in this thesis encompasses a consideration of 3D television requirements and a survey of stereoscopic and autostereoscopic methods. This confirms that although there is a lot of activity in this area, very little of this work could be considered suitable for television. The principle of operation, design of the components of the optical system and evaluation of two EU-funded (MUTED & HELIUM3D projects) glasses-free (autostereoscopic) displays is described.

Four iterations of the display were built in MUTED, with the results of the first used in designing the second, third and fourth versions. The first three versions of the display use two-49 element arrays, one for the left eye and one for the right. A pattern of spots is projected onto the back of the arrays and these are converted into a series of collimated beams that form exit pupils after passing through the LCD. An exit pupil is a region in the viewing field where either a left or a right image is seen across the complete area of the screen; the positions of these are controlled by a multi-user head tracker. A laser projector was used in the first two versions and, although this projector operated on holographic principles in order to obtain the spot pattern required to produce the exit pupils, it should be noted that images seen by the viewers are not produced holographically so the overall display cannot be described as holographic. In the third version, the laser projector is replaced with a conventional LCOS projector to address the stability and brightness issues discovered in the second version. In 2009, true 120Hz displays became available; this led to the development of a fourth version of the MUTED display that uses 120Hz projector and LCD to overcome the problems of projector instability, produces full-resolution images and simplifies the display hardware.

HELIUM3D: A multi-user autostereoscopic display based on laser scanning is also described in this thesis. This display also operates by providing head-tracked exit pupils. It incorporates a red, green and blue (RGB) laser illumination source that illuminates a light engine. Light directions are controlled by a spatial light modulator and are directed to the users' eyes via a front screen assembly incorporating a novel Gabor superlens. In this work is described that covered the development of demonstrators that showed the principle of temporal multiplexing and a version of the final display that had limited functionality; the reason for this was the delivery of components required for a display with full functionality.

Declaration

I declare that the work described in my thesis is original work undertaken by me for the degree of Doctor of Philosophy, at Imaging and Displays Research Group (IDRG), at De Montfort University, Leicester, United Kingdom. No part of the material described in this thesis has been submitted for the award of any other degree or qualification in this or any other university or college of advanced education.

Rajwinder Singh Brar

Acknowledgements

I want to give special thanks to my project supervisors, Dr Ian Sexton and Dr Phil Surman, for their guidance towards the completion of this work.

I also want to express my gratitude to all my friends for all the help and support they gave me throughout the project.

My gratitude also goes to my parents for all the encouragement and support they gave me throughout this course.

I especially want to thank God for the love and guidance He showed me, and for the strength He gave me.

Thank you so much.

Publications

[1] Brar, R., Surman, P., Sexton, I., Bates, R., Lee, W., Hopf, K., Neumann, F., Day, S. and Willman, E., "Laser-based Head-tracked 3D Display Research," Journal of Display Technology (JDT), IEEE, Vol. 6 Issue:10, pp. 531 - 543. 2010.

[2] Brar, R., Surman, P., Sexton, I. and Hopf, K., "MUTED - Multi User 3D Television Display," Journal of the Society for Information Display (JSID), Vol.18 Issue: 9, pp. 654-661. 2010.

[3] Brar, R., Surman, P. and Sexton, I., "Projection-Based Head Tracking 3D Displays," Journal of the Society for Information Display (JSID), Volume 18, Issue 10, pp. 844-854. 2010.

[4] Brar, R., Surman, P., Sexton, I. and Hopf, K., "A Time-multiplexed 3d Display Using Steered Exit Pupils," Journal of Information Display (JID), vol.11 no.2. 2010.

[5] Brar, R., Surman, P., Sexton, I. and Hopf, K., " HELIUM3D: A Laser-scanning Head-tracked Autostereoscopic Display," Journal of Information Display (JID), vol.11 no.3. 2010.

List of Tables

Table of Contents

List of Figures

List of Acronyms

CCD	Charge Coupled Device
CGH	Computer Generated Hologram
CRT	Cathode Ray Tube
DFT	Discrete Fourier Transform
DLP	Digital Light Processor
DMD	Digital Micromirror Device
DOF	Depth of Field
EASLM	Electrically Addressed Spatial Light Modulator
FFT	Fast Fourier Transform
FLA	Focussed Light Array
FLC	Ferroelectric Liquid Crystal
FPGA	Field Programmable Gate Array
HDTV	High Definition Television
HOE	Holographic Optical Element
LCD	Liquid Crystal Display
LCOS	Liquid Crystal on Silicon
LED	Light Emitting Diode
LSD	Light Shaping Diffuser
OASLAM	Optically Addressed Spatial Light Modulator
PCB	Printed Circuit Board
PDP	Plasma Display Panel
PWM	Pulse Width Modulation
RGB	Red Green Blue
SLM	Spatial Light Modulator
SMV	Super Multi-view
SVGA	Super VGA
TFT	Thin Film Transistor
VGA	Video Graphic Array

CHAPTER 1

INTRODUCTION

1.1 Preface

The ultimate aim of the research is the design, production and evaluation of two EU funded (MUTED & HELIUM3D projects) glasses-free (autostereoscopic) displays that are suitable for television applications [78, 36]. These displays will meet the particular requirements for television that are set out in this chapter. It is envisaged that the proposed displays will fulfil the demands of the third generation of television that is likely to be around for about twenty years. The time is overdue for the commencement of 3D television - our eyes have colour receptors and we also have two of them. The first generation of television, monochrome, was prominent from the nineteen thirties until the nineteen sixties and seventies, when colour took over. Once colour had been established, monochrome was considered unacceptable. The same pattern is likely to happen with 3D.

There are three broad categories of the display requirement: single-viewer for displaying on computer monitors and arcade games, two to around six viewers where television (and some arcade games) is viewed, and tens of hundreds of viewers for theatre presentations. The consensus of opinion is that a 3D television display should be autostereoscopic, i.e. it does not require the wearing of special glasses. There are several single-viewer autostereoscopic systems under development. The object of the current research is to produce a display that provides 3D without glasses to several viewers over a room-sized area. This will necessarily be more difficult to produce than a single-viewer 3D display, and will therefore be somewhat more complex.

1.2 Background

1.2.1 3D Television Requirements

Research into producing autostereoscopic television is still ongoing due to the fact that the enabling technologies required to create a comfortable, high resolution and appealing display have not been fully developed. The supporting technologies however have undergone major transformations in recent years [45]. The advances in software technology, complexity of field programmable gate array (FPGA) devices, fast light switching, laser technologies for generating a wide colour gamut, electronic/optoelectronic hardware, modulating devices at micron levels and high resolution display devices have

made the advent of a commercially available autostereoscopic system possible within the next few years.

Cost is an important consideration; there is little doubt that 3D television displays will be more expensive than current monoscopic displays. However, when colour television was introduced, the cost of a colour set was around five times that of black and white, yet this did not deter consumers from buying them [47]. The key factors for a successful 3D TV experience are the availability of content, cost of deployment, the ease of use and the quality of experience. However, the aspects mentioned in the following sections are likely to be the most important.

Display availability might appear to be a rather obvious requirement but there would have been no point, for example, in pursuing a method using a direct-view LCD if a device of sufficient size and with a low enough cost had not become available. This point seems to be rarely acknowledged in published work on stereo displays. It must be borne in mind that *any* stereo display will have to provide a minimum of twice the number of images necessary for monoscopic presentation. The current research has been carried out for a number of years and during that period LCDs have gradually increased in size and also are sufficiently fast to support 120Hz frame-sequential operation where the use of temporal multiplexing enables full resolution images to be displayed [82].

Unlike computer monitors that in general need to provide an image to only one viewer, television has to serve a maximum of around six viewers. The prototypes described here only fulfil the requirements of the television market and no attempt will be made to present stereo to a theatre-sized audience.

It is generally recognised that 3D television would not be as acceptable if special glasses had to be worn. As television is watched intermittently - usually with many interruptions - unlike the cinema, it is unlikely that viewers will want to keep putting on and taking off special glasses.

Television viewers must be able to move freely over a large viewing volume, typically between 1 to 4 metres from the screen, and up to 40 degree from the centre-line. Within this volume, stereo must be able to seen for any head position [54]. Methods such as those employing simple lenticular displays which have alternate stereoscopic and pseudoscopic zones or integral imaging which have around three or four unusable regions across the width of the viewing field would place unacceptable restrictions on the viewers' freedom of movement. In many autostereoscopic displays the viewers are restricted to being close to an optimum-viewing plane; this is the distance at which the viewers can move laterally with no interruption to the 3D effect.

The light rays in a stereo display will require some degree of manipulation that would not be necessary in a monoscopic display; therefore it is possible that the overall housing size is likely to be larger. When a direct-view LCD is used in its normal mode of operation the housing should be of 'hang-on-the-wall' size.

1.2.2 Background to MUTED and HELIUM3D

The Imaging and Displays Research Group (IDRG) at De Montfort University (DMU) has been the lead partner in two European Union (EU) funded projects, these are: MUTED (Multi-user 3D Television Display) and HELIUM3D (High Efficiency Laser-based Multi-user Multi-modal 3D Display). This thesis covers original research carried out within MUTED, work within HELIUM3D and research undertaken on the development of an improved embodiment of the MUTED prototype (Chapter 7) that was undertaken after the official end of the project In November 2009.

MUTED was a 40-month project that commenced in August 2006 and whose goal was to produce a multi-user autostereoscopic display based on the earlier EU ATTEST project, in which DMU also participated. DMU was the lead partner and other partners were: Sharp Laboratories of Europe, Fraunhofer HHI, Technical University of Eindhoven, University of West Bohemia and Light Blue Optics. The project had 30 persons per year of effort and attracted €2.8 m funding with a gross value of €4.3 m.

The 3½ year HELIUM3D project commenced in January 2008 and again DMU was the lead partner. The other partners were: Philips Consumer Electronics Nederland B.V., Barco N.V., University College London, Fraunhofer Gesellschaft Zur Foerderung Der Angewandten Forschung E.V., Technische Universiteit Eindhoven, Koc University and Nanjing University. The project received €2.8m funding that supported 32 persons per year of effort.

As the research reported in this thesis comprises distinct areas of work within the MUTED and HELIUM3D projects and also the development of the MUTED display, it is useful at this stage to describe these projects in some detail in order to place my work in context and to show its relevance and its contribution to knowledge. All the displays covered in the thesis are autostereoscopic where regions in the viewing field in front of the screen, referred to as exit pupils, are formed where either a left image or a right image is seen over the complete area of the screen. When the user is situated in the ‘sweet spot’ the viewer perceives 3D. Ultimately it is intended that several exit pupils will be formed and that these will follow the positions of the viewers’ heads under the control of a multi-user head tracker.

In MUTED the optics form the steerable backlight of a direct-view liquid crystal display (LCD). The exit pupils are formed by a series of intersecting collimated beams from an optical array (Figure 4.2) [77, 79]. Small illumination sources in the focal planes of the array lenses form the emergent beams and these effectively move laterally in order to steer the beams in the desired directions. As a viewer moves laterally the sources move in the opposite direction, and as the viewer comes closer to the screen the spacing between the sources increases (and vice-versa). Several viewers can be accommodated by producing a separate series of illumination sources for each viewer.

As 120 Hz LCDs were not available until the end of the MUTED project, in the display developed left and right images were produced simultaneously on alternate rows of LCD pixels. This scheme is called spatial multiplexing (MUX) and separation of the left and right channels is performed with the use of a horizontally-aligned lenticular screen (Figure 4.9) that separates the output from two separate steering arrays that are arranged one above the other as in Figure 4.6.

In the earlier ATTEST [76] prototype illumination was supplied from a matrix of around 5000 white LEDs in an arrangement of curved sub-arrays; the LEDs were illuminated in a pattern in accordance with a head tracker. There were various problems associated with this configuration, for example low brightness and colour variation, and in order to overcome these the MUTED display was proposed, where the illumination array was situated in a single flat plane thus enabling the possibility of using projection techniques to provide the illumination pattern.

This pattern is sparse and illumination occurs in less than 5% of its total area with the remainder dark, as shown in Figure 4.5. If a conventional projector is used the majority of the light is blocked so that the luminous efficiency is very low. For this reason it was decided to use a laser projector where the pattern is created by interference so that the energy in the complete incident wavefront is concentrated into the illumination pattern [10, 62]. The primary illumination source for the display is a set of red, green and blue (RGB) lasers.

The brief description of the display is given here in order to show where my research fits in; a more detailed description of the display optics is given in Chapter 4.

The HELIUM3D display is another head tracked display with an RGB laser source [18, 1], however the principle of operation is completely different. This display is essentially a rear projection system where the image is transferred to the front screen through via an intermediate stage where the emergent light directions are determined by a spatial light modulator (SLM) [96] that is controlled by a head tracker [11].

The key property of this system is the fact that the image is scanned by a horizontal raster where an image column moves from one side of the screen to the other over the duration of a scan. Exit pupils are formed dynamically; they are produced by the emerging light beam from the column being directed to a particular eye by changing its direction as the column traverses the screen [11]. The principle of operation is explained in more detail in Section 8.2.

1.3 Aims and Objectives of the Research

Although the majority of the research covered forms only part of the display integration work on the two projects, the amount of original research is considerable and has produced a significant contribution to knowledge. Each of the approaches is intended to develop a display that could provide the first commercially-viable multi-user autostereoscopic display. As there are two approaches being developed in parallel and some of the technology is the same for each, for example the multi-user head tracker, this technology approach stands a fairly good chance of being the first successful method.

My work within the MUTED project amounted to around one third of the total research effort of DMU and totally covered the following key areas:

1. Characterise the lenticular multiplexing (MUX) screen performance.
2. Determine the soft aperture profile that compensates for the polar plot of the horizontal diffuser.
3. Develop a method for illumination pattern correction utilising polynomial functions.
4. Characterise holographic projector image.
5. Determine the effect of birefringence of optical components and inform the decision on choice of components for second prototype.
6. Determine the requirement for the screen enhancement lens and specify parameters for custom-built units.
7. Identify the cause of patterning in observed image and source an LCD suitable for the second prototype.

The performance of the second MUTED prototype was poor, principally due to low brightness but also to projector instability and other factors. Although this prototype was able to demonstrate the operation of the head tracker it was not possible to see an image on it. In order to address this, a version was built using a non-holographic projector. The aim of this version was to show that a 3D display using an optical array as an LCD

backlight could be produced. This work was completely carried out by me and was separate to the MUTED project work.

I also contributed to the HELIUM3D project and the aims of the work were as follows:

1. Develop a method of synchronising two different display types.
2. Build and evaluate a temporal multiplexing demonstrator
3. Build and evaluate a simplified version of the HELIUM3D display where the scanned laser–illuminated projector is replaced by a 120Hz projector.

The above contributions to the projects were self-contained areas of work within the projects and were my sole responsibility.

As it was clear that the MUTED display with the holographic projector as developed within the project was far too dim to provide a viable display, conventional projector versions of this were developed and one of these, using a 60Hz LCOS projector, was capable of providing images that could be seen under reasonably high ambient lighting conditions.

In addition to the prototype display research, eight different 3D display types that are in the IDRG laboratory were characterised and the results written up. This work was for one of the HELIUM3D deliverables and included measurements of crosstalk and brightness. The objective of the research was to compare the HELIUM3D display performance with that of other 3D displays.

1.3.1 MUTED

The research questions are most clearly identified by showing where the research sits in the overall context of the MUTED project. The work is described in detail in Chapter 4 but the position of the research covered, in relation to the overall display work, is covered in the thesis. Figure 1.1 is a block diagram of the MUTED display system including the viewer and head tracker. The numbers in red indicate the area of research applicable to that region of the diagram. The figure shows the linking of the various areas of work and the remainder of this section identifies the research questions and describes the research methodologies employed.

1) Spatial MUX Analysis

In the MUTED display, left and right images are produced simultaneously on a single 60Hz display and these are displayed on alternate rows of pixels. The principle of spatial MUX with a lenticular screen is described in detail in Section 4.3. MUX is achieved with the use of a lenticular screen with horizontally-aligned lenses that is located behind the LCD. This screen was custom-built to a design of MUTED partner Sharp Laboratories of Europe (SLE).

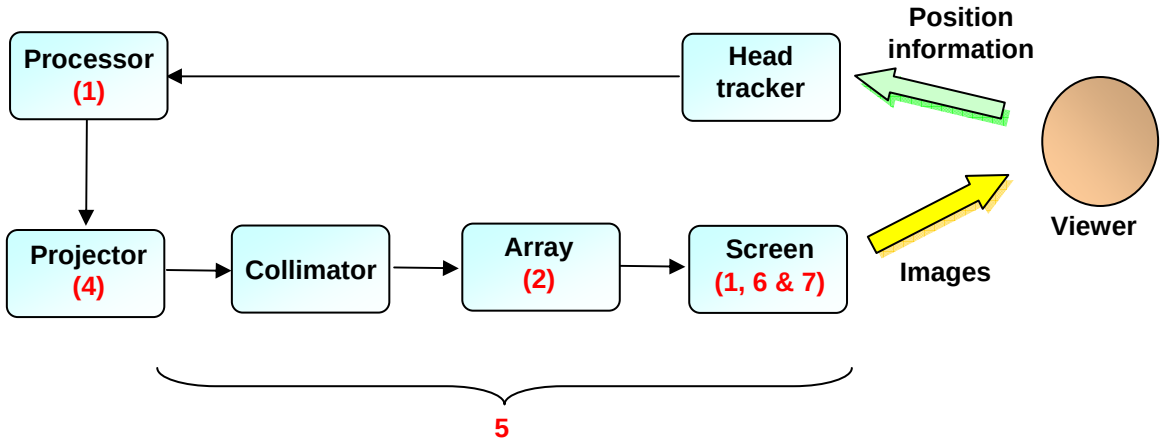

Figure 1.1: Context of research. The areas of research within the MUTED project that have been developed exclusively in this thesis are; 1) spatial MUX, 2) soft aperture characteristic, 3) polynomial spot pattern correction, 4) spot pattern powers, 5) birefringence of complete optical system, 6) brightness enhancement lens, 7) patterning in image.

In practice it was found that the screen did not perform in accordance with the design parameters. My investigations involved determining the cause of this, and it was concluded that the error was caused by the lens pitch being incorrect. It was determined that the temperature at which the screen is manufactured is critical to the pitch. A second iteration of the screen was made and this was carefully evaluated, not by measurement of the lens pitch but by the performance of the screen as an image multiplexer. This was achieved by visual analysis of photographs of the image separation as opposed to quantitative measurements. This was used to determine the optimum positioning if the screen in relation to the other display components.

2) Soft Aperture Profile

This covers original work carried out within MUTED (Chapters 4, 5 and 6) and development of an improved embodiment of the MUTED prototype (Chapter 7) after the end of the project In November 2009.

Earlier work on this approach [74] established that in order to provide a contiguous light source from an array of separate sources the profile of the overlapping emergent beams from the sources should be specially shaped. The intensity at any particular point is the summation from two adjacent array elements and the beam profile is such that illumination variations over the width of the array are imperceptible.

As explained in Section 4.5, the array aperture transmission profile is dependent on the desired output beam profile and the polar plot of the horizontal diffusers mounted the backs of the elements. In this case the output profile is chosen to be triangular and the

diffuser profile determined by the polar plot of the major axis of a Luminit elliptical diffuser that has a minor axis of 0.5°.

Normally, data supplied by the manufactures would be used but in this case the data supplied appeared to be incorrect as the major axis plot, that should be approximately Gaussian, shows large fluctuations that from previous experience indicate that coherent light was used. For this reason the diffuser was characterised using collimated light obtained from an incandescent source illuminating a pinhole of around one millimetre diameter. This produced the characteristic shown in Section 4.5.4.

3) Illumination Pattern Polynomial Correction

As described in Chapter 4, the display operates by producing exit pupils that are formed from intersecting collimated beams that originate from a pattern of spots in an illumination plane that move around in accordance with the viewer's eye position. The effective focal length of the array lenses is small in relation to the typical user distance; the effect of this is that a small error in spot position causes a large error in beam position at the viewer.

The spot pattern is generated in accordance with the users' head positions and the Matlab program developed to perform the mapping the viewers' X and Z coordinates is given in Appendix 3. This is obtained from the set of transformation equations that are used to map viewer eye into X and Y coordinates in the viewing field to X and Y spot position coordinates in the illumination plane of the optical array.

It was found that the holographic projector used to produce the spot pattern had linearity and stability problems and these had to be addressed by inserting corrections to the Matlab program. Initial studies had to be carried out to determine whether the errors were entirely produced by the projector or whether these were due to other components, for example the parabolic collimating mirror.

In addition to software solutions allowing for projector errors other strategies were investigated, for example mechanical adjustment of the parabolic mirror and the projector mounting. These enabled quick and simple adjustments to the system.

4) Characterise Holographic Projector Image

In this application the most relevant parameters in the characterisation of the projector are: spot position, spot shape and spot intensity. Spot position is covered in the previous section where this information is used in order to apply corrections. The shape of the spot is important as this determines the shape of the exit pupil. Ideally its cross-section shape would be top hat as this would give the sharpest cut off at the edge of the pupils that is

located in the region located between the viewer's eyes. As each spot provides the illumination for a vertical strip of the image it is important that the range of spot powers remains within a given range so that vertical banding is not seen.

5) Birefringence

The output of the holographic projector is polarised and the LCD has polarisers at its input and output. The output from the holographic projector is polarised and in principle the output of the projector could be matched to the projector if a half-wave plate is used to rotate the projector output to match the polariser in the projector. For this to work polarisation has to be preserved throughout the optical system. Investigation was carried out on the properties of the existing materials used at each stage. Several of these were found to be birefringent and alternative materials were sought. Where required, the use of these was specified to the component suppliers and the alternative materials incorporated.

6) Screen Enhancement Lens

In its original form it was found that the image from the MUTED display did not cover the complete height of the screen and that diagonal 'staircase' banding was observed on the image. In the MUTED project the complete system was not modelled in, for example, ZEMAX software and the reason for the banding had to be determined. It became clear that an additional lens was required at the output of the system; that is in front of the LCD screen. This lens also produces a brighter image as it concentrates light into the region occupied by the viewers. A custom-built cylindrical lens was made to the specification given and its performance was evaluated.

7) Image Patterning

On the original MUTED prototype, that had just been constructed when the work on this thesis started, the image was found to have a diagonal spot pattern. The cause of this was initially not clear but upon careful examination it became apparent that this was caused by the sub-pixel structure in the LCD. After extensive investigation an LCD was obtained that had a suitable structure. This task was fairly difficult as information on the sub-pixel structure is not available from the manufacturers.

1.3.2 HELIUM3D

1) Synchronising Different Display Types

Both the 120Hz projector version of the MUTED display and the simplified version of the of the HELIUM3D display require the synchronisation of a 120Hz LCD display and a 120Hz projector. This appeared to be useful line of research as the same development could be applied to both displays and synchronisation could be achieved relatively simply using Genlock with Nvidia Quadro graphics cards. In practice, unforeseen difficulties were encountered; these are described in Chapter 7.

2) Temporal Multiplexing Demonstrator

During the HELIUM3D project it became clear that due to the late delivery of certain key components the completion of a prototype, even with limited functionality, would be late and the decision was taken to produce a demonstrator that showed the operation of one of the key properties of the display, that is of temporal MUX. This demonstrator operates on different principles to the HELIUM3D display; the principal differences are that images are formed on an LCD located at the front screen and there is no SLM as exit pupil positions are formed by another LCD located at the SLM position. My work involved determining the display configuration that would be suitable for demonstration purposes at a project Review Meeting with the EU project officer and the two independent Reviewers, designing and building the display hardware, applying the synchronisation work described in the previous section and then testing and evaluating the display.

3) Simplified HELIUM3D Display

In addition to the demonstrator it was necessary to build a display that showed as many features as possible of the display described in the HELIUM3D Description of Work. Two important features of the HELIUM3D display are the use of a Gabor superlens and the implementation of a two-stage projection system; these are demonstrated in the prototype that was finally built. The Gabor superlens enables an image of the relatively small SLM to be magnified so that light can be controlled over a wide viewing region and the two-stage system enables light direction control to be carried out in the Fourier transform plane of a large projection lens. The display did not enable the demonstration of dynamic exit pupil formation as this requires a fast SLM and this was not available until after my research had been completed.

Again my work involved determining the display configuration that would be suitable for demonstration purposes at the Review Meeting and then designing and building the display hardware, applying the synchronisation work described in the previous section and finally testing and evaluating the display.

1.4 Thesis Overview

My contribution to the research in these projects is set out by chapter in this section.

This thesis covers four broad areas, these are:

- Survey of stereoscopic and autostereoscopic displays.
- Original research carried out within MUTED (Chapters 4, 5 and 6) and Development of an improved embodiment of the MUTED prototype (Chapter 7) after the end of the project In November 2009.
- Original research undertaken on various aspects of HELIUM3D (Chapters 8 and 9).
- Characterise the 3D displays at DMU

Apart from this introduction and the conclusions, the main body of the work carried out is summarised as follows:

Chapter 2 3D Glasses Display Survey

In this chapter the various types of 3D displays that require the wearing of special glasses are surveyed. These include anaglyph – the familiar red and green glasses, shutter glasses that are currently the technology most commonly used for 3D television and polarised glasses that are used in 3D cinema and increasingly for 3D television.

Chapter 3 Autostereoscopic Displays Survey

This survey is based on the taxonomy of autostereoscopic display types where the basic categories are: holographic, volumetric, multiple image and light field. Holography is only briefly mentioned as it is not seen as technology suited to a consumer 3D display for at least the next decade. Volumetric displays require relatively complex hardware but provide motion parallax (the ability to look around objects). Their principal disadvantage is that the images are transparent. In multiple image displays, the category that covers my research, two-dimensional images are produced on the screen but the appearance of these is directional, such that left and right images are seen by each pair of eyes. This could be the same image pair as in MUTED and HELIUM3D, or a different image pair as in multi-view displays. In light field displays, discrete beams of light that vary with angle radiate from each point on the screen. These can take several forms and integral imaging, multi-beam and dynamic apertures are described.

Chapter 4 Laser Projector Display Description

Chapter 4 describes the principle of operation, the construction of the display and the head tracker developed in the MUTED project. In order to place my own research in context the chapter describes all aspects of the display. Within this my specific contributions were:

- Develop the method to determine the efficacy of the lenticular spatial MUX screen using a matrix of photographs (this is described in Section 4.3).
- Determine the transmission profile of the soft aperture incorporated into the optical array elements. This was achieved by measuring the polar plot of the available diffusing material and then calculating the transmission profile of the soft aperture that produces the required 'triangular' output beam profile (Section 4.5).

Chapter 5 Laser Projector Display Spot Pattern Calibration

The positional accuracy of the spot pattern projected on to the back of the optical array must be high, as a small deviation from the desired position will cause a large difference to the emergent ray angle resulting in crosstalk and the appearance of banding in the image. This chapter describes the method developed to compensate for non-linearity in the system by determining the polynomial function of the error and then applying this into the Matlab program that calculates the pattern. The method proved to be successful and positional errors in the spot pattern within a tolerance of ±0.5 millimetres were achieved.

Chapter 6 Laser Projector Display – Other Performance Issues

This chapter describes the work carried out on the second iteration of the prototype in order to address the deficiencies of the first version. The areas of work covered were:

- Measure amplitude of each spot. These were found to be sufficiently uniform for the variation to be masked by the effect of the soft apertures.
- Determine the birefringence of Plexiglass optical components. This is important as the output of the laser projector is polarised and must be aligned with the LCD polariser, and led to the recommendation that Plexiglass components were replaced with crown glass and that other components be supplied on non-birefringent substrates.
- Optimise array element vertical diffuser. The original diffuser was one with a Gaussian profile and a suitable lenticular screen replacement with a 'top hat' profile was found.

- Examine original LCD panel used in order to determine cause of intensity variation on screen. Source and evaluate a replacement panel that does not produce these artefacts.

Chapter 7 Non-laser Projector Prototypes

It was found that the brightness of the MUTED prototype to be demonstrated at the final Review Meeting was only in the order of a few candelas per square metre (nits) and it was therefore decided that another display would be demonstrated as well. This work was independent to the MUTED project and produced a prototype incorporating a conventional liquid crystal on silicon (LCOS) projector. The 3D display has a brightness of around 25 nits and can be comfortably viewed in subdued ambient lighting conditions.

Work was also commenced on a 120Hz version that employs temporal MUX by using a 120Hz digital light processor (DLP) projector synchronised with an Alienware 120Hz LCD intended for shutter glasses use.

Chapter 8 HELIUM3D Prototype

The first part of this chapter briefly describes the principle of operation of the HELIUM3D prototype.

Section 8.2 describes the operation of a simple spatial multiplexing (MUX) demonstrator where a 120Hz DMD projector is used as the illumination source for images produced on a 120Hz LCD. An exit pupil pair was formed 1000 millimetres in front of the screen. This uses the same projector and LCD as the 120Hz version of the MUTED display so the synchronisation work applied to both systems.

I also built and evaluated another demonstrator that followed the HELIUM3D configuration more closely. Again this used a 120Hz projector and 120Hz LCD. This is described in Section 8.3.

Chapter 9 Scanned Light Engine Prototype

There was considerable delay in obtaining key components in the HELIUM3D project, in particular a fast linear SLM. In order to provide an interim solution a version of the display was built where the function of the SLM was performed by the Alienware 120Hz LCD. My contribution to this work was to determine that the system could not be run at greater than 60Hz, that is 30Hz per eye.

Chapter 10 Display Measurement

One of the deliverables in the HELIUM3D Description of Work was a report on the performance on existing displays. There are several 3D displays at DMU and as part of this PhD is the characterisation of these. This had the additional benefit of providing valuable input into the project as a report on the performance of existing displays was one of the deliverables.

CHAPTER 2

3D GLASSES DISPLAY SURVEY

2.1 Preface

Chapters 2 and 3 describe the current state of the art of 3D display, and the table in Appendix I shows the performance of the autostereoscopic types with respect to the MUTED display. It is useful to consider every possible way in which an autostereoscopic display can be achieved and then consider where MUTED sits in relation to the other state of the art approaches. The functionality and the likely time scales for the technology to come to market must be taken into account. It is envisaged that the MUTED display will supply a niche market and then be subsequently developed into a display suitable for television after that time.

2.2 Glasses Display Types

There are two major categories of 3D glasses, these are passive and active. Passive lenses rely on simple technology and are what generally comes to mind when the term '3D glasses' is used. The classic 3D glasses have coloured anaglyph lenses. Today, a more popular type of passive lens in movie theatres can be found in polarised glasses. On the other side, shutter glasses fall into the category of active glasses that are now widely used, for example in 3D TVs [64].

In a movie theatre, the reason 3D glasses are worn is to feed different image channels to the eyes. The screen actually displays two images and the glasses cause one of the images to enter one eye and the other to enter the other eye [70]. There are five common systems for doing this that are described further in detail: Anaglyph, Polarised, Decoder, Shutter and Pulfrich Glasses.

2.2.1 Anaglyph Glasses Displays

Anaglyph glasses use two different colour lenses to filter the images observed on the screen. The two most common colours used are red and cyan (Figure 2.2). If you were to look at the screen without your glasses, you would see that there are two sets of images slightly offset from one another. One will have a blue tint to it and the other will have a reddish hue. When viewed through the glasses a single image that appears to have depth is observed [15].

The explanation for this is as follows; the red lens absorbs all the red light coming from the screen thus cancelling out the red-hued images. The blue lens does the same for the

blue images. The eye behind the red lens will only see the blue images while the eye behind the blue lens sees the red ones as shown in Figure 2.1. Because each eye can only see one set of images the brain interprets this as both eyes are looking at the same object. However, the eyes are converging on a point that's different from the focal point -- the focus will always be at the screen; this creates the illusion of depth [15].

In anaglyph systems where the images are printed the lenses are generally red/green or red/blue as this matches the inks used for printing and the subtractive method of colour reproduction. Glasses for use with displays are generally red/cyan as this has a closer match to the primary colour spectra used in the additive colour reproduction method. In this system, two images are displayed on the screen, one in red and the other in blue (or green). The filters on the glasses allow only one image to enter each eye and your brain does the rest. You cannot have a full colour images when colour is used to provide the separation, so the image quality is not as good as with the polarised system [90].

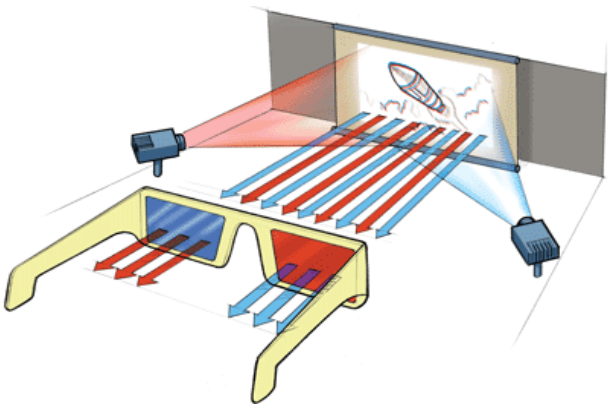

Figure 2.1: The red and blue lenses filter the two projected images allowing only one image to enter each eye.
(science.howstuffworks.com/3-d-glasses2.htm)

Figure 2.2: 3D glasses with red/blue lenses
(science.howstuffworks.com/3-d-glasses2.htm

One disadvantage with anaglyph 3D is that it can strain the eyes and can cause headaches and nausea in some people. Also, some viewers have a dominant eye and find it difficult to see the image as three dimensional [49].

The anaglyph method of displaying stereoscopic images uses a complementary colour-coding technique to send separate left and right views to an observer's two eyes. The two perspective images of a stereo-pair are stored in complementary colour channels of the display and the observer wears a pair of glasses containing colour filters which act to pass the correct image but block the incorrect image to each eye [49]. For example, if a red/cyan anaglyph is used, the left perspective image is stored in the red colour channel and the right perspective image is stored in the blue and green colour channels (blue + green = cyan), and the observer wears a pair of anaglyph 3D glasses with the left-eye filter red and the right-eye filter cyan. The main advantages of the anaglyph 3D method are its simplicity, low cost and compatibility with any full-colour display. The main disadvantages are its inability to accurately depict full-colour images and commonly, the presence of crosstalk.

The most important contributors to anaglyph crosstalk are display spectral response and anaglyph glasses spectral response. Less important contributors are image compression and image encoding/transmission. Figure 2.3 provides an illustration of the process of crosstalk in anaglyph stereoscopic images due to spectral leakage. Several papers have analysed crosstalk with anaglyph images in considerable detail [100, 102, 99].

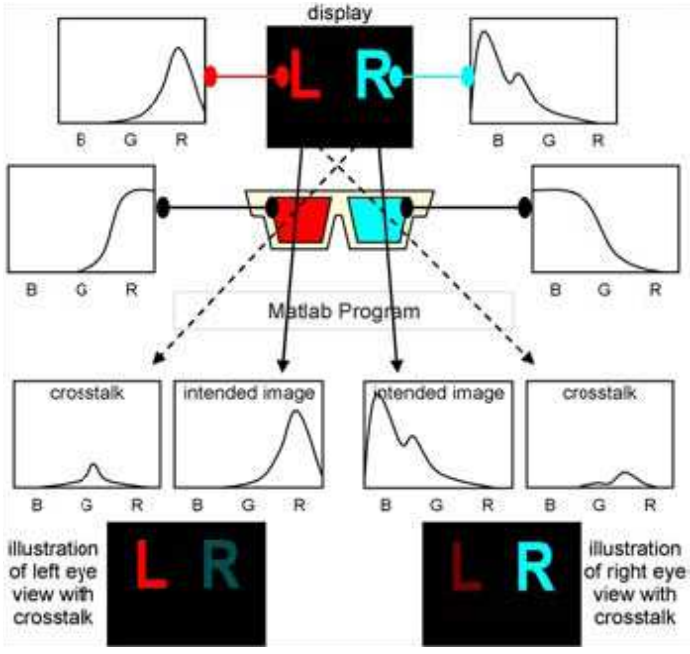

Figure 2.3: Anaglyph Crosstalk: From the top: (1) Spectral response of display, (2) spectral response of anaglyph glasses, (3) simulation of crosstalk using a computer program, (4) spectral output characteristic of crosstalk and intended image, and (5) visual illustration of left- and right-eye view with crosstalk.
(www.informationdisplay.org/article.cfm?year=2007&issue=11&file=art9)
Andrew J. Woods, Ka Lun Yuen, Kai S. Karvinen. "Characterizing crosstalk in anaglyphic stereoscopic images on LCD monitors and plasma displays", Curtin University of Technology

2.2.2 Decoder Glasses

Special lenses of Red/Red (Figure 2.4) or any identical colour for decoding secret messages (Figure 2.5). Decoder glasses are used to decipher hidden images or messages. Images or words can be encoded with dark red, blue, or green filters and computer image modifications [104].

Figure 2.4: Decoder Glasses
(www.3dglasses.net/3dglasses- How.htm)

The image in Figure 2.5 has a hidden message that becomes apparent when viewed with decoder glasses.

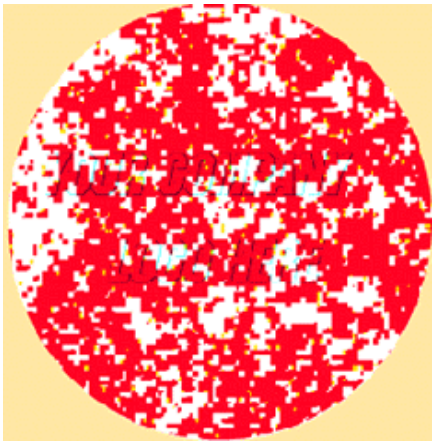

Figure 2.5: Secret decoded message
(www.theatricsupport.com/dec.html)

2.2.3 Polarising Glasses

Today, a more popular type of passive lenses in movie theatres can be found in the polarised glasses. Again, if one looks at a screen as shown in Figure 2.6 that uses this technology more than one set of images is seen [103]. The glasses use lenses that filter out light waves polarised at certain angles. Each lens only allows light through that is polarised in a compatible way. Because of this, each eye will see only one set of images on the screen. Polarised lenses are becoming more popular than anaglyph glasses because the glasses don't distort the colour of the image as much and provide a better

audience experience. This technique requires the polarisation to be retained at the screen so this is coated with a metallic paint layer.

At Disney World, Universal Studios and other 3D venues, the preferred method uses polarised lenses because they allow colour viewing. Two synchronised projectors project two respective views onto the screen, each with a different polarisation. The glasses allow only one of the images into each eye because they contain lenses with different polarisation [39].

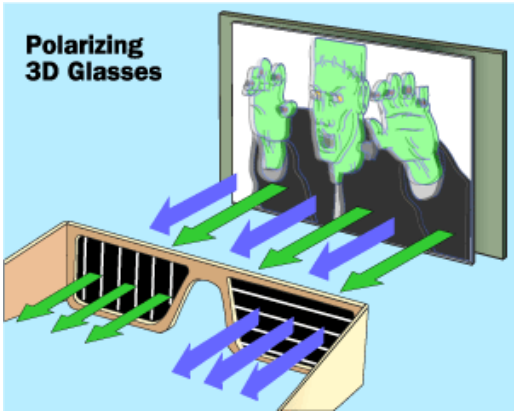

Figure 2.6: Polarising 3D Glasses & Projection Screen
(www.3dglasses.net/3dglasses- How.htm)

The difficulty arises because light reflected from a motion picture screen tends to lose some of its polarisation. However, this problem is eliminated if a 'silver' or Aluminised screen is used. This means that a pair of aligned digital light processor (DLP) projectors, some polarising filters, a silver screen, and a computer with a dual-head graphics card can be used to form a relatively low-cost (under US$10 000 in 2003) system for displaying stereoscopic 3D data simultaneously to tens of people wearing polarised glasses [91]. Such a system, called a GeoWall, has been used for several years now in the Earth Sciences application area.

When stereo images are to be presented to a single user, it is practical to construct an image combiner, using partially silvered mirrors and two image screens at right angles to one another. One image is seen directly through the angled mirror whilst the other is seen as a reflection. Polarised filters are attached to the image screens and appropriately angled filters are worn as glasses. A similar technique uses a single screen with an inverted upper image, viewed in a horizontal partial reflector, with an upright image presented below the reflector, again with appropriate polarisers [91]. Polarising techniques are most simply used with cathode ray technology, as polarisers are used within ordinary LCD screens for control of pixel presentation - this can interfere with these techniques.

Polarised lenses specially cut at opposing 45° degree angles for viewing stereo pairs projected through left and right polarising filters. These glasses are specifically used for viewing polarised 3D movies, 3D laser shows, concerts, ride simulators and multi-media displays.

Linear Polarised Glasses are the general purpose glasses as shown in Figure 2.7 used for polarised projection of slide shows, multi-media displays, concerts, movies, simulator rides, and viewing vectographs [39]. These glasses are for use in IMAX movie theatres. Linear polarised glasses have the left and right axis at 45 degrees and 135 degrees (perpendicular to each other), and a standard transmission of 37%.

Figure 2.7: Linear Polarised Glasses
(en.wikipedia.org/wiki/Polarized_3D_glasses)

An example of a linear polarised display is that produced by Planar (Figure 2.8). This display provides full native resolution images by utilising two LCD panels whose outputs are combined with a semi-silvered mirror. This is an elegant design as the silvering on the mirror has the dual function of combining the images and rotating the linearly polarised outputs from the LCDs into two orthogonally polarised beams that can be separated into the left and right channels for the appropriate eyes by the glasses.

Figure 2.8: Planar Display: Two full-resolution images are produced on a pair of LCD monitors and combined by a semi-reflecting mirror that also produces orthogonally polarised images suitable for passive glasses viewing.
(www.prlog.org/10704007-planar-3d-stereoscopic-displays-at-proflixsalescom-at-unprecedented-prices.htm)l

Circular Polarised Glasses can also be used for viewing LCD 3D images. An example of this is Stereo Graphics' Monitor ZScreen. Circular polarised glasses (Figure 2.9) have a horizontal linear axis (left and right) [91].

Figure 2.9: Circular Polarised Glasses
(www.dinodirect.com/3d-glasses-circular-polarized.html?cur=GBP)

Comparison Between Linear and Circular Polariser Technology Circular polarisation technology has the advantage over linear polarisation methods in that viewers are able to tilt their head and look about the theatre naturally without a disturbing loss of 3D perception, whereas linear polarisation projection requires viewers to keep their head orientation aligned within a narrow range of tilt for effective 3D perception; otherwise they may see double or darkened images.

2.2.4 Shutter Glasses

Liquid crystal shutter glasses (also called LC shutter glasses or active shutter glasses) are glasses used in conjunction with a display screen to create the illusion of a three dimensional image. Each eye's glass contains a liquid crystal layer which has the property of becoming dark when the voltage is applied, being otherwise transparent [51]. The glasses (Figure 2.10) are controlled by an infrared, radio frequency, DLP-Link or Bluetooth transmitter that sends a timing signal that allows the glasses to alternately darken over one eye, and then the other, in synchronisation with the refresh rate of the screen. Meanwhile, the display alternately displays different perspectives for each eye, using a technique called alternate-frame sequencing, which achieves the desired effect of each eye seeing only the image intended for it.

Figure 2.10: Shutter Glasses & IR emitter
(www.nvidia.com/object/product_geforce_3D_VisionKit_us.html)

Recently, Sony and Panasonic have introduced an ‘active shutter’ technique for high definition plasma and LCD TVs. The viewer still has to wear polarised glasses, but in this system the glasses have LCD active shutters that are synchronised with signals from the TV. The shutters rapidly block the right and left eye views alternately so each eye receives the correct image [37]. The new system gives higher resolution. Separate images for the left and right eyes are recorded with 1920 X 1080 full-HD quality and alternately played at high speed. By watching these images through special LCD glasses that are timed to open and close the right and left lenses in synchronisation with the alternating images, the viewer observes 3D.

Figure 2.11 shows shutter glasses used with an LCD display where the addressing time takes up a relatively large proportion of the frame period. During this time the shutter in front of each eye must be opaque [14]. Crosstalk occurs if there some residual image from the previous frame and if the shutter transmits some light in its ‘off’ state.

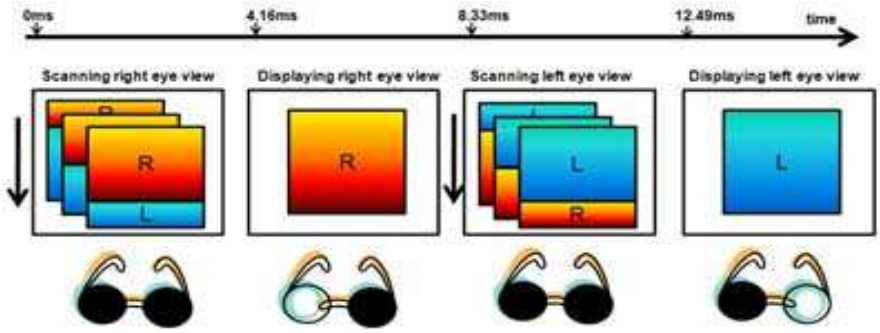

Figure 2.11: Shutter Glasses LCD Display: Left and right images are presented sequentially on the LCD. As the LCD is addressed to replace the left image with the right both shutters must be off. The right shutter is on until the left image starts addressing. Both shutters are then off until the screen is fully addressed, when this is complete the left shutter only is on.
(ieeexplore.ieee.org/xpl/freeabs_all.jsp?arnumber=1438253)

Advantages; LC shutter glasses mostly eliminate "ghosting" which is a problem with other 3D display technologies such as RealD 3D, or Dual projector setups. DIsadvantage: flicker can be noticeable except at very high refresh rates, as each eye is effectively receiving only half of the monitor's actual refresh rate. Modern LC glasses however generally work in higher refresh rates and mostly eliminate this problem.

2.2.5 Pulfrich Glasses

3D effect based on the phenomenon (named after Carl Pulfrich who never saw it!) of Dark and Clear lenses. The image through the dark lens reaches the brain slightly later than the image through the clear lens, creating the illusion of 3D. In 2000, 3D Pulfrich glasses

(Figure 2.12) were given to six million viewers in the United States and Canada for Discovery Channel's Shark Week.

Figure 2.12: Pulfrich Glasses
(www.3dglasses.net/Pulfrich 3D Glasses.htm)

The Pulfrich effect is a psycho-optical phenomenon wherein lateral motion by an object in the field of view is interpreted by the brain as having a depth component, due to differences in processing speed between images from the two eyes [61]. The effect is generally created by covering one eye with a dark filter.

In the classic Pulfrich effect experiment a subject views a pendulum swinging in a plane perpendicular to the observer's line of sight. When a dark neutral density filter is placed in front of the right eye a pendulum swinging in front of the viewer appears to make an elliptical orbit, giving the illusion that it is closer as it swings to the right, and further away as it swings to the left. When the filter is placed over the other the depth effect is reversed.

The most accepted explanation for the noticeable depth is reduced retinal illumination in terms of the other eye creating a signal delay due to the immediate spatial differences between objects in motion [94]. The most probable explanation for this is the visual latencies which are normally shorter for the visual system reacts faster to targets that are bright in contrast to targets which are dim. The moving object is observed in the retinal luminance and hence there is a difference in the signal latencies because of the distance between two eyes.

This effect can also be caused by several diseases of the eye such as cataracts, optic neuritis or multiple sclerosis. In these cases, symptoms that have been reported include having difficulty in judging the paths of cars that are coming towards the subject.

In visual media such as film and television, the Pulfrich effect is often used to produce 3D imagery with glasses. As in other kinds of stereoscopy, 3D glasses are used to create the illusion of a three-dimensional image [61]. By placing a neutral filter (by way of example, the darkened sunglass lens) covering one eye, an image, while moving back and forth to the left or to the right; the effect is not observed when the motion is in the vertical direction.

Because the Pulfrich effect depends on motion in a particular direction to instigate the illusion of depth, it is not useful as a general stereoscopic technique; for example it cannot be used to show a stationary object apparently extending into or out of the screen.

However, the novelty effect is found in the visual scenario. One advantage of material produced to take advantage of the Pulfrich effect is that it is fully compatible with regular viewing material (provided its content has the required motion) without the need for special capture cameras.

This effect was somewhat popular in the 1990's. It was used, for example, in a 3D motion TV advertisement in the 1990's where objects moving in a particular direction appeared less distant to the viewer than those moving in the opposite direction in relation to the background; the advertiser provided a large number of viewers with pairs of glasses having in a paper frame. In one eye the filter was more of a dark neutral gray and the other one was more transparent. In this instance, the commercial was restricted to objects such as skateboarders and refrigerators moving down a steep hill from left to right across the screen, a directional dependency determined by which eye was covered by the darker filter.

The effect was also used in the 1993 Doctor Who charity special entitled 'Dimensions in Time' and a 1997 special TV episode of 3rd Rock from the Sun. In many European countries, a group of short 3D movies made in the Netherlands were seen on TV. 3D Glasses were sold at a chain of gas stations. These short films were mainly travelogues of Dutch localities. An episode of The Power Rangers uses "Circlescan 4D" technology and was given away through McDonalds. Animated programs that employed the Pulfrich effect in specific segments of its programs include The Bots Master and Space Strikers; they typically achieved the effect through the use of constantly-moving background and foreground layers [94]. The famed Nintendo Entertainment System was known for using the effect along with their videogame Orb-3D through keeping the player's ship continually moving and also included a set of 3D Glasses. Another example is Jim Power in "The Lost Dimension" in 3D for the popular Super Nintendo gaming system, utilising interesting and unique scrolling backgrounds to give a particularly striking effect.

2.2.6 Market Survey

In many overseas markets, the number of 3D systems installed has doubled since January 2009. In some new markets, like Latin America, Australia, Russia and Eastern Europe, almost 100% of all digital installations are 3D. In many countries, where the multiplex- or circuit-wide 2D digital conversions have stalled due to lack of economic incentives, screen-by-screen 3D conversion is the single reason digital cinema is moving forward. Depending on how screens are counted, as of August 2009 there were between 4,800 and 6,600 3D-equipped screens, split approximately equally between the U.S. and international markets [93].

An advantage for exhibitors is that there are plenty of choices in processes and equipment. Following the 2005 debut of RealD's low-cost passive glasses and silver-screen solution, there is now competition from Dolby's reusable glasses and white-screen approach. There are also XpanD's active glasses and newcomer MasterImage's 3D solution. Increased competition in the marketplace is keeping equipment prices down and driving system performance even higher.

RealD continues to lead the market with approximately 3,400 systems installed as of July 2009. In addition, they have received orders that will bring their total to over 9,000 in the next few years. RealD estimates that 90% of US 3D box office is delivered on their 3D-equipped screens. Their new RealD XL light-doubler has been a hit with cinemas with larger screens. This is timely since more and more of the 3D titles are playing in the larger auditoriums [88].

Europe has been a particularly active market for RealD, with sales reportedly up 400% since the opening of their London office in February 2009 with industry veteran Bob Mayson at the helm. Exhibitors recently signing on to add RealD systems are Cinestar in Germany, CGR in France, Cineplex in Austria, Vue Entertainment in the U.K., Irish Multiplex Cinemas, and others.

In the fall of 2008, Sony announced they had developed a special 3D process and lens assembly for their 4K SXRD projector. It is a fairly simple and elegant solution, using their 4K chip to project two images top and bottom—one for each eye—and a special dual-lens assembly to converge the images on the screen. Sony has incorporated RealD's circular polarised filters, so the Sony 3D process is entirely compatible with the RealD glasses and the silver screen. Sony has entered an exclusive distribution plan so that the Sony lens is available through RealD's program. Since both the AMC and Regal theatre circuits have made large commitments to add Sony 4K projectors, a substantial number of these will be RealD 3D-enabled.

Dolby claims over 1,000 cinemas installed with their 3D system as of July 2009, with another 500 installations in progress. Rather than concentrating on a few key exhibitors, Dolby has been quietly building a strong base of support from many small and mid-sized exhibitor organisations, independent cinemas and specialty screening rooms [92]. With a broad and loyal geographic footprint around the globe, the Dolby system lends itself well to exhibitors where there is a desire to keep a white, non-silver screen and where managing reusable glasses is not a problem. Organisations such as the Academy of Motion Picture Arts and Sciences, the U.K.'s BAFTA, the Directors Guild of America, and a number of science centres and museums have selected the Dolby process. Dolby has also addressed the need to show their 3D on larger screens. In a joint development with

Barco, twin projectors are mounted in a custom configuration, allowing exhibitors to fill larger screens ranging from 41 to 70 feet. The Dolby and Barco large-screen solution is compatible with all of BARCO's twin-projector offerings, including their ultra-bright DP-3000.

XpanD, with what might be considered the original 3D process using active LCD shuttered glasses, has been gaining recognition, particularly in the European markets. They have around 1,000 3D screens installed. XpanD has been able to put new life into an old idea. The original shuttered glasses were large and heavy. With the acquisition of NuVision, the leading manufacturer of shuttered glasses, they have been re-engineered. XpanD's new X101 Series glasses are lighter, look stylish, and have easily replaceable batteries. Although the XpanD glasses are the most expensive, the costs are offset by the savings in basic booth equipment. All that is really needed beyond a 3D-capable digital projector and server is a fairly low-cost IR emitter for synchronising the glasses [21]. This also leads to more flexible operation as multiple screens can be equipped with the IR emitters and quickly used for 3D by bringing in the glasses. XpanD has made recent progress with exhibitor commitments from Yelmo Cinemas in Spain, Xtreme Cinemas in the Czech Republic, Euro Palaces Theatres in France and United Entertainment and Camelot Cinemas in the U.S. In Asia, XpanD has a distribution agreement with Singapore-based server manufacturer GDC Technology to incorporate their 3D systems into the growing base of digital systems in mainland China.

MasterImage, a Korean company, is the fourth and newest entry into the commercial cinema 3D business. MasterImage USA, headed by cinema veteran Peter Koplik, recently opened an office in Burbank, Calif., to specifically focus on the exhibition market. The MasterImage system, like RealD, uses a silver screen and low-cost glasses, but the filter is a spinning wheel in an enclosure positioned between the projection lens and the porthole. MasterImage claims the simplicity of their systems results in lower costs and increased flexibility, without compromising image quality.

Currently, MasterImage has approximately 130 systems in North America, bringing their total installed base to over 300 screens worldwide [20]. They have just concluded a major agreement with the U.K.'s Empire Cinemas for 40 systems. Other recent installations include 12 systems for Palace Cinemas to be installed in the Czech Republic and Hungary. Plus, they are planning on adding 30 systems in Ireland. At ShoWest 2009, MasterImage announced a distribution agreement with DTS Digital Cinema.

Another recent development facilitating the spread of 3D is progress toward a single-inventory 3D master for distribution to the cinemas. Both the RealD and Dolby 3D processes, for most excellent imaged quality, require a small but different type of pre-

processing on the files before being sent to the projector. Initially, the RealD pre-processing, referred to as ghost busting, was added to the DCP delivered to the theatres, but that caused distributors to have to identify in advance which system was being used and maintain multiple inventories of digital prints. The Dolby pre-processing was performed in Dolby's server, but that limited Dolby 3D playback to those cinemas with Dolby servers. To resolve the issue, both RealD and Dolby have begun licensing their pre-processing to server manufacturers, thereby allowing one compatible single-inventory DCP to be used for all 3D systems.

2.3 Summary

The earliest form of 3D glasses viewing was anaglyph introduced by Wilhelm Rollmann in 1853; this is the familiar red/green glasses method. Anaglyph operates by separating the left and right image channels by their color. Early anaglyph systems used red and green or red and blue. When liquid crystal displays (LCD) are used, where colors are produced by additive color mixing, better color separation is obtained with red/cyan glasses.

Left and right image channels can also be separated with the use of polarised light that can be either linearly or circularly polarised. Circular polarisation has the advantage that the separation of the channels is independent of the orientation of the polarisers so that rotation of the glasses does not introduce crosstalk.

The other method of separating the channels is with the use of liquid crystal shutter glasses where left and right images are time multiplexed. In order to avoid image flicker, images must be presented at 60Hz per eye, that is a combined frame rate of 120Hz. The earliest shutter glasses displays used a cathode ray tube (CRT) to produce the images as these can run at the higher frame rate required.

Although Pulfrich stereo can be shown on a two-dimensional image without the loss of resolution or color rendition and without the use of special cameras, its use is limited and it is only suitable for novelty applications as either the cameras have to be continually panning or the subject must keep moving in relation to its background.

CHAPTER 3

AUTOSTEREOSCOPIC DISPLAYS SURVEY

3.1 Introduction

Autostereoscopic displays are those which create a stereoscopic image without any special glasses or other user-mounted artefacts. There are various classifications of displays and the terminology is not always clear, however perhaps most useful here is the classification that divides the basic autostereoscopic display types into three principal areas, these being: holographic where the image is formed by wave-front reconstruction, volumetric where the image is formed within a volume of space without the use of light interference, and multiple image where different two-dimensional images are seen across the viewing field. These basic types, along with sub-divisions of the technologies within each group, are shown in Figure 3.0. This survey will describe the state of the art in all of them.

This chapter covers autostereoscopic displays that are likely to provide the next generation of mainstream 3D display after consumers tire of glasses displays. Simple two-view displays where a stereoscopic pair can be observed in fixed regions in the viewing field are not covered. These are less comfortable to watch than glasses displays as they require the user to remain close to a sweet spot, so are unlikely to be adopted for widespread use.

Multi-view displays are covered. These are a mature technology and if displays with a sufficiently high resolution become available, these could potentially provide a simple hardware solution. In one respect, they do not provide the most efficacious solution in terms of display usage as they require the display of redundant information due to images being directed into the viewing field where no viewers' eye is necessarily present. Integral imaging is a technique that was proposed over one hundred years ago but this may become a viable approach again if sufficiently high resolution displays become available.

Another approach is to use head position tracking in order to direct images only to those regions in the viewing field where a viewer's eye is actually present. This is necessarily more complex than other methods but its use could be unavoidable if the required high resolution display does not become available in the near future. The work carried out in the European MUTED and HELIUM3D projects, where head tracking is employed, is described below in some detail. Head tracking is also being pursued by other researchers, for example the system under development by Microsoft [83].

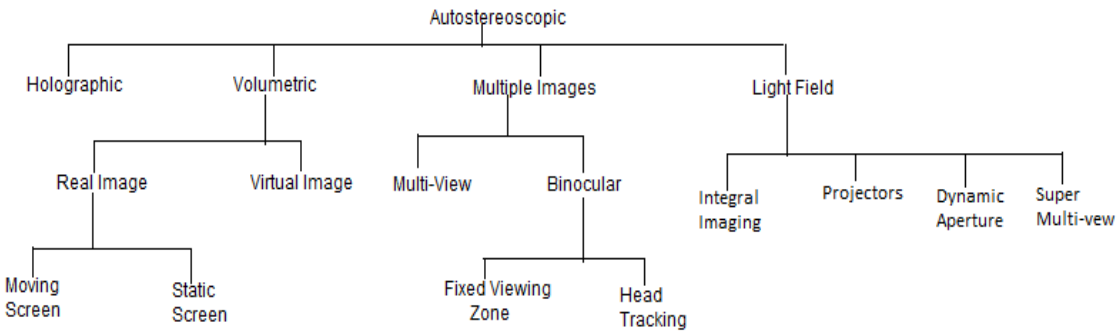

Figure 3.0: Classification of autostereoscopic types

3.2 Autostereoscopic Display Types

3.2.1 Holography

Whilst holography is well established amongst the scientific community, its impact has not yet had a great impact upon the general public. Many people are familiar with the 3D holographic images found on credit cards; however, these are low quality images that do little justice to the capabilities of holography. Colour holography produces 3D images of startling quality, with depth cues and parallax that are difficult to achieve by other techniques. Even fewer people have witnessed dynamic holograms or holographic movies that have been produced either by electro-holography or more conventional techniques. Historically, holographic movies and television have been limited by their reliance on high-resolution emulsions for recording and reconstruction. More recently, developments in CCD capture technologies and SLMs have moved the technology into the digital domain were transmission of holographic data is possible. A number of challenges need to be overcome before holographic 3D display is ready for the mass markets. However, the prospect of full wavefront dynamic reconstruction of 3D images is tantalisingly close and must be aspired to.

3.2.2 Volumetric

Volumetric displays are one interesting potential category of displays for future 3D TV. Volumetric displays are a broad and diverse collection of various methods, technologies and ideas. Most of them may be interesting only for academic purposes and few of them will hit the mainstream and become commercially available for longer periods of time. Volumetric displays produce the surface of the image within a volume of space [7]. The 3D elements of the surface are referred to as ‘voxels’, as opposed to ‘pixels’, on a 2D surface. As volumetric displays create a picture in which each point of light has a real

point of origin in a space, the images may be observed from a wide range of viewpoints. The viewer can examine the 3D image from all angles.

In principle, volumetric displays could provide realistic images that do not exhibit accommodation/convergence (AC) mismatch where the eyes converge at a different distance to their focus; however, in addition to image transparency they cannot readily portray surfaces that have a non-Lambertian distribution. Dependent on the scene, this could represent a high proportion of a natural image. Volumetric displays have the ability to display motion parallax in both the vertical and horizontal directions. The displays are of two basic types; virtual image [7] and real image [86].

Figure 3.1 shows the Volumetric Display [2]. The ICT Graphics Lab at USC has created a low-cost volumetric 3D display. The process is not simple but can be defined through a few key concepts: spinning mirrors, high-speed DLP projectors, and very precise computation that calculates the correct axial perspective needed for a 360-degree image.

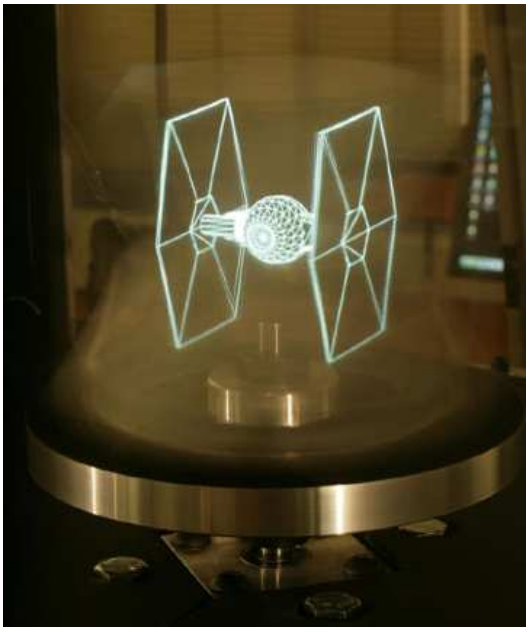

Figure 3.1: USC ICT Graphics Lab's Volumetric Display

The USC volumetric display is different and considerably more realistic. When projecting video frames into a rapidly spinning mirror, around 5,000 individual images are reflected every second within the surface area and come together to create a real-space three-dimensional object. Because the images projected from the mirror jump out ‘toward multiple viewpoints in space’, the USC team created a formula that renders individual projections at different heights and traces each projected beam back to the display area to find the correct position of the viewer.

The system also updates itself in real time at 200Hz, adjusting to the height and distance of the viewer, producing an image that will ‘stay in place’. In this way, every person in a

room will be able to have a correct perspective, as in a holographic image. It also allows for the correct image occlusion as well as the appropriate image shading necessary for each item. More importantly, it enables simultaneous viewing without the use of special glasses.

3.2.3 Two-image Display

DMU has constructed a lenticular display that has a fixed pair of viewing zones. This display was constructed by using the glass lenticular screens manufactured to FHG's specification for the Free2C display that was developed in the ATTEST project. In order to keep costs down the same screens were also used as a spatial MUX screen for DMU's multi-user display in this project. As there were some surplus screens one of these was carefully attached to the front of an NEC Multisync 2110 21″ LCD monitor in order to provide a 3D display for evaluation purposes.

The display is rotated 90° to portrait format so that the pixel rows become columns. The lenticular screen is mounted in front of the LCD and aligned with the pixels. It pitch is slightly less than double the pixel horizontal pitch in order to allow for parallax. The function of the screen is to steer light from alternate columns of the display to alternate viewing zones where an observer can view the three-dimensional image as shown in Figure 3.2. In practice multiple viewing zones are created because light from one row of pixels can travel through more than one lens. This means several observers can see a three-dimensional image at once but care has to be taken to select suitable pairs of viewing zones to avoid seeing a pseudoscopic image.

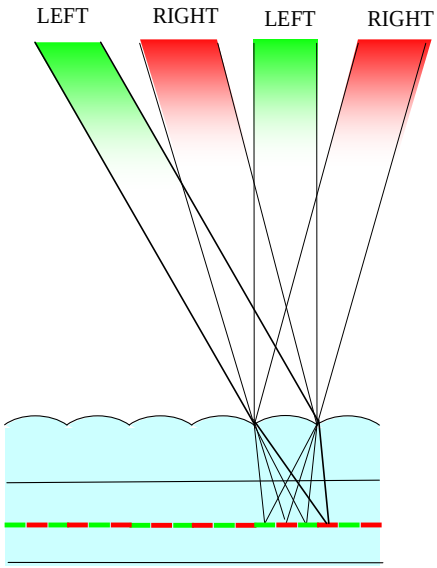

Figure 3.2: Lenticular screen forming exit pupils

3.2.4 Multi-view

In multi-view displays, a series of discrete views is presented across the viewing field. One eye will lie in a region where one perspective is seen, and the other eye in a position where another perspective is seen. By definition, the number of views is too small for continuous motion parallax. Current methods use either lenticular screens or parallax barriers to direct images in the appropriate directions.

Lenticular screens with the lenses running vertically can be used to direct the light from columns of pixels on an LCD into viewing zones across the viewing field. The principle of operation is shown in Figure 3.3. The liquid crystal layer lies in the focal plane of the lenses and the lens pitch is slightly less than the horizontal pitch of the pixels in order to give viewing zones at the chosen distance from the screen; this is the distance where uninterrupted 3D is seen across the complete width of a group of viewing zones. In this case three columns of pixels contribute to three viewing zones.

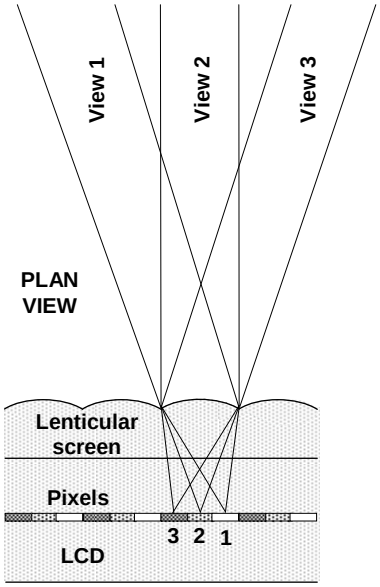

Figure 3.3: Multi-view light directing: Light from three pixels is shown as being directed in three directions. The number of views is usually greater and a parallax barrier might be used in place of the lenticular screen.

A simple multi-view display with this construction suffers from two quite serious drawbacks. Firstly, the mask between the columns of pixels in the LCD gives rise to the appearance of vertical banding on the image known as the ‘picket fence’ effect. Secondly, when a viewer’s eye traverses the region between two viewing zones, the image appears to ‘flip’ between views. These problems were originally addressed by Philips Research Laboratories in the UK by the simple expedient of slanting the lenticular screen in relation to the LCD [6]. An observer moving sideways in front of the display always sees a constant amount of black mask, therefore rendering it invisible and eliminating the

appearance of the ‘picket fence’ effect which is a moiré-like artefact where the LCD mask is magnified by the lenticular screen.

The slanted screen also enables the transition between adjacent views to be softened so that the appearance to the viewer is closer to the continuous motion parallax of natural images. Additionally it enables the reduction of perceived resolution against the display native resolution to be spread between the vertical and horizontal directions. For example, in the Philips Wow display the production of nine views reduces the resolution in each direction by a factor of three. The improvements obtained with a slanted lenticular screen also apply to a slanted parallax barrier.

It should be noted that the concept of crosstalk has a different interpretation in two-image and multi-view displays. Whereas crosstalk is a disadvantage in two-image displays where a certain amount of one channel is seen by the other eye, it is probably an advantage in multi-view displays as it enables blending of adjacent images. It is preferable to refer to the effect as ‘ghosting’. In Figure 2.12(a) the intensity of a series of 5 images with lateral position is shown. It can be seen that there is not an abrupt transition at the edge of each view; this cannot be achieved in practice and is also possibly not desirable.

The eye shown in Figure 2.12(a) will see view 4 at 100% brightness, but also views 3 and 5 at reduced brightness. The virtual position of an object is shown in Figure 2.12(b) and for view 4 this occupies the position on the screen indicated by ‘Viewing zone 4 image’. The same object occupies position ‘Viewing zone 3 image’ on the screen for the image directed towards zone 3. This results in the displaced ‘ghost’ image shown. There will also be a ‘ghost’ image of view 5 that is not shown in the figure for reasons of clarity. When a virtual object is too far from the screen the resulting image is uncomfortable to watch.

There are several companies with an interest in multi-view displays, but Philips, who was involved with these for fifteen years, finally discontinued sales and production of the 42” Wow 9-view display in March 2009. Philips Consumer Lifestyle still has an interest in consumer television in the future and is in fact a partner in the HELIUM3D project that is described later. The French Alioscopy company produces 42” and 47” 8-view displays that appear to operate on the same slanted lenticular screen principle as the Philips Wow display and arguably give superior images [23]. The Philips 42″ Wow (Figure 3.4) is a multi-view display; these displays operate by providing a series of discrete images across the viewing field with each image presenting a different view. This gives motion parallax and repeating the series of images enables a wide viewing region. This viewing region is restricted to the viewers being fairly close to the optimum viewing distance (as defined earlier) and also not being located at the boundaries of the zones where pseudoscopic images are seen.

Multi-view displays require the native resolution of the display to be reduced for each zone image. The display could consist of a vertically-aligned light-directing screen (parallax barrier or lenticular) that reduces the horizontal resolution by a factor of the number of views. A better method is to have a slanted view-directing screen. The Philips 'Wow' display provides the nine viewing zones by reducing both the vertical and horizontal resolutions by a factor of three.

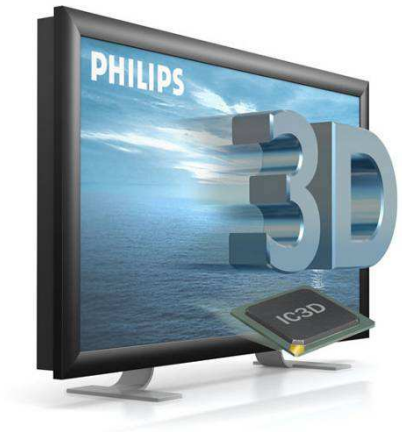

Figure 3.4: Philips 42" Wow display: This figure is taken from the Inition website and depicts 3D as it could never be seen in practice. The Wow display is no longer available.

3.2.5 Light Field Displays

In light field displays discrete beams of light that vary with angle radiate from each point on the screen. These can take several forms and integral imaging, multi-beam and dynamic apertures are considered here.

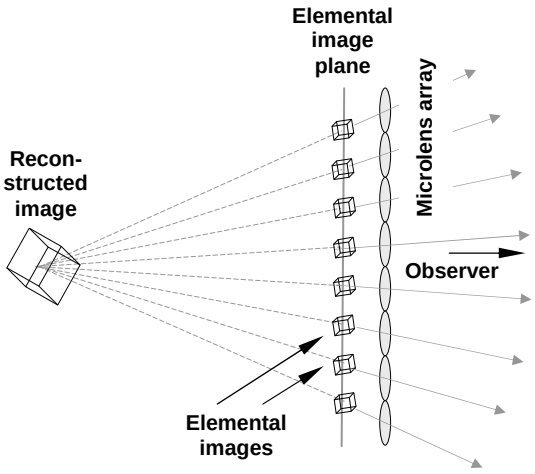

Figure 3.5: Integral imaging: orthoscopic image reconstruction. Rays from the elemental images form a reconstructed image where they intersect; in this case a virtual image is produced behind the screen.

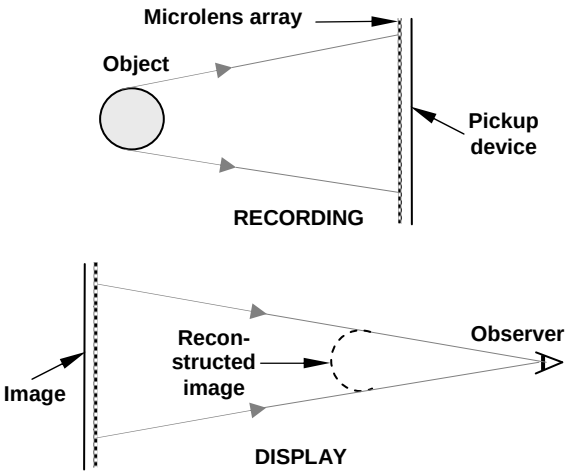

Figure 3.6: Integral imaging: pseudoscopic images. The reconstructed images are reversed in depth (pseudoscopic). If no action is taken to prevent this objects are effectively seen from the 'inside'.

Integral imaging displays were an early technique and first proposed by Gabriel Lippmann in 1908 [40] [63]. An array of small lenses is used to produce a series of elemental images

in their focal plane as shown in Figure 3.5. If the lens array is two-dimensional fly's eye lens then motion parallax in both the horizontal and vertical is provided. A fundamental problem with this technique is the production of images with reversed depth known as pseudoscopic images (Figure 3.6). The effect is unnatural and normal orthoscopic images are required; there have been methods devised to overcome this problem [46] [3] without degradation of the images.

NHK in Japan has carried out research into integral imaging for several years including one approach using projection [44]. In 2009 NHK announced they had developed an 'integral 3D TV' achieved by using a 1.34 millimetres pitch lens array that covers an ultra-high definition panel.

Hitachi has demonstrated a 10" 'Full Parallax 3D display'; that has a resolution of 640 x 480. This uses 16 projectors in conjunction with a lens array sheet [28] and provides vertical and horizontal parallax. There is a trade-off between the number of 'viewpoints' and the resolution; Hitachi uses 16 800 x 600 resolution projectors and in total there are 7.7 million pixels (equivalent to 4000 x 2000 resolution).

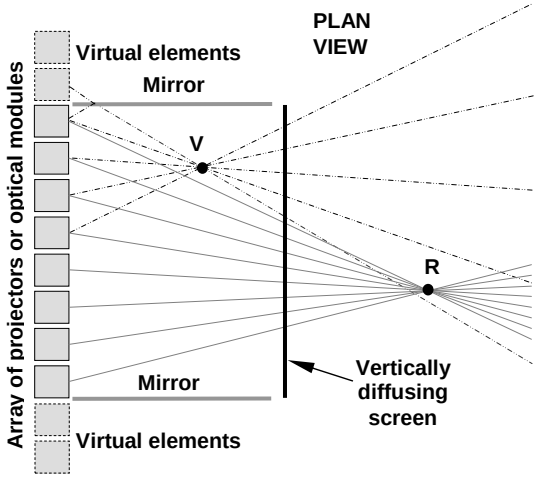

Figure 3.7: Light field: multi-beam: Optical modules provide multiple beams that converge and intersect in front of the screen to form real image voxels (R) or diverge to produce virtual voxels (V) behind the screen.

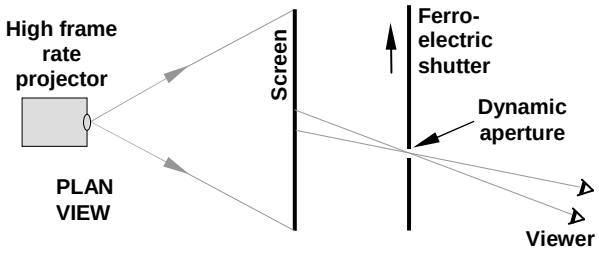

Figure 3.8 Light field; dynamic aperture: This uses a fast frame rate projector in conjunction with a horizontally scanned dynamic aperture to provide perspectives dependent on viewer position.

In multi-beam displays optical modules provide multiple beams that both converge and intersect in front of the screen to form real image voxels or diverge to produce virtual voxels behind the screen (Figure 3.7). The screen diffuses the beams in the vertical direction only allowing viewer's vertical freedom of movement without altering horizontal beam directions. As the projectors/optical modules are set back from the screen, mirrors are situated either side in order to provide virtual array elements either side of the actual array. Examples of this type of display are Holografika [4] and QinetiQ. Holografika can

currently supply a 32" display using 9.8 megapixels and a 72" version with 34.5 megapixels [29]. The QinetiQ display appears to operate on the same principles but uses projectors instead of the optical modules of Holografika. As very little has been heard of the QinetiQ display for a few years it is possible that this is not currently being developed any further.

The dynamic aperture type of light field display uses a fast frame rate projector in conjunction with a horizontally scanned dynamic aperture as in Figure 3.8. Although the actual embodiment appears to be totally different to the multi-beam approach, the results they achieve are similar. In the case of the dynamic aperture the beams are formed in temporal manner. An early version of this type of display used a mechanically scanned aperture with the images supplied by a cathode ray tube [85]. More recently this has been developed further at Cambridge University with the use of a fast digital micromirror device (DMD) projector and a ferroelectric shutter [48]. This is currently available from Setred as a 20” XGA display intended for medical applications.

3.2.6 Super Multi-view

A super multi-view (SMV) display is a multi-view display where the number of discrete images presented is sufficiently large to give the appearance of continuous motion parallax with no accommodation/convergence (AC) mismatch. AC mismatch is arguably the principal disadvantage of stereoscopic methods as it can potentially cause visual fatigue due to the eyes focusing at a different distance to their convergence. If sufficient views are provided, this mismatch does not occur and research has been carried out into the number of views required. A research group at the Telecommunications Advancement Organisation (TAO) in Japan has identified the need for a large number of views in order to overcome problems caused by AC mismatch [35]. Their approach was to provide sufficient views for the pupil to receive two or more parallax images.

In a paper from MIT [42], where multiple views across the viewing field are produced holographically are analysed, the effect of the image appearing to 'jump' between adjacent views is considered. This phenomenon is similar to aliasing when a waveform is under-sampled, i.e. when the sampling rate is less than double the maximum frequency in the original signal. This gives a result that is in the same order as the figure obtained from research at Fraunhofer HHI where it has been determined that typically, 20 views per interocular distance are required for the appearance of smooth motion parallax [52]. As AC mismatch occurs when the virtual position of an object in the image is away from the plane of the screen; there is a limit below which the mismatch is acceptable. It has been determined that the depth range should not exceed 13% of the viewing distance [12]. Another criterion is the 'one degree of disparity rule' [32]. Although multi-view displays

show motion parallax, the images are generally within the ±13% region for current readily available versions (9 views or less) as the depth of field is limited due to the visibility of adjacent viewing zones. That was mentioned in the previous section.

Although multi-view and integral imaging operate on different principles at lower screen resolutions, their principles of operation merge as the number of views increases. The depth of field will increase with increasing number of views but there has been nothing found in the literature quantifying this. If a 4K x 2K native resolution panel becomes affordable in the future, the expected resolution of each of image in a 64-view system based on this would be in the region of 500 x 250 (the exact value being dependent on the slant angle of the lenticular screen). This is not an acceptable resolution so it may be some time before SMV becomes a viable solution. A system was demonstrated at CeBIT 2010 by Sunny Ocean Studios [72] that can supply 64 viewing zones. It is not clear at present how a sufficiently high pixel count is obtained for this.

A slanted lenticular 72-view display is mentioned [30] in a presentation from the National Chaio Tung University in Taiwan but it is not clear whether this has actually been built due to the very high resolution LCD required. A 256-view display has been developed by the Tokyo University of Agriculture and Technology [81] where the outputs of sixteen 16-view Multiview displays are combined by projection lenses on to a vertical diffuser to provide a 10.3” display. The horizontal pitch of the viewing zones is 1.3 millimetres which is less than the pupil diameter therefore fulfilling one of the criteria given for continuous motion parallax.

3.3 Advantages/Disadvantages of Each Approach

3.3.1 Holography

Although in principle holographic displays have the ability to perfectly reproduce an original scene, a large amount of redundant information must be displayed in order to do this. Also, it is not clear how naturally-lit scenes will be captured. Possibly the scene could be captured with a camera array and a hologram synthesised from this. This would be computationally intensive and also has the risk of not providing a particularly natural-looking image.

3.3.2 Volumetric

These displays have the advantage that the image presented has full motion parallax and that the accommodation and convergence of the eyes are the same for every point in the image. Also they have the advantage that every voxel is only displayed once – as opposed to multi-view and multi-beam that display each image point many times. The

principal disadvantage of these displays is that the images are transparent so that voxels that lie behind a front surface are seen through it. Another difficulty that is possibly less important than transparency, but could give an unrealistic appearance to natural images, is that of the inability to display surfaces with a non-Lambertian intensity distribution. The hardware also tends to be large and moving surfaces are used in many instances.

3.3.3 Light Field

Light field displays require the presentation of a large amount of information in order to give the appearance of continuous motion parallax. There are various criteria for this and the generally agreed figure is for a different image to be presented to the eye approximately every two millimetres across the viewing field to give a usable image. Most proposed methods do not have vertical motion parallax so that there will still be rivalry in the vertical direction; and also the eyes will be attempting to focus at two different distances at the same time. This is an area that should be the subject of human factors investigations.

3.3.4 Multi-view

The construction of multi-view displays is generally simple and they do not require any form of head tracking. Resolution loss is a problem but this can be minimised with strategies such as slanted lenticular screens or stepped parallax barriers. The accommodation of the eyes is generally different to the convergence. However, as the eyes will focus at the screen and the depth of field is limited, this will possibly not be a problem. Lenticular multi-view displays have been gradually evolving for more than a decade. Due to loss of resolution, limited depth of field and restricted viewing regions current performance is limited. Higher resolution LCDs will enable performance in these areas to be improved.

3.3.5 Multi-beam

The construction of these displays is generally fairly complex and the housing size is large. The problem with these displays is that a lot of information must be displayed (100 megapixel in the case of Holografika). With the optical module/projector and integral imaging methods the depth of field is limited and in the ferroelectric barrier method the image can appear to ‘shear’. However these displays are capable of motion parallax.

3.3.6 Two Image

These displays are the simplest to construct, however they suffer from the disadvantages of accommodation / convergence rivalry, lack of motion parallax and most importantly do

not allow freedom of head movement. The limited head movement can be overcome with the use of head tracking. This can be achieved for single or multiple viewers.

3.3.7 Comparison of MUTED with other Autostereoscopic Displays

In Appendix 1 Table A.1.1 shows a summary of the technology capabilities of both multiple view and volumetric and holographic displays. The capability for multiple viewer and viewer movement is shown, together with the image display properties of each technology, the complexity and estimated costs. In Table A.1.2 various displays in each generic type are listed, along with a brief description of the technology.

As stated earlier, moving image holography is too far in the future to be a serious contender in the markets envisaged for MUTED display. Two image non-head tracked and single user head tracked displays only serve one viewer so applications for these are not covered in the potential MUTED application areas. The large housing size and image transparency of volumetric displays also makes these unsuited to anticipated applications. Therefore only the displays marked blue are likely to fulfil the same requirements.

Having determined that the generic display type's multi-view and multi-beam have the potential to compete in possible MUTED application areas, it is necessary to ascertain which examples of these will not be suitable. Five of these are not suitable and the reasons for this are given in the right hand column (Table A.2.1).

3.4 Summary

There are many autostereoscopic displays and they cannot all be described in a single chapter. There are however only a limited number of categories of glasses-free displays and their brief definitions and attributes can be summed up as follows:

Holography is a method of recording three-dimensional image of an object as a pattern created by interference from a reference laser beam and the light obtained by reflection from the object when this is illuminated with light that has been split from the reference beam. The image is recreated by illuminating the recorded interference pattern with either laser or non-laser illumination. Holography has the potential to provide a perfect reproduction of the original object. It does, however require the recording of a very large amount of information as its use for a moving image display is probably some years away.

Volumetric displays recreate an image within a volume of space where this volume can be either real or virtual. They have the advantage that the natural accommodation/ convergence relationship of the eyes is not violated so that eyestrain does not occur. The disadvantages of volumetric displays are that they generally exhibit image transparency and cannot show a non-Lambertian light distribution. These limitations have been

addressed recently by groups carrying out research into methods of producing anisotropic light distribution from the surface of the imager.

Two-view displays are simple to produce as they can be produced with only a flat display and a lenticular sheet or parallax barrier. Their principal disadvantage is that 3D can only be seen in a single ‘sweet spot’ or a series of ‘sweet spots’.

Multi-view displays are probably the most common type of autostereoscopic display at present. As a series of images is produced across the viewing field head position is not limited to the ‘sweet spot’ and 3D can be seen over a wide field. They are simple to construct as they comprise only a flat display and either a lenticular screen or a parallax barrier. Their disadvantages are that there is a trade-off between number of views and resolution, the viewing field is relatively limited and the depth of field of the image is restricted.

Super multi-view displays are a multi-view displays where a large number of views is provided. If the number of views is sufficiently large, continuous motion parallax will be seen and there will be no conflict between accommodation and convergence. This type of display will be more viable as higher resolution displays become available.

Light field displays emit light from each point on the screen that varies with direction in order to faithfully reproduce a natural 3D scene but without the use of holography. These can take several forms including integral imaging, optical modules and dynamic aperture. Light field displays require large amounts of information to be displayed

Head tracked displays can overcome many of the disadvantages of other types of display. The amount of information displayed is kept to a minimum as only two views have to be displayed if all the viewers see the same image pair, and only 2N views if motion parallax is supplied to N viewers. These displays produce exit pupils that are steered around the viewing field under the control of a head tracker in order to follow the viewer’s eye positions.

CHAPTER 4

LASER PROJECTOR DISPLAY DESCRIPTION

4.1 Background

The MUTED project ran from 2006 until 2009 and its purpose was to build a multi-user autostereoscopic display where several users can move freely over a room-sized area. The ultimate goal of the research is to produce a display suitable tor TV purposes as its name implies (Multiple User Television Display). Within the actual project the display was intended for the niche medical market, and a partner specialising in synthesising computer generated stereo images from CT and MRI scan information was taken on board.

In the MUTED display, left and right images are produced on a direct-view LCD and the conventional backlight is replaced with steering optics that can produce multiple pairs of exit pupils that follow the positions of the viewers' eyes under the control of a multi-user head tracker (Figure 4.1) [75]. The steering optics consists of arrays of optical elements that produce series of intersecting collimated beams at each eye position. Each beam is produced from a spot of light whose position is controlled in order to direct the output beam in the appropriate direction. Two arrays are required in the 60Hz version of the display; one for producing the left exit pupils and one for the right exit pupils. The reason for this is that the left and right images are produced simultaneously on the LCD on alternate rows of pixels. Light from each of the arrays, which are positioned one above the other, is separated into the correct pixel rows by a horizontally-aligned lenticular screen located behind the LCD. The spatial multiplexing method was adopted, as when the project commenced in 2006 there was no LCD available to run at the 120Hz rate necessary for temporal multiplexing.

In the first iteration of the display, spot patterns were produced by an RGB laser projector. This has the advantage that the sparse spot patterns required are produced by light interference so that the complete wavefront is utilised and concentrated into the pattern. In a conventional projector the unwanted light is blocked. The performance of this version is fairly poor in terms of brightness and stability, and for this reason a spatially multiplexed version has been built using a conventional LCOS projector. This gives a brighter image that can be viewed in reasonably high ambient light and there are no stability issues. Since 2009, 120Hz LCDs have become available and a version incorporating a 120Hz LCD and A DMD projector is currently under construction. This version is capable of providing full screen native resolution as opposed to the halved vertical resolution of the previous 60Hz versions. Also, only one steering array is required as the sets of left and

right exit pupils are produced sequentially. The lenticular multiplexing screen is no longer necessary as the images are not temporally multiplexed.

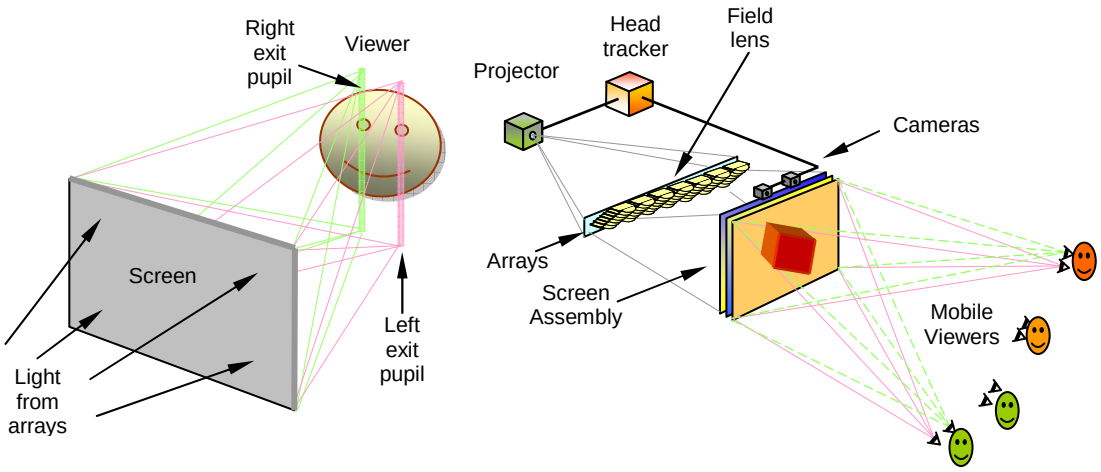

(a) Exit pupils in the region of a viewer's head are formed by intersecting collimated beams from the screen.

(b) Schematic diagram of MUTED display showing the principal components.

Figure 4.1: MUTED Display and Exit Pupils

The display optics effectively performs the function of a large lens that has several small illumination sources behind it that provide real images in the viewing field. An eye located in these regions perceives illumination over the complete area of the lens. The function of a single large lens can be performed with an array of smaller lenses with multiple light sources behind them; this overcomes the housing size and aberration problems.

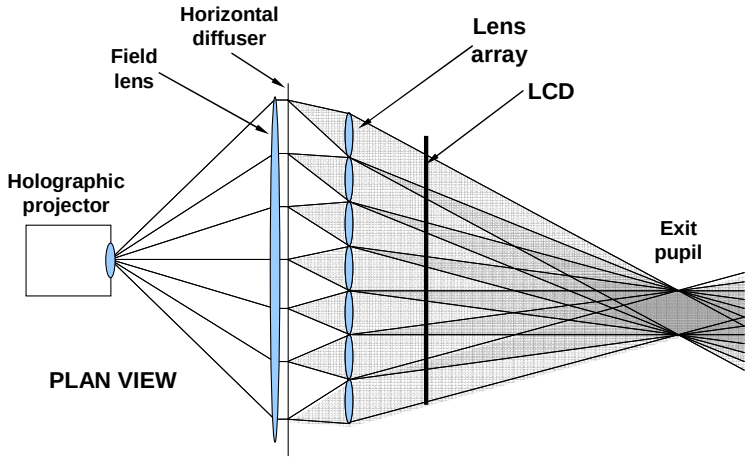

Figure 4.2: Formation of Exit Pupil. A series of illumination points are converted into a series of intersecting collimated beams.

Figure 4.2 shows the way in which a series of illumination points located in the plane of the horizontal diffuser are converted into a series of collimated beams that emerge from the front surfaces of the array elements and intersect at the viewer's eyes after passing through the LCD. A series of spots is generated for each viewer and as the viewer comes closer to the screen the spacing of the spots increases. As the viewer moves laterally the spots move in the opposite direction. Multiple exit pupils are formed by multiple series of illumination points. For simplicity of explanation, the beams from the projector are shown as being collimated with a large lens but in practice a large mirror is used for this purpose in the laser projector prototype.

4.2 Display Structure

The purpose of MUTED is to address limitations identified in previous research by replacing the curved LED illumination arrays originally used with a single projected image and to incorporate an LCD with a more suitable sub-pixel structure that produces less diffraction effects. Figure 4.3(a) shows the configuration of the display where a large mirror is used to collimate the output beam from a laser projector. An array element that produces a collimated beam is illustrated in Figure 4.3(b). Light is contained between the upper and lower surfaces by total internal reflection and the intensity across the beam width controlled by the soft aperture. The design of the transmission profile is critical and its detailed design is given in Section 4.6.

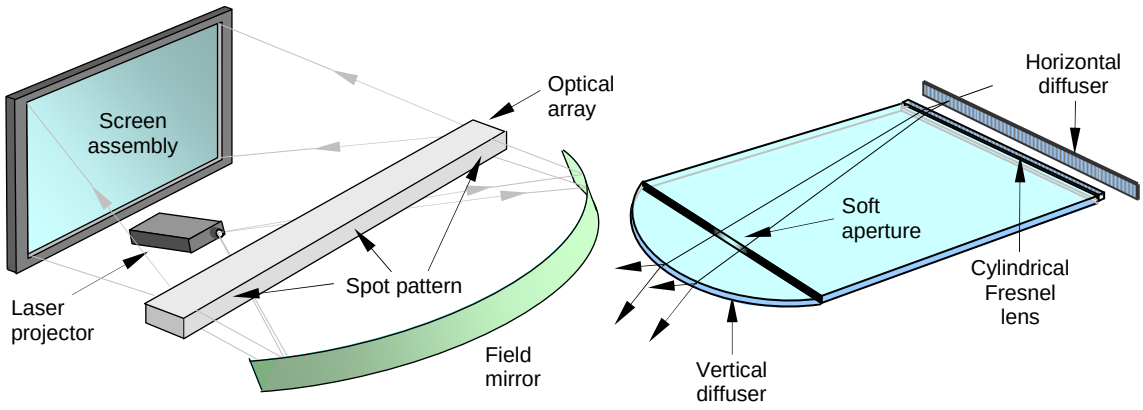

(a) Layout of MUTED Display components. The field mirror collimates the projector output.

(b) Optical Array Element. This converts the incident light spot into a vertically diverging collimated beam.

Figure 4.3: MUTED Display Layout and Array Element

Left and right images are presented on alternative pixel rows on the LCD and light for each set of images is obtained from two horizontally displaced sources (upper and lower

array as shown in Figure 4.4). The picture also shows the head tracker camera array and the screen height adjustment mechanism.

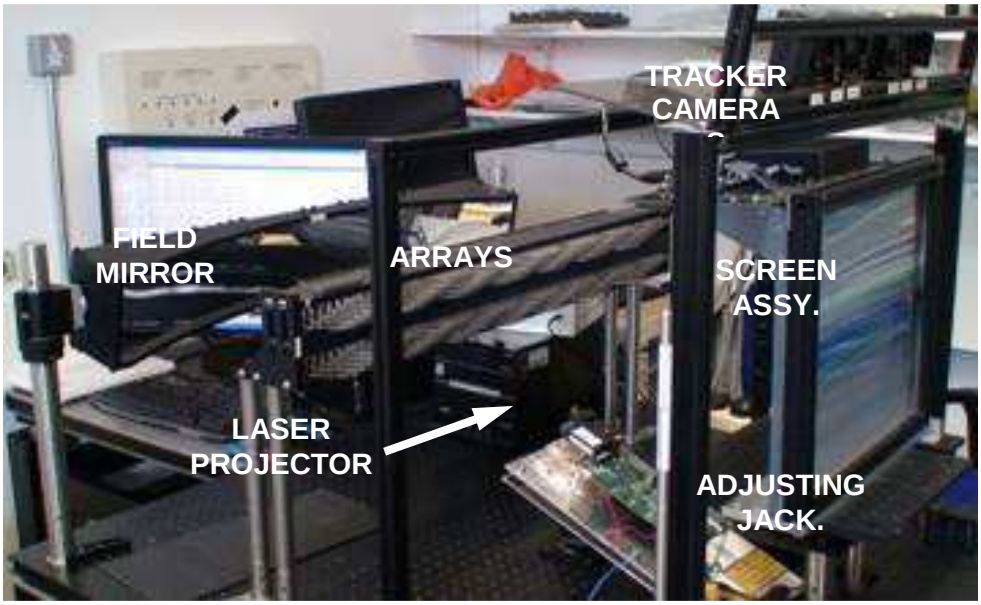

Figure 4.4: MUTED LCOS Projector Prototype showing the configuration including the tracking cameras and screen height adjustment.

Two 49-element optical arrays are mounted around 350 millimetres behind the screen assembly and illuminated by a pattern as shown in Figure 4.5; the spot pattern is sparse around 95% would be blocked if a conventional projection is used. A laser projector is used as it utilises the complete wavefront and concentrates this energy into the region of the spots. The efficiency is less than 100% due to the formation of a conjugate image but it is still considerably more than conventional projection.

Figure 4.5: Spot patterns from projector showing the pattern of 49 spots from the laser projector.

.

In the prototype the conventional backlight of an LCD with the holographic laser projector shown in Figure 4.6 that generates series of spots of light using a hologram rendering technique. Laser projectors were supplied by MUTED project partner Light Blue Optics. The light spots are used to create exit pupils using MUTED display optics. Laser

projection has an advantage over the conventional projection as only around 5% of the area is illuminated; if conventional projection was used an SLM would block around 95% of the light however the laser projector utilises the complete wavefront. Three Laser projectors designated Y34, Y44, and Y43 were supplied by MUTED project partner Light Blue Optics (LBO). These projectors are a sealed unit whose output is Class 1; this means that even when the display is operated with no housing around it there is no danger to users or to researchers working on the display.

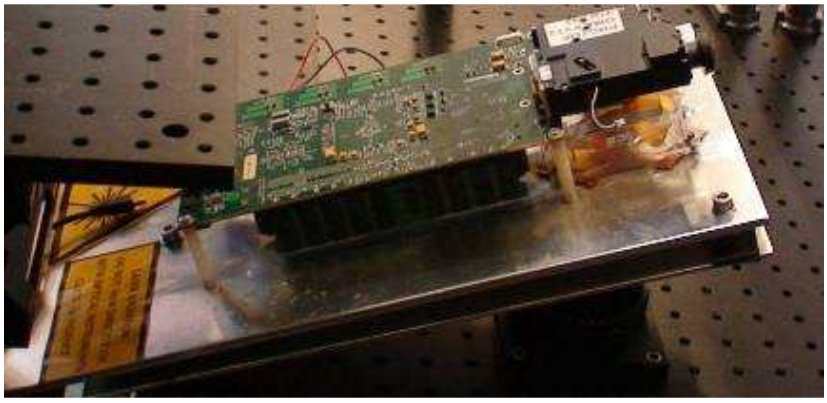

Figure 4.6 Laser Projector: Compact RGB laser projector developed by Light Blue Optics and adapted for use in the MUTED display.

4.3 Steering Array and Field Mirror

The steering optical arrays each consist of 49 elements as shown in Figure 4.7; this acts as viewing zone forming optics. Two different view images are required and each of these must be directed to its corresponding eye; this achieved using an optical array whose role is to form the exit pupils that are formed by converting a series of spots of light into intersecting collimated beams from the array that is situated around 400mm behind the LCD screen assembly.

The elements are mounted in a ‘staircase’ configuration; the pitch between the adjacent elements is less than the element width so that the majority of the width of adjacent elements overlaps. This is necessary as the emergent beam width is equal to the array pitch and the array must provide source that is contiguous across its width.

Light must enter at normal incidence on the back of the array so it must be collimated. The use of a Fresnel to perform was initially ruled out as it was feared that the faceted structure of the lens would interfere with the spot pattern. For this reason a large parabolic mirror was constructed (Figure 4.8).

Figure 4.7: Optical Steering Arrays. Two vertically-separated 39-element arrays illuminate alternate LCD pixel rows.

Figure 4.8: Parabolic field mirror collimates the projector output so that light enters the array elements at normal incidence.

The mirror incorporated into the prototype incorporated a matrix of 175 tapped holes in its back panel in order to allow for fine adjustments if necessary with the use of 80 threads per inch ball-ended adjusters contacting with the back of the surface-silvered plastic mirror. In practice this was not found to be required when a second higher quality mirror replaced the first version and the principal purpose of the adjusting screws is to enable the front surface of the mirror to be in light contact with the front of the parabolic retaining groove. This adjustment was delicate and it was difficult to achieve this contact without causing rippling of the mirror surface.

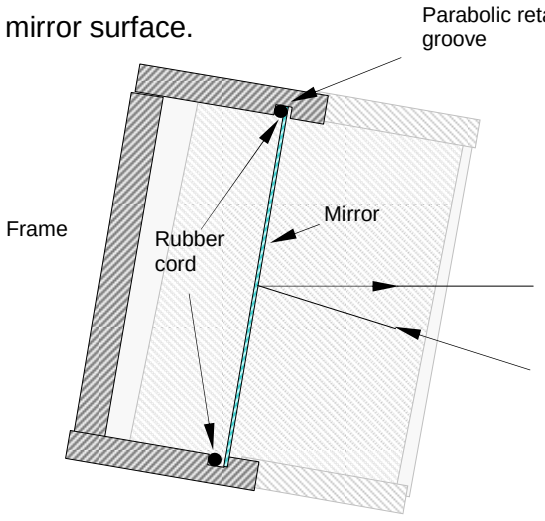

Figure 4.9: Sections through Second Field Mirror

Some of the adjusters at the ends are used to counteract the effect of barrelling where the surface becomes slightly curved in the vertical direction. On the basis of the second iteration uses two millimetre diameter rubber cord to press the mirror against the front of the groove as shown in Figure 4.9. There are fifteen adjustment holes either end to allow for barrelling. A visual examination of the image formed does not exhibit the slightly rippled appearance of the first version.

4.4 Spatial Multiplexing

This light is separated at the screen with a Lenticular spatial MUX screen with its lenses running horizontally that is attached to the back surface of the LCD as shown in Figure 4.10; its pitch is slightly less than twice the LCD vertical pixel pitch. Lenticular screen lenses enable almost 100% of the light from the steering optics to be focused on to the LCD pixels. The performance of the lenticular screen is determined by displaying alternate red and green rows of pixels on the LCD and mounting the backlight to the front face of the LCD.

Passing the light in the opposite direction to that of normal use enabled the series of photographs in Figure 4.11 to be taken at array to screen distance that appears to give the best performance. Note that the X and Y directions refer to the camera position axes i.e. the series of photographs is for the camera traversing vertically; the orientation of the axes of the screen depicted are at right at right angles to these (they are shown here in their operating orientation). Examination of this pattern revealed that there must be a vertical spacing in excess of 30 millimetres between the arrays in order for a transition zone to be completely located between the upper and lower array; the vertical position of the screen is adjustable in order to locate this zone in the correct position.

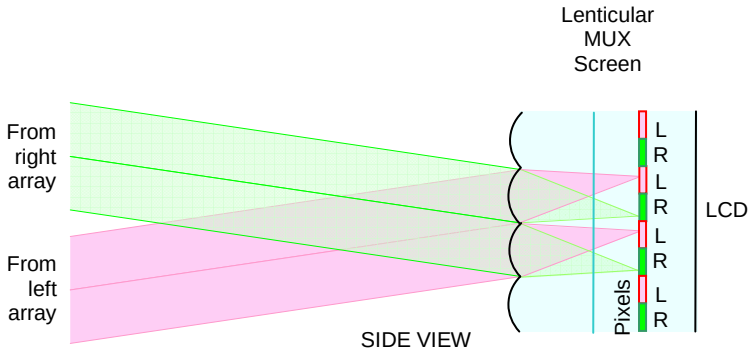

Figure 4.10: Section of Lenticular MUX Screen. Light from two arrays is directed to the appropriate pixel rows.

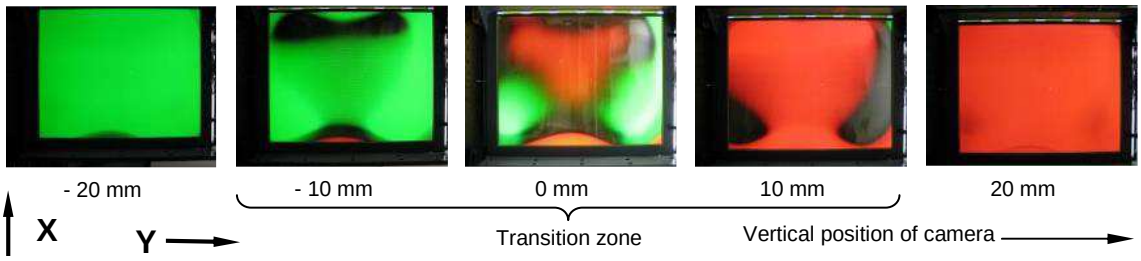

Figure 4.11: Lenticular MUX Separation: Patterns seen when light is passed in the reverse direction through the MUX screen.

Due to manufacturing inaccuracy the pitch of the lenticular screen was slightly larger than its design value and this resulted in an increase in the array to screen distance. Another effect of this was that an increased vertical separation was required between the two arrays. A clear indication of the performance of the MUX screen can be obtained by illuminating the entire front of the screen with a diffuse source. An image of red and green pixels on alternate rows was presented on the LCD and when observed from a point that lies within the region corresponding to the area of an array output, either a red or a green image should be seen over the complete area of the screen.

A matrix of photos that represents vertical traverses of the illumination field is used to establish the vertical locations of the arrays that would give the most even images and hence minimum crosstalk. Photos taken in 5mm vertical increments and at the horizontal positions indicated are used to obtain Figure 4.12. This was found to be 490mm by placing a white screen in the region where the camera lens is located and noting the plane at which the sharpest image of red and green bands is formed. Series of photos were taken on the central axis and at 100mm either side of the axis. The areas marked as ‘regions of interest’ in Figure 4.12 are those that correspond to an incident angle of < 25°; the areas outside these regions correspond to angles of incidence that are greater than can be obtained from the array.

Examination of the Photographs in Figure 4.12 indicates that increasing the vertical separation of the arrays by 10mm (increasing the total separation to 34mm) will enable light pass into the appropriate pixel rows without undue crosstalk. Unlike Figure 4.11, in this case the X and Y axes for the images and the capture positions are both shown in their normal orientation.

As the lenticular screen was designed for an array to screen distance of 320mm the effect of the increased distance required by the lenticular screen having a slighter greater pitch than its design must be considered. From the document MUTED LCD Optics the approximate value of the refractive index is 1.5 and the lens to pixel distance is 3.333mm.

Using the thin lens equation it can be shown that:

$$\frac{1}{V} = \frac{1}{1.5}\left(\frac{1}{320} - \frac{1}{S}\right) + \frac{1}{3.333}$$

Where:

S = array to screen distance (mm)

V = lens to image distance within the lenticular/screen assembly

If S = 490mm then V = 3.324mm.

This shows that changing the screen to array distance from 320mm to 490mm the focal point within the LCD substrate moves from 3.333mm to 3.324mm from the lens surface. This difference of 0.009mm is small and will not cause noticeable effects due to defocusing.

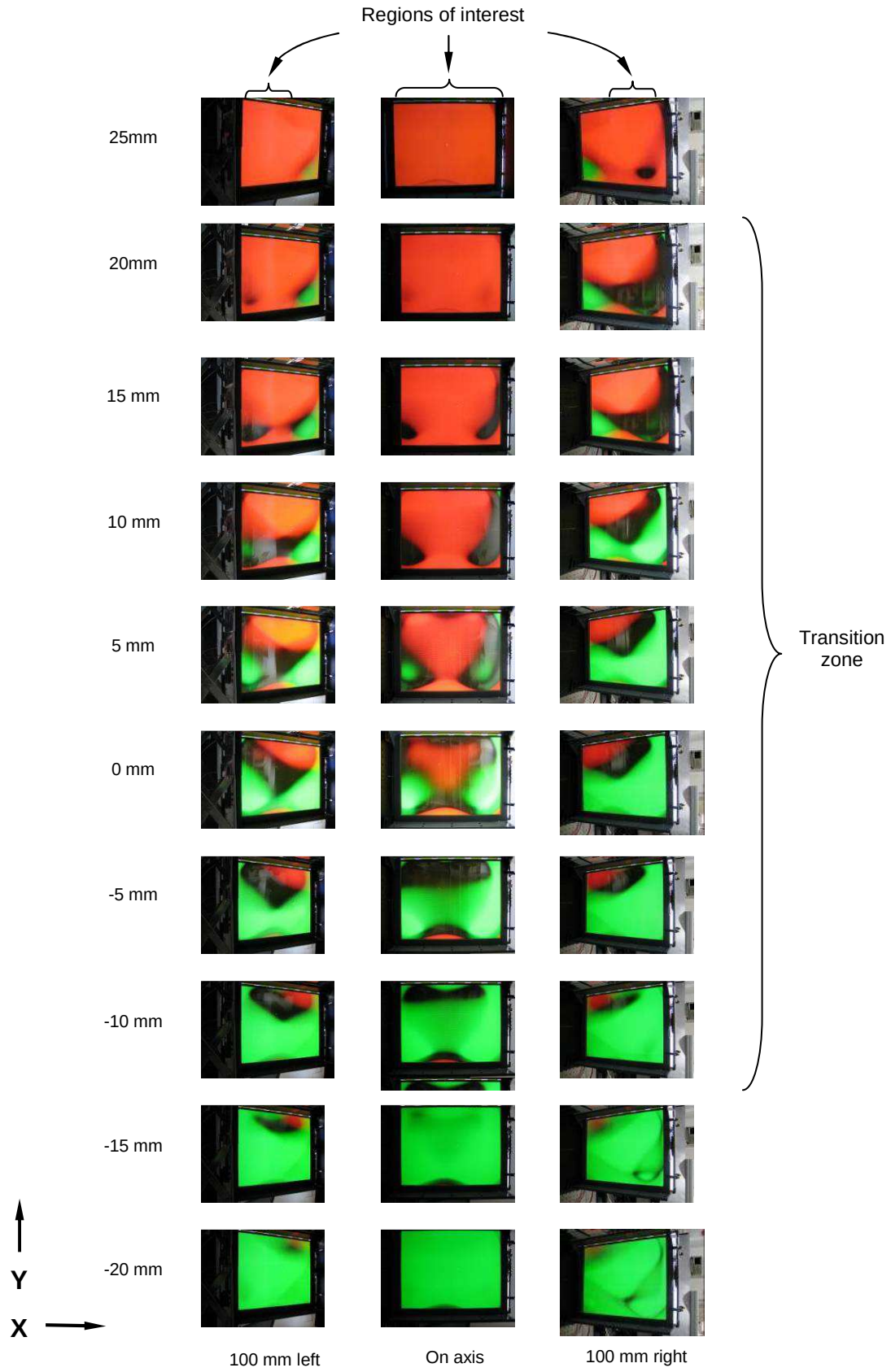

Figure 4.12 Lenticular MUX: This matrix of photographs shows the appearance of the screen from different positions behind the screen assembly.

4.5 Screen Enhancement Lens

As the effective backlight is effectively originating from a source that is less than 100 millimetres high it must be diffused in the vertical direction in order to fill the complete height of the viewing region. This occurs to a certain extent with the use of the lenticular multiplexing screen. Table A 4.1 shows measurements of this effect taken by observing the screen at a given distance above the axis from 0mm to 150mm. The observation is made at 460mm from the LCD.

The values in the table were determined by visual examination of the assembled system where the upper and lower rays of the illuminated section of the screen coincided with markers on the screen positioned in 50mm increments. Simple geometry shows that the opening angle of these rays is around 15º and is in accordance with the predicted angle determined from the F number of the lenticular that is necessary to locate images of the upper and lower arrays on alternate pixel rows.

Observations in Table A 4.1 show that the axes of the ray bundles emerging from the LCD are not deflected by the lenticular or LCD. A 15° divergence of the rays leaving the array, at a distance of 450mm indicates that only around 1/3 of the LCD will appear to be illuminated from any given viewing position. The divergence of the rays emerging the LCD will be too small to allow the entire display to appear illuminated for any given observation position. Although initial assessment suggested a correcting element would not be required these results prove that a correcting element is necessary.

Distance on screen above axis (mm)	Distance above axis at 460 mm from screen (mm)		Emergent opening angle (º)
	Upper ray	Lower ray	
0	-60	56	14.4
50	51	177	15.3
100	184	319	15.1
150	294	447	15.5

Table 4.1 measurements of this effect taken by observing the screen

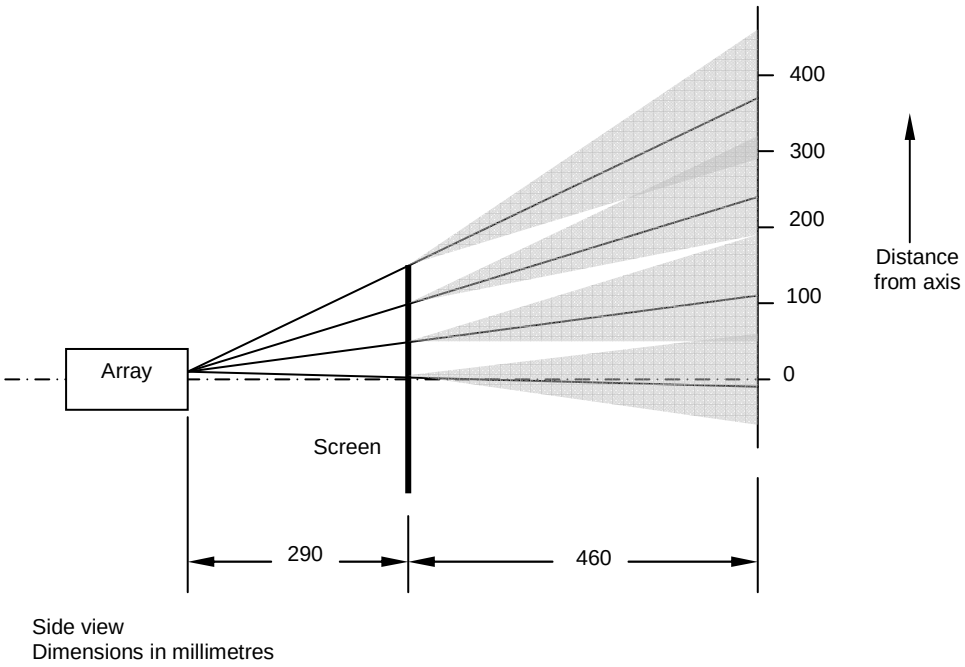

Figure 4.13: LCD Vertical Diffusion

Figure 4.13 shows the values in the table plotted as a side view of the emergent rays. It can be seen that each ray bundle axis diverges from the horizontal and must be concentrated towards the central axis with the use of a field lens.

Figure 4.14 indicates that a suitable cylindrical enhancement lens could be designed to allow the opening angle of 15º to provide a sufficiently high viewing region. This could be used as an alternative to a vertical diffuser in front of the screen to correct the problem.

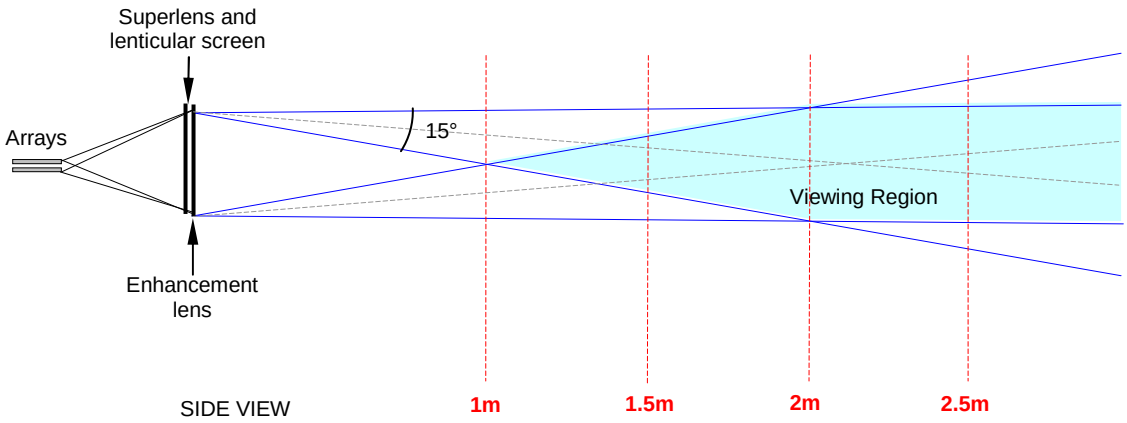

Figure 4.14: Cylindrical enhancement lens

The measurements were obtained with the screen 290mm in front of the arrays; this was the original design distance. However it has been found that with the final manufactured version of the lenticular screen this distance is 450mm, this is due to issues relating to reliable manufacture of the lenticular sheet. The specification of a lens to expand the 15° opening to fill the screen height is as follows when the screen is 450mm from the optical arrays:

Clear aperture:	385mm x 310mm, lines parallel to the long side
Plano conjugate:	450mm
Fresnel conjugate:	2000mm
Focal length:	334.2mm
Pitch:	0.1mm
Refractive index:	1.493805 at 546nm
Thickness:	1.8mm +/- 0.3mm
Material:	PMMA

The focal length of the lens was specified to the manufacturer to fit the other given parameters. The conjugate positions are known from the display dimensions, the pitch is chosen to be the finest that can be made in order to avoid it having an impact on the display quality.

The focal length of this lens is 334.2mm. As an off-the-shelf spherical lens with a focal length in this region is unavailable, the use of a spherical lens in this application has been considered. Although in principle it would be possible to compensate for the effect of the lens on the angle the beams for the exit pupils as they pass through the LCD, in practice the short focal length of the lens would necessitate horizontal rays to emerge at >25º from the array axis. The array design allows for a maximum exit angle of 25º.

A method of multiplexing the left and right eye views is required. A lenticular sheet has been designed to fulfil the spatial multiplexing requirement of the display design.

The constraints of the design of the optical system require an additional component in front of the LCD to ensure the entire screen is illuminated when seen from all viewpoints. Without this only about 1/3 of the LCD will be visible from any given location. A vertical enhancement lens has been designed to ensure the entire screen is viewable in the main viewing region.

Due to the capabilities of commercially available LCDs spatial multiplexing was used to mix left and right views on the display. This has involved design of a lenticular array to attach to the screen. The optical films on the LCD have been assessed for suitability and

a replacement polariser found which does not have anti-glare properties. The use of a lenticular screen coupled with the rest of the MUTED optics has required investigation for the need of an enhancement lens. The enhancement lens has been determined to be necessary and has also been designed. The LCD pixel has been modelled to identify the effect the design is likely to have on crosstalk and illumination of the viewing zone due to any black bands though it.

4.6 Soft Aperture

4.6.1 Introduction

The object of the soft apertures in the array elements is to reduce the effect of banding in the image. In the ATTEST prototype that was a forerunner of MUTED the beams had flat profiles with faded edges. Due to the closer spacing of the elements in the MUTED array the beam profiles are triangular as in Figure 4.15. At any particular position along the array the perceived intensity on the screen over a given column of the LCD is determined by the light emitted from two adjacent elements. For example, the image columns receive illumination from the array in the region denoted by the line AA will receive around 40% of this from Element (N +1) and around 60% from Element (N +2).

The soft aperture is required for two reasons:

1. To allow for aperture image width variation. As the aperture is viewed from different directions the apparent width of the aperture will vary.
2. To allow for constructional variations.

The image of the aperture seen through the front of the array element forms the backlight of the LCD. This image varies in width as the observer's position moves horizontally and vertically; measurements made from photographs for the virtual aperture width for an actual width of 13mm are given in Table 4.2.

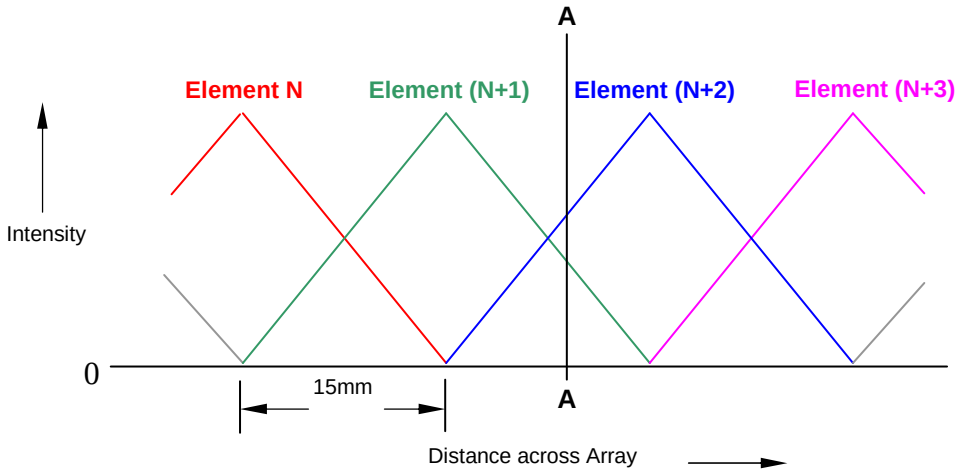

Figure 4.15: Overlapping Intensity Profiles

The fading width required in order for the effect of overlap to be imperceptible has been determined [74]. Based on these findings a fading width of 12.8mm will be required. As the array pitch is 15mm the fading region can be 15mm; this gives the triangular profile shown in Figure 4.15.

	Measurements from photographs		Magnific--ation	Aperture image width
Position	**13 mm on scale**	**Aperture Image**		
On axis	24	27.5	1.15	14.9
On axis, ± 25° horizontal	21.5	24	1.12	14.51
On axis, ± 10° vertical	29	34.5	1.19	15.47
± 25° horizontal ± 10° vertical	23	26	1.13	14.7

Table 4.2 Aperture Magnification

4.6.2 Experimental Setup

The profile of the Luminit 10º x 0.5º FWHM elliptical diffuser that is located behind the array elements has been measured previously by both Luminit and DMU using coherent light. This produces a characteristic with a spiky and irregular appearance. The results of these are not particularly useful and the expected profile with a smooth Gaussian-like shape needs be used to determine the soft aperture transmission function. Due to this the latest measurements were carried out using a non-coherent halogen lamp source.

The illumination source comprised a halogen lamp behind a 0.5mm pinhole. The diffuser was placed between two 200mm focal length lenses as in Figure 4.16. The light pattern formed in the plane where the power meter is located is the Fourier transform of the light emitted from the diffuser. The collimated beam from L_1 passes through the diffuser; the angle of the emergent light is converted to a position in the measurement plane by L_2.

Figure 4.16: Experimental Setup

4.6.3 Theory

The positions of the readings taken on the power meter must be mapped to the equivalent positions on the soft aperture. The measurements were made with the power meter located 260mm away from the lens L_2. Figure 4.17 shows where a particular ray crossing the measurement plane would land if directed to the soft aperture. The light path from the source to the aperture in the actual display is 10mm in air and 120mm in Plexiglass that has a refractive index of 1.49.

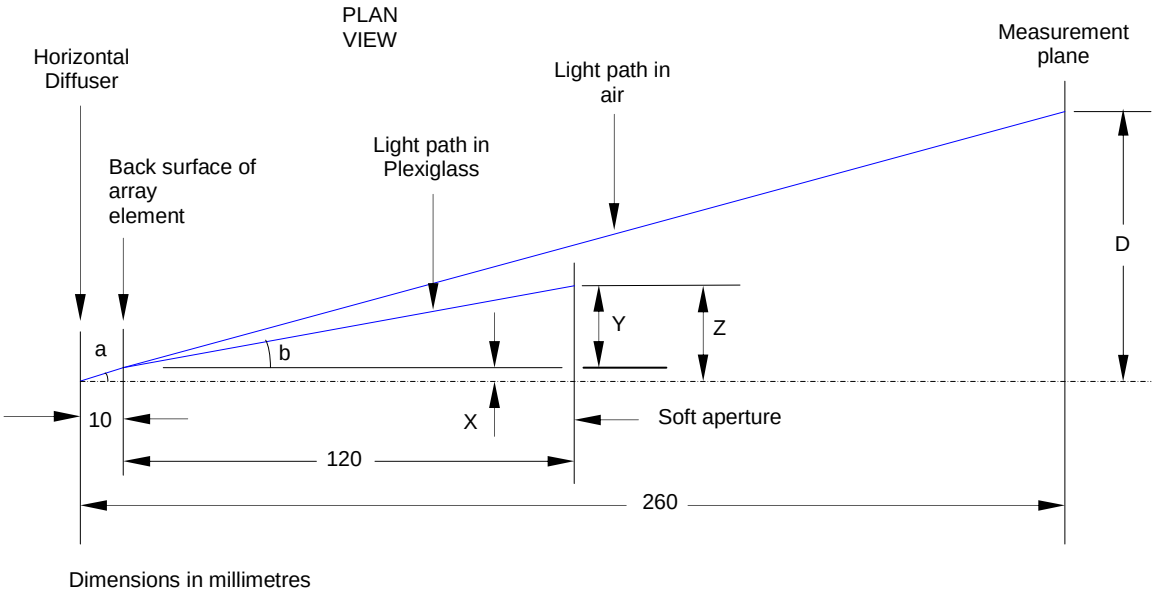

Figure 4.17: Mapping the Measurement Plane to the Soft Aperture Plane

The equations below are used to calculate the relationship between the positions.

$$A = ATN\left[\frac{D}{260}\right] \quad \text{…….. (1)}$$

By similar triangles,

D / 260 = X / 10

$$\frac{D}{260} = \frac{X}{10}$$

$$X = \frac{D}{26} \quad \text{…….. (2)}$$

Refraction at array element surface:

$$1.49 = \frac{SIN(a)}{SIN(b)}$$

$$b = SIN^{-1}\left(\frac{SIN(a)}{1.49}\right) \quad \text{…….. (3)}$$

Path in element from surface to aperture:

$$TAN(b) = \frac{Y}{120}$$

$$Y = 120TAN(b) \quad \text{…….. (4)}$$

Distance of ray from axis at aperture:

$$Z = X + Y \quad \text{…….. (5)}$$

As the maximum emergent angle from the diffuser is <10° it is safe to assume that there is a linear relationship between the measurement plane and soft aperture positions. The distance of the outermost ray is 15mm as shown in Figure 4.18(a). This is set by the transmission profile of the soft aperture. The image of the soft aperture is magnified by the front refracting surface of the array element. Figure 4.18(b) shows the appearance of the soft aperture.

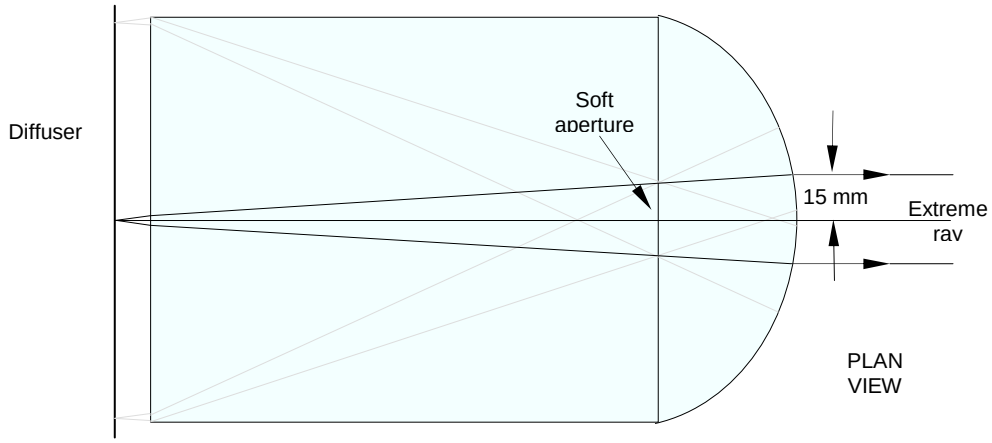

(a) Extreme Ray

(b) Front View of Soft Aperture

Figure 4.18: Soft Aperture and Extreme Rays

Equations (1) to (5) are used to calculate Z from the value of D. As it is not simple to find D from Z the value of D is adjusted to give Z = 12.99mm. This gives the value of D at the extreme ray position as 41.93mm. The scaling factor of 0.310 (D / Z) is used over the complete range of values to convert the power meter position to the equivalent position on the soft aperture.

D = Input	a = ATAN(D /260)	X = a /26	b = ASIN(a) /1.49	Y = 120.TAN(b)	Z = X + Y	Scaling factor
41.93	0.160	0.006	0.108	12.983	12.989	0.310

Table 4.3: Mapping Aperture Position to Measurement Position

4.6.4 Measurements

The power meter was moved in 2.5mm increments over a length of 110mm at a distance of 260mm from the lens L_1. The background illumination with the illumination source switched off was >1nW so no corrections were necessary. The results are shown in Table 4.4 and plotted in Figure 4.19.

Distance across traverse	Power (nW)
-57.5	3
-55	5
-52.5	7
-50	10.5
-47.5	14
-45	20.5
-42.5	27
-40	39
-37.5	51
-35	69.5
-32.5	88
-30	97.5
-27.5	107
-25	120.5
-22.5	134
-20	145.5
-17.5	157
-15	169
-12.5	181
10	190.5
-7.5	200
5	205.5
-2.5	211

Distance across traverse	Power (nW)
0	211
2.5	211
5	206
7.5	201
10	192
12.5	183
15	171
17.5	159
20	145
22.5	131
25	117.5
27.5	104
30	91.5
32.5	79
35	57
37.5	35
40	28.5
42.5	22
45	16
47.5	10
50	6
52.5	2

Table 4.4: Power Meter Readings

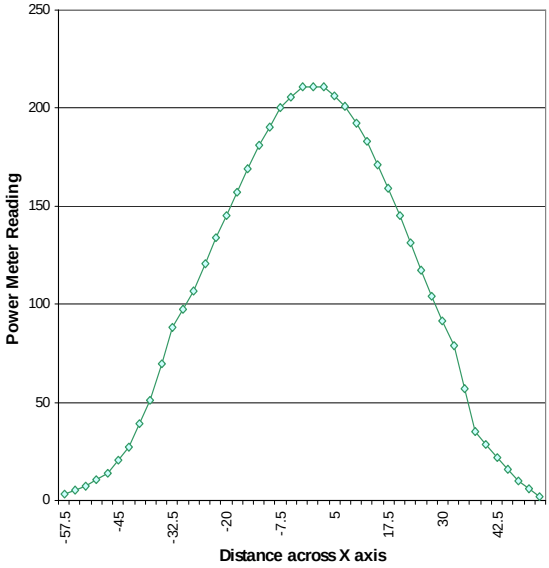

Figure 4.19: Intensity across Diffuser Major Axis

4.6.5 Processing Results

The readings plotted in Figure 4.20 show that the output appears to be slightly asymmetrical. This is due to either manufacturing defects or experimental error. The soft aperture transmission profile will be symmetrical so effect of the diffuser asymmetry is reduced by averaging results obtained at the same distance either side of the axis. The normalised readings and the averaged values are shown in Figure 4.20. The values on the X axis are obtained by multiplying the distance across the measuring traverse by the scaling factor of 0.310.

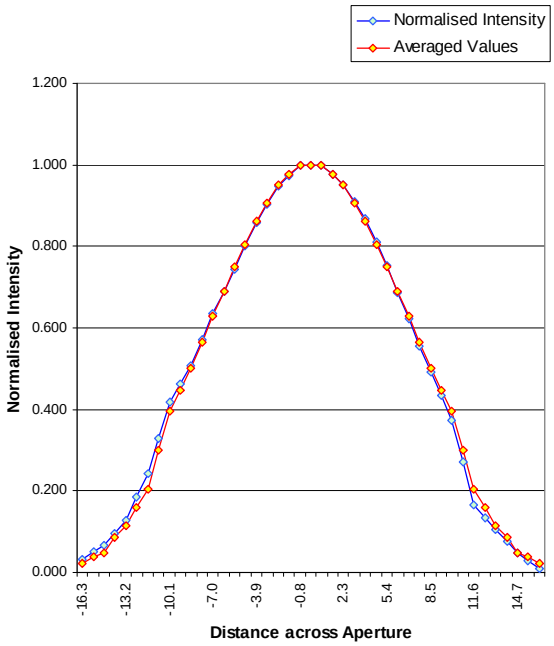

Figure 4.20: Normalised Intensities

4.6.6 Calculation of Aperture Profile

The total width of the aperture profile is 30mm which is double the array pitch. If this width is divided by the magnification of the front surface then the overall width of the aperture is 30/1.155 = 25.96mm. Figure 4.21 shows the intensity profile of the 10° horizontal diffuser and the output beam profiles. The diffuser profile is shown as 'Averaged profile' in Figure 4.21 as it was obtained from measurements made at DMU where slight asymmetries were averaged in order to even out any measurement errors; this is based on the assumption that the diffuser output is actually symmetrical. Complete plots were not made for off-axis beams but rotation of the diffuser up to ±25° and with a power meter located at various angles to the to the axis up to ±25 ° gave no discernable variation with rotation angle. The region between plots represents the light absorbed by the aperture and the ratio of the integration of the two yields a value of 76.5% efficiency.

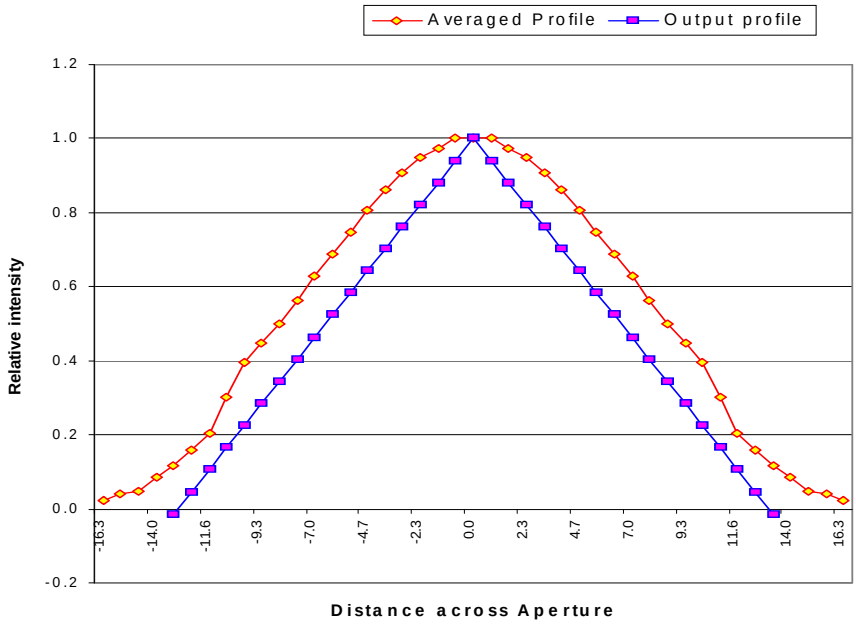

Figure 4.21: Diffuser and Output Profiles

Aperture Profile Calculation

In Table 4.5 the average normalised values, the output intensity and soft aperture profiles are given for given positions on the aperture. The aperture transmission profile plot is given in Figure 4.22.

As the output intensity profile function is triangular its values are obtained by subtracting the modulus of the distance from the centre from half the aperture width and dividing this by half the aperture width i.e.

P = (Z – | w |) / Z …….. (6)

P = profile intensity

Z = half aperture width

W = distance across aperture

The transmission profile of the soft aperture shown in Figure 4.22 is obtained by dividing the required output (plot ‘Output profile’ in Figure 4.21) at any given distance across the aperture by the value of the relative intensity from the 10° diffuser (‘Averaged profile’ in Figure 4.21) at that position.

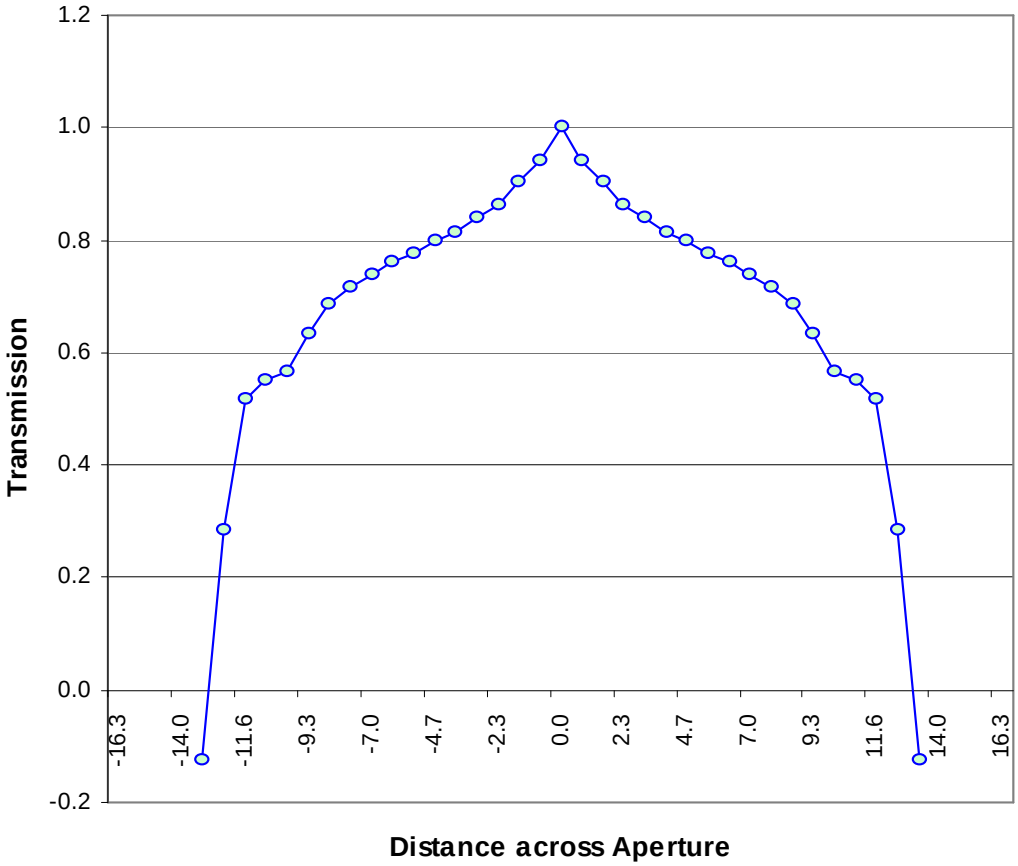

Figure 4.22: Soft apertures Transmission Profile

Distance across aperture	Left/right average normalised	Output intensity profile	Soft aperture transm-ission profile
-15.5	0.039		
-14.7	0.049		
-14	0.086		
-13.2	0.116	-0.014	-0.123
-12.4	0.16	0.045	0.283
-11.6	0.204	0.105	0.515
-10.9	0.3	0.165	0.549
-10.1	0.396	0.224	0.567
-9.3	0.448	0.284	0.634
-8.5	0.5	0.344	0.687
-7.8	0.564	0.403	0.715
-7	0.628	0.463	0.737
-6.2	0.688	0.523	0.759
-5.4	0.749	0.582	0.778
-4.7	0.806	0.642	0.797
-3.9	0.863	0.702	0.813
3.1	0.906	0.761	0.84
-2.3	0.95	0.821	0.864
1.6	0.975	0.881	0.903
-0.8	1	0.94	0.94
0	1	1	1

Distance across aperture	Left/right average normalised	Output intensity profile	Soft aperture transm-ission profile
1.6	0.975	0.881	0.903
2.3	0.95	0.821	0.864
3.1	0.906	0.761	0.84
3.9	0.863	0.702	0.813
4.7	0.806	0.642	0.797
5.4	0.749	0.582	0.778
6.2	0.688	0.523	0.759
7	0.628	0.463	0.737
7.8	0.564	0.403	0.715
8.5	0.5	0.344	0.687
9.3	0.448	0.284	0.634
10.1	0.396	0.224	0.567
10.9	0.3	0.165	0.549
11.6	0.204	0.105	0.515
12.4	0.16	0.045	0.283
13.2	0.116	-0.014	-0.123
14	0.086		
14.7	0.049		
15.5	0.039		
16.3	0.021		

Table 4.5 Soft aperture profile

4.6.7 MUTED Head Tracker

The Fraunhofer Heinrich Hertz Institute (FHG) Free2C display shown in Figure 4.23 provides free positioning of a single viewer within an opening angle of 60°. Crosstalk between left and right views is the most important artifact with this type of display. The optics for the display has been designed such that extremely low crosstalk, excellent color reproduction and high brightness are achieved.

Figure 4.23: FHG Free2C Display: The head tracked display allows freedom of head movement of a single viewer. The two tracker cameras can be seen above the screen.

Exit pupils in the Free2C display are formed in a similar manner to the DMU display described in the following section where alternate left and right viewing zones are formed across the viewing field (Figure 4.26) by a vertically-aligned lenticular screen. This is located in front of an LCD that is in the portrait orientation so that the RBG sub-pixels run horizontally across the screen. This allows even distribution of each colour primary across the viewing field.

In the Free2C display the viewing zones follow a viewer's eye positions in both the X and Z directions (Figure 4.24) by moving the lenticular screen also in the X and Z directions. This is achieved with the use of voice coil actuators controlled by the output of a non-invasive head position tracker that processes the output of a pair of cameras mounted above the display.

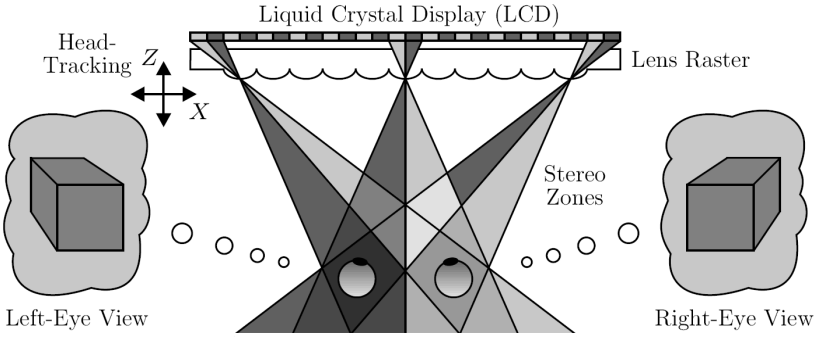

Figure 4.24: Free2C Display: display the viewing zones follow a viewer's eye positions in both the X and Z directions

Figure 4.25 is a close-up the positioning device for the mechanical adjustment of a lens plate that is moved by actuators controlled by the output of the head tracker.

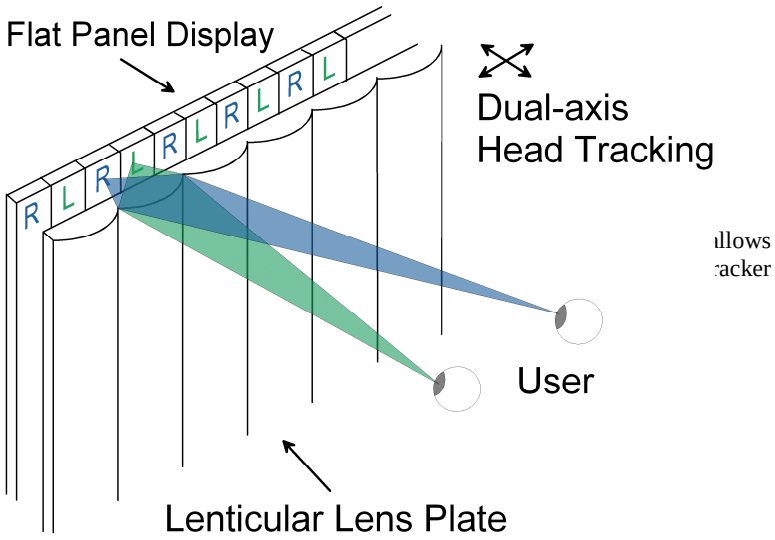

Figure 4.25: Mechanical lens plate positioning: The vertically-aligned lenticular screen is moved in the X and Z directions to enable the movement of an exit pupil pair in the X and Z directions

A high-precision single-user 3D video head tracker was developed several years ago that uses high-speed cameras with a frame rate of 120Hz. It employs an appearance-based method for initial head detection and a modified adaptive block-matching technique for head and eye location measurements in the tracking phase. The head tracking system must provide; (a) high accuracy in terms of located head position, (b) robustness with respect to different users, fast head movements as well as changes in scene background and illumination and (c) automatic initialisation procedure. The tracker is based on an adaptive block-matching approach that compares the current image with eye patterns of various sizes, which are stored during initialisation. Tracking results for different users are shown in Figure 4.26. As can be seen from the figure, the tracking algorithm also works reliably for viewers wearing glasses.

Figure 4.26: FHG Head Tracker: Tracking results for several users with some wearing glasses are shown.

Figure 4.27 shows the graphical user interface where the positions of the viewer's eyes obtained by the head tracker are indicated by the green rectangles

Figure 4.27: Graphical User Interface. This includes the facility to show the detected positions of the user's eyes.

The tracking area of the Free2C technology is suitable only for one person and the boundary of this is shown in 4.28. It can be seen that the user has a high freedom of movement that enables comfortable viewing.

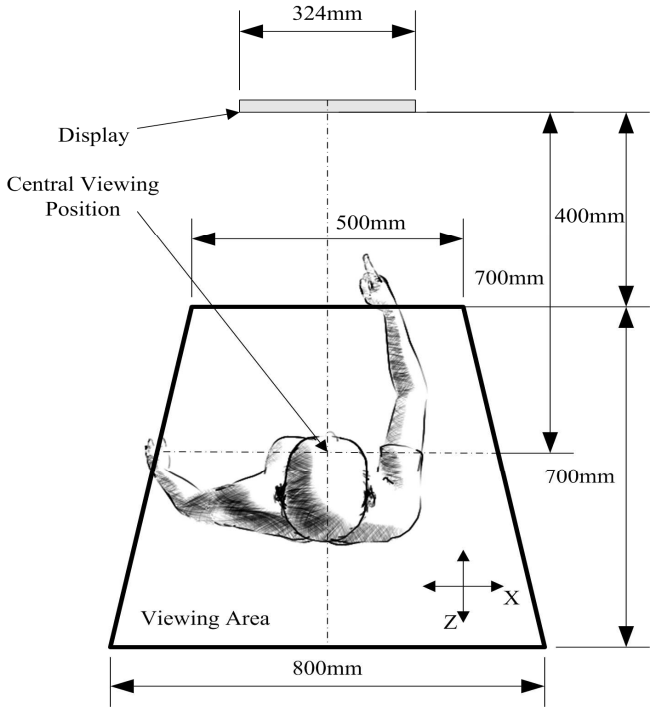

Figure 4.28: Free2C User Area: A single user is able to see stereo over a comfortably large area as the exit pupils can be steered between 400 and 1100 mm from the screen as opposed to merely laterally

Head positions are determined using the multi-user head tracker whose capture camera array is shown in Fig. 4.29. This has been built by MUTED partner Fraunhofer HHI and is a development of the earlier single user ATTEST display tracker.

A non-contact non-intrusive video-based system that provides a near to real-time high-precision single-person 3D video head tracker has been developed by one of the MUTED partners for use in a single viewer head tracked display. This has been adapted for use as a multi-user tracker.

The multi-user tracking implementation is divided into fully automated initial face detection and subsequent feature tracking. The initial face detection is based on a decision cascade of Haar basis functions [89]. By combining these simple functions it is possible to construct a classifier which is also able to discriminate classes with more complex distributions with sufficient accuracy. An essential advantage against other methods is the high speed in the detection process. The decision cascade is preliminary learned by boosting [22] on a large face dataset and a very large dataset of a complementary non-face class.

After the initial face detection has been done specific facial feature points are detected by several image processing methods. One method used is the calculation of the radial symmetry to detect pupils [41]. After a set of facial features has been successfully detected the information is used to track these features in a computationally inexpensive and fast tracking process. The tracking is done by enhanced adaptive block matching methods. For that purpose tracking features (image elements around a facial feature with properties that make this element simple and reliable to track) for the specific facial feature are selected and tracked. The combination of the tracking results of these tracking features increases the accuracy of the facial feature up to sub-pixel accuracy. The use of calibrated stereo camera pairs provides spatial position data with sufficient accuracy in all dimensions.

A fundamental problem in video-based tracking technology is the limitation of the camera optics. A limited depth of focus and a constant focal length restrict the possible detection area to unsuitable dimensions. A single optic of a system that tracks an object with an adequate accuracy provides a limited variation of the tracking distance. For that reason our approach uses multiple cameras, a camera system with large focal length to observe far areas and a short focal length system with large opening angle to observe near areas.

Alternatively we evaluated an approach using high resolution cameras. The costs of high resolution cameras, a high amount of unused data traffic and the goal to develop an effective hardware version led to a tracking system that uses multiple cameras with common TV (PAL) resolution.

The basic design of the tracking system supports the use of multiple, almost independent stereo camera pairs. These camera pairs observe a sub-area of the overall tracking area. The detection and tracking results are sent to a data manager which collects the data of all camera pairs, evaluates the data and merges all information to globally defined instances of the tracked individuals. As a result, a person is constantly tracked even though he moves from one sub area to another. Fig. 4.30 shows camera images of tracked users in a fragmented tracking area. One camera pair with short focal length (lower two images in Fig. 4.30) is tracking persons in a near area and another camera pair with a longer focal length (upper two images in Fig. 4.30) is tracking persons in a more distant area. Fig. 4.30 shows the projections of the coordinates of the globally unique objects into the specific view. The blue markers show the face detection results, the green markers show the eye tracked area and the red markers indicate small squared markers on forehead.

This concept implies high scalability and high robustness compared to the sensitivity of a single camera-pair approach. The only limiting criteria are the available processing power and the corresponding number of cameras. The overlapping between the camera capturing areas of the multi-camera approach provides additional processing features. In future developments possible improvements of the overall tracking performance will be investigated by combining the measurement results of competing camera pairs for a same sub-area. In a further step it is planned to adapt the whole tracking software system to a hardware implementation which will be directly integrated into the multi-user display set-up.

Figure 4.29: Head tracker camera array: Six cameras are employed to track users from 1000 to 3000 mm distance.

Figure 4.30: Multi-user head tracker: Images captured on six-camera array

In the FHG Free2C display left and right images are produced on alternate pixel columns and directed to the viewer by a vertically aligned lenticular screen. The viewer is able to move in both the X and Z directions by shifting the lenticular screen in relation to the LCD. If the viewer moves to the left the lenticular screen moved to the left and vice versa. If the viewer moves closer to the screen the gap between the LCD and the lenticular screen increases and vice versa. The lenticular screen is moved by voice coil actuators that are controlled by the output of a head position tracker. The tracker processes the output from two cameras that are mounted above the display as shown in Figure 4.31.

Figure 4.31: Free2C display: showing its use in the interactive mode where virtual buttons are pushed.

The head tracker for the MUTED display was developed from the single-user tracker used in the Free2C display that was developed by FHG in the ATTEST 3D TV display project. This is a non-intrusive tracker that does not require the wearing of any special headgear by the user. The Free2C display only serves a single viewer who only has a relatively small degree of movement compared to MUTED. This means that tracking can be achieved with a single camera pair mounted above the display as can be seen in Figure 4.23.

As the user area that has to accommodate four viewers is much larger (upper diagram in Figure 4.32) several cameras are necessary to accommodate the greater range of distances and angles. It can be seen that with the six-camera capture arrangement shown in the lower photograph in Figure 4.32 provides capture over a 60º opening angle with a 1000 to 3000 millimetre range of distances.

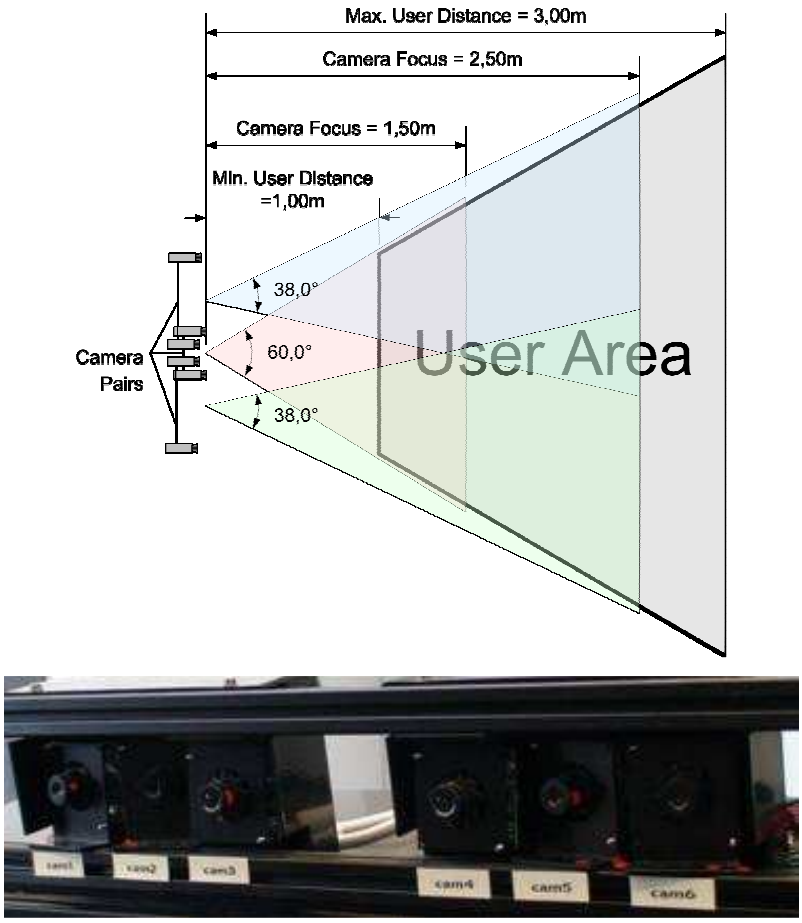

Figure 4.32: MUTED Multi-user Head Tracker: The large opening angle of 60º and range of distances of 1000 to 3000 mm of the user area require the use of six cameras in the configuration in the upper figure. The photograph shows the cameras mounted above the MUTED display.

The concept of head tracking has been around for many years and the earliest reference found by the authors is that of Alfred Schwartz in 1985 [65]. This utilises two CRT projection modules that project the left and right images on to a Fresnel lens that acts as the screen. The Fresnel lens produces real images of the projection module lenses, these are the exit pupils. In order for the display to track the viewer the lens is moved laterally in accordance with the viewer's head position. Several variations based on this principle have been developed over the years. Sharp Laboratories of Europe developed an LCD version that uses separate LCDs for the left and right images therefore providing full resolution [19, 98]. The two images are viewed via a semi-silvered beam combiner screen. MIT developed a display [5] where the left and right images are produced on one screen with the optical paths separated with the use of a micro-polariser array. Other similar displays include the use of monochrome 2D displays for the light source with twin screens and a beam combiner [25], a micro-polariser and linear arrays of white LEDs [26] and projection of a pair of 6.5" LCD panels on to a Fresnel lens [67].

Lenticular screen displays can be used in conjunction with a head tracker to allow greater freedom of head movement and the earliest reference found is that of NTT in 1989 [31] where columns of pixels of a conventional lenticular 3D display are switched in order to eliminate pseudoscopic images when the head is in certain positions. However, when an eye is located between viewing zones the head tracking cannot enable a good image to be seen. This can be overcome by making the exit pupil width around 2/3 of the intraocular separation. Another approach is to move the lenticular sheet in order for the viewing zone to follow the eye positions. Fraunhofer HHI has developed a display that can track the viewer's head position in both the X and Z directions as mentioned previously [55].

There are various other means by which a head tracked display can be implemented; Dimension Technologies Inc. produced a display where controlled narrow vertical lines of illumination behind an LCD enable the viewing regions to follow the viewer [17]. Moving projectors in front of a retro-reflecting screen can be used [84, 24] or the projectors can be located behind a double lenticular screen acting as a Gabor superlens [50, 33]. A dynamic parallax barrier is employed in the New York University display [53] and a virtual dynamic barrier in the Varrier display from the University of Illinois [58]. SeeReal produce a head tracked display where a moving prismatic screen controls the exit pupil positions.

An interesting development is that of SeeReal which combines the use of holography with head tracking in order to reduce the large amount of redundant information presented with conventional holography [60]. It is claimed that by producing viewing windows ten millimetres diameter the display pixel size required is in the order of 25-50 micrometers; this is much larger than the requirement for conventional holography.

4.7 Summary

The MUTED display operates by providing an active backlight for a direct-view LCD where exit pupils are formed at the positions of viewers' eyes. The exit pupils follow the positions of the eyes under the control of a multi-user head position head tracker. In this way, the customary 3D glasses required to channel the appropriate images to the left and right eyes can be dispensed with so that the display is autostereoscopic. Exit pupils could be created with a large lens in conjunction with a vertical diffuser so that vertical regions are formed in front of the screen where a viewer's eye can be located. Although this method does work the lens suffers from aberrations that limit its performance in terms of viewing field size. MUTED overcomes this limitation by replacing a single large lens with an array of smaller lenses where collimated beams are formed that intersect at the viewers' eyes.

In order to perform this function the complete display comprises:

- Projector to produce a spot illumination pattern that provides the illumination sources for the output beams from the projector.
- Large collimating mirror that produces a parallel beam that enters the steering lens array.
- Two lens arrays comprising 49 optical elements each that produce the intersecting parallel beams. One array produced the left exit eye pupils and the other array the right pupils.
- Screen assembly comprising a spatial multiplexing lenticular screen, an LCD, a vertical diffuser and an enhancement lens.
- Multi-user head tracker.

The laser projector was built by MUTED partner Light Blue Optics and is briefly described in this Chapter. My contribution to the operation of the projector was in its calibration; this is described in Chapter 5.

The collimating mirror design was crucial as the parabolic profile of the flexible surface-silvered plastic mirror had to be maintained accurately over its height with no irregularities, as these would cause the spots in the illumination pattern to land in the wrong positions on the back of the array.

MUTED partner Sharp Laboratories of Europe carried out the optical design of the array elements and it was DMU's role to design the components that determine the beam intensity profile. This is important as this gives a homogeneous image with no vertical striations. The profile is determined by the polar plot of the horizontal diffuser located at the back of the steering array and a soft aperture whose transmission profile had to be calculated. As the information supplied by the diffuser manufacturer appeared to be unreliable the characterisation was carried out at DMU.

In the screen assembly, the performance of the lenticular multiplexing screen is critical as any dimensional errors could lead to image crosstalk. Careful measurement of the performance using a red/green pattern on the LCD revealed that the screen pitch was incorrect and other components in the display should be modified to accommodate this.

In order to concentrate the light from the screen to the axial region where the viewers are located a cylindrical Fresnel lens was custom-built for the display. The parameters for this were determined from measurements on the system.

The last part of the chapter describes the multi-user head tracker developed by MUTED partner Fraunhofer HHI. Although DMU assisted in the integration of the tracker into the complete display, the work described in the last section is entirely that of HHI.

CHAPTER 5

LASER PROJECTOR DISPLAY SPOT PATTERN CALIBRATION

5.1 Preface

In the four iterations of the MUTED Display, a pattern of spots is projected onto the back of optical arrays and these are converted into a series of collimated beams that form exit pupils after passing through LCD. The principal goal of this chapter is to describe the spot pattern correction and calibration of the laser projector*. It should be noted that in this chapter all X and Y coordinates refer to positions in their normal orientation, that is: X across the display and Y the vertical direction.*

The pattern projected on to the back of the array exhibited non-linearity in the X direction and positional variations in the Y direction. It was necessary to determine the magnitude and source of these by careful measurement. The main aim of this chapter is to discuss two types of spot pattern corrections. These are:

- **X Corrections:**

  X Coordinates - Projector Only

  X Coordinates - Projector and Mirror using Grid

  X Coordinates - Projector and Mirror using Spot Pattern

- **Y Corrections:**
- **Discuss results**

5.2 Spot Profile

A two-dimensional plot of a spot from projector Y44 was carried out using the set-up shown in Figure 5.1 where the pattern was magnified by the bi-convex lens. A low-power detector is traversed across the image in the X and Y directions on two stages. Some degree of spatial filtering will be caused by the 10mm diameter of the detector but visual observation has indicated that there are no significant high frequency components that would be filtered out.

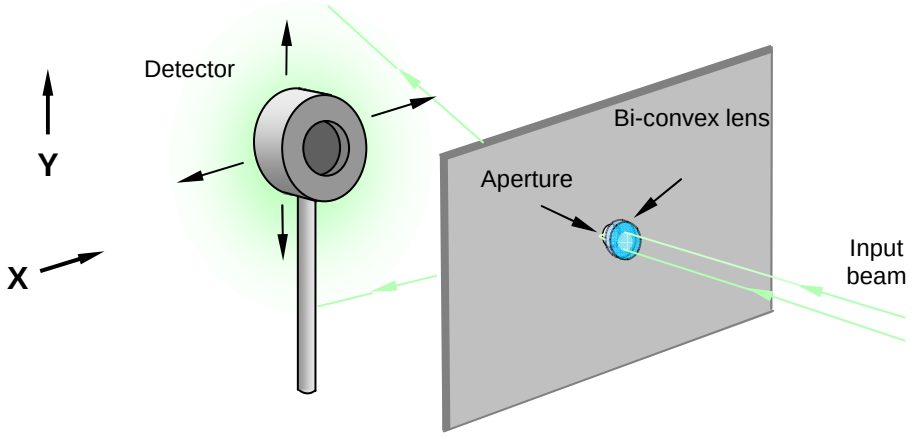

Figure 5.1: Measurement of Spot Profile

Table 5.1 gives the measurements of an X-Y traverse of the spot. The values are normalised to the maximum value. The spot was for the equivalent of one 'pixel' from a projector Y44 image. Note that the spot is higher than its width due to the action of the field mirror where the emergent beam continues to expand vertically after being reflected from the field mirror but is collimated in the horizontal direction. The vertical and horizontal FWHM dimensions are around 2.7 and 2.4mm respectively.

		Y (mm)										
		-2.6	**-2.2**	**-1.7**	**-1.3**	**-0.9**	**-0.4**	**0**	**0.4**	**0.9**	**1.3**	**1.7**
X (mm)	**-1.7**	0.093	0.181	0.2	0.208	0.19	0.139	0.097	0.074	0.042	0.032	0.083
	-1.3	0.148	0.259	0.4	0.356	0.366	0.352	0.273	0.208	0.144	0.06	0.162
	-0.9	0.181	0.287	0.5	0.509	0.597	0.722	0.685	0.542	0.31	0.171	0.227
	-0.4	0.19	0.306	0.4	0.56	0.722	0.931	0.94	0.718	0.588	0.375	0.269
	0	0.181	0.181	0.4	0.546	0.676	0.958	**1**	0.912	0.736	0.519	0.333
	0.4	0.171	0.236	0.3	0.463	0.639	0.894	0.917	0.824	0.722	0.463	0.282
	0.9	0.144	0.176	0.2	0.361	0.491	0.639	0.778	0.778	0.69	0.454	0.222
	1.3	0.097	0.167	0.2	0.236	0.315	0.458	0.514	0.556	0.519	0.361	0.111
	1.7	0.074	0.102	0.1	0.167	0.231	0.287	0.31	0.407	0.329	0.259	0.056
	2.2	0.046	0.088	0.1	0.111	0.144	0.19	0.185	0.227	0.218	0.176	0.032

Table 5.1: Spot Pattern 2D Profile Measurements

The three-dimensional plot of Figure 5.2 shows the spot to have an approximately Gaussian profile in each direction.

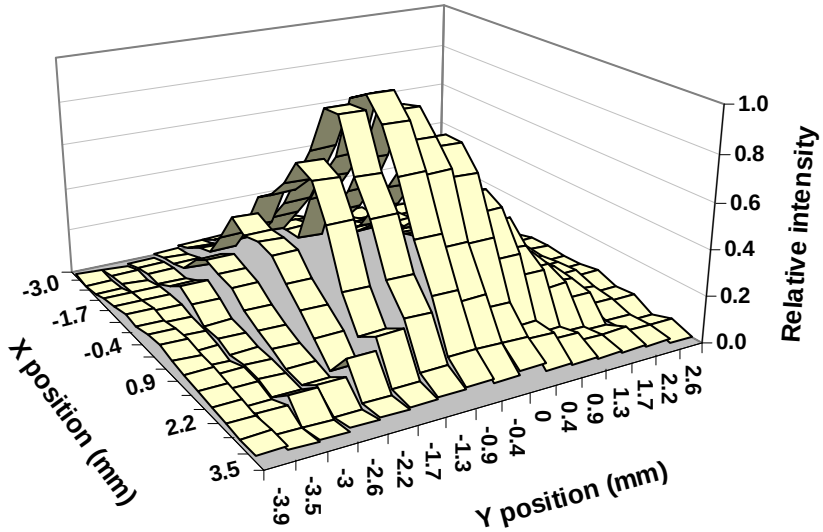

Figure 5.2: Spot Pattern Profile

The effect of vertical spot position can be estimated from the data used to provide Table 5.1. The values summed for each value of Y are used in Figure 5.3 to obtain a moving average that represents the integration of a region 2mm high. The resulting plot gives an indication of the effect of moving the spot position in relation to the capture region (the back surface of an array element). From the figure it can be shown that if the spot vertical positional accuracy is ±0.5mm the output variation is ±3% and if it is ±1mm the output variation is ±13%. The estimated spot position accuracy is in the region of 0.5% to 1%.

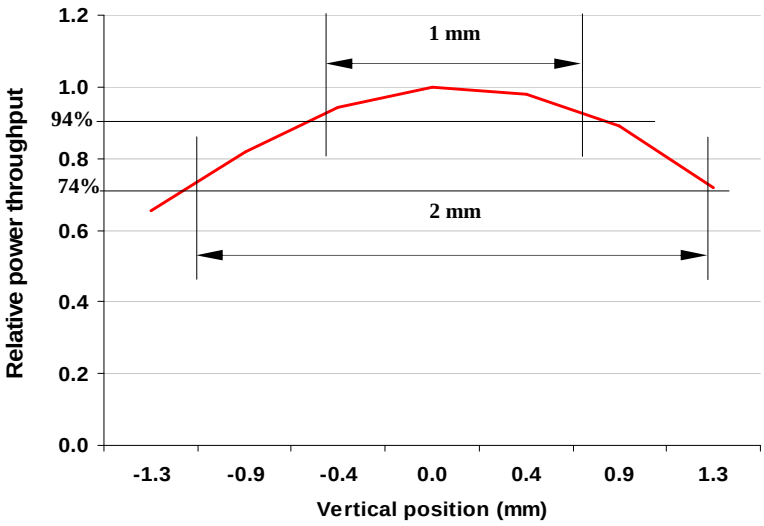

Figure 5.3: Light Capture by 2mm high Element

5.3 Spot Pattern Corrections

5.3.1 Introduction

The pattern projected on to the back of the array exhibited non-linearity in the X direction and positional variations in the Y direction. It was necessary to determine the magnitude and source of these by careful measurement. Potential causes of variation are:

- Errors in the Matlab program
- Hologram rendering
- Projector optics
- Field mirror

Examination of the Matlab program did not reveal any obvious errors and initially a pattern obtained directly from the projector was measured in order to isolate the effect of this from that of the field mirror. Following this, measurements were made with a screen placed at the back of the array so that the effect of both the projector and field mirror were taken into account. All measurements were made with the green channel only operating.

5.3.2 X Coordinates - Projector Only

The projector was removed from the display where it is mounted at an angle of around 20° and secured with its axis horizontal to an optical breadboard. The image was projected on to a vertically-aligned screen located 560mm located in front of the projector lens. The pattern used was of spots located at 10mm intervals along each of the 49 array elements. This gives 163 spots that are effectively placed with a horizontal spacing of 5mm at the array input (with the exception of the second in from either end that are produced by interpolation for graph plotting purposes).

The linearity of the output can be more readily determined by comparing the positions of the spots in relation to a straight line. This is achieved by calculating the coordinates for the best-fit line and subtracting these from the measured values. By using the extreme left spot as the reference and assigning the value of zero to this it was found that the best-fit line is found by multiplying the spot position number by the factor 4.165. The difference values are plotted in Figure 5.4 where the trend line (degree 6 polynomial) is shown by the red line. When allowance is made for the lack of correction it can be seen in Figure 5.4 that some asymmetry is present in the characteristic.

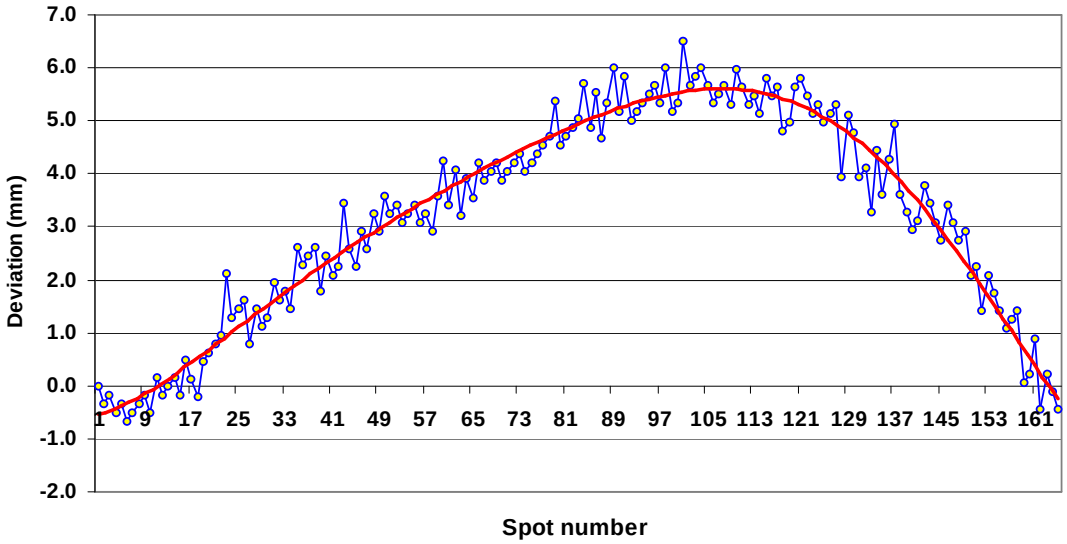

Figure 5.4: Spot X Coordinates Direct from Projector

5.3.3 X Coordinates - Projector and Mirror Using Grid

It is necessary to determine the difference in non-linearity over the height of the reflected image from the field mirror as it is possible that if perceptible irregularities are present in the mirror they could vary over the height as well as the width of the image. Projecting the image a grid provides the most visibly clear means of displaying this. The image on the back of the array of a grid with vertical lines having a pitch of 7 pixels showed that at the left end of the image (looking from the back) these lines exhibited a curvature. It was determined that a possible cause of this was barrelling of the field mirror surface in the region of the end of the mirror. A ball-ended adjuster with a pitch of 80 threads per inch was positioned so that it enabled the centre of the mirror surface on the left side to be moved slightly forward. Careful adjustment enabled the vertical gridlines to be rendered close to being straight and vertical.

The X positions of the gridlines on the axis and around 42mm above and below the axis were measured and the differences from the best-fit straight line plotted in Figure 5.5. These measurements cover the centre and the upper and lower boundaries of the region of the mirror that is actually used. In Figure 5.5 the black plot is the moving average trendline with a period of 3 of the average of the upper, lower and centre measurements. The measurement error is ±0.5mm and the rounding error in converting the calculated spot coordinate value to the nearest pixel is of the same order. This indicates that it is probably valid to apply a correction function that approximates to the trendline as this is virtually always within one millimetre of the extreme upper and lower values. Correction values that range from -1 to 1.5mm are small compared to the total 820mm width of the image.

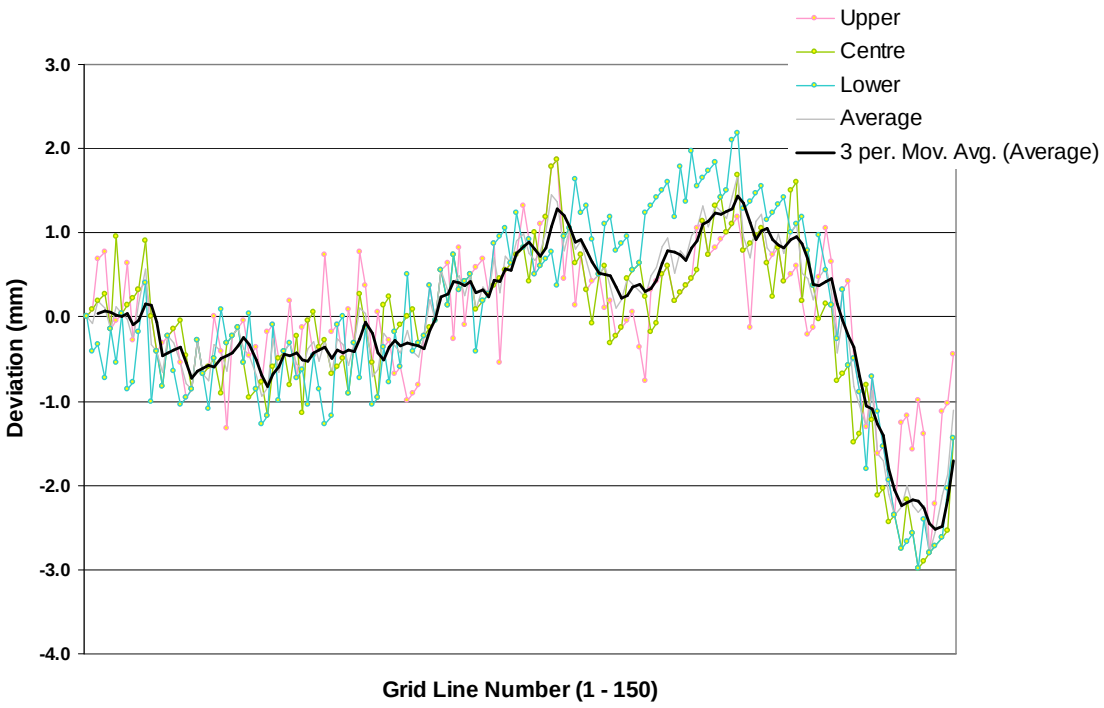

Figure 5.5: Grid Pattern X Coordinates with Projector and Mirror

5.3.4 X Coordinates - Projector and Mirror Using Spot Pattern

Having determined that it is valid to apply a correction function to the calculated X values that apply to the usable area of the image, measurements were then carried out using the same spot pattern. This provides a 5mm pitch pattern and the results for the deviation from the actual position over the complete 820mm width are shown in Figure 5.6. In this case the actual intended positions are used (as opposed to the best-fit straight line) as this provides correction values that can be applied directly into the Matlab program.

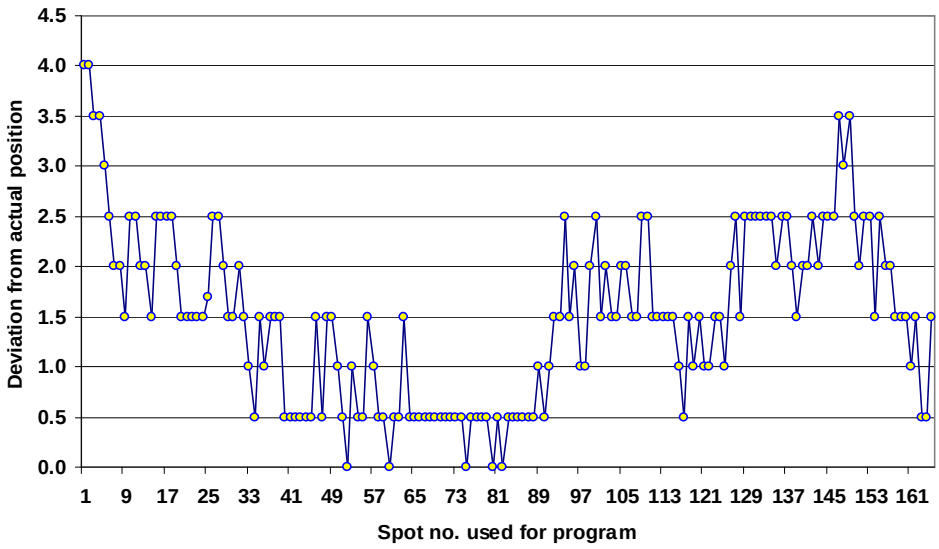

Figure 5.6: X coordinates with Projector and mirror using spot pattern

A function that provides a good fit to the difference values obtained in Figure 5.6 can be used in the program in order to correct the combined non-linearity. This plot is obtained using figures inputted into Excel, one of whose features is to obtain the best-fit polynomial. In the data for Figure 5.6 the first and third spots are outside the usable region of the array as the first 11mm of the array is not used due to the Fresnel lenses on the back of the array elements being only 78mm. The second spot is obtained by interpolation and also falls within the unused region. The same considerations also apply to the 160th, 161st and 162nd spots. Therefore only spot numbers 4 to 159 are required for the purposes of obtaining a correction function.

As best-fit polynomials of degree 2 through to 6 can be obtained with Excel it is necessary to determine which order is most appropriate to the measured data values. Figure 5.7 shows the trendline for each degree and examination of these reveals that the degree 6 trendline provides the best fit.

Excel will only calculate the polynomial coefficients from the data number (an integer), as opposed to the actual data value. These values are determined by Equation (i)

$$AA = 1 + \frac{R + 395}{5} \quad \text{..... (i)}$$

The polynomial coefficients are calculated to 25 significant digits, however it was found that rounding the coefficients to 5 significant digits provides sufficiently accurate results.

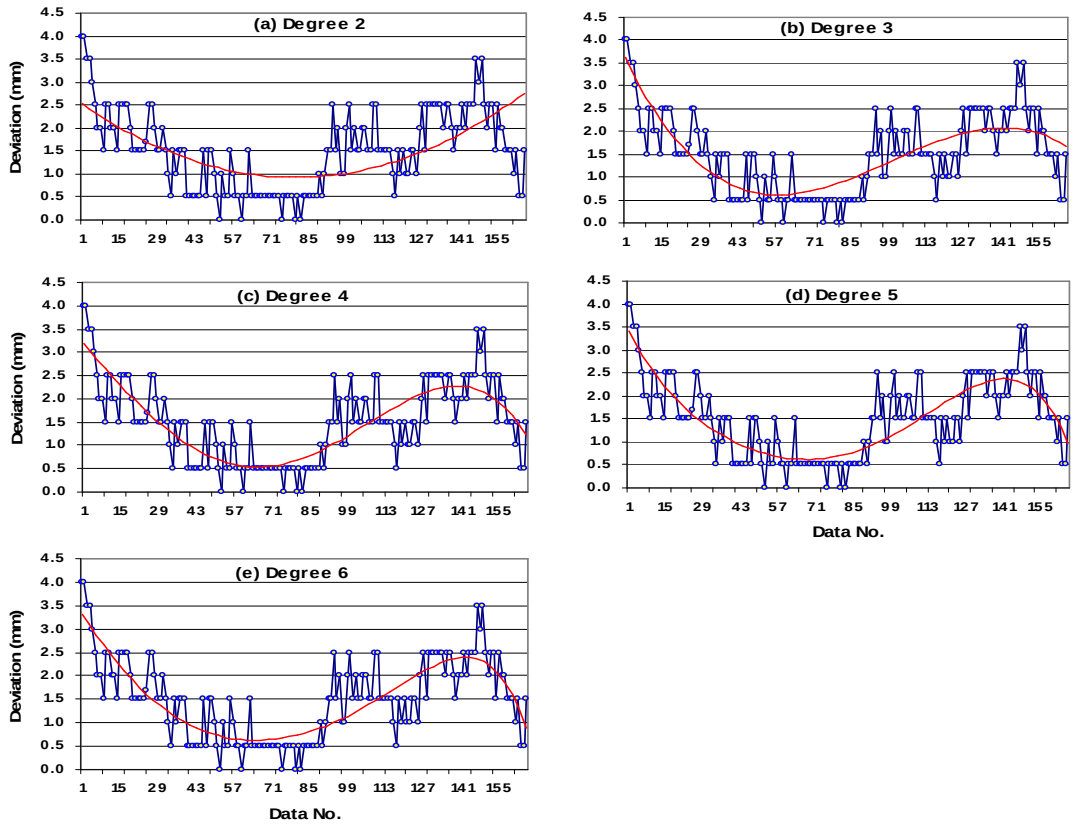

Figure 5.7: Effect of polynomial degree

5.3.5 Simplified Data Function

When the polynomial derived from the data plotted in Figure 5.6 was used to correct the function it was found that errors of around 2mm still occurred at either end of the image. The cause of these is could possibly be due to the effect of measurement and rounding errors. It was decided that final optimisation would use a simplified function based measured data in order to produce minimum deviations from the required spot positions. The Y values of this function are in increments of 0.5mm and the optimised function shown in Figure 5.8 gives values of X. This function was obtained by fine tuning the limits of each discrete Y value so that the spots are within ±0.5mm of the required positions over the width of the image. The correction value AB is given by Equation (ii):

$$AB = -2.7371E\text{-}12AA^{6} + 1.15550E\text{-}09AA^{5} - 3.3363\text{-}07AA^{4} + 2.8383E\text{-}05AA^{3} - 8.5651E\text{-}07AA^{2} - 0.097485AA + 3.3752 \quad .....(ii)$$

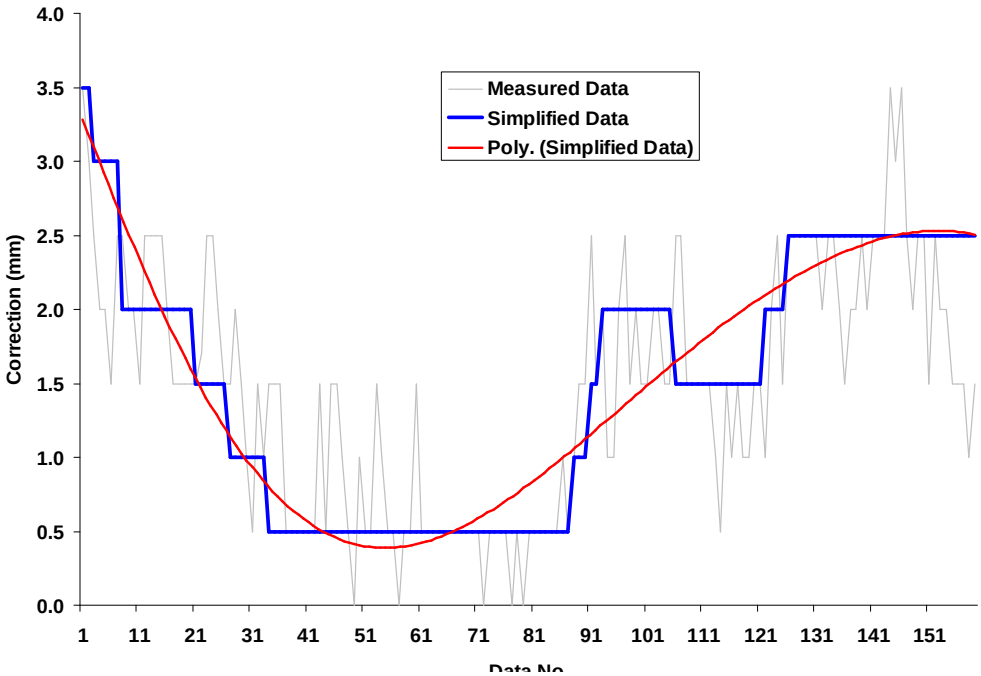

Figure 5.8: Simplified Data

A section of the pattern used to obtain the measurements is shown in the photograph in Figure 5.9(a). This pattern is obtained by generating spots in 10mm increments for every element. This pattern is fairly complex and it was found that a series of vertical lines with a spacing of 15mm as in Figure 5.9(b) enabled deviation from the correct X locations to be clearly observed.

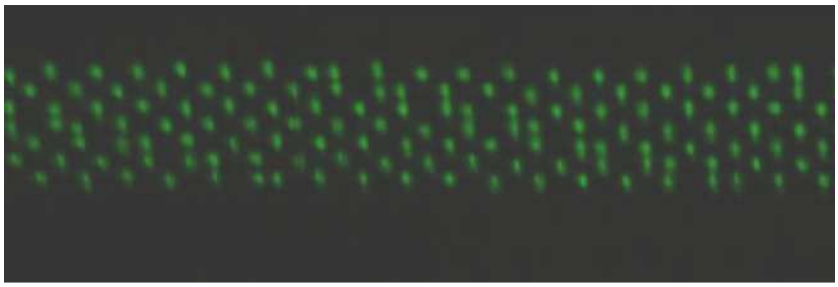

(a) Section of Test Pattern

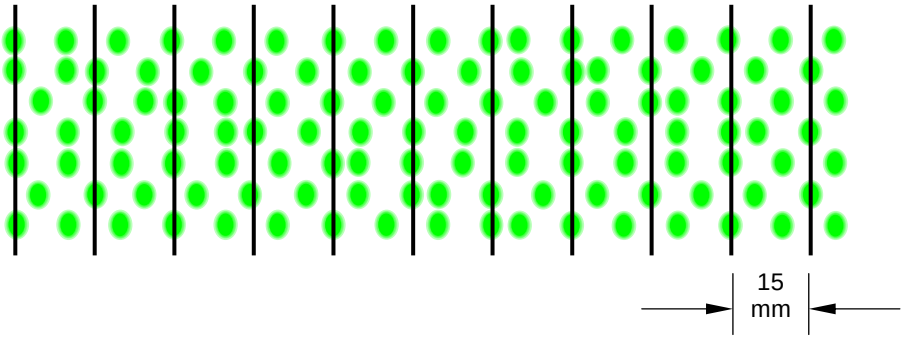

(b) Measurement Grid

Figure 5.9: X Coordinate Measurement

5.3.6 Changes to Matlab Program

The complete Matlab program to produce the spot pattern is given in the Appendix. In order to perform the polynomial correction the following lines in the program were added:

```
R=J+Q;
AA = 1+(( R + 395)/5);
AB = (- 0.0000000000027371*(AA.^6) + 0.00000000115550*(AA.^5) –
0.00000033363*(AA.^4) + 0.000028383*(AA.^3) – 0.0000008.5651*(AA.^2) - 0.097485
*(AA) + 3.3752);
AC= R + AB;
V=AC+mirror_half;
```

5.3.7 Y Correction

Allowance is made in the program to apply a Y correction to every element in the upper and lower arrays. Correction is made by measuring the actual positions of the spots in relation to their intended positions and entering these values into the program matrices.

5.3.8 Measurements

In this case a simpler spot pattern was generated that enabled spots on adjacent elements to be differentiated from each other. This comprised a central spot for each

element and spots at ±40mm either side of this; this gives the pattern shown in Figure 5.10 where the lateral separation of the outer spots in adjacent elements makes measurement easier. The positions of these spots are just outside the active area of the back of the elements which is around the ±39mm determined by the width of the cylindrical Fresnel lenses attached to the back of the elements. The pattern is projected on to a screen with lines marking the positions of the centres of the array element layers. The corresponding positions of the elements and the central spacer are also shown. The measurement results are given in Appendix 2.

5.3.9 Current Status

With the corrections applied the X and Y coordinates of the spot positions are generally within ±0.5mm of their intended positions. It is concluded that as the corrections applied are all within a maximum limit of 3mm it is reasonable to carry out all the corrections in the software. At the time of writing there were still some issues that required addressing, these were:

- Projector instability: The pattern normally remained stable with the exception of couple of occasions when it has drifted vertically by several millimetres. Rather than change offsets, the projector was adjusted on its two front mechanical adjustment screws.
- Change of Y offsets in the program causes horizontal grid lines to curve. The offsets are currently 3.5mm for the upper array and 4mm for the lower array. When these are set to zero as required for the patterns to be in the correct positions in relation to the central reference point at the array, there is a pronounced curvature of the horizontal grid lines. Currently the pattern is set to the correct vertical position by setting the projector adjustment screws; this does not produce any keystoning of the image or curvature of the grid lines.
- When the vertical corrections were last applied into the program, corrections of one millimetre caused the spots to move by several millimetres.
- The blue and green patterns are fairly well aligned with each other but the red pattern is poorly aligned.
- Certain correction strategies were considered before the work was carried out but it was found in practice these were not necessary. For future reference these are as follows:
    - Apply a Gaussian function for the X corrections: it was not known initially whether local corrections would be necessary, due to possible

irregularities in the mirror surface. If polynomials had been unable to cope with these, Gaussian functions with their flexibility in varying their position, amplitude and FWHM could have been applied.

- Use $f_c(x)$ to provide Y corrections: if the variations over the width of an array element were excessive, an additional Y correction based on lateral position could potentially rectify this.
- Apply local constant values between limits: instead of calculating a polynomial correction function it could also be possible to add a given correction value when x is between certain limits i.e. if $x_1 < x < x_2$ then add K.

5.4 Summary

The dimensions of the spots in the illumination pattern are important in determining the shape of the exit pupil profile, and the actual positions of the spots must be closely controlled in order to provide good image quality.

The two-dimensional profile of the spot was measured as being approximately Gaussian in profile with dimensions of 2.7 millimetres FWHM in the vertical direction and 2.4 millimetres horizontally (Figure 5.1). This pattern is used to illuminate the back of an array element that is two millimetres high and it was determined from the profile that a positional variation of ±0.5 millimetres gives an output variation of ±3 % and ±1 millimetre gives an output variation of ±13%. This shows that the vertical positional accuracy should be within ±0.5 millimetres in order to keep the illumination of the image columns formed by each element within acceptable limits.

The linearity of the projector alone was measured as deviating 6 millimetres (Figure 5.4) and the results indicated that this could be readily rectified with a simple correction function. As the mirror can introduce deviations to the beams from the projector the most relevant linearity profile is that of the overall projector/mirror combination. From experience it was known that the mirror can be prone to local surface variations so 3 plots at different Y positions were made (Figure 5.5). These showed that although there are small variations for different Y values the trend is the same in each case.

The linearity plot of the projector/mirror combination was applied directly into the Matlab program in order to compensate for the linearity errors. In principle this should correct the spot X positional errors but it was found in practice that errors still occurred at the extreme ends. In order to overcome this, a simplified correction function (Figure 5.8) was applied.

The correction function was calculated by obtaining a polynomial using Excel, and examination of the results showed that the degree 6 polynomial trendline provided the closest result (Fig 5.7).

It was found that the most effective means of making the Y corrections was made by adjusting the screws on the laser projector mounting.

CHAPTER 6

LASER PROJECTOR DISPLAY - OTHER PERFORMANCE ISSUES

6.1 Preface

The principle goal of this chapter is to check the performance of the major components used in the first two iterations of the MUTED Display and these are:

- Vertical Diffuser
- Birefringence
- LCD Sub pixel Structure

6.2 First Iteration

The original version of the display was built with Plexiglas array elements, a Samsung LCD display and optical components on non-birefringent components.

The spot powers at the back of the array were measured so that the combined effect of both output spot power and mirror reflectivity are allowed for. This was also simpler to perform as the detector is always in the same orientation; it is more difficult to aim it at the projector lens when the direct powers are measured. The power meter was used that takes averages for one second sampling periods. This eliminated the varying readings caused by the projector LCOS device switching. The variation of the spot pattern brightness is important as the spots provide the backlight for the LCD where each spot illuminates a column of the screen. When the powers shown in Figure 6.1 (from Table 6.1) were measured on projector Y44 the red laser was not functioning at the time the measurements were made.

As light was observed bleeding through the field mirror when this was viewed from behind, the reflectivity of the mirror was measured in order to determine whether the light loss was significant. Power meter readings showed that this light, although visible, was too low to be measured by the Newport power meter, even when used with a low power detector.

Direct beam = 357.9μW

Passing through screen = 487nW

Background =499nW

Power reflected at 45° = 265.9nW

Therefore reflectivity = **74.3%**

Power reflected at 20° = 288.1nW

Therefore reflectivity = **80.5%**

The measurements above show that light loss in the mirror is due to absorption in the material so that improvement could possibly be obtained by changing the material but not increasing the deposition thickness. It was not particularly easy to measure the reflectivity at normal incidence but this in fact is not necessary as this condition does not occur in practice.

	Green		Blue	
	Upper	**Lower**	**Upper**	**Lower**
Total power (mw)	491.9	497	180.4	189.3
Mean power (μW)	10.04	10.14	3.68	3.86
Standard deviation (μW)	0.38	0.41	0.35	0.29
Fractional Variation (± %)	9.1	9.6	18.9	7.4

Table 6.1: Spot Powers

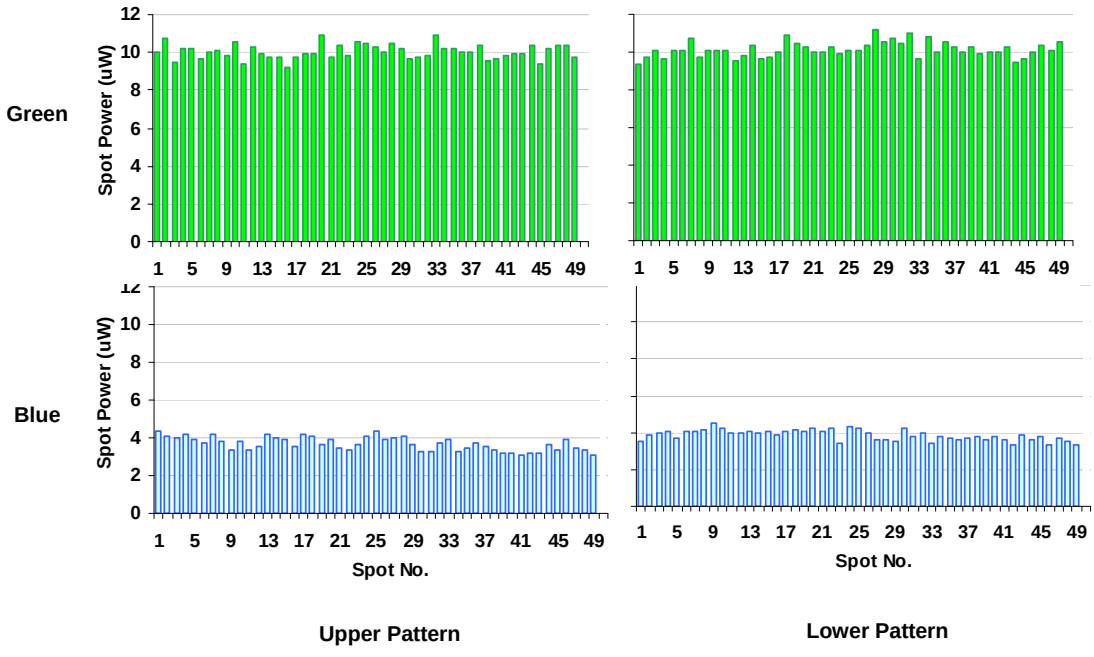

Figure 6.1: Spot Powers

6.2.1 Vertical Diffuser

Emergent light from the front surface of the array elements is spread out vertically with the use of a Luminit 'holographic' diffuser. If all the array elements were situated in one plane the Gaussian spread from these diffusers would give an image whose brightness falls away from the centre. However, the 'staircase' nature of the array means that adjacent columns of the effective backlight formed by the array output have vertical brightness profiles that are displaced relative to each other. The effect is most pronounced every seventh element where the vertical displacement of adjacent elements is 26mm.

There is also the effect of clipping where the extreme uppermost rays from the lower elements are unable to reach the top of the screen (and vice versa). This gives the appearance of dark jagged regions at the top or the bottom of the image. These effects would be worse with the reduced array to screen distance if steps were not taken to alleviate this.

6.2.2 Birefringence

In the first arrays built the elements were made from Plexiglass as this material could be readily fabricated into components with sufficient accuracy to give well-collimated emergent beams. The problem with this material is that it is birefringent and therefore alters the linearly polarised light from the projector which cannot then be matched to the back polariser of the LCD.

The Plexiglass exhibits birefringence when light passes lengthwise through it. This is not unexpected as it is extruded when manufactured. For this reason 2mm thick cast acrylic material was tested as it appeared possible that the different process used to produce the material could potentially overcome the birefringence problem. A test piece with dimensions of 80mm x 80mm and having opposite sides polished was place between crossed polarisers. This displayed very similar transmission characteristics to Plexiglass and was therefore also not suitable for this application.

6.2.3 LCD Sub-pixel Structure

The effect of the black region in the Samsung LCD sub-pixels can be determined by reference to Figure 6.2. P is the point projected back from all the black regions via the lens centres. In Figure 6.3(a) this is situated at the front surface of Element D and every black region over the height of the illuminated region of the screen blocks the light from this element. In Figure 6.3(b) P is situated within the array resulting in the projected lines passing through the front of elements A and F. Figure 6.3(c) shows the lateral positions of the elements. When the screen is at this 'correct'* distance a vertical dark line is produced

in line with the position of the illuminated region of Element D as depicted in Figure 6.4(a). In Figure 6.4(b) the dark area indicated by the letter A is the 'shadow' formed by the dark region. Similarly, the dark areas B to F are shadows formed by the dark regions in areas of the screen where the point P aligns through the lens centres with the dark regions. It should be noted that the lenses shown in Figure 6.3 are only representations of the actual lenses which have a different configuration in reality.

*The term 'correct' is used to distinguish between the array position that corresponds to the correct parallax and the distance where the image is subjectively superior.

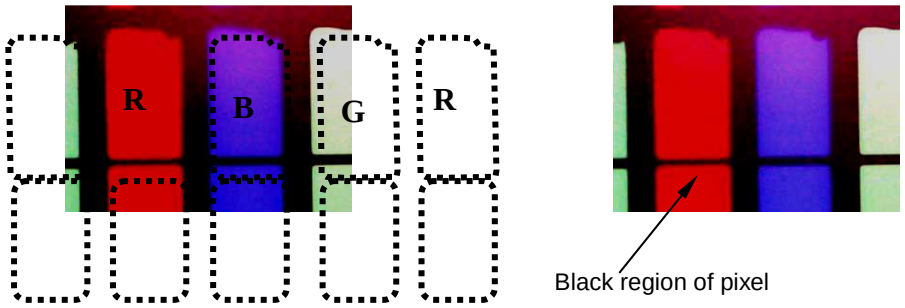

Figure 6.2: Samsung LCD Sub-pixels

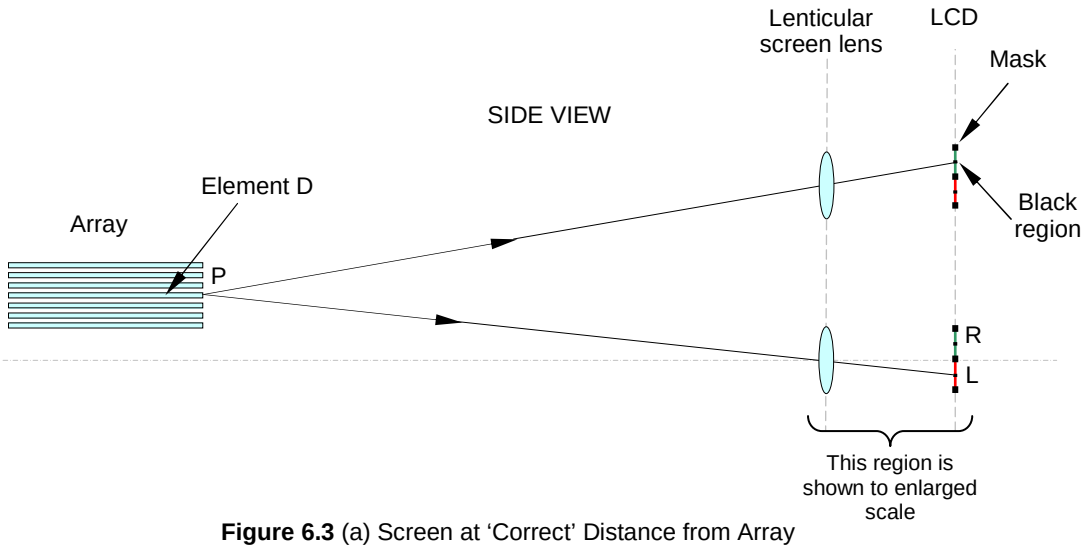

Figure 6.3 (a) Screen at 'Correct' Distance from Array

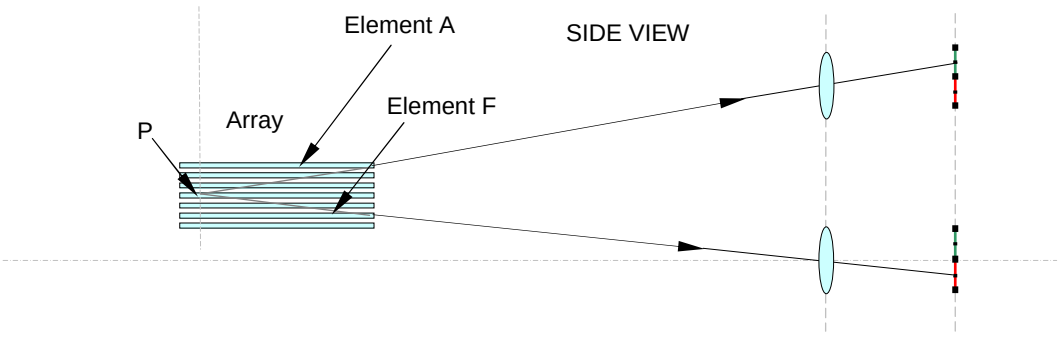

Figure 6.3 (b) Screen closer than 'Correct' Distance

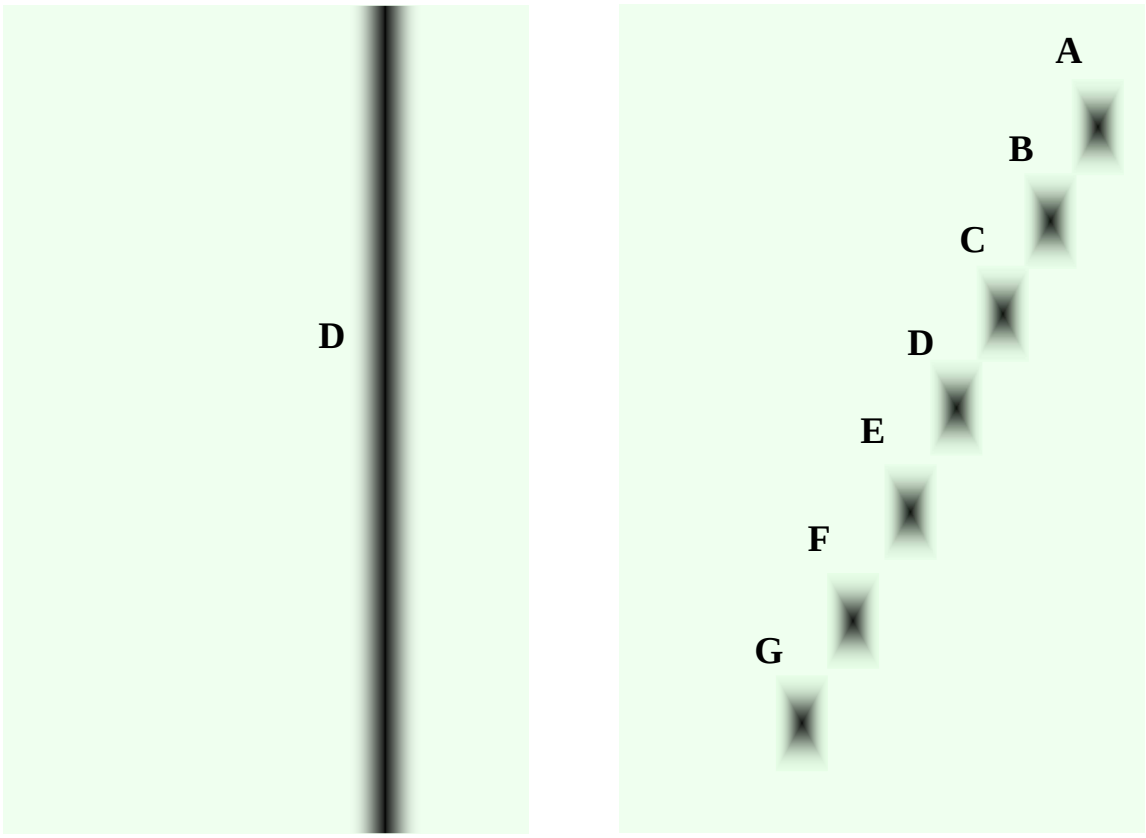

(a) Screen at Optimum Distance

(b) Screen Closer

Figure 6.4: Predicted Appearance of Screen

For the best subjective results position of the screen should be determined by actual observation of the appearance on the screen rather situating it at its geometrically 'correct' distance of 490mm. The spots used to produce the photos in Figure 6.5 were obtained using a conventional projector providing red and green spots for the upper and lower arrays. The enhancement lens and 10° diffuser were positioned in front of the screen. The array to screen distance Z_S was varied from 400 to 510mm in 10mm increments and photographs were taken on the central axis and at 135mm above and below this.

Unfortunately it is fairly difficult to see from the photos where the images are most uniform but actual observation by two viewers indicated that the value of Z_S is around 460mm for the most uniform appearance. Comprehensive trials with a larger number of observers was not considered necessary as is was not intended for the Samsung display to be employed in any evaluation work.

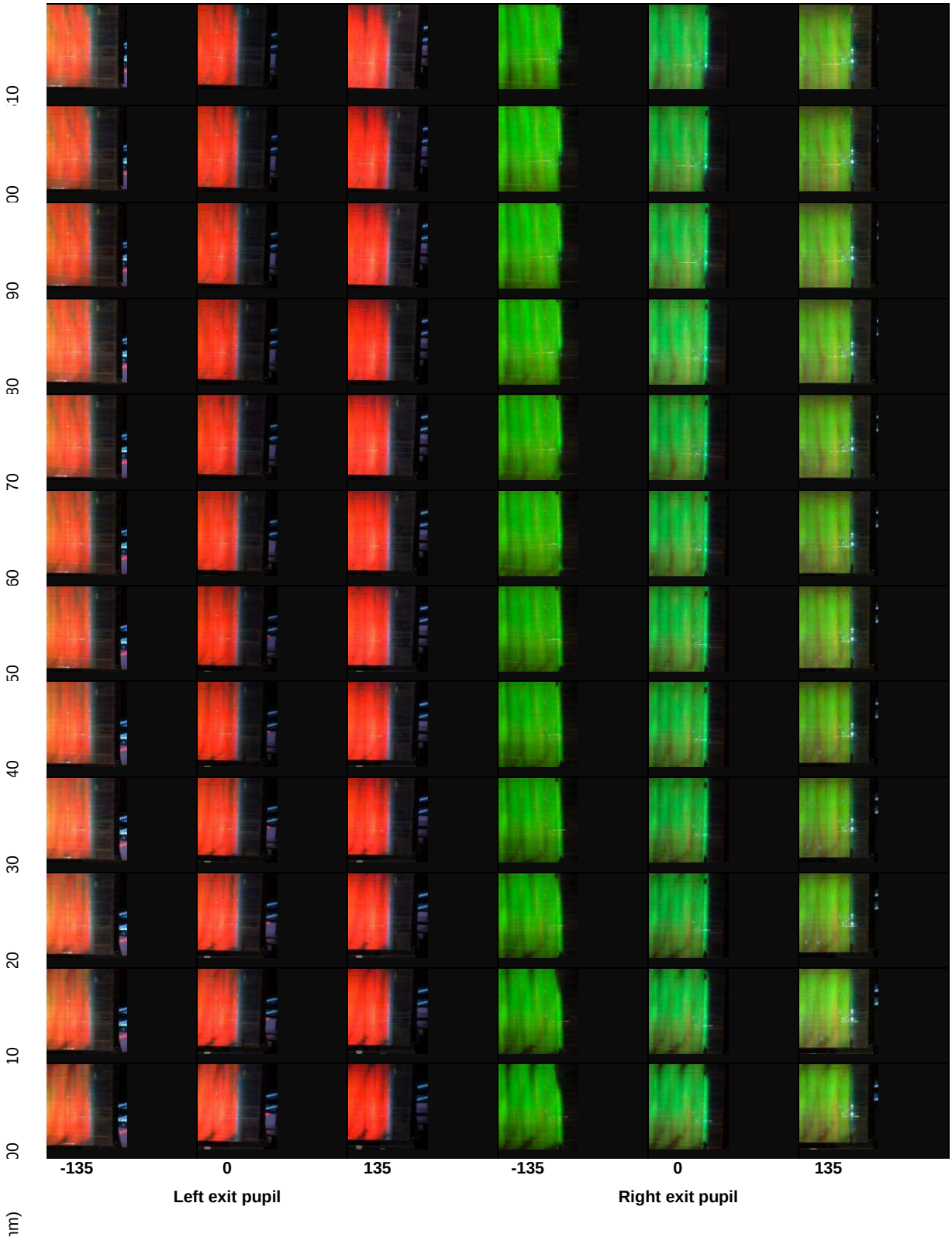

Figure 6.5: red and green spots for the upper and lower arrays

6.3 Second Iteration

The image observed in the first version of the display was very dim and measurements were made to identify the reasons for this. The principal factors thought to be contributing to this were; insufficient power in the spot pattern, light loss in the array elements and losses due to birefringence and mismatch of the projector polarisation with that of the LCD.

6.3.1 Vertical Diffuser

Screen variation brightness problems can be solved by replacing the Luminit diffuser with a horizontally-aligned lenticular screen that has a 'top hat' function as shown in Figure 6.6. This is a 275 LPI screen supplied by Microsharp Corporation. The figure shows that the lenses are optimised for collimated light falling on the lens surfaces. The lenticular screens are therefore attached with their lens face toward the element. In order to function an air gap is left between glass and the lens surfaces therefore the 2mm high diffuser strips are attached at either end out of the light path.

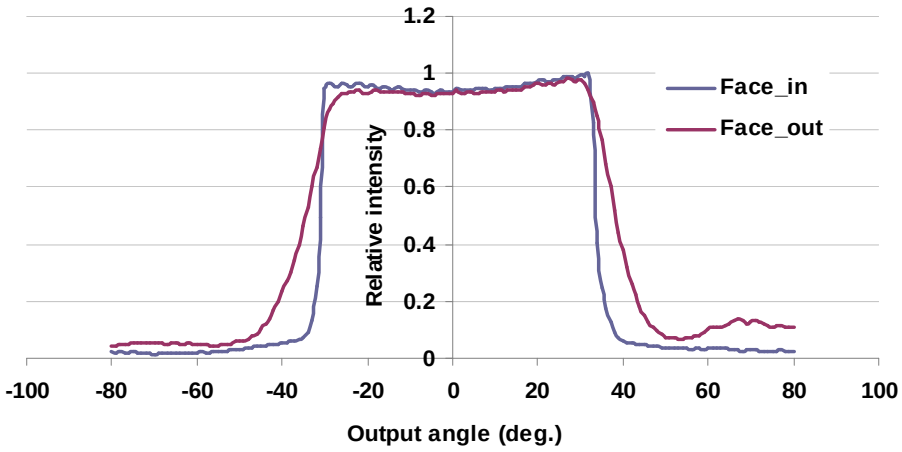

Figure 6.6: Lenticular Diffuser Profile

6.3.2 Birefringence

The disadvantage of the Plexiglass material used in the original array is that it is birefringent and upsets the vertically polarised light from the projector which cannot be matched to the back polariser of the LCD, therefore causing considerable light loss. This can be solved by making the array elements from glass and has the additional benefit of having much more consistent thickness therefore avoiding the previous necessity of rejecting around 80% of the acrylic material whose thickness did not fall within specified limits.

The photographs in Figure 6.7 are of a Plexiglass and a glass element taken through crossed polarisers. The lower/right element is Plexiglass and the birefringence can clearly be seen. The glass element shows slight transmission at 45°.

Figure 6.7: Comparison between Glass and Plastic array Elements

It is useful to compare the throughput of several elements in a stack in order to get an indication of any possible birefringence effects. Figure 6.8 shows a stack of six glass array elements arranged at 45° between crossed polarisers. This indicates low birefringence as only a small amount of light can be seen in the central region; this is passing through the soft apertures. The banding seen is due to leakage between adjacent elements and not to variation from element to element.

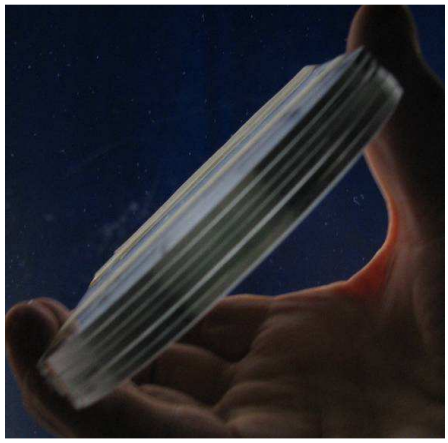

Figure 6.8: Comparisons of Glass Array Elements

In order to gain advantage from the use of glass elements every component in the light path between the projector and the LCD back polariser must also be non-birefringent. These components in order are: field mirror, horizontal diffuser, Fresnel lenses, array rectangular piece, soft aperture, array D-piece, vertical diffuser and lenticular MUX screen. The array components are shown in side elevation in Fig. 6.10 and the screen components in Fig. 6.11.

In order to gain advantage from the use of glass elements every component in the light path between the projector and the LCD back polariser must also be non-birefringent. These components in order are: field mirror, horizontal diffuser, Fresnel lenses, array rectangular piece, soft aperture, array D-piece, vertical diffuser and lenticular MUX screen. The array and screen components are shown in side elevation in Figure 6.9. In order to match the projector polarisation to the LCD a half wave plate optimised for 532nm is located immediately in front of the projector lens and rotated in order to give maximum image brightness.

The field mirror is constructed from a surface-silvered sheet that does not affect the polarisation and the Fresnel lenses attached to the back surface of the array elements are not birefringent. However the other components used had to be replaced with non-birefringent versions.

1.	Horizontal diffuser	Pokalon substrate
2.	Fresnel lens	polymethylmethacrylate (PMMA)
3.	Rectangular piece	BK7 glass
4.	Soft aperture	triacetylcellulose (TAC) substrate
5.	D-piece	BK7 glass
6.	Vertical diffuser	triacetylcellulose (TAC) substrate
7.	Lenticular MUX	triacetylcellulose (TAC) substrate

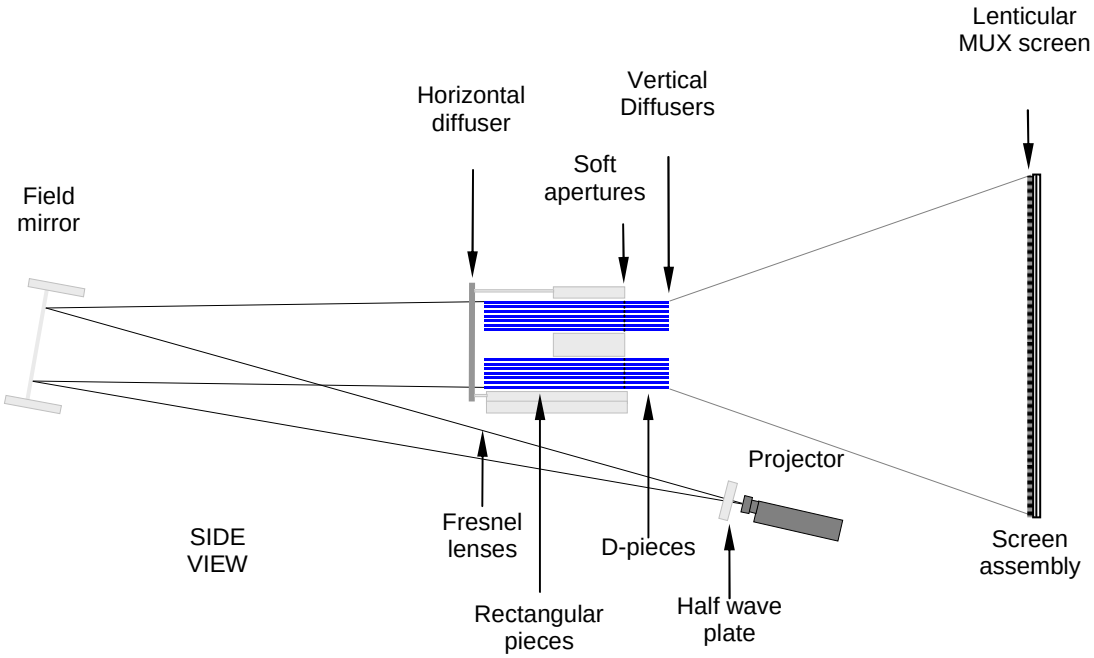

Figure 6.9: MUTED Laser Projector Prototype

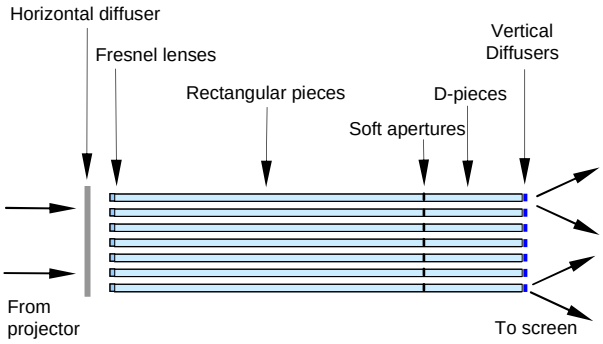

Figure 6.10: Side elevation of array: This shows the six array components that must be non-birefringent

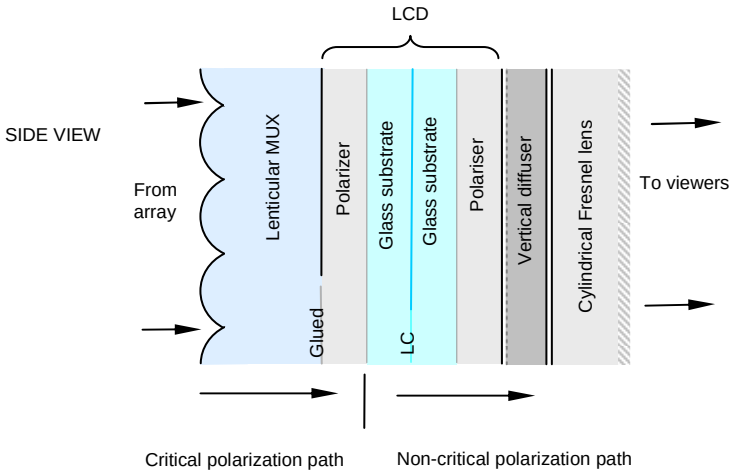

Figure 6.11: Screen components: This is a side elevation of a section of the screen and shows the components in the critical polarisation path.

6.3.3 LCD Sub-pixel Structure

The shapes of the sub-pixels of the original Sony monitor used are shown in Figure 6.12. The prototype incorporating this did not exhibit patterning in the image and this supports the view that the source of the pattern is due to the LCD black mask. The transmitting areas are clear apart from the regions in two of the corners that give them a ‘D’ shape; and there is also no fine microstructure visible within the transmitting areas.

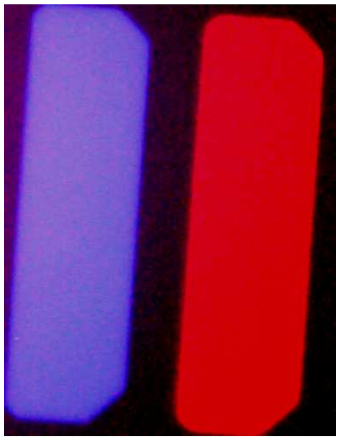

Figure 6.12: Sony LCD Sub-pixels

6.4 Measurements

The maximum brightness measured with the power meter was 16nW. For the 10mm diameter aperture sensor, positioned at 1m from the display (which was only half illuminated due to poor spot alignment) this corresponds to 1.8 nits. This is around 8% of the theoretical prediction of 21 nits and 1.8% of the 100 nit target. LBO has measured the speckle contrast to be in the range 60+/-4% (out of a maximum value of 100%) taking samples at various points across the display. This is less than 100% due to the multiple scattering surfaces in the system and the nature of the laser projection which rapidly superposes uncorrelated speckle patterns. All measurements are summarised for convenience in Appendix 4**.**

6.5 Summary

Two iterations of the laser projector version have been built. The first version revealed various improvements that were required in the following version. The shortcomings of the first display were identified as low brightness and luminance variation over the screen area

As each spot in the illumination pattern corresponds to a vertical illumination strip behind the LCD the variation in spot powers was measured (Figure 6.1). The fractional variation was ±9.1% and 9.6% for the green patterns and ±7.4% and 18.9% for the blue pattern. The maximum variation for blue is large but it was not clear how this could be rectified.

The irregular pattern observed at the top and bottom of the images on the first prototype was due to the vertical diffusers attached to the front of the array elements having too small a diffusing angle and also having a Gaussian distribution. The pattern of dark rectangles (Figure 6.4) was caused by the black mask in the sub-pixel structure (Figure 6.2) of the Samsung display. Another model display without this mask was required.

The images were extremely dim and the only action to mitigate this was to use non-bi-refringent optical components in the light path, and to match the resulting linearly polarised components to the polariser in the LCD by using a half wave plate at the projector output.

In the second iteration of the prototype the diffusers on the front of the array elements were replaced with 80° opening angle lenticular screens on a non bi-refringent substrate (Figure 6.6). The LCD was replaced with a Sony monitor that does not have the black mask in the sub-pixel (Figure 6.12). The non-bi-refringent replacement component materials were as follows: Horizontal diffuser - Pokalon substrate, Fresnel lens - polymethylmethacrylate (PMMA), Rectangular piece - BK7 glass, Soft aperture-

triacetylcellulose (TAC) substrate, D-piece - BK7 glass, Vertical diffuser - triacetylcellulose (TAC) substrate, Lenticular MUX - triacetylcellulose (TAC) substrate.

The refinements were carried out principally to improve the brightness and uniformity of the display. It was not anticipated that the replacement of the components with non-birefringent versions would make a very substantial improvement in brightness but this action did enable the projector to be operated under the most favourable conditions with the use of a half-wave plate to match the linearly polarised projector output to the polariser of the LCD. It was found that it was necessary to rotate the projector polarisation by only 10° in order to match the orientation.

CHAPTER 7

CONVENTIONAL PROJECTOR PROTOTYPES

7.1 60Hz LCOS Projector Prototype

7.1.1 Introduction

In order to overcome the brightness problems with the laser projector, versions using conventional lamp projectors were built. A 60Hz LCOS projector version has been built and a 120Hz DLP projector version is under development. Figure 7.1 is a simplified schematic diagram of the 60Hz version. At present this produces a single pair of exit pupils 1000 millimetres directly in front of the screen that are not head tracked. The display does however provide images that are sufficiently bright for use for comparative evaluation purposes.

As the output of this projector is elliptically polarised and the polarisation is different for each of the primary colours there was nothing to gain by using non-birefringent optics. For this reason the Plexiglass array is used in this version. The configuration of this prototype is similar to the holographic projector-based prototype with two exceptions: the replacement of the laser projector with a Canon 60Hz LCOS conventional projector, and the replacement of the parabolic field mirror with a large one metre focal length Fresnel lens. Originally it was anticipated that the faceted structure of a Fresnel lens would create fringing artefacts but subsequent investigation showed this not to be the case. Conventional projection also allows the pattern to be a series of rectangles as opposed to the spots from the laser projector that have a Gaussian profile. This enables greater control over the exit pupil intensity profile.

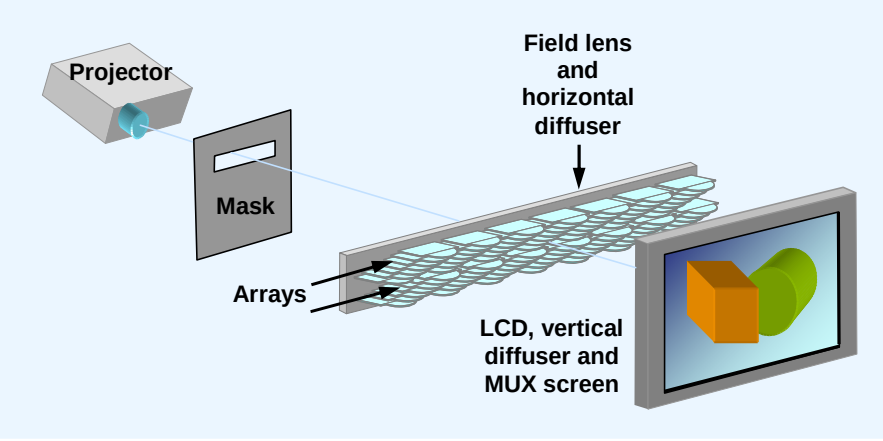

Figure 7.1: MUTED LCOS Projector Prototype: The projector produces a series of illuminated rectangles on the back surface of the arrays that are transformed into intersecting collimated beams that form exit pupils at the viewer's eyes

The conventional projector-based working MUTED prototype is shown in Figure 7.2. Head tracking has not yet been applied to this prototype but the optical performance can be determined without this. The screen brightness of 25 nits enables it to be viewed under reasonably bright ambient lighting conditions as Figure 7.3 indicates.

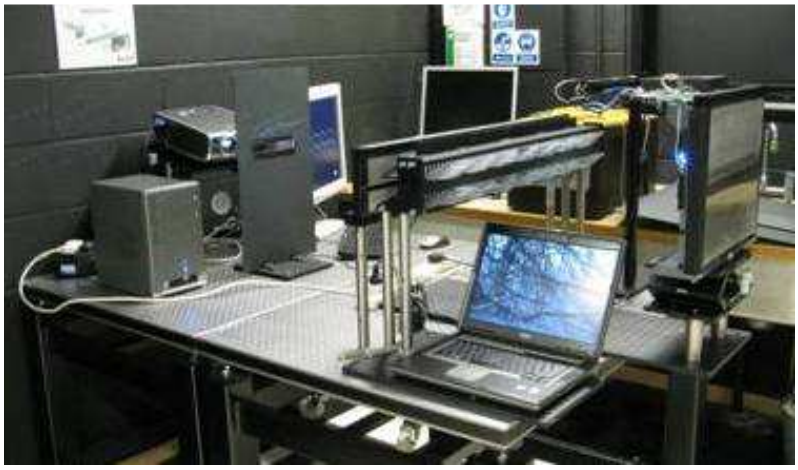

Figure 7.2: MUTED LCOS Projector Prototype: This uses a conventional LCOS projector (on left) illuminating the back of the arrays via a mask that cuts off extraneous image regions.

7.1.2 Left Right Images

Left/right pairs of images shown in Figure 7.3 are produced; the difference in horizontal camera position can be seen by observing the relative positions of the array behind the screen. The photographs were taken in typical indoor lighting conditions. Some vertical banding is visible in the images; this due to the use of an LCD panel with the bar in the sub-pixel and will be eliminated in the next version of the display with the use of a panel that has a clear sub-pixel aperture. Results show this approach to be promising; for example the extreme letterbox shape of the image only utilises around 10% of the available image. It is possible that a projector light engine designed specifically for this application could give screen brightness in the order of 250 nits.

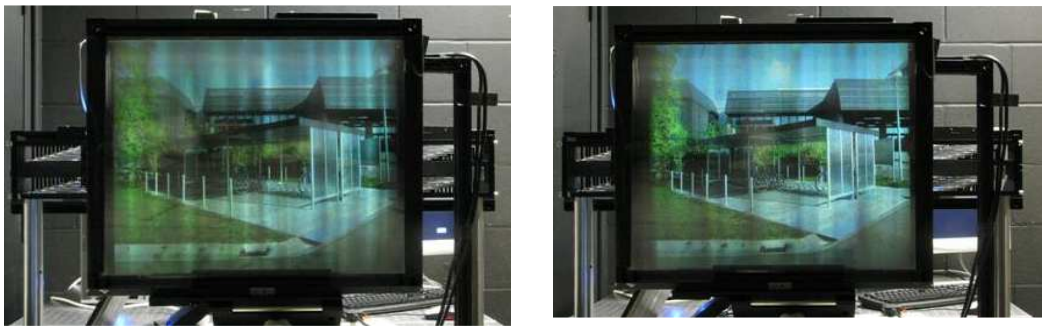

Figure 7.3: MUTED LCOS Projector Prototype Images: These show vertical striations caused by mask in LCD sub-pixels of original Samsung screen. These are not present in the replacement Sony LCD.

7.1.3 Medical Test Images

Figure 7.4 shows a typical medical image, in this case the blood vessels in the Circle of Willis that has been used in initial evaluation work. These overlaid left and right images are produced by dynamic contrast-enhanced magnetic resonance imaging (MRI) where the stereo pair is synthesised from this information in order to provide a non-invasive method of examination.

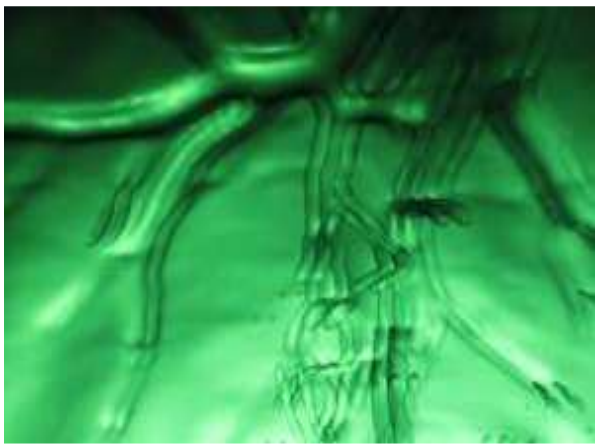

Figure 7.4: Medical Test Images: Test images of blood vessels in the Circle of Willis supplied by MUTED partner Biotronics 3D. These are synthesised from MRI scans in order to provide non-invasive examination.

7.1.4 Crosstalk Measurements

The intensity profiles of the left and right exit pupils are shown in Figure 7.5(a). These were measured at a distance of 1000 millimetres from the screen with the pupils centred on the central axis. Due to asymmetry it is better to determine crosstalk from these plots by the values at points separated by the eye spacing rather than measuring levels at two fixed points. The reason for this is that the tracking capability of the display in its final form enables exit pupils to be located in relation to the viewers' eyes in a position that gives minimum crosstalk. The values obtained from these plots are 4.6% for the right channel and 7.3% for the left channel.

The relatively high levels of crosstalk could be reduced by changing the relative positions of the exit pupils. This is possible in the MUTED display by altering the spot pattern that produces the exit pupils in accordance with the results of either objective measurements or with subjective tests. In this case, increasing the separation by 16 millimetres as shown in Figure 7.5(b) could reduce the crosstalk to 5.6% in the left channel and 1.5% in the right channel.

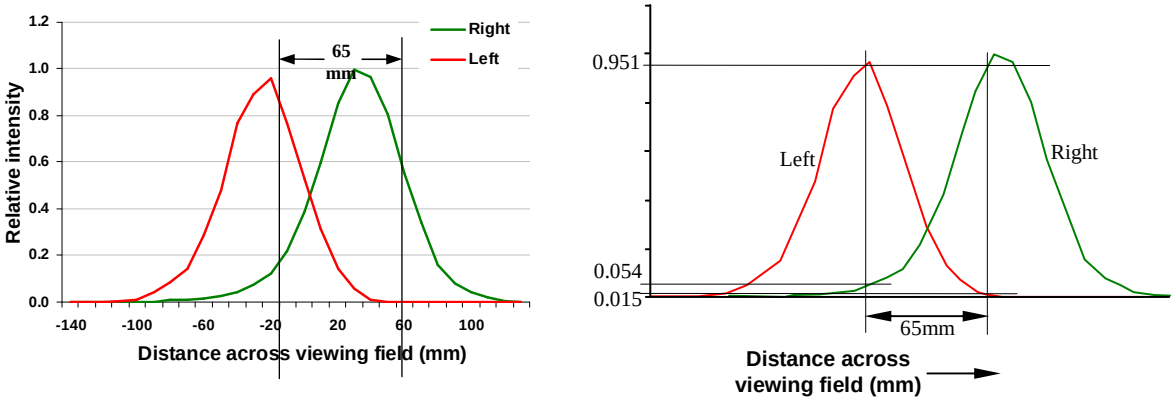

(a) MUTED LCOS Projector Prototype Crosstalk: The plots for the left and right exit pupil intensity profiles show that crosstalk is dependent

(b) Crosstalk Reduction: The plots in Figure 5.2.1 indicate that increasing the exit pupil separation could reduce the crosstalk.

Figure 7.5; LCOS projector prototype crosstalk

The use of a laser projector at this stage of currently available technology is not possible but its use in the future should not be ruled out. Conventional projection shows promise as the current version utilises only a small proportion of the available image and a redesigned projector light engine would allow at least an order of magnitude increase in screen brightness. The display is inherently 2D/3D switchable but with halving of the vertical resolution. Another version of this display is currently under construction that incorporates a 120Hz projector and LCD. This will provide full resolution so will be truly 2D/3D switchable.

7.2 120Hz DLP Projector

7.2.1 Introduction

This section presents construction and operation of a multi-user autostereoscopic 3D display system using the time multiplexing approach. This prototype has three main advantages over previous versions developed by the authors:

- Hardware is simplified as only one optical array is used to create viewing regions in space.
- Lenticular multiplexing screen is not necessary as images can be produced sequentially on a fast 120Hz LCD with full resolution.
- The laser projector is replaced with a high frame rate digital micromirror device (DMD) projector.

The whole system in this prototype consists of four major parts:

- 120Hz high frame rate DMD projector.
- 49-element optical array.
- 120Hz screen assembly.
- Multi-user head tracker.

The display images for left/right eyes are produced alternatively on a 120Hz direct-view LCD and are synchronised with the output of the projector which acts as a backlight of the LCD. Novel steering optics controlled by multi-user head tracker system directs the projector output to regions referred to as exit pupils that are located at the viewers' eyes. The display has the capability of being developed into in 'hang-on-the-wall' form.

7.2.2 Temporal MUX

The prototype described in this chapter uses time multiplexing where three-dimensional images are produced by presenting left and right images sequentially to the users' eyes. There are three types of multiplexing schemes, these are; time, spatial and spatiotemporal. In time multiplexing the image data is arranged time sequentially, in spatial-multiplexing the image data is arranged in parallel and spatiotemporal multiplexing uses a combination of both of these. The previous three versions of the prototype discussed in this paper were built using spatial multiplexing. Time multiplexing has typically been applied to the projection-type 3D systems based on high-speed projectors; spatiotemporal multiplexing uses both time and spatial multiplexing simultaneously to display more views than a high-speed projector can handle [66].

To display N-view images with time multiplexing the display device should display 60N frames/sec for progressive scanning in order to display flicker-less image at usual TV brightness. This scheme is generally used in multi-view, binocular and volumetric displays; a two-image display which uses this scheme to present left/right images from an image pair alternatively to one viewer left/right eyes or for several viewers using head tracking is described in this paper. Images are presented in a layered configuration in volumetric methods [38, 71], they are sampled for a very short period and then arranged in a specific time sequence.

Spatial multiplexing is the most commonly used scheme in two-image, multi-view, volumetric and holographic displays. In this scheme either a specific image column or a pixel from each view image or different view images in the multi-view images [13] to be displayed, are sampled and then arranged in a spatial image sequence. The multi-view images can also be arranged in either a zigzag [87] or slanted [59] line style. A two-image display may use this approach to display two images to the viewers simultaneously where

the viewing regions may occupy fixed positions [16] or may allow for viewers' moving head positions under the control of a head tracker [56]. Volumetric displays, where images are formed within a volume of space using this approach [8], are capable of providing autostereoscopic images but the hardware tends to be complex. They currently provide only transparent images, although it is possible this problem may be overcome in the future. Holography uses phase variation in the reflected light from the object for recording an object image and reconstructing the image by phase conjugation [43].

Spatiotemporal multiplexing is used to enhance the performance of currently-available display devices [69, 34]. Typical examples are electro-holographic systems based on a single acousto-optic modulator (AOM) with many parallel input channels and multiple AOMs aligned in parallel. A multi-view system based on combining two time multiplexed multi-view image channels spatially such that viewing regions of each channel is joined to each other without any overlapping [9].

7.2.3 Prototype Background

Three iterations of this display were built in the MUTED European Commission-funded project, with the results of the first used to inform the design of the second and third versions. The first three versions of the display use two 49-element arrays, one for the left eyes and one for the right eyes. A pattern of spots is projected on to the back of the arrays and these are converted into series of collimated beams that form exit pupils after passing through the LCD. An exit pupil is a region in the viewing field where either a left image or a right image is seen across the complete area of the screen.

The spot pattern is sparse and the proportion of the spot area in relation to the total projected area is in the region of 10%. For this reason a holographic projector was chosen for the first prototype as this uses the complete wavefront from a combined RGB laser beam and concentrates all of the energy into the bright regions. A mirror-image conjugate that cannot be used is also produced but the overall efficiency is still greater than for a conventional projector where the unwanted light is simply blocked. This system suffered from problems of projector stability and low power output [9] [80].

The laser projector used in the first two prototypes was replaced with a conventional LCOS projector to address the stability and brightness issues. The first display used a laser projector constructed on an optical breadboard and exhibited some mechanical instability. It was also found that the first LCD used had a sub-pixel structure that contained a horizontal bar that made it unsuitable for use with a lenticular MUX screen. A suitable LCD with clear sub-pixels was obtained to replace this.

The principal problems found with the first version of the first prototype were: low brightness, projector positional instability and banding in the image. In order to combat these problems the following improvements were carried out:

- The laser projector was constructed in a custom-built mechanically stable die-cast housing.
- Non-birefringent annealed BK7 glass replaced the Plexiglas elements of the original array.
- All optical components in critical path fabricated on non-birefringent substrates.
- A half wave plate was mounted at the projector output to match the linearly polarised projector output to the LCD polariser.
- The LCD panel was replaced with one having clear sub-pixel apertures.
- Improved design parabolic field mirror.
- Gaussian vertical diffuser on the front of the elements replaced with ‘top hat’ diffuser.
- Speckle reduction using an actuator at the array input.

Even with these improvements incorporated into the design of the second iteration the performance was relatively poor. The principal shortcoming of this display is the brightness that is only around 2 nits. This limitation, at least at the present time, is due to the necessity of the laser projector to be illuminated with single mode lasers; the power of these is limited to around 300mW. The display brightness was sufficient to enable useful evaluation to be carried out but insufficient for user trials. The head tracker performs well and demonstrates the viability of tracking more than one user.

In order to overcome the brightness constraints of the laser projector a third version of the display was built incorporating a conventional LCOS projector with a 2500 lumen projector. In this prototype the parabolic mirror is replaced with a Fresnel lens as it was determined that its faceted structure would not noticeably affect performance as was initially anticipated. Head tracking has not yet been applied to this prototype but the optical performance can be determined without this. The screen brightness of 25 nits enables it to be viewed under reasonably bright ambient lighting conditions. Results show this approach to be promising; for example the extreme letterbox shape of the image only utilises around 10% of the available image. A projector light engine designed specifically for this application could give screen brightness in the order of 250 nits.

When the MUTED project kicked-off in 2006 it was anticipated that LCDs would be sufficiently fast for 120Hz frame-sequential operation. Although fast response times were quoted by manufacturers at that time none were found to be suitable when response time

measurements were carried out. In 2009 true 120Hz displays became available. These make the MUTED principle of operation much more viable and simplifies the display hardware.

Three major changes are required to produce this prototype:

- The laser projector is replaced with a conventional 120Hz DMD projector.
- The conventional LCD operating with a lenticular MUX screen is replaced with a 120Hz Alienware AW2310 LCD in order for left and right images to be seen sequentially with full resolution.
- The double optical array is replaced with single optical array as the projector is capable of producing spot patterns for left and right eyes sequentially.

Head positions are determined using the multi-user head tracker whose capture camera array is shown in Fig. 7.6. This has been built by MUTED partner Fraunhofer HHI and is a development of the earlier single user ATTEST display tracker.

Figure 7.6 Head tracker camera array: Six cameras are employed to track users from 1000 to 3000 mm distance.

The multi-user tracking implementation is divided into fully automated initial face detection and subsequent feature tracking. The initial face detection is based on a decision cascade of Haar-basis functions [16]. By combining these simple functions it is possible to construct a classifier which is also able to discriminate classes with more complex distributions with sufficient accuracy.

After the initial face detection has been done specific facial feature points are detected by several image processing methods. After a set of facial features has been successfully detected the information is used to track these features in a computationally inexpensive and fast tracking process. The tracking is done by enhanced adaptive block matching methods. For that purpose tracking features (image elements around a facial feature with properties that make this element simple and reliable to track) for the specific facial feature are selected and tracked. The combination of the tracking results of these tracking features increases the accuracy of the facial feature up to sub-pixel accuracy. The use of

calibrated stereo camera pairs provides spatial position data with sufficient accuracy in all dimensions.

(a) Single User (b) Multiple Users

Figure 7.7: Head Tracker output: Overlaid rectangles show the positions of the detected head centre and eye positions.

Figure 7.7 shows camera images overlaid with squares indicating the detected positions of the eyes of a single user and for two users in a fragmented tracking area. One camera pair with short focal length is tracks persons in a near area and another camera pair with a longer focal length tracks persons in a more distant area.

7.2.4 Principle of Operation

The purpose of the display optics is to provide a backlight for a direct-view LCD that produces multiple exit pupils whose positions follow the viewers' eyes and are controlled by the output of a head tracker. The display optics includes a 120Hz View-Sonic PJD6381 stereo projector, a single 49-element array, an Alienware LCD screen and a head position tracker. These give the full multi-user capability with a large viewing field; the complete set-up is shown in Figure 7.8.

The hardware is simplified as only one optical array is required and a lenticular MUX screen is not necessary as left and right images can be presented sequentially. The images can be seen at full resolution, as opposed to being halved by the MUX screen in previous versions.

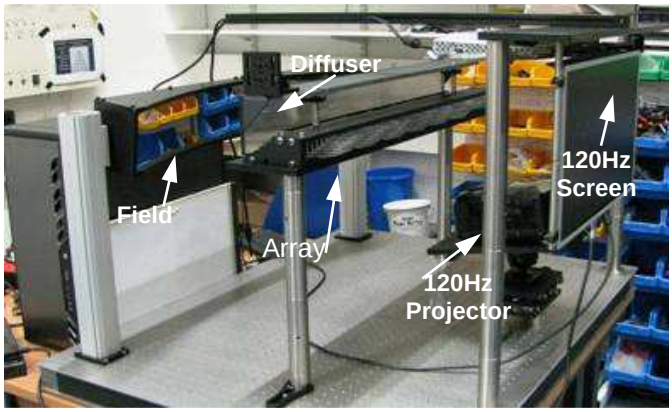

Figure 7.8 MUTED Prototype: This shows the principal components: 120 Hz DLP projector, 120 Hz LCD, field mirror, vertical diffuser and a single array.

Figure 7.9: Optical array Front & Back View: The array controls the light to the right and left exit pupils alternatively; it comprises 49 elements in a 'staircase' configuration.

The novel steering optical array consists of 49 elements as shown in Figure 7.9; this acts as viewing zone forming optics. Two different view images are required and each of these must be directed to its corresponding eye. The 120Hz Viewsonic projector is shown in Figure 7.10. The images produced by the projector are shown in the upper illustration Figure 7.11 and typical LCD images in the lower illustration.

Figure 7.10: ViewSonic 120Hz Conventional Projector: Provides a backlight for a direct-view LCD by producing a spot pattern controlled by the head tracker and MUTED optics.

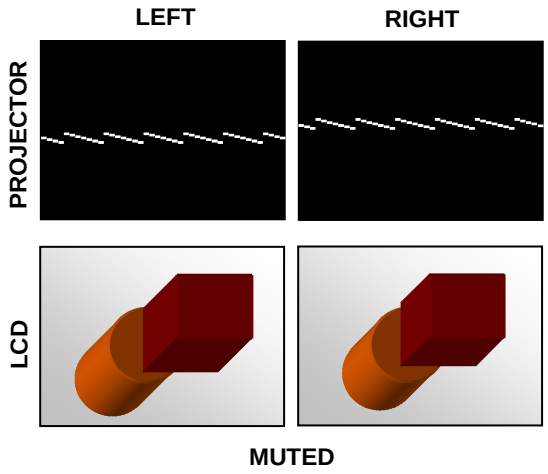

Figure 7.11: MUTED Images: The projector provides the exit pupil position information and the LCD provides the image.

A horizontal diffuser seen in Figure 7.8 is mounted behind the array; this allows narrow beams from the projector to spread out in order to form diverging beams within the elements. These are shaped into the collimated beams by the front array surfaces. Vertical diffusers are attached to the front surfaces of the array elements in order for the output to cover the full height of the screen.

7.2.5 Synchronisation Methods

In order to synchronise the projector and the LCD an NVIDIA Quadro FX4600 graphics card that has a dual head video card capable of supporting two 120Hz displays is used. Both heads of the card are locked together to release frames at the same time to both screens. This is used in conjunction with a G-Sync II card which allows external driving of the Vsync shown in Figure 7.12. If necessary, these can be over-clocked to run faster than 120Hz. Initially, in order to operate the projector and LCD in unison and to create the appearance of single display, the following two processes were performed using an Nvidia Control Panel and OpenGL extension; these are:

Frame Lock: - Synchronising the rendering of frames across projector and LCD; this involves the use of hardware to synchronise the frames on both displays in a connected system. When two separate applications are displayed across LCD/projector, frame locked system help maintain image continuity to create a virtual canvas.

Swap Sync: - Synchronising the swapping of front and back buffers; two separate applications running on LCD/projector can synchronise the application buffer swaps between them. Swap Sync, that uses OpenGL, always requires that both systems are frame locked.

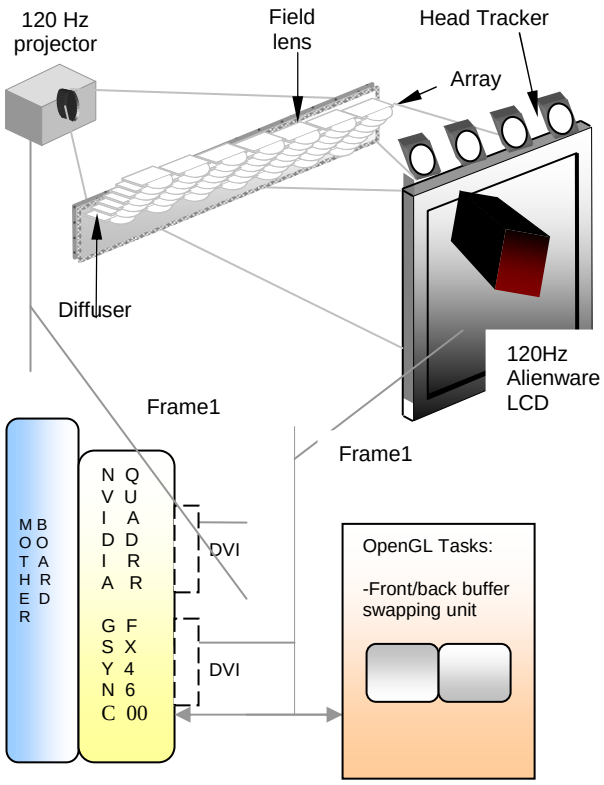

Figure 7.12: MUTED 120 Hz Prototype: The prototype incorporates: a 120Hz DLP stereo projector, a 120Hz LCD screen and an Nvidia Quadro & Gsync card for synchronisation. Only a single array is necessary, no lenticular MUX screen is needed and images are full resolution.

Difficulty was encountered in synchronising the LCD and projector using this approach as the Samsung LCD does not support custom resolution. Other projectors with resolutions close to that of the LCD were tried but also could not be synchronised as the process not only requires the refresh rates of the LCD and projector to be synchronised but also require horizontal pixel refresh rates and internal pixel clock of both devices to be synchronised. Adding blank pixels to each frame was also tried but this did not work either. The best match was obtained by creating custom resolution and adding some blank pixels to each frame of projector as follows:

DepthQ_projector:-	Samsung LCD:-
Refresh Rate = 119.997Hz	Refresh Rate = 119.997Hz
Horizontal Pixel Refresh Rate = 97.55Hz	Horizontal Pixel Refresh Rate = 97.55Hz
Pixel clock = 115.1208Hz	Pixel clock = 115.5000Hz

Due to the difference in pixel clock rate the frames start drifting after 30 minutes; attempting to match the pixel rate by adding some extra active blank pixels upsets the refresh rate of projector.

Another approach, called Genlock, could also be used for frame synchronisation. Nvidia boards can lock to an external pulse and synchronise the video formats to that pulse. Genlock is the process of synchronising the pixel scanning of one or more displays to an external synchronisation source. A Horita BSG-50 Sync pulse generator is used as an external sync source which produces synchronisation signals by adding slight delay of few microseconds in one application buffer to match it to the other application buffer. Once proper connection is established, buffer swapping (left/right images) is very easily achieved by using OpenGL extension. This allows the projector left-right light pattern to work in conjunction with the left-right image of the LCD and enables the alternate switching of light to one eye and then the other, while the display alternately in order to show the different perspectives for each eye.

It was found that Alienware display can also support custom resolution. In order to simplify the prototype hardware by avoiding the use of external sync pulse generator the Samsung LCD replaced with the Alienware LCD. By creating custom resolution and adding extra blank pixels into each frame of both projector and LCD, the following best match was obtained and two displays were synchronised very easily without the use of extra sync. pulse generator.

ViewSonic 120Hz projector:	Alienware AW2310 120Hz LCD:-
Refresh Rate = 119.997Hz	Refresh Rate = 119.997Hz
Horizontal Pixel Refresh Rate= 97.56Hz	Horizontal Pixels Refresh Rate= 97.56Hz
Pixel clock = 115.1208Hz	Pixel clock = 115.1208Hz

The use of the texture mapping technique is currently being investigated for use in OpenGL. This renders left/right camera images at 60Hz refresh rate that are then displayed on both the projector and the LCD. This is a graphic design process in which a 2D surface, called a texture map, is ‘wrapped around’ a 3D object. Thus the 3D object acquires a surface texture similar to that of the 2D surface.

7.2.6 Time MUX & Synchronisation Test of Projector & LCD

Simple tests have been carried out on an intact ViewSonic projector and an Alienware LCD to check the frame synchronisation and time multiplexing of projector and LCD by showing a white rectangle on a black background in the left half of the image in first frame and a white rectangle on the right in the second frame. The projector was full-screen red in the first frame red and green in the second frame. These images were displayed for all odd and even frames as explained in schematic diagram shown in Figure 7.13.

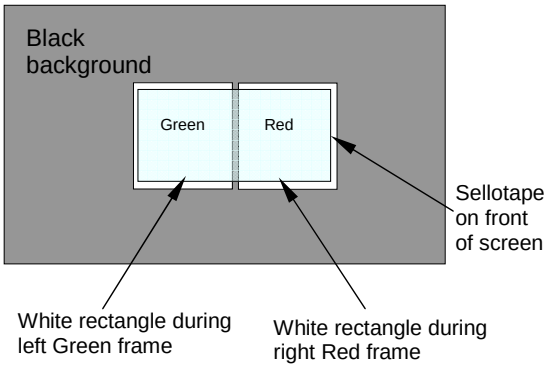

Figure 7.13: LCD & Projector Frames Synchronisation: Frames Green and Red are alternative frames of projector synchronised with alternating white rectangle images of LCD. Film attached to front surface to eliminate scattering from the anti glare surface.

7.2.7 Results

Currently this version does not incorporate head tracking but this can be implemented fairly easily as the spot patterns can be calculated in real time, as opposed to using the look-up tables employed with the laser projector prototype. Pictures of six camera head tracker and single and multiple user tracking deployed in the previous version can be seen in Figure 7.14. It can also accommodate more than one viewer and work on this is ongoing.

Figure 7.14: Head Tracker and Output: The top figure shows Head tracker camera array. Six cameras are employed to track users from 1000 to 3000 mm distance.The left picture shows detection of single user's eyes (smaller green rectangles) and the right picture, two users.

Multiple viewers can be supported by producing a spot pattern for each viewer. In the 120Hz version of the display a separate pattern of 49 spots is produced for each user. For example, if there are three viewers a pattern of 147 spots is produced for each image so that three exit pupils can be produced simultaneously. This pattern changes at 120Hz so

that left and right patterns are produced at a rate of 60Hz for each of the sets of left and right eye exit pupils. Each set of 49 spots can move independently to the others so that in this case three independently controllable exit pupils can be produced that follow the viewers' eye positions. The number of viewers that can be served is dependent on the head tracker but in principle the number of viewers that can be handled by the optics is limited to the number that can physically fit into the available viewing field.

Tests were conducted to check the sub-pixel structure; Figure 7.14 shows the clear sub-pixel aperture of the Alienware LCD panel used in this prototype. Images have been obtained on this display but these are currently fairly dim due to light losses from the projector output; the back of the array captures only a small proportion of the output as the majority of light is currently lost in the regions above and below the array. Future redesign of the light engine will rectify this.

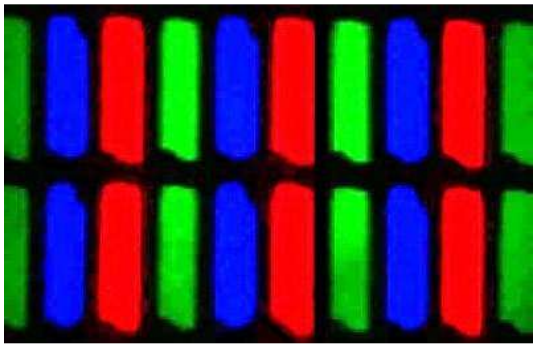

Figure 7.15: LCD sub-pixel structure: This shows clear sub-pixel structure of the Alienware LCD.

7.2.8 Future Development

The 3D display application area is very wide, this includes: virtual world presentations, advertising, education & entertainment, air traffic control, medical operations, telemarketing etc. In the near future these displays will be commercially available; it is anticipated that a display will be ready for commercialisation around four years time, this will be around the time other 3D displays will be available in the market and consumers will also be ready to discard wearing the glasses that are inconvenient in 3D television viewing situations.

The 120Hz prototype will be developed into a viable commercial product (Figure 7.16) by simplifying the display hardware and making it smaller. The projector is a stripped-down DMD light engine with the RGB colour wheel removed as only monochrome is required. As the backlight is essentially a projection system the prototype has a large volume between the array and the screen; this will be reduced to make the display 'hang-on-the-

wall' with the use of light piping where the horizontal angles emerging from the array output are preserved over the complete height of the screen as shown in Figure 7.17.

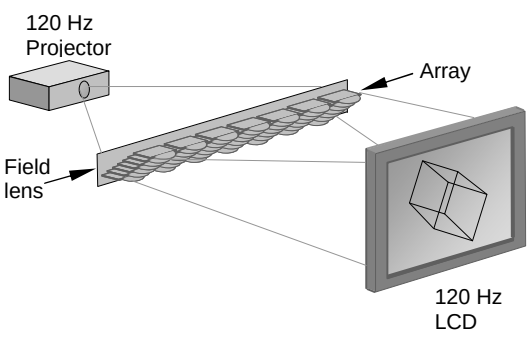

Figure 7.16: MUTED 120 Hz display: This version is simplified as it uses a field lens, a single array and has no spatial MUX screen. Full-resolution images are obtained by frame sequential temporal MUX.

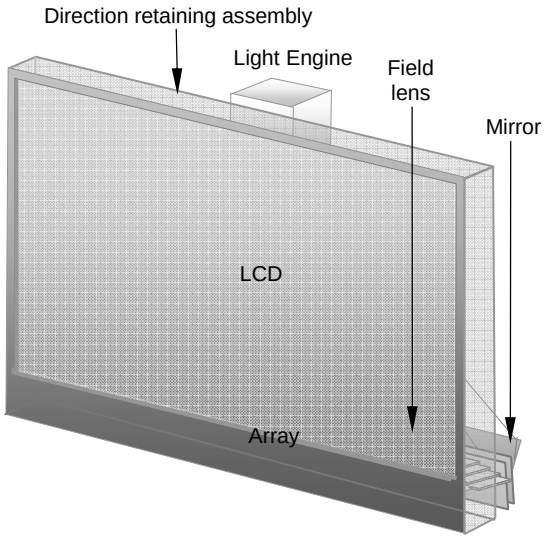

Figure 7.17: Folded MUTED Display: Method of folding with direction-retaining screen; in this case the array width is around that of the screen

The volume between the light engine output and the array input is small as its height is determined by the diameter of the light engine lens and the height of the array that is less than 30 millimetres. This can be readily compressed with the use of narrow folding mirrors. Methods of simplifying the optics, for example; the replacement of the original field mirror with a Fresnel lens and the use moulded plastic components with integral supporting spacers will also be incorporated.

7.3 Summary

The first non-laser projector version built uses a 2500 lumen 60Hz LCOS projector. Two optical arrays are still necessary as the patterns for the left and right exit pupils are produced simultaneously. As the light exiting the projector does not have a single polarisation angle and appears to be a combination of both linear and elliptical polarisation, the arrays incorporate Plexiglass optical elements. The construction is simplified by replacing the parabolic collimating mirror with a large Fresnel lens. The use of this component that has a periodic structure did not cause the detrimental fringing effects that were predicted originally. Unlike the laser projector prototype, the images on this version can be seen with ambient lighting on as its output is 25 nits. The crosstalk is quite high with 4.6% and 7.3% for the right and left channels respectively.

A 120Hz prototype incorporating a digital micromirror device (DMD) projector is under development and this offers the following advantages: hardware is simplified as only one optical array is required, no lenticular MUX screen is necessary and it has full resolution

as images are produced sequentially. The LCD is a panel from an Alienware AW2310 monitor and the projector is a Viewsonic 120Hz model.

The projector and LCD are synchronised using an NVIDIA Quadro FX4600 graphics card that has a dual head video card capable of supporting two 120Hz displays. Both heads of the card are locked together to release frames at the same time to both screens. External driving of the Vsync is achieved using a G-Sync II card. The projector and LCD are run in synchronism by the following two processes using an Nvidia Control Panel and OpenGL extension:

Frame Lock: - Synchronising the rendering of frames across projector and LCD. This involves the use of hardware to synchronise the frames on both displays in a connected system. When two separate applications are displayed across LCD/projector, a frame locked system is used to maintain image continuity to create a virtual canvas.

Swap Sync: - Synchronising the swapping of front and back buffers. Two separate applications running on LCD/projector can synchronise the application buffer swaps between them. Swap Sync, that uses OpenGL, always requires that both systems are frame locked.

CHAPTER 8

HELIUM3D PROTOTYPE

8.1 Preface

The first part of this chapter describes the principle of operation of the HELIUM3D display that has the potential to provide several users motion parallax (the ability to 'look-around' objects) and other interesting modes of operation if a fast light engine can be obtained that provides the images at a frame rate of 240Hz or more. As with the MUTED display, this also operates by providing exit pupils that follow the positions of the viewers' eyes under the control of a multi-user head tracker. The display is illuminated with an RGB laser illumination source whose output beam is scanned into the light engine. Light directions are controlled by a spatial light modulator and a front screen assembly incorporates a novel Gabor superlens. A 120Hz demonstrator that provides sequential left and right images to exit pupils is described.

8.2 Principle of Operation

Head tracked displays that operate on a different principle to HELIUM3D have been developed in the European MUTED project. In this case left and right images are produced on a direct-view LCD and the conventional backlight is replaced with steering optics that can produce multiple pairs of exit pupils that follow the positions of the viewers' eyes under the control of a multi-user head tracker.

The steering optics consists of arrays of optical elements that produce series of intersecting collimated beams at each eye position. Each beam is produced from a spot of light whose position is controlled in order to direct the output beam in the appropriate direction. Two arrays are required, one for producing the left exit pupils and one for the right exit pupils. The reason for this is that the left and right images are produced simultaneously on the LCD on alternate rows of pixels. Light from each of the arrays, which are positioned one above the other, is separated into the correct pixel rows by a horizontally aligned lenticular screen located behind the LCD.

Spatial MUX is used as when the project commenced in 2006 there was no LCD available to run at the 120Hz necessary for temporal multiplexing. The spot patterns are produced by an RGB laser projector. This has the advantage that the sparse spot pattern is

produced by light interference so that the complete wavefront is utilised and concentrated into the pattern; in a conventional projector the unwanted light is blocked.

The performance of the laser projector version was poor in terms of brightness and stability and for this reason a spatially multiplexed version has been built using a conventional LCOS projector. This gives a brighter image that can be viewed in reasonably high ambient light and there are no stability issues. Since 2009 120Hz LCDs have become available and a version incorporating a 120Hz LCD and digital light processor (DLP) projector is currently under construction. This version is capable of providing pull screen native resolution as opposed to the halved vertical resolution of the previous 60Hz versions. Also, only one steering array is required as the sets of left and right exit pupils are produced sequentially and the lenticular multiplexing screen is no longer necessary.

The HELIUM3D display operates by forming regions referred to as exit pupils where a particular image can be seen over the complete area of the screen. In this way a stereo image pair can be directed to each viewer. The display can operate in two modes; if a single image pair is formed the same pair can be directed to the left and right eyes of all uses. In this mode the display acts in a similar manner to a conventional glasses display, with the exception that the glasses are not necessary. Images are produced sequentially so that they must have a frame rate of 120Hz in order to eliminate flicker. Higher frame rates can enable more than one viewer to see their own dedicated images. For example a 240Hz frame rate allows four images to be presented every 1/60th second so that two viewers can see two separate image pairs; this would enable motion parallax and other interesting modes of operation to be obtained.

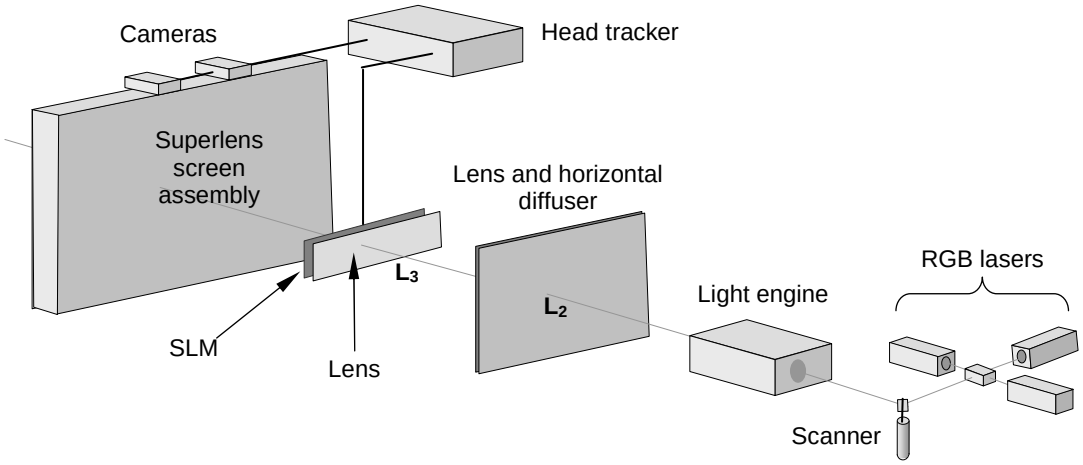

Figure 8.1: HELIUM3D Prototype Schematic Diagram: The projector is illuminated with a horizontally scanned white beam giving a scanned image column on L_2 that is transferred to the screen via L_3. Light directions are controlled by the SLM.

Figure 8.1 is a simplified schematic diagram of the display. It is essentially a projection display where images are formed in a light engine and transferred to a viewing screen via a relay lens system that contains an SLM. In the figure L_2 is a field lens that concentrates the light from the light engine projection lens (L_1) on to the second projection lens L_3. A horizontal diffuser spreads the real image of L_1 across the complete width of L_3. L_3 relays the image on L_2 on to the screen and is adjacent to a linear SLM. This SLM controls the light input to the screen but its image is not seen as it is in the Fourier transform plane of L_3. A real image of the SLM is produced in the viewing field and the images of the transmitting regions form the exit pupils.

The exit pupils are created dynamically; in MUTED the pupils are formed simultaneously so that the complete width of the screen is illuminated at any one time and in HELIUM3D the an image column scans the screen horizontally and the directions of the light emerging from the column controlled by an SLM as in Figure 8.2. This shows light being diverted to two viewers eyes by opening two transmitting apertures in the SLM.

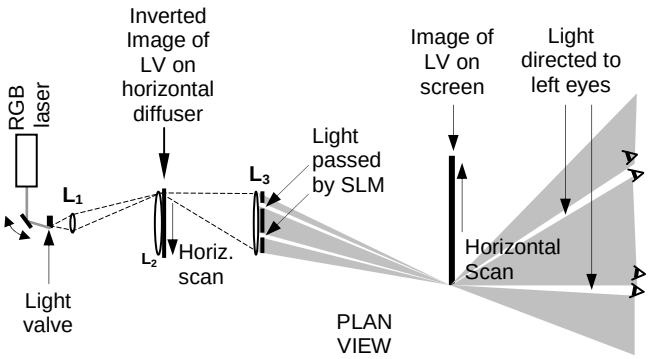

Figure 8.2: Exit pupils in the HELIUM3D display are formed by allowing light to pass through clear apertures in the SLM. These are effectively focused at the viewers' eyes by the screen.

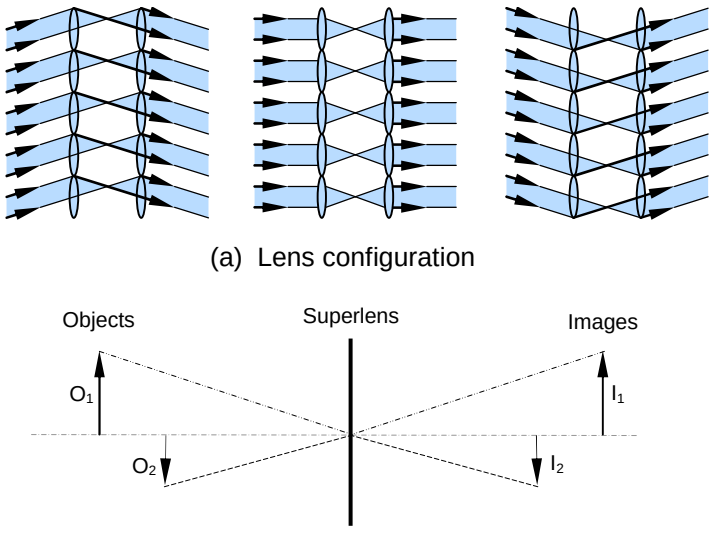

Figure 8.3: Gabor superlens: showing (a) the microlens configuration and ray paths and (b) the unique image formation properties.

The front screen assembly includes a Gabor superlens [27]. This is a type of lens invented by Denis Gabor in the 1940s that comprises two sets of microlens arrays as shown in Figure 8.3(a). This has different imaging properties to conventional lenses as input and output ray angles remain on one side of the normal to the lens surface and image distances become less as the object distance is reduced (Figure 8.3(b)).

The purpose of the superlens screen in the display is to effectively magnify and focus an image of the SLM into the viewing field so that this fills its complete width. Magnification is achieved with the use of a superlens having different focal lengths as in Figure 8.4 and located in between two collimating spherical lenses. Each superlens element acts as a telescope where the first lens acts as the 'objective 'and the final lens as the 'eyepiece'. In order to prevent light passing into adjacent elements a field lens is located in the focal plane of the 'objective'. The lens surfaces are only curved in one direction so that a complete lens array is a lenticular screen having vertically aligned lenses. Angular magnification takes place only in the horizontal direction and its value is equal to the ratio of the objective focal length to the eyepiece focal length.

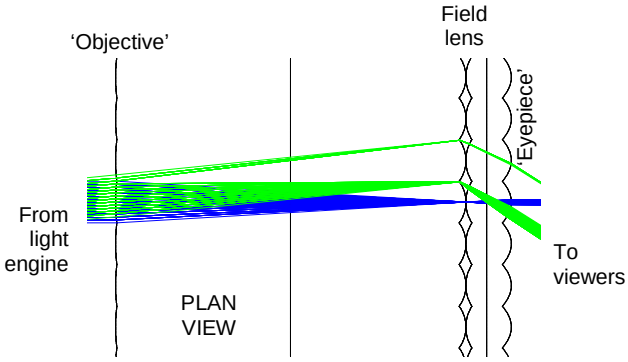

Figure 8.4 : x 6 Gabor superlens: showing ray paths through the 'objective', 'field lens' and 'eyepiece' equivalent lens layers. The angular magnification equals the 'objective' to 'eyepiece' focal length ratio.

With reference to Figure 8.3(b) it can be seen that the SLM will form a real image in the viewing field, the position of which will also be determined by the focal lengths of the collimating lenses in the screen assembly. The position of this image is referred to as the conjugate plane and when an eye is located in this plane the position of the transmitting region in the SLM does not change position over the duration of a scan. When however the eye is away from the conjugate plane the transmitting region must traverse the SLM during the scan with the distance traversed being proportional to the distance of the eye from the conjugate plane.

In figure 8.5 the case for an eye closer than the conjugate plane is shown. As the effective position of the source must be closer than the SLM in this case, a point C must be formed where the light always passes over the scan period. In order to achieve this it can be seen that the transmitting region in the SLM must move from point A to point B. If the eye is further than the conjugate plane the point C must lie behind the SLM so that it is a virtual intersection point.

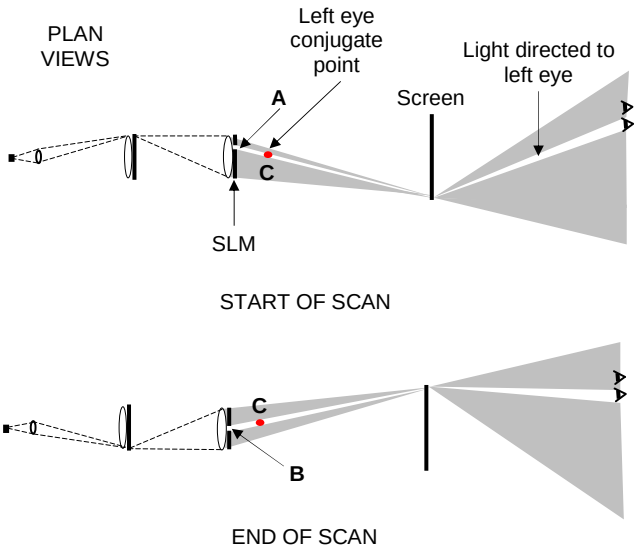

Figure 8.5 Dynamic Exit Pupil: Light to the left eye is transmitted by the SLM at region A at the start of the scan & region B at the end give virtual source at C, the conjugate point of the left eye.

Originally the intention was to use a linear diffractive light valve in the display as this is capable of running at a high frame rate and is designed to operate in the horizontally scanned image column mode with illumination from a laser source. Unfortunately these are not readily available now and the HELIUM3D prototype uses an analogue LCOS light engine with a scanned laser illumination source. A DLP light engine cannot be used as grey scale is obtained by pulse width modulation (PWM) and this requires a constant illumination on each pixel which scanned Illumination does not provide. The illumination beam is a vertical fan of rays from a combined RGB laser source that is concentrated into a narrow beam and scanned horizontally. The light engine produces a horizontally scanned image on L_2.

8.3 Temporal MUX Demonstrator

A setup that demonstrates temporal MUX has been constructed. This uses the images from a 120Hz projector to provide illuminated regions on a Fresnel lens/vertical diffuser (Figure 8.6) screen that can be focused into real images in the viewing field that are the exit pupils. This focusing is carried out by a Fresnel lens located adjacent to a 120Hz

LCD. The mirror shown in the figure is used to enable the complete display to be conveniently located on a bench and performs no other function.

The projector images are white rectangles on a black background that alternate in left and right positions at 120Hz thus enabling adjacent left and right exit pupils to be created at the viewer's eyes. Images are formed on the 120Hz LCD and the other components constitute its steerable backlight; moving the rectangles enables the exit pupils to move laterally at a fixed distance from the screen. Synchronisation between the projector and LCD is achieved by running them both from an Nvidia Quadro FX4600 graphics card. Although it is possible for users to observe 3D on this demonstrator this is not its primary purpose and 3D is only seen over a relatively small region of the screen due to lens aberrations.

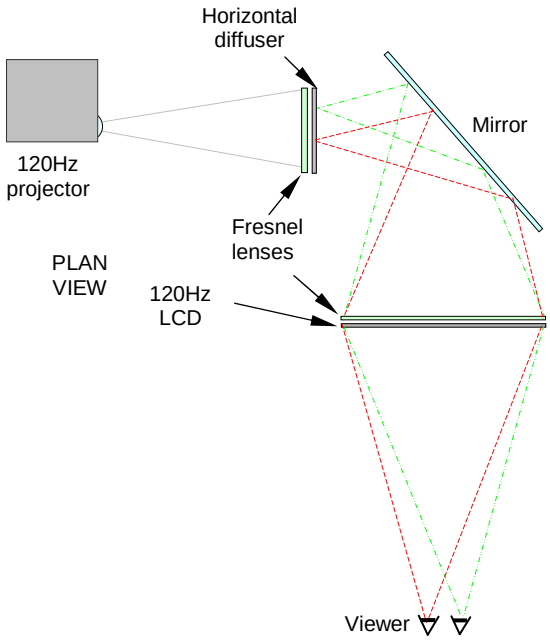

Figure 8.6: Temporal MUX demonstrator: White rectangles projected on to the vertical diffuser are focused by the front Fresnel lens on to the viewer's eyes.

8.4 120Hz Non-scanned Demonstrator

Two of the components for the planned first prototype, the light engine and the SLM, have proved difficult to obtain and in interim version of the display has been built using a 120Hz projector as the light engine and a 120Hz LCD as the SLM. The 120Hz projector does not enable more than two-image stereo to be seen and the 120Hz SLM does not allow dynamic exit pupil formation. Dynamic exit pupil formation provides the ability to steer exit pupils in the Z direction and this depends on both the light engine supplying a horizontally scanned image column and the SLM to effectively shift a transmitting aperture along the

SLM over the duration of a scan. The purpose of this prototype is to demonstrate the basic operating principles using passive optical components similar to those on the final versions.

The functions of lenses L_2 and L_3 are split into two lens-pairs, L_{2A}/L_{2B} and L_{3A}/L_{3B}, shown in Figure 8.7. These are off-the-shelf aspherical Fresnel lenses whose profiles are optimised for collimated light to pass between each pair and the plano-conjugates equal to the external conjugates of each pair; the focal length of L_{2A} is equal to the separation between L_{2A} and L_1, the focal lengths of L_{2B} and L_{3A} are equal and the focal lengths of L_{3B} and L_4 are equal. As L_2 is a field lens its performance is not particularly critical but L_3 is a projection lens and Fresnel lenses are not ideal for this purpose.

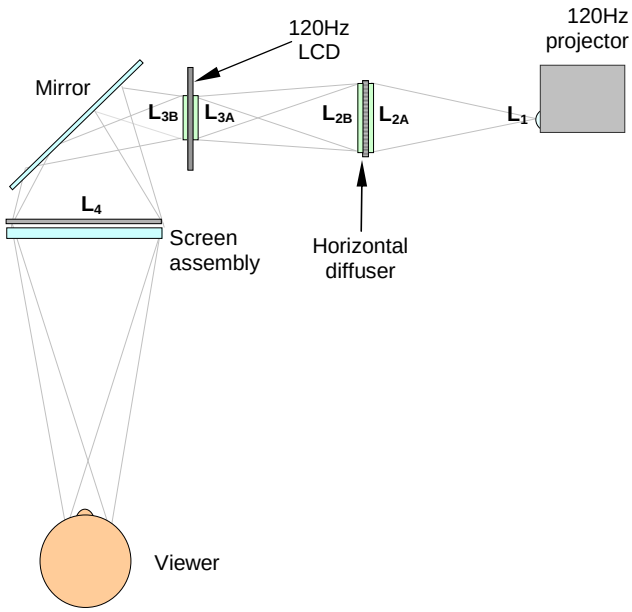

Figure 8.7: 120 Hz prototype: Images are provided by a non-scanned 120 Hz projector and the SLM is a 120 Hz LCD. Dynamic exit pupil formation is not possible.

The screen assembly comprises a x2 magnification superlens, a vertical diffuser and a one metre focal length field lens. The superlens is constructed from two off-the-shelf lenticular screens that have the same pitch and focal lengths but with a factor of two differences; this enabled low-cost units to be built. Synchronisation between the projector and LCD is carried out in the same way as in the temporal MUX demonstrator.

Simple images showing the letters L and R are shown in Figure 8.8. A traverse of the viewing field at one metre from the screen shows a sharp transition between the two exit pupil regions. As the screen comprises five layers scattering is reasonably high and this results in crosstalk which is in the order of 8%. Crosstalk can be observed in the figure where a ghost letter R can be seen superimposed on the letter L. Head tracking is not incorporated into this version and the viewing region is provided by a fixed exit pupil pair one metre from the screen.

Figure 8.8: Images in 129 Hz prototype: Ghosting can be seen as vestigial images in the opposite channels. The lines are reflections from the surface of the front Fresnel lens.

8.5 Temporal Performance of Canon Projector

Given the apparently poor temporal performance of the dismantled Canon light engine at UCL, tests have been carried out on an intact Canon SX7 projector at DMU. This is the 4000 lumen version of the 2500 lumen SX60 projector at UCL. It is fairly reasonable to assume that the LCOS devices have similar characteristics as they are both have SXGA+ resolution and therefore probably use the same LCOS devices. The effect of LCOS response times on image quality is assessed by producing sequential images on the projector and using a synchronised 120Hz Alienware OptXTM AW2310 3D monitor as effective shutter glasses as shown in Figure 8.9.

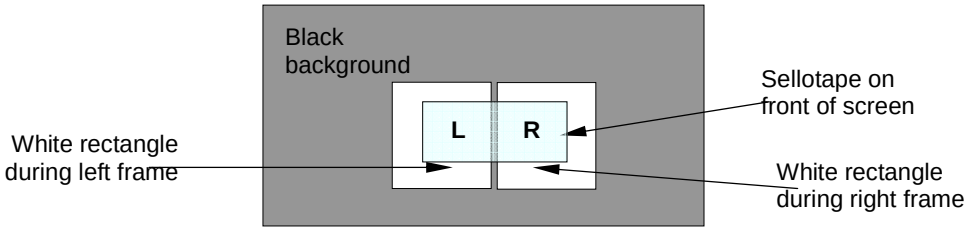

Figure 8.9: Use of LCD as Shutter Glasses: Regions L and R act as shutter glasses with alternating white rectangle images and film attached to front surface to eliminate scattering from the anti glare surface.

In Figure 8.10 the projected image on a screen is viewed through the LCD. The right side of the LCD passes light when the projector is showing a right image on a screen behind the LCD. When a left image is projected the left side of the LCD passes light. Simple images showing ‘L’ and ‘R’ can be shown to be separated by temporal MUX. In order to prevent the camera saturating a polariser orientated at 45º is placed in front of the screen. The projector is located just behind, and lower than, the LCD.

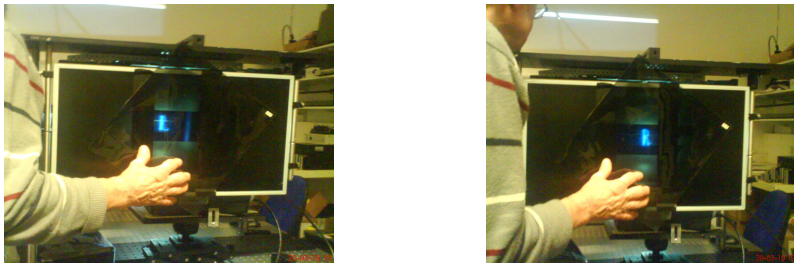

Figure 8.10: Setup: The letters L and R are projected sequentially at the same position on a screen located behind the LCD. A 45º polariser attenuates the light to prevent camera saturation. These pictures were taken from two different viewpoints to separate the images.

The photographs in figure 8.10 are taken with a frame rate of 60Hz. Figure 8.11 shows close-ups of the images of the letters.

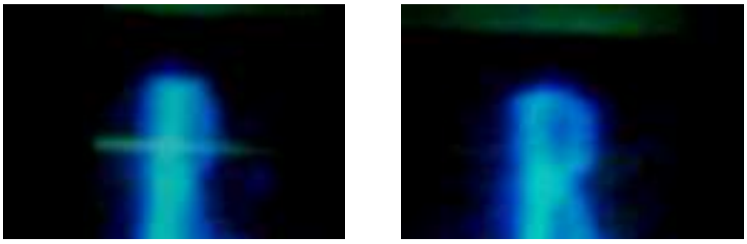

Figure 8.11: Close-ups of 60 Hz Images: These are close-ups of the letters L and R in Figure 2. Crosstalk from the right channel into the left channel appears to be greater than from the right to the left.

When the procedure is repeated for 75Hz the images of Figure 8.12 were obtained. These show a greater degree of crosstalk as might be expected given the effects of response time. It was not possible to run the LCD and projector above 75Hz.

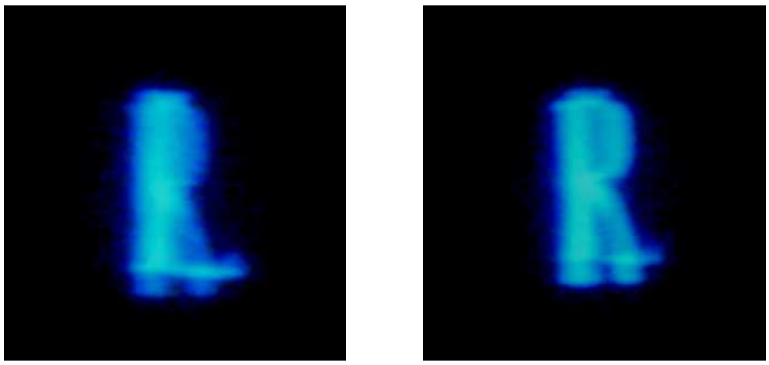

Figure 8.12: Close-u of 75 Hz Images: The crosstalk appears to be greater in this case with the left channel appearing to be virtually unusable; this to be verified by objective measurements.

The provisional conclusions from this initial study are as follows:

- The projector cannot be used at 75Hz due to very high crosstalk levels. This was verified by HELIUM3D partner UCL.
- The projector *could* be used at 60Hz (30Hz per eye). The images will exhibit flicker and high crosstalk levels but will be sufficient to demonstrate proof-of-principle of temporal MUX with a scanned light engine. If the images are comparable to those of Figure 8.12 this would suffice for the first prototype.
- Pursue the fast light engine approach and consider the use of some form of frame rate doubling in conjunction with this.

8.6 Summary

The first part of this chapter describes the principle of operation of the HELIUM3D display. This provides a background to the research carried out in this PhD and was pre-existing work. Like MUTED, the display provides multiple exit pupils that are steered to the positions of the viewers' eyes. In this case images are produced in a light engine and the system is effectively a rear projection display. Unlike a conventional display, the image is scanned by a vertical raster and exit pupils are built up in a dynamic manner (Figure 8.2). At any instant the light radiating from the column travels only in the directions of the selected eyes. In the stereoscopic mode, light is directed to the right during one scan and towards all the left eyes during the next scan.

Illumination is supplied from an RGB laser light engine. Lasers are not used for their coherence as the display does not employ interference. The low étendue source enables close control of light directions with the use of a horizontally aligned linear fast SLM. The image of the SLM is effectively focussed into pupils in the viewing field using a Gabor superlens front screen (Figure 8.3) that provides angular magnification.

Components for the final HELIUM3D display, in particular the SLM and the superlens screen, took longer than anticipated to be built and three lower performance demonstrators were built to show at the project Review Meeting.

The first demonstrator showed the principle of temporal MUX where left and right images are shown sequentially. In this, left and right images are produced sequentially on an Alienware 22" 120Hz LCD. Illumination is provided from a 120Hz Viewsonic projector that produces left and right rectangles on a black background (Figure 8.6). The rectangle shifts position at 120Hz so that two exit pupils are formed at the viewer's eyes by a Fresnel lens located adjacent to the LCD. Simple images showing the letters 'L' and 'R' were placed at the left and right exit pupil positions.

A second demonstrator was built that was a simplified version of the final display. In this case the output from the projector is not scanned and the fast SLM is replaced with a 120Hz LCD (Figure 8.7). This does not employ the novel dynamic pupil formation but showed a sufficient number of the display's features to present this at the Review Meeting. Again, 'L' and 'R' images were displayed.

It was planned that the first HELIUM3D prototype would incorporate a Canon LCOS projector and two of these were dismantled for use at DMU and at HELIUM3D partner Koc University. At first it was anticipated that the projectors would run faster than 60Hz, and this was tested visually at DMU by projecting an image on to a screen and viewing this through an LCD that was driven to effectively act as a pair of shutter glasses (Figure 8.9).

CHAPTER 9

SCANNED LIGHT ENGINE PROTOTYPE

9.1 Preface

A version of the display with a scanned light engine and x4 magnification superlens is currently under construction. A head tracker will be incorporated into this version to enable a single viewer. The layout is similar to Figure 8.7 but with an additional mirror, a beam expander and a cylindrical convex lens. The light engine consists of red, green and blue lasers that are combined into a white beam by an X-cube (Figure 9.1 left). The width of this beam is increased by a x10 beam expander and converted to a 200 micron wide scanned illumination line by a cylindrical convex lens with a vertical axis and a mirror scanner (Figure 9.1 right).

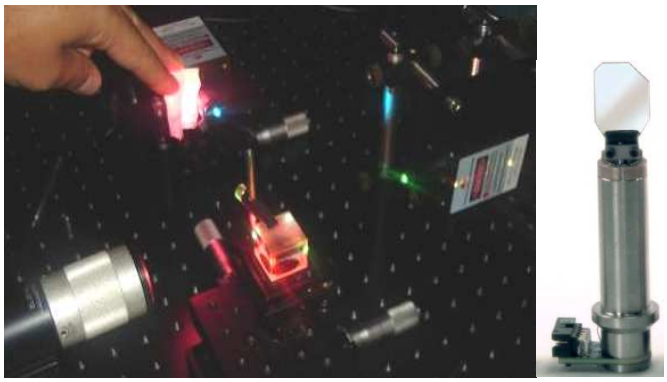

Figure 9.1: RGB Laser source and scanner: The outputs of three lasers are combined with an X-cube (left) and scanned by a rotating mirror (right).

The light engine is taken from a Canon 3 LCOS projector that has been dismantled and the lamp removed in order to allow the scanned laser beam to enter. Within the engine, the white beam is split into the three component primary colours by an X-cube and a separate LCOS device controls each channel. The images are then recombined by another X-cube. Although the combination of the lasers with one external X-cube and its splitting with another appears to be unnecessary, it is simpler to do this as the light engine with its precise alignment can remain undisturbed.

The 120Hz LCD is used in this prototype as well with the synchronisation carried out in the same way as the other versions. The superlens design was optimised after extensive modelling. Ideally the angular magnification would be very high, however diffraction limits

this and it was determined that a value of four is sufficient as this requires an SLM of a length that can be manufactured fairly easily. Good collimation of the output beam is required in order to keep crosstalk to a reasonable level and a value of 0.2º is obtained with the use of four refracting surfaces where each surface is acylindrical. As the diamond tooling required for producing the master from which the sheets are made is expensive, the two field lens components have the same profile. Aligning the four lens layers is fairly difficult and a technique using a diverging laser beam has been developed.

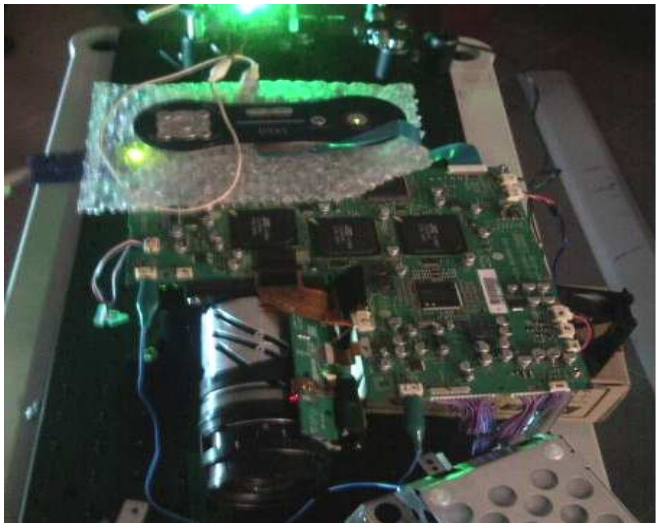

Figure 9.2: Light engine: This is a 3-channel LCOS unit from a Canon X60 projector. The lamp unit is removed to allow input from the scanned laser source.

9.2 60Hz Canon Light Engine

In the extract from the data sheet (Figure 9.3) for the Canon SX60 projector the vertical scanning frequency is given as 50–100Hz. Although the projector can accept frames up to 100Hz this does not necessarily mean that the LCOS devices can run at this rate and perform properly in the HELIUM3D light engine. In normal operation slow device response will produce motion blur; in HELIUM3D slow response will cause the residual image from one channel to be seen in the other channel. This will cause crosstalk in a similar manner to that produced by phosphor decay times in earlier shutter glasses CRT systems.

Input Signals	Analog PC Input	UXGA/SXGA+/WXGA/SXGA/XGA/SVGA/VGA	
	Digital PC Input	SXGA+/WXGA/SXGA/XGA SVGA/VGA	XGA/SVGA/VGA
	Scanning Frequency	H:15 - 100 kHz, V: 50 - 100 Hz, Dot clock: 170 MHz	
	Video/S-Video Input	NTSC/PAL/SECAM/NTSC4.43/PAL-M/PAL-N	
	Component Input	1080i/1035i/720p/575p/480p/575i/480i	
	Digital Video Input	1080i/1035i/720p/575p/480p	

Figure 9.3: Extract from Canon Data Sheet: The vertical frequency is given as 50 – 100Hz in the Data Sheet; this does not necessarily mean that it can perform satisfactorily at 100 Hz in the HELIUM3D light engine.

At the response of the light engine was determined by supplying alternate white and black frames at 60Hz. A red laser was passed through the engine and the output measured with a photodetector. The upper plot in Figure 9.4 shows that the white frames are only completely addressed for a small proportion of the period T. The lower timing diagrams show a possible means of dealing with this problem. As the lasers cannot be modulated the beam must not fall on the LCOS active areas during the addressing time; with this scheme the reflected beam will be beyond one end or the other in this time. The unavoidable disadvantage with this is the reduced duty cycle as shown in the lower plot.

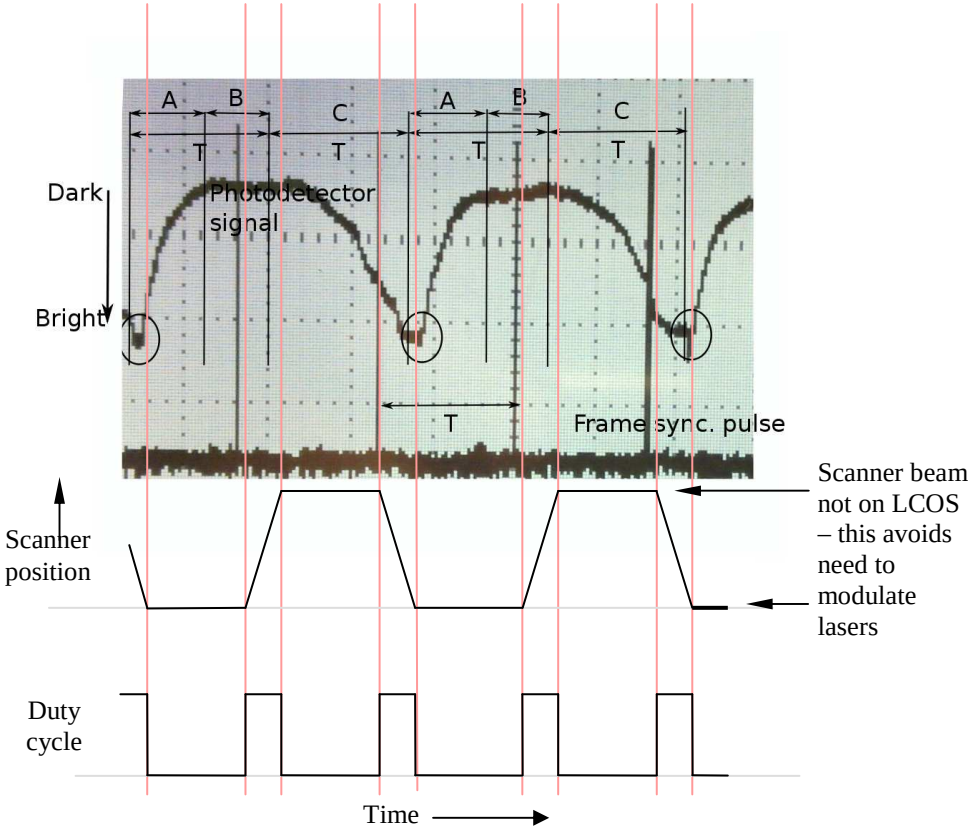

Figure 9.4: Canon Light Engine Response and Possible Fix: The upper plot shows the light throughput of alternate black and white images at 60 Hz. The lower plots show a means of not illuminating during addressing time but with unmodulated lasers.

- Given the poor measured performance of the dismantled Canon light engine and the fact that this might not be the worst-case, tests were carried out on an intact Canon SX7 projector at DMU. This is the 4000 lumen version of the 2500 lumen SX60 projector that was tested at UCL. It is fairly reasonable to assume that the LCOS devices have similar characteristics as they are both have SXGA+ resolution (1400 x 1050) and therefore probably use the same LCOS devices. The effect of

LCOS response times on image quality is assessed by producing sequential images on the projector and using a synchronised 120Hz Alienware OptXTM AW2310 3D monitor as effective shutter glasses. Actual images are used and an assessment of performance was made by examination of photographs of these.

- The provisional conclusions from this initial study are as follows:
- The projector cannot be used at 75Hz due to very high crosstalk levels. This can be verified by objective measurements made at UCL [95] (note that this paper covers all the work carried out by UCL that is referred to in this thesis.
- The projector *could* be used at 60Hz (30Hz per eye). The images will exhibit flicker and high crosstalk levels but will be sufficient to demonstrate proof-of-principle of temporal MUX with a scanned light engine.
- It is not worth applying the proposed frame rate doubling configuration to this projection engine as it would still not be possible to achieve the minimum 200Hz necessary for two user-multi modal operations.
- It was not possible to run the projector at 30Hz in order to determine whether frame rate doubling could be used to obtain good 60Hz operation. However even if this was a possibility its use could not be justified as a single light engine might well be available that could do this.
- Pursue the fast light engine approach and consider the use of frame rate doubling in conjunction with this.

9.3 120Hz DepthQ Projector

The first version of this prototype incorporating a 120Hz DepthQ DLP projector as the light engine and a 120Hz Alienware OptXTM AW2310 3D monitor as the SLM has been built at DMU (Figure 9.5). Lenses L_{2A} and L_{2B} have a combined focal length of 250 millimetres and focus the image of the projector into a horizontal line with the use of a horizontal diffuser mounted between them. This line is focused on to the LCD where white rectangles on a black background are formed into real images in the viewing field by the x2 magnification superlens screen; these are the exit pupils. The image on the horizontal diffuser is projected on to the screen assembly by the lenses $L3_A$ and $L3_B$ that are

attached to the LCD surface. Pupil steering in the Z direction is not possible and the X positions are held in fixed positions at this stage.

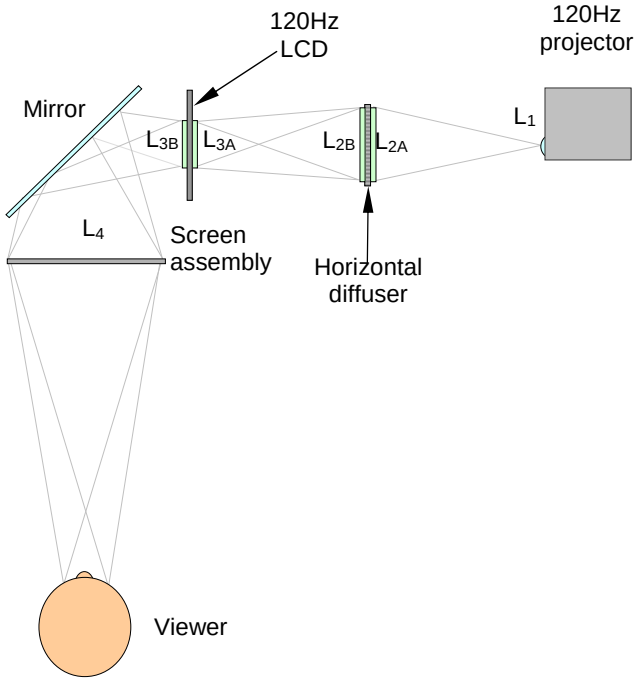

Figure 9.5: HELIUM3D Prototype: Plan of first version using a 120 Hz DLP projector as a light engine and a 120Hz LCD as an SLM; this only allows lateral viewer mobility.

9.4 SLM: 120Hz LCD

It is necessary to synchronise the images on the projector and LCD in order for this system to work. The two devices are driven by an Nvidia Quadro FX4600 graphics card (Figure 9.6). The 120Hz development of the MUTED display also requires a 120Hz LCD and 120Hz projector to be synchronised. In this case the projector is a ViewSonic high throw-angle projector but the same technique using the same Nvidia graphics card is used. This is useful as the development work on synchronisation has been applicable to both displays. In the MUTED display a spot pattern that controls the exit pupil positions is produced by the projector and converted into exit pupils produced by intersecting collimated beams. These pass through the LCD that displays the stereo image pair sequentially.

The spot pattern and stereo pair are shown in the left four figures in Figure 9.7. The HELIUM3D prototype operates in the opposite manner by displaying the stereo pair on the projector and the rectangles on the LCD (the exit pupil control component) as depicted in the figures on the right side of Figure 9.7. The synchronous operation of the projector is demonstrated by illuminating the LCD with alternate red and green frames from the

projector. The LCD displays alternate images that show a white rectangle that is on the left of centre when the projector displays red and on the right when the projector displays green. Figure 9.8 is the appearance of the screen; note that the red and green rectangles in the photograph are seen reflected in the folding mirror.

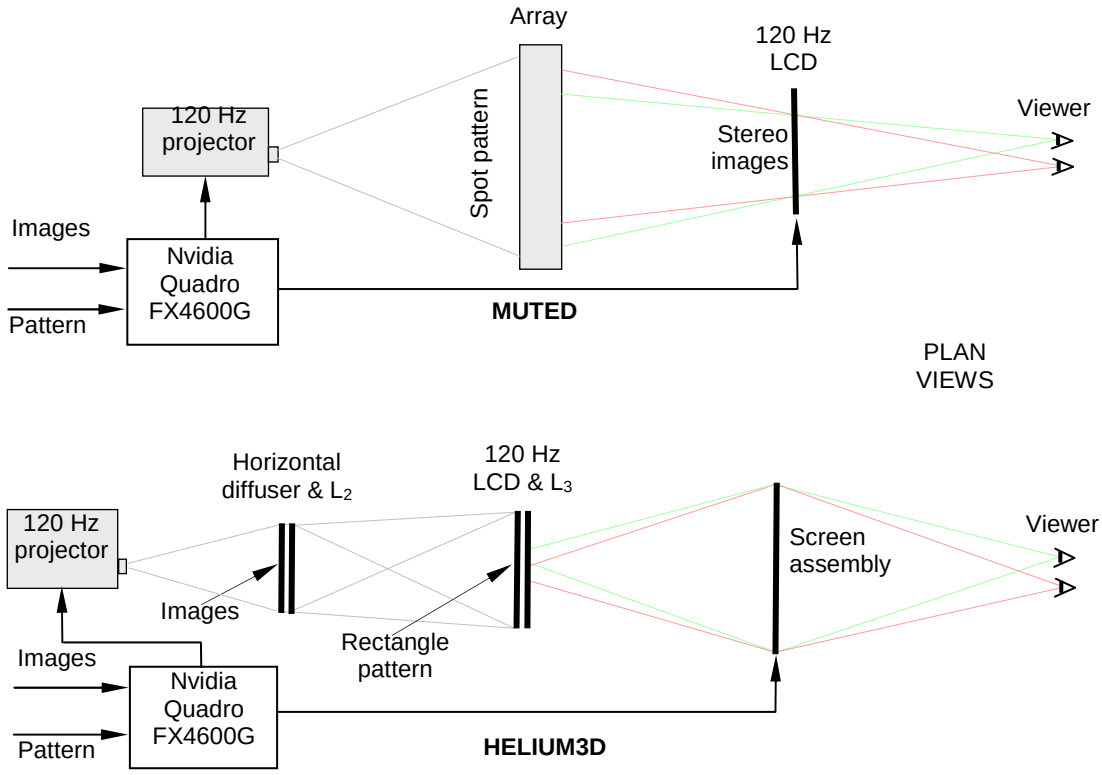

Figure 9.6: MUTED/HELIUM3D Common Components: Using a 120 Hz projector and 120 Hz LCD in the first HELIUM3D prototype enables the use of common components and drivers.

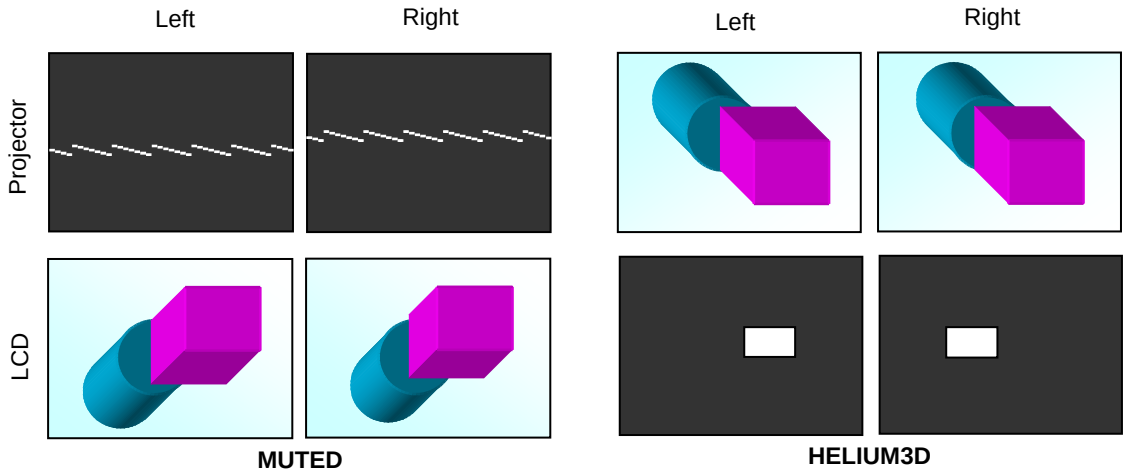

Figure 9.7: MUTED/HELIUM3D Images: In MUTED the projector provides the exit pupil position information and the LCD the image. In HELIUM3D the LCD controls the directions in which the projector images are directed.

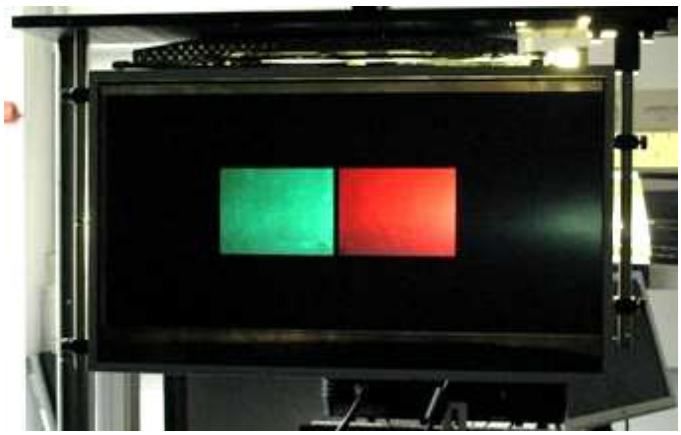

Figure 9.8: Temporal MUX: The projector displays alternate complete green and red frames and the LCD displays white rectangle on right and left side alternately.

- In order to synchronise a 120Hz projector to a 120Hz LCD an Nvidia Quadro FX4600G graphics card that has a dual head video card capable of supporting two 120Hz displays is used. Both heads of the card are locked together to release frames at the same time to both screens, one for each Alienware/projector is used in conjunction with G-Sync II card which allows external driving of the Vsync shown In Figure 9.9. They can be over-clocked to go higher than 120Hz.
- Initially, in order to operate the projector and LCD in unison and to create the appearance of single display the following two processes were performed using an Nvidia Control Panel and OpenGL extension:
- Two methods of performing synchronisation were investigated:
    - Frame Lock: - Synchronising the rendering of frames across projector and LCD: this involves the use of hardware to synchronise the frames on both displays in a connected system. When two separate applications are displayed across LCD/projector the frame-locked system helps maintain image continuity to create a virtual canvas.
    - Swap Sync: - Synchronising the swapping of front and back buffers, which means two separate applications running on LCD/projector, can synchronise the application buffer swaps between them. Swap Sync, that uses OpenGL, always requires that both systems are frame locked.
- Difficulty was encountered in synchronising the LCD and projector using this approach as the original Samsung 120Hz LCD used does not support custom

resolution. Other projectors with resolutions close to that of the LCD were tried but did not work as the process not only requires the refresh rates of the LCD and projector to be synchronised but also require horizontal pixel refresh rates and internal pixel clock of both devices to be synchronised; for that purpose adding some blank pixels to each frame was also tried but that also did not work. The best match, obtained by creating custom resolution and adding some blank pixels to each frame of projector is as follows:

- DepthQ projector:-

Refresh Rate = 119.997Hz

Timing Horizontal Pixels Refresh Rate = 97.55Hz

Pixel clock = 115.1208Hz

Samsung LCD:-

Refresh Rate = 119.997Hz

Timing Horizontal Pixels-
Refresh Rate = 97.55Hz

Pixel clock = 115.5000Hz

Due to difference in pixel clock rate the frames start drifting after 30 minutes; attempting to match the pixel rate by adding some extra active blank pixels upsets the refresh rate of projector.

Another approach called Genlock could also be used for frame synchronisation. Nvidia boards are able to lock to an external pulse and synchronise the video formats to that pulse. Genlock is the process of synchronising the pixel scanning of one or more displays to an external synchronisation source. A Horita BSG-50 Sync pulse generator can be used as an external sync source which produces synchronisation signals by adding slight delay of few microseconds in one application buffer to match it to the other application buffer. Once proper connection is established, buffer swapping (left/right images) is very easily achieved by using OpenGL extension. This allows the projector left-right light pattern to work in synchronism with the left-right images on the LCD. This enables the alternate switching of light to one eye and then the other controlled by the LCD while the projector alternately shows the different perspectives for each eye.

It was found that the Alienware AW2310120Hz LCD monitor can also support custom resolution. In order to simplify the prototype hardware by avoiding the use of external sync pulse generator the Samsung LCD was replaced with an Alienware AW2310 LCD. By creating custom resolution and adding extra blank pixels into each frame of both projector and LCD the following best match was obtained and two displays were synchronised very easily without the use of an extra sync. pulse generator.

ViewSonic 120Hz projector:-

Refresh Rate = 119.997Hz

Alienware AW2310 120Hz LCD:-

Refresh Rate = 119.997Hz

Timing Horizontal Pixels Refresh Rate = 97.56Hz

Pixel clock = 115.1208Hz

Timing Horizontal Pixels Refresh Rate = 97.56Hz

Pixel clock = 115.1208Hz

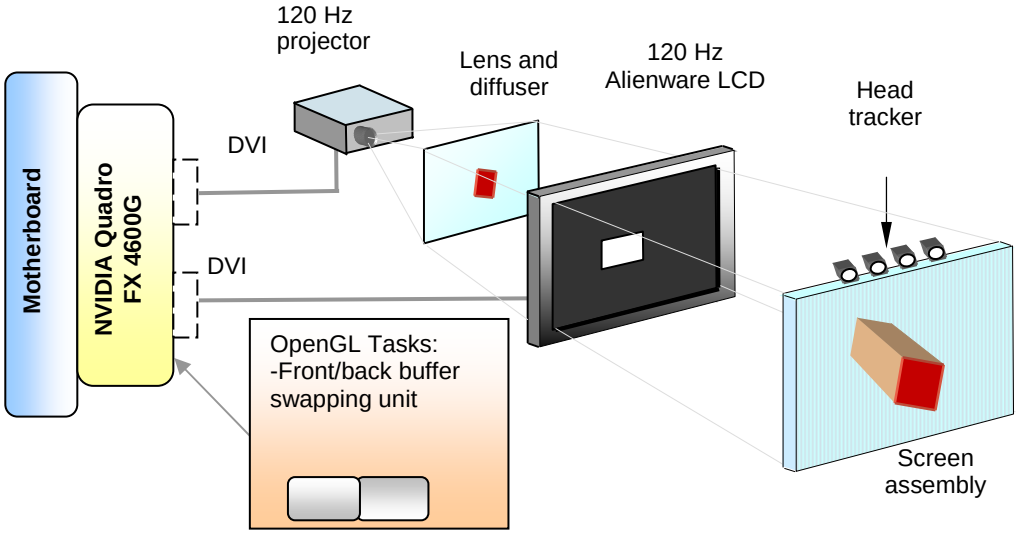

Figure 9.9: 120 Hz Prototype : The prototype incorporates a: 120Hz ViewSonic digital light processor (DLP) stereo projector, 120Hz Alienware Optx AW2310 LCD screen, Nvidia Quadro & Gsync card for synchronisation, lens/diffuser assembly and superlens screen assembly.

The synchronisation is checked by presenting white rectangles on a black background in two different lateral positions on alternate LCD frames as shown in Figure 9.10 which is a front view of the LCD. Complete red and complete green images are displayed on the projector whilst the right and the left rectangles respectively are displayed on the LCD. When synchronisation is achieved a stable red and green pattern is obtained as shown in Figure 9.8. Although the projector is capable of fast switching between images this is not the case for the LCD. This creates the appearance of a transition region on the LCD if the image from the projector changes whilst that region is being addressed. As only the central region of the LCD is being used in the SLM mode the transition regions are above and below the transmitting area and therefore have no effect on its operation.

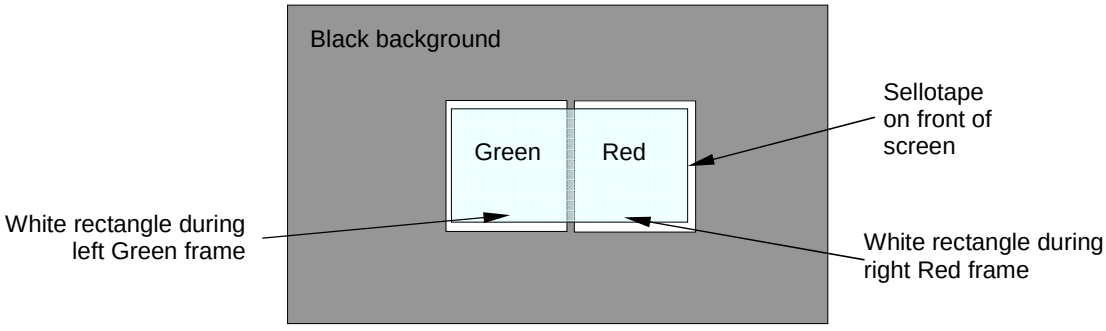

Figure 9.10: LCD & Projector Frame Synchronisation: This is tested by showing left and right rectangles on a black background on the LCD and synchronising this with alternate red/green projector images. Anti-scattering Sellotape layer is applied to front of LCD.

System Requirements:

Windows Vista Professional

Quadro FX4600 graphics card

Gsync card

Frame Lock (with Swap Sync)

Proper synchronisation of applications running on multiple displays involves the following two processes:

Frame lock involves the use of hardware to synchronise the frames on each display (LCD/projector) in a connected system. When an application is displayed across multiple monitors, frame locked systems help maintain image continuity to create a virtual canvas. Frame lock is especially critical for stereo viewing, where the left and right fields must be in sync across all displays.

Swap sync. refers to the synchronisation of buffer swaps of multiple application windows. By means of swap sync, applications running on multiple systems can synchronise the application buffer swaps between all the systems. Swap sync requires that the systems are frame locked.

The following are the basic steps to frame locking LCD & projector using the new Nvidia control panel. Detailed instructions follow this:

Set up the hardware Using first approach, synchronisation of projector and LCD can be achieved by connecting the both systems using standard CAT5 patch cabling. Two QuadroFX series cards are required for that purpose to bring identical systems into a network. As the voltage and signal on the frame lock ports are different from Ethernet signals a Frame lock port must not be connected to an Ethernet card or network hub otherwise damage could be caused to hardware.

9.5 Summary

The first part of the chapter describes some work carried out by partners Koc University and UCL. The light engine is a projector that must provide a horizontally scanned image 500 millimetres in front of its lens. The illumination source comprises red, green and blue 300mW lasers whose outputs are combined with an X-cube (Figure 9.1). The emergent white beam is expanded with a x10 beam expander and this is focussed into a narrow vertical line with a cylindrical lens. This line illumination passes to the projection engine via a scanner (Figure 9.1). The engine is from a disassembled Canon projector and contains a beam splitter, three LCOS cells, a beam combiner and a lens. The response time of the engine was measured at UCL (Figure 9.4).

Work on synchronisation that would apply to both the MUTED and HELIUM3D projects is described. When the projector and LCD are running synchronously in the MUTED application the illumination spot pattern is produced by the projector and this is the backlight for the LCD via the optical array. In HELIUM3D the LCD acts as the SLM to control the light directions and images are generated in the projector.

Difficulty was encountered in synchronising the LCD and projector using the approach described in Chapter 7 as the original Samsung 120Hz LCD used does not support custom resolution. The process not only requires the refresh rates of the LCD and projector to be synchronised but also requires horizontal pixel refresh rates and internal pixel clock of both devices to be synchronised. For that purpose adding some blank pixels to each frame was also tried but that also did not work. The best match was obtained by creating custom resolution and adding some blank pixels to each frame of the projector.

The frame synchronisation was tested by showing a white rectangle on a black background in the left half of the image in the first frame, and a white rectangle on the right in the second frame on the LCD. The LCD was illuminated by the projector that showed full-screen red in the first frame and full screen green in the second frame. Static red and green colour appearing on the rectangles on the LCD indicated that the two devices were running in synchrony.

CHAPTER 10

DISPLAY MEASUREMENT

10.1 Preface

The principal goal of this chapter is to describe and characterise the displays at DMU. The main aim of this chapter is to:

- **List display devices:** There are eleven devices in total and Section 1 lists these with their specifications.
- **Provide results of tests:** The results of these tests are given and these can be used as a benchmark with which to compare the results of the HELIUM3D evaluations.
- **Discuss results**

Due to the nature of the HELIUM3D display that operates on an entirely different principle to the displays under test and to the added capabilities such as gesture recognition, only a certain range of HELIUM3Ds parameters can be covered in this chapter.

10.2 Relevant Objective Measurements

The parameters considered in this chapter are crosstalk and brightness; brightness variation across the screen area (known as mura) only appears to be a problem in the MUTED prototype and this is an area of ongoing research. None of the displays are illuminated by lasers and therefore do not exhibit speckle. Table 10.1 shows the objective measurements made on the eight suitable displays that are relevant to HELIUM3D.

Crosstalk is defined as the amount of unwanted image that is visible to the wrong eye is due to:

- The system crosstalk: This is a measure of the optical performance for a stereo system and is independent of the contrast of the individual images.
- The viewer crosstalk: This is defined as the ratio of luminance of the ‘wrong’ image to the luminance of the ‘correct’ image as seen by the observer. It will be a function of the image contrast and the disparity.

	Display	Parameter			
		Brightness	Crosstalk	Speckle	Tracker performance
Autostereoscopic	Philips 42" Wow	Measured	N/A	N/A	N/A
	FHG Free2C	Measured	Measured	N/A	Measured
	DMU lenticular	Measured	Measured	N/A	N/A
	MUTED	Measured	Measured	N/A	Measured
Glasses	Planar PL2010-BK	Measured	Measured	N/A	N/A
	Anaglyph	Not measured as dependent on display device	Depends on glasses and screen parameters	N/A	N/A
	DepthQ WXGA projector	Not measured as dependent on screen distance	Measured	N/A	N/A
	Nvidia sequential	Measured	Measured	N/A	N/A

Table 10.1: Objective Measurements made in D3.3

10.3 Available Devices

This section describes the displays that are in the Imaging and Research Group's demonstration area at DMU where there are eight 3D displays that have been purchased and prototypes that were developed by DMU in the ATTEST and MUTED projects. Out of these displays, two are not included in this report: the performance of the ATTEST display is relatively poor and not really suitable to be used for meaningful comparison purposes.

Table 10.2 lists all the available displays along with their descriptions and known parameters. With the MUTED display the tracker is used in conjunction with the laser projector version of the display. The performance is not sufficiently good to be used for evaluation purposes although it is sufficient to demonstrate the multi-user tracking capability. Display performance was measured on a version of this display that incorporates a conventional LCOS projector.

			Display specification					
	Display	Technology	Number of users	Frame rate (Hz)	Resolution		Screen size	Viewing distance (mm)
					Native	Per view		
Autostereoscopic	**ATTEST prototype**	Fresnel lens and spatial MUX LCD	1	60	1600 x 1200	1600 x 600	21.3" 3:4	1000
	Philips 20" multi-view	Slanted lenticular	Several	60	1600 x 1200	649 x 360	20.1 3:4	800
	Philips 42" Wow	Slanted lenticular	Several	60	1920 x 1080	640 x 360	42" 16:9	3000
	FHG Free2C	Head tracked lenticular	1	60	1600 x 1200 (portrait)	1600 x 600	21.3" 3:4	450 – 1100
	DMU lenticular	Lenticular	1	60	1600 x 1200 (portrait)	1600 x 600	21.3" 3:4	800
	MUTED	Optical array backlight	1	60	1280 x 1024	1280 x 512	19" 4:3	1000
		Non-intrusive multi-user head tracker	4	60	1280 x 1024	1280 x 512	19" 4:3	1000 – 2500
Glasses	**Planar PL2010-BK**	Passive polarised glasses	Several	60	1600 x 1200	1600 x 1200	20" 4:3	Variable
	Anaglyph	Colour filter glasses	Several	Depends on device	1280 x 1024	1280 x 1024	19" 4:3	Variable
	DepthQ WXGA projector	Active shutter glasses	Several	1/2 x 120 (frame seq.)	1280 x 720	1280 x 720	Variable 16:9	Variable
	Nvidia sequential	Active shutter glasses	Several	1/2 x 120 (frame seq.)	1680 x 1050	1680 x 1050	22" 16:9	Variable

Table 10.2: Display Specifications

10.4 Test Regimes

The Planar, DepthQ 120Hz projector and Nvidia shuttered glasses displays were measured with a stationary power meter detector and the MUTED display with the detector attached to a translation stage mounted parallel to the screen. Barco performed measurements on the Free2C display with an Eldim 3D display analyser and the DMU lenticular display was measured with a Spectroradiometer. Crosstalk and ghosting results for anaglyph and the Philips Wow displays are obtained from previously published papers on their performance.

10.4.1 Free Space – MUTED LCOS Projector Prototype

Crosstalk was determined by displaying a white image on the left frame and a black image on the right frame. The exit pupil profile was measured at 10 millimetre intervals across the field 1000 millimetres from the screen with the power meter detector mounted on a translation stage (Figure 10.1). The process was then repeated with a white image on the right frame and a black image on the left frame.

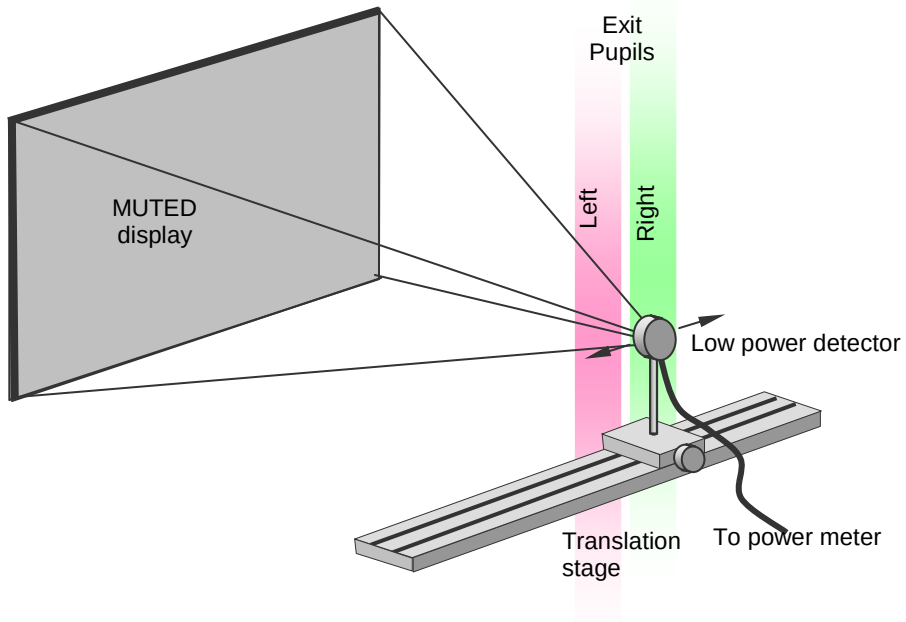

Figure 10.1: MUTED Exit Pupil Profile Measurement: The power meter detector traverses the exit pupils in order to measure the intensity profiles. This enables allowance for profile asymmetry.

10.4.2 Free Space - Glasses Displays

Glasses displays that are not anaglyph operate on three different principles, these are; linearly polarised, circularly polarised and shuttered. In linearly polarised displays one of the channels has linear polarisation with the other polarised orthogonally to this. Circular polarisation is where the electric field vector has a phase shift of π/2 in relation to the magnetic field vector. The resultant of this vector plotted in time is a helix and the polarisation is referred to as right-handed if the helix forms a right-handed screw and vice versa. If right and left-handed circularly polarised light is used for each of the channels these can be separated with the use of polarising sheets. The advantage of this approach is that the separation is unaffected by the orientation of the glasses.

When linearly polarised light is used the orientation of the glasses must be correct in order to provide minimum crosstalk. The only polarised light display amongst those under test here is the Planar that is linearly polarised. Care must therefore be taken to obtain the

minimum reading of the blocked channel by rotating the glasses when determining the level of crosstalk.

Shutter glasses projector systems operate in a similar manner. The difference is that the DLP projector switches much faster than the addressing time of an LCD and also it has no residual image from the previous frame. The DLP projector is inherently crosstalk free; any crosstalk will be caused by leakage in the shutter glasses and by the way in which they are driven. In early CRT shutter glasses displays crosstalk was caused by the persistence of the phosphor.

For all the glasses displays measurements were made by displaying a white image on the right channel and a black image on the left channel. The leakage on the left channel was measured by placing the left eyepiece of the glasses in front of the power meter detector and taking a reading and then placing the right eyepiece in front of the detector and taking another reading. The process was repeated for right channel crosstalk by displaying a black image on the right channel and a white image on the left channel. All readings were taken 1000 millimetres from the screen.

10.5 Applicability of Test Results

The tests provide useful benchmarks against which the performance of the HELIUM3D display can be compared. Unfortunately the only laser illuminated display available is the MUTED prototype with the laser projector illumination source and this does not perform sufficiently well for valid comparisons to be made. There is considerable amount of information on acceptable levels of speckle contrast and the performance of the HELIUM3D display can be compared against this. What is not clear at present is the effect of speckle on subjective stereoscopic performance. It could be that an effect similar to that caused by metallic painted surfaces is seen where binocular is rivalry caused by the difference between images that have high spatial frequency. This should be investigated.

Measurements of the other parameters of crosstalk, brightness and tracker performance are all applicable for use as benchmarks and an indication of their relevance can be obtained from Table 10.3. It should be noted that the Philips Wow display has now been discontinued.

Display	Parameter			
	Comm-ercially available	Autostereo-scopic	Head tracked	Multi user
Philips 42" Wow	X	X		X
FHG Free2C	X	X	X	
DMU lenticular		X		
MUTED LCOS projector		X		
MUTED Laser projector		X	X	X
Planar PL2010-BK	X			X
Anaglyph	X			X
DepthQ WXGA projector	X			X
Nvidia sequential Samsung 2233RZ	X			X

Table 10.3: Applicability of Display Tests

10.6 Results: Brightness

Out of the eight displays covered in this report, brightness measurements were not made on anaglyph as this is a generic type where the brightness is dependent on the actual display used. They were also not made on the DepthQ 120Hz WXGA projector as brightness has not got a fixed value but dependent on the projector to screen distance.

In Table 10.4 the measured brightness and the manufacturer's figures for the remaining six displays is given. Measurements were made with the power that has a ten-millimetre diameter detector capture area. Readings were taken 1000 millimetres from the screens. Background readings were taken in each case and were found to be negligible with the exception of the MUTED display where a very small correction was necessary. The power readings were converted to nits (candelas per square metre) by allowing for the detector capture area, the screen to detector distance and the screen area. In all but one of the measurements (Free2C) white images were shown on the screen.

The measurement of 409 nits for the Philips 42" Wow display is a little lower than the manufacturer's figure of 460 nits. This could possibly be accounted for by the fact that the detector capture region is set back within its housing so that off-axis rays cause a shadow around the outer part of the capture area. This is generally not a problem but in the case of the 42" Philips display being measured at 1000 millimetres a significant proportion of the rays may not reach the detector. The measurements were made in the sequence of

material originating from Philips when the screen the screen showed white over its complete area.

The 142 nit measurement of the Free2C is less than the 200 nit figure quoted for the NEC Multisync 2110 LCD display on which it is based. Considering the geometry of the Free2C display that uses a lenticular screen to separate left and right images it is unlikely that there is ant significant loss in the display optics. It is almost certain that the lower figure is due to the image content. It was not straightforward to present a pure white image on this display so a maximum reading was taken for the brightest images supplied by FHG with the display.

The DMU lenticular display uses the same NEC LCD as the Free2C display. In this case it was possible to present white images on the display. The reduction in brightness against the manufacturer's figure is possibly due to ageing of the backlight fluorescent tubes as the panel was purchased in 2003.

The 25 nit brightness of the MUTED LCOS Projector Prototype display is low compared to the others; however this display in its LCOS projector embodiment is considerably brighter than the 1.8 nits of the laser projector version. The value if 25 nits is encouraging as the display in its current form only utilises around 1/10th of the area of the projected image. Therefore, the display has the potential to provide around 250 nits with a redesigned projector light engine adapted to handle the extreme 'letterbox' shaped image.

The planar display was measured by supplying the left channel with a white image and measuring the screen output with the left lens of the polarised glasses supplied with the display mounted in front of the detector. The manufacturer's figure of 280 nits is for the LCD used in the display as Planar do not quote the figure for the overall 3D system. It would be expected that the action of the semi-silvered mirror would produce an effective brightness of 140 nits. The small difference between the measured and manufacturer's figures is probably accounted for by absorption in the image-combining screen and the linear polariser in the glasses. The measured power was highly dependent on the orientation of the glasses due to the linear polariser and the maximum measured value of 1.21μW was used.

The manufacturer's figure of 300 nits for the Nvidia system is for the Samsung Sync Master 2233RZ LCD monitor as a figure is not available for the complete 3D system including the shutter glasses. If anything, the value of 128 nits appears to be high as the duty cycle for the image being visible to an eye will be 50% (to allow for the right image to be blocked) less the percentage of the 8.3ms period where the shutter must be opaque in order to block the LCD image whilst it is being addressed (Figure 10.1).

	Display	Screen size (inches)	Aspect ratio	Screen area (m2)	Power at 1000 mm (µW)	Back-ground (nW)	Corrected power (µW)	Measured brightness (nits)	Manu-facturer's figure (nits)
Autostereoscopic	**Philips 42" Wow**	42	16:09	0.486	15.8	2.2	15.8	**409**	460
	FHG Free2C	21.3	04:03	0.14	1.59	6	1.59	**142**	200
	DMU lenticular	21.3	04:03	0.14	1.67	4.3	1.67	**149**	200
	MUTED Proto. 3	19	04:03	0.112	0.227	2.6	0.224	**25**	n/a
Glasses	**Planar PL2010-BK**	20	04:03	0.124	1.21	3.9	1.21	**123**	280
	Nvidia sequential	22	16:09	0.133	1.36	3.6	1.36	**128**	300

Table 10.4: Summary of Brightness Measurements

10.7 Results: Crosstalk

10.7.1 Laser Projector Prototype

An objective measurement of crosstalk was obtained from the plots in Figure 10.2 made from a power meter detector traversing the viewing field at 1000mm from the screen. Table 10.5 shows the crosstalk, estimated from the plots in Figure 10.2 that would be observed by eyes at the positions marked by the vertical lines that correspond to a spacing of 65mm. Lower estimated values were obtained by 'moving' the spacing of the centres of these profiles to 80mm. Therefore in this particular case increased separation of the exit pupils could reduce the crosstalk.

X position (mm)	Eyes in positions marked in Figure 20		With spacing increased by 15 mm	
	Left	Right	Left	Right
-200	3.5	8.7	2.2	7.0
0	2.7	8.2	0.6	5.4
200	2.2	6.4	2.2	6.4

Table 10.5: Crosstalk (%) at 1000 mm from Screen

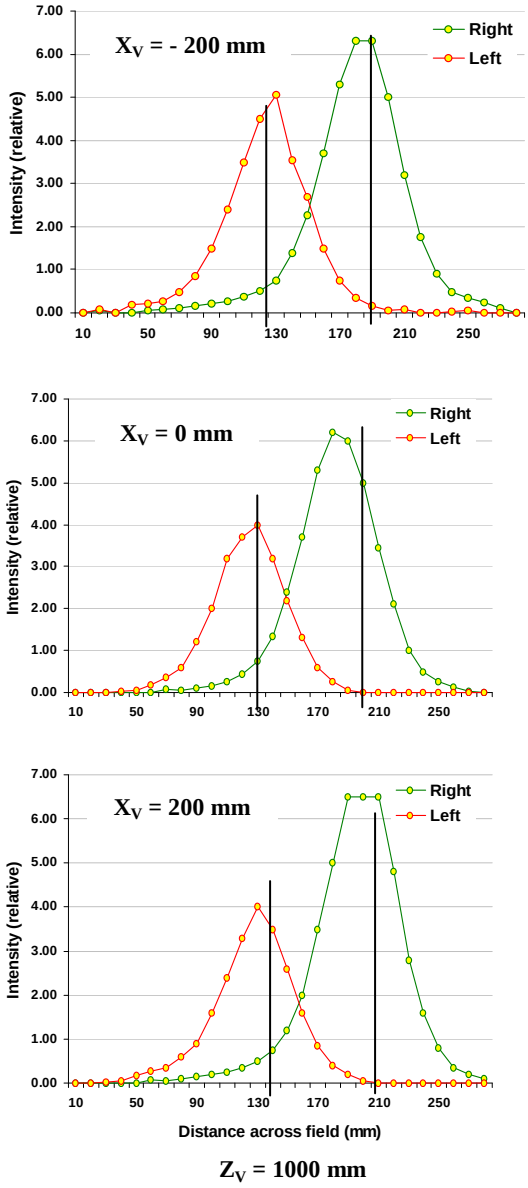

Figure 10.2: Exit Pupil Profiles 1000 mm from Screen

10.7.2 Polarised Glasses Displays

As with brightness, the crosstalk of the planar display is highly dependent on the orientation of the glasses; these were rotated to give a minimum values of 5.7% and 4.9% respectively for the left and right channels.

DepthQ Crosstalk values were 3.4% and 3.7% respectively for the left and right channels. Crosstalk on the Nvidia display was 4.4% and 4.8% respectively for the left and right channels.

10.7.3 Anaglyph Glasses Displays

Anaglyph crosstalk has been studied in some detail in research led by Curtin University of Technology in Australia [71].The effect of pixel and anaglyph glasses spectral response on the level of crosstalk has been calculated for plasma, LCD and CRT displays. In this report we are principally concerned with LCD displays and the results of the calculations in their SID paper of 2007 [71] are summarised in the column charts of Figure 10.5. The red crosstalk is the amount of the cyan channel bleeding through the red filter and cyan crosstalk the red channel passed by the cyan filter.

In this paper the spectral responses of 31 different red/cyan anaglyph glasses are matched with 14 LCDs in order to calculate the crosstalk. Some combinations give crosstalk in excess of 90%, however the values used to obtain Figure 10.5 are for red crosstalk values less than 9% and cyan crosstalk values of 1.5% or less. The lowest calculated values were 6.4% and 0.2% for the red and cyan crosstalk respectively.

It can be seen in Figure 10.3 that red crosstalk is usually significantly greater than cyan crosstalk – on average over all the glasses/display combinations almost four times greater. Red crosstalk usually therefore dominates the overall crosstalk value. This can be attributed to the shape of the spectral curves for the display and glasses, but will also be due to the fact that the green channel is usually much brighter than the red channel. It was also determined that there is considerable variation in the amount of anaglyph crosstalk exhibited by different displays. For example, on average CRT monitors exhibit approximately 45% more crosstalk than LCD monitors. This study was for red/cyan glasses only and there are others, for example red/green and blue/orange.

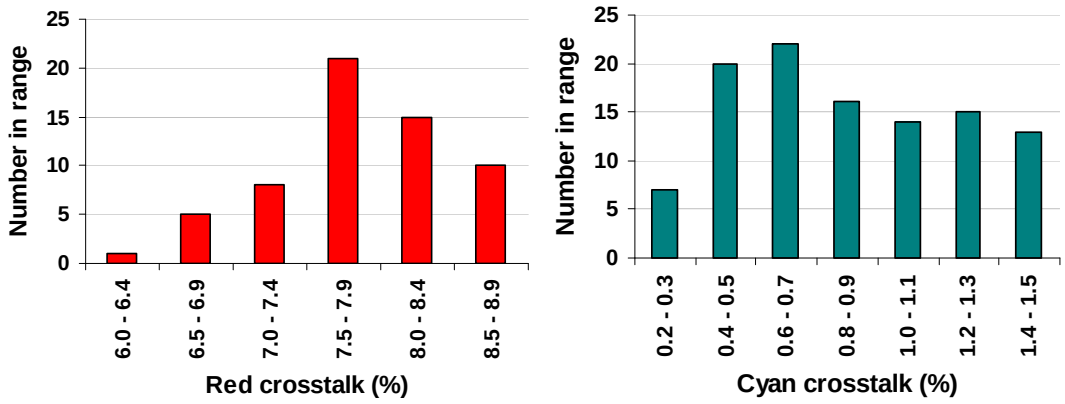

Figure 10.3: Calculated Red/cyan Anaglyph Crosstalk: Results obtained by calculation from the spectral responses of 31 glasses and 14 LCDs. Values of red crosstalk less than 9% and cyan crosstalk 1.5% and less are used.

10.7.4 Crosstalk Summary

Table 10.6 is a summary of the measurements and also the results from external reports on crosstalk for a representative selection of displays.

	Display	Comments	Crosstalk
Autostereoscopic	**Philips 42" Wow**	Information obtained from reference [79]	Multi-view display - not applicable
	FHG Free2C	Measurements carried out by Barco on Eldim analyser	6.3% at 500 mm 4.2% at 700 mm
	DMU lenticular	Measured with spectroradiometer	1.7%
	MUTED LCOS Projector Prototype	Measured by DMU with power meter	Left: 7.3% Right: 4.6%
Glasses	**Planar PL2010-BK**	Measured by DMU with power meter	Left - 5.7% Right – 4.9%
	Anaglyph	Information obtained from papers	Left: ~ 6.4 to 8.9% Right: ~ 0.2 to 1.5%
	DepthQ WXGA projector	Measured by DMU with power meter	Left - 3.4% Right – 3.7%
	Nvidia sequential	Measured by DMU with power meter	Left - 4.4% Right – 4.8%

Table 10.6: Summary of Crosstalk Values

10.8 Discussion

The results obtained from objective measurements carried out by the partners DMU, BAR and FHG and from results of reports on multi-user and anaglyph displays from other researchers provide a useful benchmark against which the HELIUM3D display can be judged.

The crosstalk figures for the Planar, DepthQ projector and Nvidia LCD displays show small differences between the left and right channels that can probably be accounted for by measurement error. The precise measurements on the DMU lenticular display made with the spectroradiometer give close figures of 1.6% and 1.7% for the channels.

The different levels of 7.3% and 4.6% for the MUTED display can be accounted for by the asymmetry of the exit pupil intensity profiles.

Figure 10.4 is a summary of the results obtained and provides an indication of crosstalk that the HELIUM3D display should achieve in order to be comparable to existing displays. The anaglyph values used here are the mean of those given in Table 5 and are used to provide an approximate value for comparison purposes. The mean of all values is 4.4% and the mean of the Autostereoscopic displays is **4.3%**; this appears a realistic level of crosstalk to be expected from the HELIUM3D display. If the Eldim measurements are subsequently found to be high then the overall average would be slightly less and the autostereoscopic average substantially less.

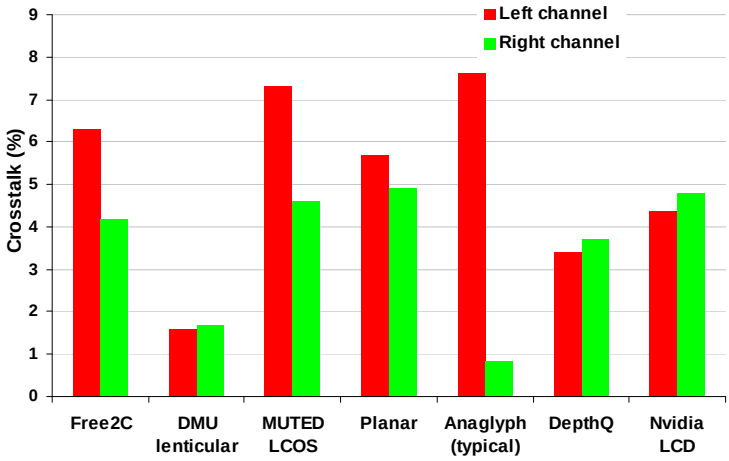

Figure 10.4: Summary of Crosstalk Measurements: The average of the seven display types is 4.4% and the average of the three Autostereoscopic displays is 4.3%.

Six displays were used for brightness measurements (Figure 10.5) As the DMU lenticular display has the same components as the Free2C display it is expected that their brightness would be similar; this is confirmed by the power meter measurements. The mean brightness of the four commercially-available displays is 200 nits; this includes the Philips Wow display which is fairly high at 409 nits. A reasonable figure for the HELIUM3D display to aspire to would be **150 nits** which is comparable to the Free2C display. If a version of the MUTED display with higher brightness is available within the duration of the HELIUM3D project useful comparisons between them will be made.

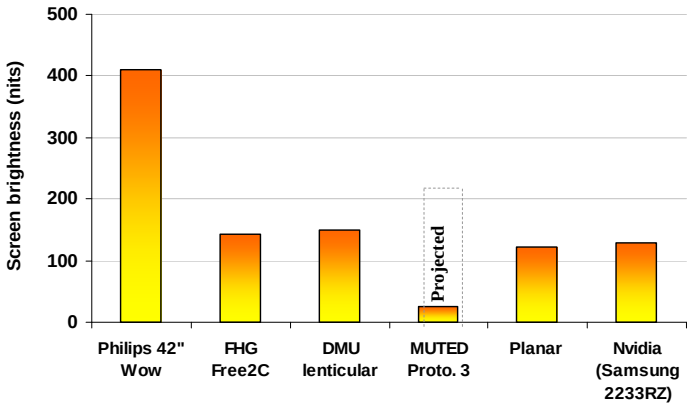

Figure 10.5: Summary of Brightness Measurements: The average of all six display types is 163 nits and the average of the four commercially-available displays is 200 nits.

10.9 Summary

One of the deliverables in the HELIUM3D Description of Work was a report on the performance of existing displays. There are seven 3D displays at DMU: three glasses types and four autostereoscopic. Measurements of brightness and crosstalk were made on these. Head tracker performance was supplied by HHI where this applied. The glasses displays are: Planar, DepthQ projector and the Nvidia 3D shutter glasses kit. Anaglyph glasses are included in the report but as this is a generic type of display, brightness measurement is not applicable. The autostereoscopic displays are: Philips 42”Wow multi-view, Fraunhofer Free2C, DMU lenticular and the MUTED LCOS projector display described in Section 7.1.

All measurements, apart from those on the DMU lenticular display which were with a spectroradiometer, were made on a Newport power meter with a low power detector. All measurements were radiometric and these were converted to photometric units where necessary.

The mean crosstalk for the MUTED LCOS projector display is 5.5%. This figure is obtained by taking the square root of the product of the left and right channel values. The average for all displays tested is 4.4%. This includes a mean value taken from references for anaglyph displays that were not measured at DMU. The MUTED display is slightly high but this could possibly be reduced with different placement of the exit pupils in relation to the viewer’s eyes.

CHAPTER 11

CONCLUSION

The research carried out so far has provided a valuable starting point for ongoing work whose ultimate goal is the production of a 3D display that will be used in the first commercially feasible 3D television broadcasting system. The surveys of other autostereoscopic methods carried out in Chapter 2 indicates that at the present time, at least amongst work that is published, there is no other 3D display being developed that is suitable for this purpose.

Although holographic wavefront reconstruction of the image could *possibly* provide a solution in the long term, it is unlikely to be used for the next generation of television display that will probably be on the market within the next ten years or so. The major problem with this approach is that, even when vertical motion parallax is dispensed with, large amounts of information still have to be displayed.

Volumetric displays suffer from image transparency, and multi-view display has a restricted depth of viewing field that becomes smaller with increasing screen width. Head tracking appears to provide the solution to providing a television display in the foreseeable future as the minimum amount of information, that is two images only, need to be displayed. This places the least demands on the display and also enables image capture with a simple camera-pair that need not occupy a large width.

The disadvantage of a simple two-image system is the lack of motion parallax and the difference between the accommodation and convergence of the eyes. This can cause fatigue and eyestrain, but it appears that insufficient research has been carried out into the *prolonged* viewing of 3D that would occur with 3D television. It is possible that some researchers have overstated this problem, as there may be strategies, for example the reduction of disparity that can overcome this.

An interesting example of the effect of reduced disparity was demonstrated at Philips Research Laboratories in Eindhoven in March 2002. A 3D image with a maximum disparity of only three pixels was presented on a polarised glasses type 3D display. This disparity is sufficiently small for the two views to be observed without the use of the glasses with no noticeable blurring. However, when the screen was viewed with the glasses, a 3D image was seen. The 3D effect had a slightly unnatural appearance, but

gives a striking example of the stereo effect of disparities that are possibly sufficiently small to cause no viewing problems.

On balance, it appears that any problems associated with a two-image display method are far outweighed by the advantages. The only way the same image-pair can be presented to one or more viewers, who do not have fixed viewing positions, is to use head position tracking to steer the regions where these images are seen (the exit pupils) to the positions occupied by the eyes.

Given the points referred to in this section, it does appear that a two-image head tracking display, using a direct-view LCD with a novel backlighting assembly to steer the positions where the images are seen, is likely to provide a viable solution for 3D television.

The research described in this thesis demonstrates that the MUTED and HELIUM3D approach can provide a viable display that can be used for the next-generation of 3D. The use of a laser projector at this stage of currently available technology is not possible but its use in the future should not be ruled out. Conventional projection shows promise as the current version utilises only a small proportion of the available image and a redesigned projector light engine would allow at least an order of magnitude increase in screen brightness. The display is inherently 2D/3D switchable but with halving of the vertical resolution. Another version of this display is currently under construction that incorporates a 120Hz projector and LCD. This will provide full resolution so will be truly 2D/3D switchable.

HELIUM3D is a longer-term prospect but there is an enormous potential market for a display that can offer so much more than straightforward 3D. Its development is at an early stage but as MUTED enabling technology is becoming available, this approach can be used for a commercial product. The demonstrators built so far have shown that the approach of using a controlled light path in conjunction with a fast LCD is a viable means of providing an autostereoscopic display. In the final prototype that will be produced within the duration of the project, there are three components whose design has proved to be challenging. These are: the light engine, the SLM and the superlens screen. The SLM is on target for completion and the first example of the superlens has been built. The current system is bulky and further work is required in order to provide some form of light path folding between the SLM and front screen. The system is currently fairly complex although this is justified by the addition of the extra functionality.

The work covered by this thesis falls into several broad areas, some of which have involved more original work than others. For example, the characterisation of various existing displays covered in Chapter 10 did not involve very much original research as such. The contributions to the MUTED work involved some work that was closely related

to pre-existing research but was necessary in the refinement of the display; the results of this work are summarised in Section 11.3.1. Other work on MUTED was of a more original nature and is summarised in Section 11.3.2. The remainder of my work was on displays that were completely original and not part of the original work plans of the projects; these are the MUTED conventional projector display (Section 11.3.3) and the HELIUM3D demonstrators (11.3.4). The results obtained show benefits with competing technologies as 3D images have been displayed and limited evaluation carried out on displays where there is no direct equivalent, that is displays that have the potential to ultimately provide a commercially-viable multi-user autostereoscopic display.

The areas of work that did not make a highly significant contribution to knowledge but nevertheless were important to the project were: the characterisation of the spatial MUX screen, the characterisation of the holographic projector image, optical component birefringence effects and reduction of the patterning on the image.

As there was a dimensional error in the lenticular MUX screen the effect of this had to be carefully determined and recommendations made for the construction of the next iteration of the screen. The performance of the screen is fairly difficult to determine and a method to visualise the effect was developed. This was with the use of a matrix of colour photographs where the separation of red and green images can be clearly seen.

The characterisation of the holographic projector image was an important part of the project as its performance is crucial to the operation of the display. In addition to characterising the brightness and shapes of the spots in the pattern this work identified a positional stability problem that was eventually to prove very difficult to resolve.

In order to provide the maximum light throughput between the holographic projector and the LCD the polarisation orientation had to be preserved. In the original set-up the components that were birefringent were identified and the information used to organise the sourcing of appropriate replacements.

Although not immediately obvious, the source of visible patterning on the original screen set-up was identified as being due to a horizontal black mask in the sub-pixel structure of the LCD. The solution to this was to locate an LCD that did not have this structure. As information on the sub-pixel structure is not available from manufacturers, several displays had to be purchased and examined under a microscope before a suitable one was located.

As mentioned in Section 4.4, an enhancement lens was required at the screen in order to allow illumination to fill the complete height of the screen. This area of work was within partner SLE's remit and initially they could see the necessity for the use of the

enhancement lens, however, previous research [73] indicates that such a lens is necessary in order to concentrate light towards the region of the vertical plane close to which the viewers will be positioned. Having determined the most suitable distance between the array and the screen, the focal length of the enhancement lens could be readily determined.

The other work carried out that was essential for the MUTED prototype demonstrated at the project final Review Meeting was the compensation for the positional error caused by the non-linearity of the holographic projector. Under normal usage where images are produced by the projector for displaying to viewers, the issue of non-linearity does not pose a problem. However, in the MUTED application this is of crucial importance. The technique of calculating the polynomial expression relating the expected to the actual position and applying this to provide acceptable overall errors enabled the projector to be used in this system. The projector was also subject to relatively long-term positional drift and this was compensated for with the use of a three point mechanical adjustment system.

The MUTED conventional projector prototypes were an extension of the research required in the MUTED project where a projector with a holographically-produced spot pattern was employed. The LCOS projector version was shown at the MUTED Review Meeting in order to show that a display operating on this principle is viable. The display did not include head tracking but there is no reason in principle for this not to be incorporated with some additional effort.

Further research is required for improving the image quality. The results in Section 7.2.2 show that the images have vertical striations. These are probably due to spot pattern alignment errors and also possibly due to misalignment of the optical components in the array elements, for example the diffusers.

The temporal MUX version using a 120Hz projector produced 3D images but there was not sufficient time available to fully evaluate the performance of this. The fact that 3D could be seen at all demonstrated that synchronisation between the projector and the 120Hz LCD was functioning correctly. Further research is required on this version as in the display produced no allowance was made for the addressing time of the LCD so consequently 3D could only be seen in the central region of the screen. This version also did not incorporate head tracking.

These two displays form the basis for future research in this area.

The 120Hz demonstrator was used at the second HELIUM3D Review Meeting to show the Reviewers that temporal MUX can be achieved by synchronising a 120Hz projector with a 120Hz LCD. The optics of this demonstrator is not particularly novel as it is essentially

forming exit pupils in the viewing field by producing real images of a rectangle with the use of a Fresnel lens.

Unlike the HELIUM3D display which is essentially a rear projected system, in this case images are formed on an LCD and the optics forms an active backlight. No evaluation work was carried out on this display as its purpose was purely to demonstrate temporal MUX.

The reduced functionality HELIUM3D display was also demonstrated at the second Review Meeting. The reason for this prototype being necessary was that a fast SLM that shows the novel dynamic exit pupil formation ability was not yet available at the time of the meeting.

The differences between this model and the final version are: a x2 Gabor superlens as opposed to a x4 superlens, a 120Hz instead of the fast FLC linear array, and a 120Hz DMD projector replaces the projection engine and laser scanner. Although there are several differences from the final dynamic version using a scanned laser light engine and fast SLM, the display proved the general principle of operation and also enabled subjective and objective evaluation to be carried out.

References

[1] Aksit, K., Olcer, S., Baghsiahi, H., Erden, E., Kishore, V. C., Selviah, D. R., Surman, P. and Urey, H., “Laser Scanning Based Light Engine for Auto-stereoscopic Display System”, (in preparation for Optics Express).

[2] Andrew, J., Ian, M. D., Hideshi, Y., Mark, B. and Paul, D., "Rendering for an Interactive 360 Light Field Display", SIGGRAPH Papers Proceedings, pp. 34 - 39, 2007.

[3] Arai, J., Kawai, H. and Okano, F., "Microlens Arrays for Integral Imaging System", Applied Optics, Vol. 45, No. 36, pp. 9066 - 9078, 2006.

[4] Baloch, T., “Method and Apparatus for Displaying Three-dimensional Images”, United States Patent No. 6,201,565 B1, 2001.

[5] Benton, S. A., Slowe, T. E., Kropp, A. B. and Smith, S. L., “Micropolarizer-based Multiple-viewer Auto-stereoscopic Display”, SPIE Proceedings, Stereoscopic Displays and Applications X, Vol.3639, pp. 76 - 83, 1999.

[6] Berkel, C., Parker, D. W. and Franklin, A. R., “Multiview 3D-LCD”, “SPIE Proceedings, Stereoscopic Displays and Virtual Reality Systems IV”, Vol.2653, pp. 32 - 39, 1996.

[7] Blundell, B. and Schwartz, A., “Volumetric Three Dimensional Display Systems”, (Wiley-Interscience), pp 316-324, (2000).

[8] Blundell, B. and Schwartz, A, “Volumetric Three Dimensional Display Systems”, (Wiley-Interscience), pp 333-336, (2000).

[9] Brar, R. S., Surman, P., Sexton, I., Bates, R., Lee, W. K., Hopf, K., Neumann, F., Day, S. E. and Willman, E., "Laser-Based Head-Tracked 3D Display Research", Journal of Display Technology, Vol.PP, Issue: 99, pp. 1 - 14,(2010).

[10] Buckley, E., Corbett, A., Sexton, I. and Surman, P., “Multi-Viewer Autostereoscopic Display with Dynamically Addressable Holographic Backlight”, SID 2008, 18 May 2008 (Display winner of SID Distinguished paper award).

[11] Chao, Y. and Yuanqing, W., “Robust Real-time Multi-user Pupil Detection and Tracking Under Various Illumination and Large-scale Head Motion”, Computer Vision and Image Understanding, Vol 115, Issue 1, pp. 1223 – 1238, (2011).

[12] Choi, H., Kim, J., Park, J. B. and Lee, B., “Analysis on the Optimized Depth of 3D Displays Without an Accommodation Error", IMID 07 Digest, pp. 1811 – 1814, 2007.

[13] De Zwart, S. T., IJzerman, W. L., Dekker, T. and Wolter, W. A. M., “A 20-in. Switchable Auto-Stereoscopic 2D/3D Display”, Proceedings of the 11th International Display Workshops, Niigata, Japan, pp. 1459 - 1460, (2004).

[14] Delaney, B., "Forget the Funny Glasses [Autostereoscopic Display Systems]", IEEE, Computer Graphics and Applications, pp 14 - 19, 2005.

[15] Dubois, E., "A Projection Method to Generate Anaglyph Stereo Images", IEEE, Acoustics, Speech, and Signal Processing, 2001. Proceedings. (ICASSP '01). 2001 IEEE International Conference on, pp. 1661 - 1664 vol.3, 2001.

[16] Eichenlaub, J. “A Lightweight Compact 2D/3D Autostereoscopic LCD Backlight for Games, Monitor and Notebook Applications”, SPIE Proceedings “Stereoscopic Displays and Virtual Reality Systems IV” Vol.3012: 274 - 281. (1997).

[17] Eichenlaub, J. and Hutchins, J. “Autostereoscopic Projection Displays”, SPIE Proceedings, Stereoscopic Displays and Virtual Reality Systems II, Vol.2409, pp. 48-54, 1995.

[18] Erden, E., Kishore, V. C., Ürey, H., Baghsiahi, H., Willman, E., Day, S. E., Selviah, D. R., Fernandez, F. A. and Surman, P., “Laser Scanning Based Autostereoscopic 3D Display with Pupil Tracking”, Proceedings of the IEEE Photonics 2009, Antalya, Turkey, pp. 10 - 11, (2009).

[19] Ezra, D., Woodgate, G. J., Omar, B. A., Holliman, N. S., Harrold, J. and Shapiro, L. S., “New Auto Stereoscopic Display System”, SPIE Proceedings, Stereoscopic Displays and Virtual Reality Systems II, Vol.2409, pp. 31 - 40, 1995.

[20] Film-Tech Articles, "Straight to Video", entitled "Master Image VS. Real D." November 23, 2010.

[21] FilmJournal articles "The Best is Yet to Come: 3D Technology Continues to Evolve and Win Audience Approval", Jan. 1, 2010.

[22] Freund, Y. and Schapire, R. E., “A Short Introduction to Boosting”, Journal of Japanese Society for Artificial Intelligence, 14(5):771-780, September 1999.

[23] Hanazato, A., “Subjective Evaluation of Cross Talk Disturbance in Stereoscopic Displays”, 20th International Display Research Conf. San Jose 25 - 28, Sept 2000.

[24] Harman, P., “Autostereoscopic Teleconferencing System”, SPIE Proceedings, Stereoscopic Displays and Virtual Reality Systems VII, Vol.3957, pp. 293 - 301, 2000.

[25] Hattori, T., “Sea Phone 3D Display”, http://home.att.net/~SeaPhone/3display.htm, pp. 1 - 6, 2000.

[26] Hattori, T., “Sea Phone 3D Display”, http://home.att.net/~SeaPhone/3display.htm, pp. 7 - 9, 2000.

[27] Hembd, C., Stevens, R. and Hutley, M. “Imaging Properties of the Gabor Superlens”, European Optical Society, Topical Meetings Digest Series: 13 “Microlens Arrays”, NPL Teddington, May 15-16 1997, pp. 101 - 104, 1997.

[28] Hitachi, "Hitachi Shows 10" Glasses-free 3D Display", article published in 3D-Display-Info website pp. 67 - 69, 2010.

[29] Holografika Display Technology, "Real 3D Display by Holografika", Holografika Website.

[30] Huang, Y. P., “3D Introduction and Project”, Photonics Global Conference. pp. 10 - 12, IEEE, 2007.

[31] Ichinose, N., Tetsutani, N. and Ishibashi, M., “Full-colour Stereoscopic Video Pickup and Display Technique Without Special Glasses”, Proceedings of the SID, Vol.3014, pp. 319 - 323, 1989.

[32] IJsselsteijn, W. A., Seuntiëns, P. J. H. and Meesters, L. M. J., “Human Factors of 3D Displays”, 3D Videocommunication: Algorithms, Concepts, and Real-Time Systems in Human-Centered Communication, John Wiley, ISBN 0-470-02271-X, pp. 219 - 234, 2005.

[33] Imai, H., Imai, M., Yukio, O. and Kubota, K., “Eye-position Tracking Stereoscopic Display Using Image Shifting Optics”, SPIE Proceedings, Stereoscopic Displays and Virtual Reality Systems IV, Vol.2653, pp. 49 - 55, 1996.

[34] Jang, J. S. and Javidi, B., “Spatiotemporally Multiplexed Integral Imaging Projector for Large-scale High Resolution Three-dimensional Displays,” Opt, Express. Vol.12 no.4, pp. 557 - 563, Feb. 23, (2004).

[35] Kajik1, Y., Yoshikawa, H. and Honda, T., “Three-Dimensional Display with Focused Light Array”, SPIE Proceedings, “Practical Holography X”, Vol.2652, pp. 106 - 116, 1996.

[36] Kishore, V. C., Erden, E., Urey, H., Willman, E., Baghsiahi, H., Day, S. E., Selviah, D. R., Fernández, F. A. and Surman, P., “Laser Scanning 3D Display with Dynamic Exit Pupil”, Proceedings of the 29th International Display Research Conference, Rome, Italy, pp. 492 - 495, (2009).

[37] Kunz, A. M. and Spagno, C. P., "Modified Shutter Glasses for Projection and Picture Acquisition in Virtual Environments", IEEE, Virtual Reality, 2001. Proceedings. IEEE, pp. 281 - 282, 2001.

[38] Langhans, K., Bahr, D., Bezeeny, D., Homann, D., Oltmann, K., Guill, C., Rieper, E., and Ardey, G., “FELIX 3-D Displays: An Interactive Tool for Volumetric Images,” Proc SPIE, vol. 4660, pp. 176 - 190, (2002).

[39] Lawton, G., "3D Displays Without Glasses: Coming to a Screen Near You " IEEE, Computer, pp. 17 - 19, 2011.

[40] Lippmann, G., "Epreuves Reversibles. Photographies Intégrales", Comptes-Rendus de l'Académie des Sciences 146, no. 9, pp. 446 - 451, 1908.

[41] Loy, G., “Computer Vision to See People: A Basis for Enhanced Human Computer Interaction”, Thesis submitted for the degree of Doctor of Philosophy at the Australian National University, January 2003.

[42] Lucente, M. and Galyean, T. A., “Rendering Interactive Holographic Images”, Computer Graphics Proceedings, Annual Conference Series, 1995, pp. 387-393, 1995.

[43] Lucente, M., “Interactive Three-dimensional Displays; Seeing the Future in Depth”. Siggraph “Computer Graphics - Current, New and Emerging Display Systems”, 1997.

[44] Makoto, O., Jun, A. and Fumio, O., "New Integral Imaging Technique Uses Projector", SPIE Proceedings, pp. 81-92, 2007.

[45] McCormick, M., Davies, N., Aggoun, A. and Brewin, M., "Examination of the Requirements for Autostereoscopic, Full Parallax, 3D TV", Broadcasting Convention, 1994. IBC 1994., International, pp. 477 - 482, 2002.

[46] McCormick, M., Davies, N. and Chowanietz, E. G., “Restricted Parallax Images for 3D T.V.”, IEE Colloquium “Stereoscopic Television”, Digest No: 1992/173, pp. 3/1 - 3/4, 1992.

[47] Meesters, L. M. J., IJsselsteijn, W. A., Seuntiens, P . J .H., "A Survey of Perceptual Evaluations and Requirements of Three-dimensional TV", Circuits and Systems for Video Technology, IEEE Transactions on, pp. 381 - 391, 2004.

[48] Moller, C. and Travis, A. R. L. “Flat Panel Time Multiplexed Autostereoscopic Display Using an Optical Wedge Waveguide”, Proceedings of the 11th International Display Workshops, Niigata, Japan: 1443 - 1446, 2004.

[49] Omeltshenko, S., "3-D-display", IEEE Modern Problems of Radio Engineering, Telecommunications and Computer Science (TCSET), 2010 International Conference on, pp. 108, 2010.

[50] Omura, K., Shiwa, S. and Tsutomu, M., “Lenticular Autostereoscopic Display System: Multiple Images for Multiple Viewers”, Journal of the SID, 6/4, pp. 313 - 324, 1998.

[51] Park, D., Kim, T. G., Kim, C. and Kwak, S., "A Sync Processor with Noise Robustness for 3DTV Active Shutter Glasses", IEEE, SoC Design Conference (ISOCC), 2010 International, pp. 147 - 149, 2010.

[52] Pastoor, S., “Human Factors of 3DTV: An Overview of Current Research at Heinrich-Hertz-Institut Berlin”, IEE Colloquium “Stereoscopic Television”, Digest No. 1992/173, p. 11/3, 1992.

[53] Perlin, K., Poultney, C., Kollin, J. S., Kristjansson, D. T. and Paxia, S., “Recent Advances in the NYU Autostereoscopic Display”, SPIE Proceedings, Stereoscopic Displays and Virtual Reality Systems VIII, Vol.4297, pp. 196 - 203, 2001.

[54] Quan Huynh-Thu, Barkowsky, M., Le Callet, P., "The Importance of Visual Attention in Improving the 3D-TV Viewing Experience: Overview and New Perspectives", Broadcasting, IEEE Transactions on, pp. 421 - 431, 2011.

[55] Ralf, T., HHI 3D Displays, "3D Displays”, IEEE, pp. 20 - 22, 2002.

[56] Ralf, T., HHI 3D Displays, "3D Displays", IEEE, pp. 23 - 27, 2002.

[57] Ralf, T., HHI 3D Displays, "iPoint3D - 3D Realtime API", IEEE, pp. 23 - 27, 2009.

[58] Sandin, D. J., Margolis, T., Dawe, G., Leigh, J. and DeFanti, T. A., “Varrier Autostereographic Display”, SPIE Proceedings Stereoscopic Displays and Virtual Reality Systems VIII, Vol.4297, pp. 204 - 211, 2001.

[59] Schmidt, A. and Grasnick, A., “Multi-viewpoint Autostereoscopic Displays from 4D-vision,” Proc. SPIE, vol.4660, pp. 212 - 221, (2002).

[60] Schwerdtner, A., “Video Hologram and Device for Reconstructing Video Holograms Using a Fresnel Transform”, Unites States Patent 20060238843, 2007.

[61] Scotcher, S. M., Laidlaw, D. A., Canning, C. R., Weal, M. J. and Harrad, R. A., "Pulfrich's Phenomenon in Unilateral Cataract", Br J Ophthalmol., 81(12):1050-5.

[62] Sexton, I., Bates, R., Lee, W., Surman, P., Hopf, K., Neumann, F., Corbett, A. and Buckley, E., “Laser Illuminated Multi Viewer 3D Displays”, Proc. IMID 2008, pp. 1423 - 1426, Seoul, (2008).

[63] Sexton, I., “Parallax Barrier Display Systems”, IEE Colloquium, Stereoscopic Television, Digest No: 1992/173, pp. 5/1 - 5/5, 1992.

[64] Sexton, I., Surman, P., “Stereoscopic and Autostereoscopic Display Systems”, Signal Processing Magazine, IEEE, 16 Issue3, pp. 85 - 99, 1999.

[65] Shwartz, A., “Head Tracking Stereoscopic Display”, Proceedings of IEEE International Display Research Conference, pp. 141 - 144, 2005.

[66] Son, J. Y., Bah Javidi, J. and Kwack, K.-D., “Methods for Displaying Three-dimensional Images”, Proceedings of the IEEE, Vol. 94, No. 3, (2006).

[67] Son, J. Y., Shestak, S. A., Kim, S. and Choi, Y. J., “A Desktop Auto-stereoscopic Display with Head Tracking Capability”, SPIE Proceedings, Stereoscopic Displays and Virtual Reality Systems VIII, Vol.4297, pp. 160 - 164, 2001.

[68] Son, J. Y., Shestak, S. A., Kim, S. and Choi, Y. J., “A Desktop Auto-stereoscopic Display with Head Tracking Capability”, SPIE Proceedings, Stereoscopic Displays and Virtual Reality Systems VIII, Vol.4297, pp. 168 - 172, 2001.

[69] Son, J. Y., Smirnov, V. V., Kim, K.-T., and Chun, Y.-S., “A 16-views TV System Based on Spatial Joining of Viewing Zones,” Proc. SPIE, vol. 3957, pp. 184 - 190, (2000).

[70] Srivastava, A. K., de Bougrenet de la Tocnaye, J. L. and Dupont, L., “Liquid Crystal Active Glasses for 3D Cinema” IEEE, 6 Issue:10, pp. 522 - 530, 2010.

[71] Stupp, E. H. and Brennesholtz, M. S., "Projection Displays". Chichester, (U.K.: Wiley, 1999), ch.14, pp.330 - 333.

[72] Sunny Ocean Studios, "3D Developments, Sunny-Ocean Website, 2006.

[73] Surman, P., “Head Tracking Two-image 3D Television Displays”, PhD thesis submitted to De Montfort University, pp. 135 - 151, June 1992.

[74] Surman, P., “Head Tracking Two-image 3D Television Displays”, PhD thesis submitted to De Montfort University, pp. 167 - 176, June 1992.

[75] Surman, P., Hopf, K., Sexton, I., Lee, W. K. and Bates, R., “Solving the Problem - The History and Development of Viable Domestic 3DTV Displays”, Three-Dimensional

Television, Capture, Transmission, Display (edited book). Springer ‘Signals and Communication Technology' series, 2008.

[76] Surman, P., Sexton, I., Bates, R., Yow, K. C. and Lee, W. K., “The Construction and Performance of a Multiviewer 3D Television Display”, Advanced Display Technologies, ’04 Moscow, 7 – 10 Sep 2004.

[77] Surman, P., Sexton, I., Hopf, K., Buckley, E., Lee, W. K. and Bates, R., “Laser-based Multi-user 3D Display”, ASID 2007, 10th Asian Symposium on Information Display, Singapore, 03 Aug 2007.

[78] Surman, P., Sexton, I., Hopf, K., Buckley, E. and IJsselsteijn, W., “Head Tracked Multi-user 3D Display using an RGB Laser Illumination Source”, ASID’06 Proceedings of the 9th Asian Symposium on Information Display, (2006).

[79] Surman, P., Sexton, I., Hopf, K., Buckley, E. and IJsselsteijn, W., “Head Tracked Single and Multi-user Autostereoscopic Displays”, The 3rd European Conference on Visual Media Production, (2006).

[80] Surman, P., Sexton, I., Hopf, K., Lee, W. K., Buckley, E., Jones, G. and Bates, R., "European Research into Head Tracked Autostereoscopic Displays", 3DTV Conference: The True Vision - Capture, Transmission and Display of 3D Video, pp. 161 - 164, (2008).

[81] Takaki, Y. and Nago, N., “Multi-projection of Lenticular Displays to Construct a 256-view Super Multi-view Display”, Optics Express, Vol. 18, No.9, 2010.

[82] Tam, W. J., Speranza, F., Yano, S., Shimono, K., Ono, H., "Stereoscopic 3D-TV: Visual Comfort", Broadcasting, IEEE Transactions on, pp. 335 - 346, 2011.

[83] Technology reviews, Article published by MIT, "Microsoft's New Display", article published, VID 579, 06 November 2010.

[84] Tetsutani, N., Ichinose, S. and Ishibashi, M., “3D-TV Projection Display System with Head Tracking”, Japan Display ’89, pp. 56 - 59 1989.

[85] Tilton, H. B., “Large-CRT Holoform Display”, Proceedings of IEEE International Display Research Conference, pp. 145 - 146, 1985.

[86] Traub, A. C., “Stereoscopic Display Using Rapid Varifocal Mirror Oscillations”, Applied Optics, Vol. 6 No. 6, pp. 1085 - 1087, June 1967.

[87] Van Berkel, C. and Clarke, J. A., “Characterization and Optimization of 3D-LCD Module Design,” Proc. SPIE, vol.3012, pp. 179 - 186, (1997).

[88] Verrier, R. "3-D Technology Firm RealD has Starring Role at Movie Theaters", Los Angeles Times, 2009.

[89] Viola, P. and Jones, M., “Rapid Object Detection Using a Boosted Cascade of Simple Features”, Proceedings of IEEE Conference on Computer Vision and Pattern Recognition. 2001.

[90] Volbracht, S., Shahrbabaki, K., Domik, G. and Fels, G., "Anaglyph Stereo and Shutter Glass Stereo?", IEEE, Visual Languages, 1997. Proceedings., IEEE Symposium on, pp. 190 - 194, 1997.

[91] Volbracht, S., Shahrbabaki, K., Domik, G. and Fels, G., "Perspective Viewing, Anaglyph Stereo or Shutter Glass Stereo?", IEEE, Visual Languages, 1996. Proceedings., IEEE Symposium on, pp. 192 - 193, 1996.

[92] Wiki articles "Wikipedia Dolby 3D", article published 27 July 2007.

[93] Wiki articles "Wikipedia Stereoscopy", article published 11 June 2003.

[94] Williams, J. M. and Lit, A. (1983) “Luminance-dependent Visual Latency for the Hess Effect, the Pulfrich Effect, and Simple Reaction Time”, Vision Res. 23(2):171-9.

[95] Willman, E., Baghsiahi, H., Fernández, F. A., Selviah, D. R., Day, S. E., Kishore, V. C., Erden, E., Urey, H. and Surman, P., “The Optics of an Autostereoscopic Multiview Display,” Digest of SID Annual Meeting, Paper: 16.4, pp. 222 - 225, Seattle, USA, May 2010.

[96] Willman, E., Baghsiahi, H., Fernández, F. A., Selviah, D. R., Day, S. E., Kishore, V. C., Erden, E., Urey, H. and Surman, P. A. “The Optics of an Autostereoscopic Multiview Display”, The Society for Information Display, International Symposium, Seminar, and Exhibition, Washington State Convention Center, Seattle, WA, USA, (2010).

[97] Willman, E., Baghsiahi, H., Fernández, F. A., Selviah, D. R., Day, S. E., Kishore, V. C., Erden, E., Urey, H. and Surman, P. A., “The Optics of an Autostereoscopic Multiview Display”, The Society for Information Display, 2010 International Symposium, Seminar and Exhibition, 2010.

[98] Woodgate, G. J., Ezra, D., Harrold, J., Holliman, N., Jones, G. R. and Moseley, R. R., “Observer Tracking Auto stereoscopic 3D Display Systems”, SPIE Proceedings, Stereoscopic Displays and Virtual Reality Systems IV, Vol.3012, pp. 187 - 198, 1997.

[99] Woods, A. J. and Harris, C. R., “Comparing Levels of Crosstalk with Red/cyan, Blue/yellow, and Green/magenta Anaglyph 3D Glasses” in Proceedings of SPIE Stereoscopic Displays and Applications XXI, vol. 7253, pp. 0Q1- 0Q12, January 2010.

[100] Woods, A. J. and Rourke, T., “Ghosting in Anaglyphic Stereoscopic Images” presented at Stereoscopic Displays and Applications XV, published in Proceedings of SPIE Stereoscopic Displays and Virtual Reality Systems XI, vol. 5291, pp. 354 - 365, January 2004.

[101] Woods, A. J., Yuen, K. L. and Karvinen, K. S., “Characterizing Crosstalk in Anaglyphic Stereoscopic Images on LCD Monitors and Plasma Displays”, J SID, Vol 15, Issue 11, pp. 889 - 898, November 2007.

[102] Woods, A. J., Yuen, K. L. and Karvinen, K. S., “Characterizing Crosstalk in Anaglyphic Stereoscopic Images on LCD Monitors and Plasma Displays” in Journal of the Society for Information Display, vol 15, issue 11, pp. 889 - 898, November 2007.

[103] Zervas, M. N., Markatos, S. and Giles, I. P., "Polarizing Beam Splitter Utilising Surface Plasmon Waves", IEEE, All-Fibre Devices, IEE Colloquium on, pp. 4/1 - 4/4, 1988.

[104] Zhu, Y. and Zhen, T., "3D Multi-view Autostereoscopic Display and its Key Technologie", IEEE Information Processing, 2009. APCIP 2009. Asia-Pacific Conference on, pp. 31 - 35, 2009.

Appendix 1 Display Capabilities and Descriptions

Generic Type			Multi-user	Viewer movement	Motion parallax	acc/con rivalry	Image trans-parency	Depth of field	Comp-lexity	Estimated cost
Multiple view	Two image non-HT		No	Small	No	Yes	No	Good	Low	Low
	Two image HT	Single-user	No	Sufficient	Possible	Yes	No	Good	Medium	Medium
		MUTED	Yes	Large	Possible	Yes	No	Good	Medium	Medium
	Multi-view		Yes	Limited	Yes	Yes	No	Limited	Low	Low
	Multi-beam		Yes	Large	Yes	Yes	No	Limited	High	High
	Light field		Yes	Large	Yes	Possibly	No	Good	High	Very high
Volu-metric	Virtual image		Yes	Large	Yes	No	Yes	Good	High	High
	Real image	Moving screen	Yes	360°	Yes	No	Yes	Good	High	High
		Static screen	Yes	360°	Yes	No	Yes	Good	Medium	Medium
		Volume	Yes	360°	Yes	No	Yes	Good	High	High
Holographic			Yes	Large	Yes	No	No	Good	Very high	Very high

Table A1.1 Possible technology capability matrix

Generic Type			Organisation	Technology
Multiple view	Two image non-head tracked		Dimen	LCD, parallax barrier
			DTI	LCD, parallax illumination
			Iris-3D	Dual channel projection - no crosstalk
			Kodak	2 LCDs with mirrors and lenses
			RealityVision	LCD, spatial MUX, HOE
			SeeReal	LCD with prismatic screen
			Sharp	LCD, parallax barrier, 2D/3D
			Tridelity	LCD and probably parallax barrier
	Two image head tracked	Single-user	Fraunhofer	LCD, spat. MUX, moving lenticular scn.
			SeeFront	LCD, lenticular scn, switched pixels
			SeeReal	LCD with prismatic screen
			Sanyo	LCD, optics unknown (possibly barrier)
			NTT (DoCoMo)	LCD, lenticular (with motion parallax)
		Multi-user	MUTED	LCD, optical array and RGB laser
	Multi-view		NewSight (X3D)	LCD & plasma, wavelength filter, 8-view
			Philips 9-view	LCD, slanted lenticular, 9-view
			Alioscopy	LCD, slanted lenticular, 8-view
			Sanyo	LCD & plasma, parallax bar. 4 & 7-view
			Stereographics	LCD, slanted lenticular, 9-view
			Tridelity	LCD, possibly parallax bar., 9-view
			LG	LCD, lenticular, 25-view
			Mitsubishi	Multi-projectors, lenticular screen, 16 views
	Multi-beam		Setred	DMD projector & dynamic FE barrier
			Fraunhofer PST	DMD projector & dynamic FE barrier
			Holografika	Optical modules & quasi holo. Screen
			Toshiba	Horiz. LCD with integral imaging lenses
			QinetiQ	~40 projectors & vert. diffusing screen

Generic Type			Organisation	Technology
Volum-etric	Virtual image		Strathclyde Uni.	Deformable mirror
	Real image	Moving screen	Actuality	DMD projector & rotating screen
			Felix	RGB laser, X-Y scanner, rotating screen.
			Hitachi	Projector and rotating screen
			Holoverse	DMD projector and rotating screen
			SeeLinder	Rotating barrier & LED arrays
		Static screen	DepthCube	DLP projector & LC stack
			Lebedev	Laser Projector & LC stack
		Volume	AIST	Laser-addressed plasma 'voxels' in air
			Felix	Laser addressed 'voxels' in crystal
			Fogscreen	Projection on to water vapour screen
			Stanford Univ.	Laser addressed voxels in doped glass
			Cheoptics	Images reflected off glass pyramid

Table A 1.2 Examples of generic display types

Appendix 2 Spot Pattern Corrections

Array element no.	Measured values			Lower value	Upper value	Mean of Upper and Lower Values
	- 45 mm	0 m	45 m			
1	0.00	0.50	1.00	0.00	1.00	0.50
2	0.00	0.00	0.50	0.00	0.50	0.25
3	0.00	0.00	0.00	0.00	0.00	0.00
4	0.00	0.00	0.00	0.00	0.00	0.00
5	0.00	0.50	0.00	0.00	0.50	0.25
6	0.00	0.00	-0.50	-0.50	0.00	-0.25
7	0.00	0.00	0.00	0.00	0.00	0.00
8	0.50	0.00	0.00	0.00	0.50	0.25
9	0.00	0.00	0.00	0.00	0.00	0.00
10	0.00	0.50	0.00	0.00	0.50	0.25
11	0.00	0.00	0.00	0.00	0.00	0.00
12	0.00	0.00	0.00	0.00	0.00	0.00
13	0.00	0.00	0.00	0.00	0.00	0.00
14	0.00	0.00	0.00	0.00	0.00	0.00
15	0.50	1.00	1.00	0.50	1.00	0.75
16	1.00	0.50	0.00	0.00	1.00	0.50
17	1.00	0.00	0.00	0.00	1.00	0.50
18	0.00	1.00	0.50	0.00	1.00	0.50
19	0.00	0.00	0.00	0.00	0.00	0.00
20	0.00	1.00	0.00	0.00	1.00	0.50
21	0.00	1.00	0.00	0.00	1.00	0.50
22	1.00	0.50	0.00	0.00	1.00	0.50
23	0.00	1.50	0.50	0.00	1.50	0.75
24	0.00	1.00	0.00	0.00	1.00	0.50
25	0.00	0.00	0.00	0.00	0.00	0.00
26	0.00	0.00	0.00	0.00	0.00	0.00
27	0.00	0.00	0.00	0.00	0.00	0.00
28	1.00	0.50	0.00	0.00	1.00	0.50
29	0.00	0.50	0.00	0.00	0.50	0.25
30	0.00	0.00	0.00	0.00	0.00	0.00
31	0.00	0.50	0.00	0.00	0.50	0.25
32	0.00	0.00	0.00	0.00	0.00	0.00
33	0.00	0.00	0.00	0.00	0.00	0.00
34	0.00	0.00	0.00	0.00	0.00	0.00

35	0.00	0.00	0.00	0.00	0.00	**0.00**
36	0.00	0.00	0.00	0.00	0.00	**0.00**
37	0.00	0.00	0.00	0.00	0.00	**0.00**
38	0.00	0.00	0.00	0.00	0.00	**0.00**
39	0.00	0.00	0.00	0.00	0.00	**0.00**
40	0.00	0.00	0.00	0.00	0.00	**0.00**
41	0.00	0.00	0.00	0.00	0.00	**0.00**
42	0.00	0.00	0.00	0.00	0.00	**0.00**
43	0.00	0.00	0.00	0.00	0.00	**0.00**
44	0.00	0.00	0.00	0.00	0.00	**0.00**
45	0.00	0.00	0.00	0.00	0.00	**0.00**
46	0.00	0.00	0.00	0.00	0.00	**0.00**
47	0.00	0.00	0.00	0.00	0.00	**0.00**
48	0.00	0.00	0.00	0.00	0.00	**0.00**
49	0.00	0.00	0.00	0.00	0.00	**0.00**

Table A 2.1: Upper Array Y Corrections

Appendix 3 Matlab Program for MUTED Spot Pattern

This appendix contains the Matlab program used to produce the spot pattern for the MUTED holographic projector display. Projects All applications have been developed with Matlab and additional software packages such as C and Java have been used where it has been necessary and appropriate. In order to run the program, all files need to be implemented in Matlab with .xrp extension.

The MUTED Application contains a multiple set of Matlab programs used to generate bitmaps and holograms to form an image on the back of LCD. This appendix includes five set of main programs that were used for generation of bitmaps and hologram rendering.

1. Main Program to initialise the bitmap parameters & launch the application
2. Main Program used to Generate Bitmaps
3. Program Used to Define Coordinates
4. Program Used to Define Grid
5. Matlab Program for Combining the Upper and Lower array holograms of the MUTED display

1. Main Program to Initialise the Bitmap Parameters & Launch the Application

```
%05/03/09: GenHolos: Ties together the code needed to generate analytical holograms for Y43
clear all
close all
%currentpath=cd;
%cd('C:\projects\SVN_common')
%add_dirs_to_path
%cd(currentpath)
% **** File Path Parameters ***
moduledatapath='D:\LBO\ModuleData\YO44';
%outputfilepath='C:\projects\xrender\Holograms\analytical\';
bitmapfilepath='D:\xsuite\Bitmaps\YO44_FirstSet_10June';
%*******************************
%**** Exit Pupil Parameters ***
v_nwidth=400; % (675 used before) viewing area width at point closest to the screen
near_point=1000; % (1400 used before) closest position to LCD
far_point=2500; % (1600 used before) furthest point from LCD
no_hologs=1500; % **APPROXIMATE** number of exit pupils
%*******************************
%**** Rendering Parameters ***
ED=0; %determines whether to use error diffusion or not
N=1280;%the size of the hologram being used.
RGB_sets_per_video_frame=4; %number of multiple of RGB holograms per video frame
%*******************************
%obtaining the exit pupil box centres
[x_cent,z_cent,box_w,box_d]=EP_coords(no_hologs,near_point,far_point,v_nwidth);
disp(['Total number of exit pupils = ',num2str(2*length(x_cent))]);
placenum=0;
for upper=0:1
```

```
   for k=1:length(x_cent)
      %calculating the target spot coords for a given exit pupil centre
      [R_YX, G_YX, B_YX, BMP_filename]=
GenArrayBitmap_050309(placenum,z_cent(k),x_cent(k),upper,bitmapfilepath);
      placenum=placenum+1;
   end
end
```

2. Main Program Used to Generate Bitmaps

```
function [R_YX, G_YX, B_YX, BMP_filename] = GenArrayBitmap_050309(placenum, z_pupil,
x_pupil, upper, bitmapfilepath)
%DMU's matlab program to generate array bitmap pattern for hologram generation
%FIXED PARAMETERS
%%%%%%%%%%%%%%%%%%%%%%%%%%%%%%%%%%%%%%%%%%%%%%%%%%%%%%%%%%%%%%%%%%%%%%%%%%%%%%%%
%upper = 1;   % Actually the LOWER array on the prototype display
%lower = 0;   % Actually the UPPER array on the prototype display
LCD2Array = 490+34;
mirror2array = 330;     %the separation between the mirror and the array in mm
f_mirror_ang = 10.5;    %tilt angle of the spherical mirror in degree
xres = 1280;            %horizontal resolution of the projected image(**must be EVEN number)
yres = 512;             %vertical resolution of the projected image

% Following two lines account for the difference in throw angle of the
% projector (88 degrees) and the acceptance angle of the mirror (80 degrees)
% adjust the numbers if either angle is found to differ
m_xres = round(xres*1.06); % Horizontal resolution of the image region covering the mirror
m_yres = round(yres*1.06); % Vertical resolution of the image region covering the mirror

% Variable for the array width, and half the width
array_width = 820;
array_half_width = array_width/2;

% Variable for the mirror focal length
mirror_f = 564;
% Spot positions assume mirror is a flat plane 'mirror_f' away from the projector
% and 'mirror2array' from the array.
% This calculates the effective planar mirror width which accounts for ray
% hitting the real curved mirror in the correct place
% Rays leave the mirror collimated so usable real mirror width is same as
% the array width
pcorr = array_half_width.^2/(4*mirror_f);
pcorr_2 = (pcorr./cos(pi*(f_mirror_ang/180)))*(array_half_width/mirror_f);

% Variable for half the simulated planar mirror width
mirror_half = (array_width+pcorr_2*2)/2;
% Effective resolution pix/mm for the simulated mirror using the adjusted
% pixels/mm
pixelpmm = m_xres/(array_width+pcorr_2*2); % Use the xres modified by 80/88 (used angular
range)

% Pixels/mm to use for the grid calculation since that will cover the
% entire projector throw angle / image.
m_pixpmm = xres/(array_width+pcorr_2*2);

% Pixel offsets to shift the reduced region of the image covering the
% mirror to the centre of the whole image sent to the projector.
x_pix_offset = ((xres - m_xres)/2);
```

```
y_pix_offset = ((yres - m_yres)/2);

%VARIABLE PARAMETERS
%%%%%%%%%%%%%%%%%%%%%%%%%%%%%%%%%%%%%%%%%%%%%%
%%
maxSpotWidth = 3;
if upper==0      %vertical offset of the projected spot pattern
   yoffset = -55;      % offset for lower array "-" shift dots downward in millimeter
   x_pupil = x_pupil; %45;           % Shift the pupil by half the eye offset to create a left eye pupil
else
   yoffset = -55;      % offset for upper array in mm
   x_pupil = x_pupil; %45;           % Shift the pupil by half the eye offset to create a right eye pupil
end;
GridOn = 0;         % Put a grid on the image or not
G_Dot = 0;          % using Dot rather line of the grids
http://www.hindustantimes.com/Homepage/Images/slidenext.gif
GCompensat = 1;      % Grid with compensation or not
ACompensat = true;      % Dot pattern with compensation or not
WriteBitmap = true;     % writing the bitmap to disk or not
White = 1;  Red = 0; Green = 0; Blue = 0;      % which colour of bitmap is writing to disk
Ycorrection = false;    % enable Y correction for each indivdual element

Y_Cali = false;         % generate series of calibration dot patterns with -3 to +3 pixels in Y axis only
DrawElements = false;    % Draw Element's pattern on the bitmap or not
E_FillOn = false;       % flood fills element pattern or not
% Y correction for each elements (in pixels =============
%======  1 ==== 2 ==== 3 ==== 4 ==== 5 ==== 6 ==== 7 ====
uyc = ...                                          % for upper stack in unit of pixel
 [  0     0     0     0     0     0     0
    0     0     0     0     0     0     0
    0     0     0     0     0     0     0
    0     0     0     0     0     0     0
    0     0     0     0     0     0     0
    0     0     0     0     0     0     0
    0     0     0     0     0     0     0];

%======  1 ==== 2 ==== 3 ==== 4 ==== 5 ==== 6 ==== 7 ====
lyc = ...                                          % for lower stack in unit of pixel
 [  0     0     0     0     0     0     0
    0     0     0     0     0     0     0
    0     0     0     0     0     0     0
    0     0     0     0     0     0     0
    0     0     0     0     0     0     0
    0     0     0     0     0     0     0
    0     0     0     0     0     0     0];

%======  1 ==== 2 ==== 3 ==== 4 ==== 5 ==== 6 ==== 7 ====
%END OF VARIABLE PARAMETERS
%%%%%%%%%%%%%%%%%%%%%%%%%%%%%%%%%%%%%%%%%%%%%%

if GridOn
   ArrayBitmap = GridMap(xres,yres,15,GCompensat,f_mirror_ang, ...
      m_pixpmm, G_Dot, DrawElements, array, E_FillOn,mirror2array,mirror_half);
   ArrayBitmap = ArrayBitmap.*0.25;
else
   R_ArrayBitmap = zeros(yres, xres);
   G_ArrayBitmap = zeros(yres, xres);
   B_ArrayBitmap = zeros(yres, xres);
end;

xoffset = 0;                          %horizontal offset of the projected spot pattern in mm
```

```
%"-" shift dots to the left in millimeter

%GENERATING THE SPOT COORDS FROM DISPLAY PARAMETERS
%%%%%%%%%%%%%%%%%%%%%%%%
%ALL PARAMETERS ARE AS DESCRIBED IN PHIL'S EXCEL SPREADSHEET OTF
A=1:49;
B=repmat(1:7,1,7);
C=x_pupil*ones(1,49);
D=15*(A-25);
E=D-C;
F=z_pupil*ones(1,49);
G=F+LCD2Array;
H=(180/pi)*atan(E./G);
%I=0;
I=97.27*tan(H*pi/180);
% Line below - remove I to ignore element position to angle transfer
% function put spots in centre of elements when J = D; while testing also
% while testing apply xoffset in range +/- 50 to move spot along back of
% element
J=D + I + xoffset;                    % spot x-coordinates in mm
%J=D + xoffset;                        % spot x-coordinates in mm

% ******** NOT SURE ABOUT THIS SUBSTITUTION FOR UPPER ***************
L=45-(4*B)-(60*upper) + yoffset;            % spot y-coordinates in mm ( for 30mm central piece)
%L=41-(4*B)-(50*array) + yoffset;            % for 20mm centre piece

if ACompensat
   M=J.^2/(4*564);
   N=mirror2array*ones(1,49);
   O=f_mirror_ang*ones(1,49);
   P=(pi*(O/180));
   Q=((M./cos(P))-L.*tan(P)).*(J/564);
   R=J+Q;
   %YO44 Projector Upper & Lower Polynomials
   AA=(R+375)/15;
   if upper
   AF =  (0.00000003588400097014*(AA.^6) - 0.00006660939104952379*(AA.^5) +
0.00045016027289213100*(AA.^4) - 0.01365399228755850000*(AA.^3) +
0.17587771433034000000*(AA.^2) - 0.79990059915962800000*(AA) +
2.86321573235546000000);
   AE =  (0.00000002954217507862*(AA.^6) - 0.00003474511640955514*(AA.^5) +
0.00012552691216427500*(AA.^4) - 0.00098391418760002100*(AA.^3) -
0.04508262362105600000*(AA.^2) + 3.36039078057365000000*(AA) -
62.36714960716200000000);
   AC= R-AE-AF;
   else
   AD = (0.00000004065134570695*(AA.^6) - 0.00006540346938015830*(AA.^5) +
0.00039330603464038400*(AA.^4) - 0.01035570715529840000*(AA.^3) +
0.10217509237872900000*(AA.^2) - 0.14002215635810000000*(AA) +
1.32064102841377000000);
   AB = (-0.00000000203234618631*(AA.^6) + 0.00000057093023936305*(AA.^5) -
0.00004436699082788210*(AA.^4) + 0.00105458906864442000*(AA.^3) -
0.01730649323872060000*(AA.^2) + 2.66996459536313000000*(AA) -
61.31240608784720000000);
   AC= R-AB-AD;
   end;
   %Y43 Projector Upper & Lower Polynomials
   %AA=(R+375)/15;
   %if upper
   %AF = (-0.00000002404789035357*(AA.^6) + 0.00003674039844990540*(AA.^5) -
0.00023183176607322100*(AA.^4) + 0.00778606194501208000*(AA.^3) -
```

```
0.14399304363678300000*(AA.^2) + 1.35948087086854000000*(AA) -
9.20908872460313000000);
   %AE = (0.00000009230956337362*(AA.^6) - 0.00001438434445643480*(AA.^5) +
0.00084937414555819000*(AA.^4) - 0.02347938211777030000*(AA.^3) +
0.27933883616538000000*(AA.^2) - 0.09620092254590420000*(AA) -
14.57519263221370000000);
   %AC= R-AE-AF;
   %else
   %AD = (-0.00000000583015863251*(AA.^6) + 0.00000096619077667726*(AA.^5) -
0.00007146443072691970*(AA.^4) + 0.00312574939822241000*(AA.^3) -
0.08057667472894540000*(AA.^2) + 1.05805566967956000000*(AA) -
9.27195963717713000000);
   %AB = (0.00000003789970272688*(AA.^6) - 0.00000618793247906049*(AA.^5) +
0.00038821511668674100*(AA.^4) - 0.01159666968648310000*(AA.^3) +
0.14332039905480100000*(AA.^2) + 0.40555909945896900000*(AA) -
15.40373670200100000000);
   %AC= R-AB-AD;
   %end;

   S=(L.*(564+M)./(564+N));
   T=2*(M.*sin(P));
   U=S+T;
   % Remove semi-colons after V and W to print spot locations calculated
   % in mm.
   V=AC+mirror_half;
   W=U+(yres/pixelpmm/2);
   X=x_pix_offset + V*pixelpmm;
   Y=yres-W*pixelpmm;
else
   W=L+(yres/pixelpmm/2);
   X=x_pix_offset+(J+mirror_half)*pixelpmm;
   Y=yres-W*pixelpmm;
End;
% Y43-Positive correction in these offsets gives a downward movement of the
% spots.
%=================== upper ============================
%======  1 ==== 2 ==== 3 ==== 4 ==== 5 ==== 6 ==== 7 ====
%G_uycor =...                                  % in mm unit
%      [-11.00   -09.50  -10.70  -10.20  -7.90   -5.30   -3.60
%       -11.00   -10.30  -10.70  -9.70   -7.20   -5.40   -3.00
%       -11.20   -10.60  -10.50  -9.80   -7.30   -4.30   -3.20
%       -11.10   -11.00  -10.40  -9.60   -6.80   -4.00   -2.60
%       -10.50   -11.10  -10.60  -9.40   -6.90   -4.00   -2.40
%       -10.20   -10.60  -10.60  -8.50   -6.30   -3.00   -2.00
%       -10.40   -10.60  -10.30  -8.60   -6.20   -2.90   -1.00 ];
%uycor = 0;
%======  1 ==== 2 ==== 3 ==== 4 ==== 5 ==== 6 ==== 7 ====
%=========================================================

%=================== lower ============================
%======  1 ==== 2 ==== 3 ==== 4 ==== 5 ==== 6 ==== 7 ====
%G_lycor =...                                   % in mm unit
%      [-8.80   -7.40   -8.50   -7.30   -5.40   -3.60   -2.00
%       -8.20   -8.00   -8.00   -7.40   -5.50   -3.40   -2.00
%       -8.80   -8.10   -8.20   -7.00   -5.30   -3.40   -1.20
%       -8.80   -9.20   -8.60   -7.00   -5.00   -3.20   -0.50
%       -8.50   -8.90   -8.50   -6.90   -4.90   -3.00   -0.30
%       -8.20   -9.10   -8.70   -6.70   -4.90   -2.70   -0.20
%       -8.70   -9.00   -8.90   -6.40   -4.70   -2.30    0.00 ];
%lycor=0;
%======  1 ==== 2 ==== 3 ==== 4 ==== 5 ==== 6 ==== 7 ====
```

```
%=====================================================

% Y43-Positive X correction
%=================== upper ============================
%======  1 ==== 2 ==== 3 ==== 4 ==== 5 ==== 6 ==== 7 ====
%G_uxcor= ...                                % for upper stack in unit of pixel
%     [  0     0     2     0     1     1     2
%       -1     0     2     0     0     0     1
%        0    -1     2     0     1     1     1
%        0     0     2     0     1     1     1
%        1     0     2     0     1     1     0
%        1     0     2     0     1     2     0
%        1     1     1     0     1     1     0];
%uxcor = 0;
%======  1 ==== 2 ==== 3 ==== 4 ==== 5 ==== 6 ==== 7 ====
%=====================================================

%=================== lower ============================
%======  1 ==== 2 ==== 3 ==== 4 ==== 5 ==== 6 ==== 7 ====
%G_lxcor = ...                                % for lower stack in unit of pixel
%     [  0     1     1     0     1     0     2
%        0     0     2     0     1     0     2
%        0     0     2     0     2     0     2
%        0     0     2     0     1     0     2
%        0     0     2     0     1     0     2
%        1     0     2     0     1     2     1
%        0     0     1     0     1     1     1];
%lxcor=0;
%======  1 ==== 2 ==== 3 ==== 4 ==== 5 ==== 6 ==== 7 ====
%=====================================================

% YO44 Positive Y correction in these offsets gives a downward movement of the
% spots.
%=================== upper ============================
%======  1 ==== 2 ==== 3 ==== 4 ==== 5 ==== 6 ==== 7 ====
G_uycor =...                                 % in mm unit
      [-13.40   -13.00  -14.60  -14.50   -12.20   -10.00   -7.60
       -13.70   -13.70  -14.80  -13.90   -12.30    -9.70   -7.30
       -13.70   -14.60  -15.30  -14.10   -12.60    -9.80   -7.20
       -14.30   -14.80  -15.70  -14.40   -12.60    -9.50   -6.20
       -14.40   -15.20  -15.80  -14.10   -12.60    -9.00   -6.70
       -14.80   -15.90  -15.90  -14.00   -12.20    -9.40   -5.90
       -14.90   -16.20  -15.50  -14.00   -12.20    -8.80   -5.40 ];
   %uycor = 0;
%======  1 ==== 2 ==== 3 ==== 4 ==== 5 ==== 6 ==== 7 ====
%=====================================================

%=================== lower ============================
%======  1 ==== 2 ==== 3 ==== 4 ==== 5 ==== 6 ==== 7 ====
G_lycor =...                                 % in mm unit
      [-6.10   -6.80   -7.60   -7.60   -6.00    -3.90    -1.40
       -6.80   -7.40   -8.70   -7.70   -6.10    -4.40    -0.80
       -7.70   -8.20   -8.80   -8.50   -6.30    -4.90    -0.80
       -7.70   -9.00   -9.70   -8.20   -6.00    -4.40    -0.60
       -8.00   -9.40   -9.90   -7.90   -6.30    -4.20     0.00
       -8.60  -10.40  -10.30   -8.00   -6.70    -4.20    -0.70
       -8.80  -10.70  -10.20   -8.30   -6.90    -4.30    -0.50 ];
%lycor=0;
%======  1 ==== 2 ==== 3 ==== 4 ==== 5 ==== 6 ==== 7 ====
%=====================================================
```

```
% Y044 -Positive X correction
%=================== upper ============================
%======  1 ==== 2 ==== 3 ==== 4 ==== 5 ==== 6 ==== 7 ====
G_uxcor= ...                                % for upper stack in unit of pixel
    [ 0    0    1    0    0    0    0
      -1   0    1    0    0    0    0
      -1   0    1    0    0    1    0
       0   0    0    0    1    0    0
       0   0    1    0    0    0    1
       0   0    1    0    1    1    1
       0   0    0    0    1    1    2];
%uxcor = 0;
%======  1 ==== 2 ==== 3 ==== 4 ==== 5 ==== 6 ==== 7 ====
%=====================================================

%=================== lower ============================
%======  1 ==== 2 ==== 3 ==== 4 ==== 5 ==== 6 ==== 7 ====
G_lxcor = ...                               % for lower stack in unit of pixel
    [ 2    0    0    0    0    0    0
      0    0    0    0    1    0    0
      0    0    1    0    1    0    0
      0    0    1    0    1    0    0
      0    0    1    0    1    0    1
      0    0    0    0    1    0    1
      0    0    0    0    0    0    1];
%lxcor=0;
%======  1 ==== 2 ==== 3 ==== 4 ==== 5 ==== 6 ==== 7 ====
%=====================================================



%Inserting the possibility for colour-dependent correction
R_uycor=G_uycor; B_uycor=G_uycor;
R_lycor=G_lycor; B_lycor=G_lycor;

R_uxcor=G_uxcor; B_uxcor=G_uxcor;
R_lxcor=G_lxcor; B_lxcor=G_lxcor;

if upper
   R_ycor = R_uycor(:)'*pixelpmm;
   G_ycor = G_uycor(:)'*pixelpmm;
   B_ycor = B_uycor(:)'*pixelpmm;

   R_xcor = R_uxcor(:)'*pixelpmm;
   G_xcor = G_uxcor(:)'*pixelpmm;
   B_xcor = B_uxcor(:)'*pixelpmm;

else
   R_ycor = R_lycor(:)'*pixelpmm;
   G_ycor = G_lycor(:)'*pixelpmm;
   B_ycor = B_lycor(:)'*pixelpmm;

   R_xcor = R_lxcor(:)'*pixelpmm;
   G_xcor = G_lxcor(:)'*pixelpmm;
   B_xcor = B_lxcor(:)'*pixelpmm;
end
% remove the semi-colon at the end of the next line to print the final spot
% coordinates after any corrections for mirror or mm offsets and coversion
% to unrounded pixel coordinates
R_YX = [(Y+R_ycor); (X+R_xcor) ]';
G_YX = [(Y+G_ycor); (X+G_xcor) ]';
```

```
B_YX = [(Y+B_ycor); (X+B_xcor) ]';

% Quatize real into dicreet co-ordinates
R_coords=round(R_YX);
G_coords=round(G_YX);
B_coords=round(B_YX);
%Flipping the data about the centre of the image.
hw=(size(R_ArrayBitmap,2)/2);
R_YX(:,2)=hw-(R_YX(:,2)-hw)+1;
G_YX(:,2)=hw-(G_YX(:,2)-hw)+1;
B_YX(:,2)=hw-(B_YX(:,2)-hw)+1;
% %Including the effect of Phil's hack
% half_spot_width=floor(maxSpotWidth/2);
% R_YX2=
% for k=1:size(R_YX,1)
%     new_block=[0 0];
%
%     for l=-half_spot_width:half_spot_width
%         new_block=[new_block;[R_YX(k,1)+l,R_YX(k,2)]];
%     end
%
%
% end
%
% half_spot_length=length([-half_spot_width:half_spot_width]);
% R_YX2=zeros(half_spot_length*size(R_YX,1),2);
% for k=1:length(R_YX)
%           [(k-1)*half_spot_length+1:k*half_spot_length];
%           [-half_spot_width:half_spot_width];
%           R_YX2((k-1)*half_spot_length+1:k*half_spot_length,1)=R_YX(k,1)+[-
half_spot_width:half_spot_width];
%           R_YX2((k-1)*half_spot_width+1:k*half_spot_width,2)=R_YX(k,2);
% end
%
% figure(1); plot(R_YX2(:,2),R_YX2(:,1),'r*'); axis ij; axis([0 1280 0 512])

if Ycorrection                      % Y correction for each elements (in pixels)
   if array
      ycc = uyc(:);
   else
      ycc = lyc(:);
   end;
else
   ycc = 0;
end;

R_coords(:,1) = R_coords(:,1) + ycc;
G_coords(:,1) = G_coords(:,1) + ycc;
B_coords(:,1) = B_coords(:,1) + ycc;

% Remove semi-colon at end of next line to print truncated rounded pixel
% locations of spots
%31/03/09: Ammendment to ensure that even the stretched spots remain within the image
%region
R_coords(R_coords(:,2)>(xres-maxSpotWidth) | R_coords(:,2)<(1+maxSpotWidth),:)=[];
G_coords(G_coords(:,2)>(xres-maxSpotWidth) | G_coords(:,2)<(1+maxSpotWidth),:)=[];          %
truncates the out of range coordinates
B_coords(B_coords(:,2)>(xres-maxSpotWidth) | B_coords(:,2)<(1+maxSpotWidth),:)=[];

%Hack to make the spot a number of pixels wider
for sw = 0:maxSpotWidth-1
```

```
   if upper
      R_ArrayBitmap(((R_coords(:,2)-1+sw).*yres)+(R_coords(:,1)))=1;
      G_ArrayBitmap(((G_coords(:,2)-1+sw).*yres)+(G_coords(:,1)))=1;
      B_ArrayBitmap(((B_coords(:,2)-1+sw).*yres)+(B_coords(:,1)))=1; % put dots in the bitmap in a
1-D sequence format
   else
      R_ArrayBitmap(((R_coords(:,2)-1-sw).*yres)+(R_coords(:,1)))=1;
      G_ArrayBitmap(((G_coords(:,2)-1-sw).*yres)+(G_coords(:,1)))=1;
      B_ArrayBitmap(((B_coords(:,2)-1-sw).*yres)+(B_coords(:,1)))=1; % put dots in the bitmap in a
1-D sequence format
   end;
end;

R_ArrayBitmap = fliplr(R_ArrayBitmap);
G_ArrayBitmap = fliplr(G_ArrayBitmap);                    % Flip matrix LR (mirroring the image)
B_ArrayBitmap = fliplr(B_ArrayBitmap);

if xres > 1280            % Clip the bitmap to 1280, if it > 1280 pixel, xres must be even number
   R_ArrayBitmap = R_ArrayBitmap(:, (xres/2)-639:(xres/2)+640,:);
   G_ArrayBitmap = G_ArrayBitmap(:, (xres/2)-639:(xres/2)+640,:);
   B_ArrayBitmap = B_ArrayBitmap(:, (xres/2)-639:(xres/2)+640,:);

   R_coords(:,2) = R_coords(:,2)-((xres/2)-640);            % for Y_Cali
   G_coords(:,2) = G_coords(:,2)-((xres/2)-640);            % for Y_Cali
   B_coords(:,2) = B_coords(:,2)-((xres/2)-640);            % for Y_Cali

   xres = 1280;                                  % for Y_Cali

   R_coords(R_coords(:,2)>xres | R_coords(:,2)<1,:)=[];
   G_coords(G_coords(:,2)>xres | G_coords(:,2)<1,:)=[];
   B_coords(B_coords(:,2)>xres | B_coords(:,2)<1,:)=[];       % for Y_Cali, truncates the out of
range coordinates
end;
if WriteBitmap
   %Formatting the bitmap filename
   if upper
      ssA='U_';
   else
      ssA='L_';
   end;
   ss = [ ssA num2str(z_pupil,'%04.0f') 'x' num2str(x_pupil,'%04.0f') '_xos'...
         num2str(xoffset,'%02.1f') '_yos' num2str(yoffset,'%02.1f') '_r' num2str(f_mirror_ang) '_w'
num2str(maxSpotWidth)];

   %05/03/09: Changing to allow for a colour-dependent correction
   if White
      BMP_filename=[num2str(placenum,'%04d') ,'_','BMP_W_',ss,'.bmp'];
      TBmp = zeros(yres,xres,3); TBmp(:,:,1) = R_ArrayBitmap; TBmp(:,:,2) = G_ArrayBitmap;
TBmp(:,:,3) = B_ArrayBitmap;
      outfilename = fullfile(bitmapfilepath,[sprintf('%04d',placenum),'_','BMP_W_',ss,'.bmp']);
      imwrite(TBmp, outfilename, 'bmp')
      disp(' ');
      disp([outfilename ' image is successfully generated!']);
      disp(' ');
   end;
   if Red
      TBmp = zeros(yres,xres,3); TBmp(:,:,1) = ArrayBitmap;
      eval(['imwrite(TBmp,''Bitmaps\BMP_R_' ss '.bmp'',''bmp'');']);
      disp(' ');
      disp([cd '\Bitmaps\BMP_R_' ss '.bmp image is successfully generated!']);
      disp(' ');
```

```
    end;
    if Green
        TBmp = zeros(yres,xres,3); TBmp(:,:,2) = ArrayBitmap;
        eval(['imwrite(TBmp,''Bitmaps\BMP_G_' ss '.bmp'',''bmp'');']);
        disp(' ');
        disp([cd '\Bitmaps\BMP_G_' ss '.bmp image is successfully generated!']);
        disp(' ');
    end;
    if Blue
        TBmp = zeros(yres,xres,3); TBmp(:,:,3) = ArrayBitmap;
        eval(['imwrite(TBmp,''Bitmaps\BMP_B_' ss '.bmp'',''bmp'');']);
        disp(' ');
        disp([cd '\Bitmaps\BMP_B_' ss '.bmp image is successfully generated!']);
        disp(' ');
    end;
    if Y_Cali                                   % only generate Green channel bitmap
        TBmp = fliplr(ArrayBitmap);                 % Flip matrix LR (mirroring the image)
        TBmp(((coords(:,2)-1).*yres)+coords(:,1))= 0;     % put dots in the bitmap in a 1-D sequence
format
        sc = {'m4' 'm3' 'm2' 'm1' '0' 'p1' 'p2' 'p3' 'p4'};
        for i = [-4 -3 -2 -1 0 1 2 3 4]                 % -3 to +3 pixels
            eval(['coords_' sc{i+5} ' = zeros(size(coords));']);
            eval(['coords_' sc{i+5} ' = [coords(:,1)+i coords(:,2)];']);
            eval(['TBmp(((coords_' sc{i+5} '(:,2)-1).*yres)+coords_' sc{i+5} '(:,1))= 1;']);
            TBmp = fliplr(TBmp);
            TBmp = repmat(TBmp,[ 1 1 3]); TBmp(:,:,[1,3]) = 0;
            eval(['imwrite(TBmp,''Bitmaps\BMP_G_' sc{i+5} '_' ss '.bmp'',''bmp'');']);
            TBmp = TBmp(:,:,2);
            TBmp = fliplr(TBmp);
            eval(['TBmp(((coords_' sc{i+5} '(:,2)-1).*yres)+coords_' sc{i+5} '(:,1))= 0;']);
            disp(' ');
            disp([cd 'Bitmaps\BMP_B_' sc{i+5} '_' ss '.bmp image is successfully generated!']);
            disp(' ');
        end;
    end;
end;
end
```

3. Program Used to Define Coordinates

```
% 05/03/09
% mapping function to obtain a hologram number for a given exit pupil size
function [x_cent,z_cent,box_w,box_d]=EP_coords(no_holograms,near_point,far_point,v_nwidth)
array_ang=25*(pi/180); % maximum angle that rays emanate from near point
box_aspect=4; %ratio of box depth to box width
zrange=far_point-near_point; %zrange of viewing area
view_area=zrange*(v_nwidth + zrange*tan(array_ang));
box_area=view_area/no_holograms;
box_w=sqrt(box_area/box_aspect);
box_d=box_w*box_aspect;
box_hd=box_d/2;
%number of boxes to fit within the depth (z) of viewing area
no_boxd=ceil(zrange/box_d);

holo=1;
for D=1:no_boxd
    %distance z from front of viewing area
    z=(D)*box_d;
    %number of boxes across the viewing area at dist z
    no_boxw(D)=ceil(curr_width(v_nwidth,(z),array_ang)/box_w);
```

```
    %left hand offset for boxes to be set centrally
    L_excess(D)=(0.5*(box_w*no_boxw(D)-curr_width(v_nwidth,(z),array_ang)));
    for W=1:no_boxw(D)
        %calculation of box limits
        L_box(holo)=((W-1)*box_w)-(0.5*curr_width(v_nwidth,z,array_ang)+L_excess(D));
        R_box(holo)=L_box(holo)+box_w;
        T_box(holo)=z+near_point;
        B_box(holo)=z-box_d+near_point;
        %calculation of box centres
        x_cent(holo)=0.5*(L_box(holo)+R_box(holo));
        z_cent(holo)=0.5*(T_box(holo)+B_box(holo));
        holo=holo+1;
    end
end
end
```

4. Program Used to Define Grid

```
function ABitmap = GridMap(xres, yres, gspace, compensat, f_mirror_ang, pixelpmm, dot, DrawE,
array, fill, mirror2array, mirror_half)
    centX =round(xres/2); centY = round(yres/2);
    ABitmap = zeros(yres,xres);
    if DrawE
        ABitmap = DrawRectM(ABitmap, xres, yres, pixelpmm, fill, array);
    end;
    if dot
        ABitmap([(centY:-gspace:1) (centY:gspace:yres)],[(centX:-gspace:1) (centX:gspace:xres)]') =
1;
    else
        ABitmap(1:yres,[(centX:-gspace:1) (centX:gspace:xres)]') = 1;
        ABitmap([(centY:-gspace:1) (centY:gspace:yres)]',1:xres) = 1;
    end;
    if compensat
        [Y,X] = find(ABitmap == 1);
        [X,Y] = XCompensation(X, Y, xres, yres, f_mirror_ang, pixelpmm, mirror2array,mirror_half);
        YX =round([Y X]);
        YX(YX(:,2)>xres | YX(:,2)<1,:)=[];
        YX(YX(:,1)>yres | YX(:,1)<1,:)=[];
        ABitmap = zeros(yres, xres);
        ABitmap(((YX(:,2)-1).*512)+YX(:,1))=1;      % put dots in the bitmap
    end
  ABitmap((centY-2:centY+2)',centX-2:centX+2)=1;    % Mark Centre of Image with a 5x5 square
function [X, Y] = XCompensation(X, Y, xres, yres, f_mirror_ang, pixelpmm,
mirror2array,mirror_half)
FL = 564;
X = ((X-(xres/2))./pixelpmm); Y = ((Y-(yres/2))./pixelpmm);
M=X.^2/(4*FL);
N=mirror2array;
O=f_mirror_ang;
P=(pi*(O/180));
Q=((M./cos(P))-Y.*tan(P)).*(X/FL);
R=X+Q;
S=Y.*(FL+M)./(FL+N);
T=2*(M.*sin(P));
U=S+T;
V=R+mirror_half;
W=U+(yres/pixelpmm/2);
X=V*pixelpmm;
Y=yres-W*pixelpmm;
function ArrayBitmap = DrawRectM(ArrayBitmap, resX, resY, pixelpmm, FillOn, array)
```

```
ArrayBitmap = ArrayBitmap;
```

5. Matlab Program for Combining the Upper and Lower Array Holograms of the MUTED Display

```
%05/03/09: Generating holograms based on the addition of phase ramps
function
analytical_holos2(targ_coords,ED,N,outputname,moduledatapath,outputfilepath,RGB_sets_per_vi
deo_frame)
load kernels
%create the coordinate matrices
x=1:N;
x=repmat(x,N,1);
y=x';
abers=zeros(N,N,3); %aberration matrix
%holos=zeros(N,N,3*RGB_sets_per_video_frame); %the holograms to be converted into a bin file
T=cputime;
%retrieving the coefficients from the ModuleData folder
[coeffs,indices] = read_aber_from_xrn([moduledatapath,'aber.xrn']);
disp(['time to read in aber coeffs: ' num2str(cputime - T) 's']);
targ_coords2=targ_coords;
targ_coords(:,1)=targ_coords2(:,2);
targ_coords(:,2)=targ_coords2(:,1);
for col=1:3
   %converting spot locations using stored geo files %%%%%%%%%%%%
   T=cputime;
   %converting the Zernike coefficients into a 1280x1280 phase profile
   [phasors] = make_aber_zernike_tilts(N,-coeffs{col},indices{col});
   abers(:,:,col)=phasors;
   abers(1:10,1:10,:);
   disp(['time to contruct aber holo from coeffs: ' num2str(cputime - T) 's']);
   %Summing phase ramps %%%%%%%%%%%%%%%%%%%%%%%%%%%%%%%%%%%%
   T=cputime;
   %reading in the geo files
   if col==1
      g = GeometryMap.read_from_geo_file([moduledatapath,'red.geo']);
   elseif col==2
      g = GeometryMap.read_from_geo_file([moduledatapath,'green.geo']);
   elseif col==3
      g = GeometryMap.read_from_geo_file([moduledatapath,'blue.geo']);
   end
   disp(['time to read in geo file: ' num2str(cputime - T) 's']);
   T=cputime;
   %converting ideal to pre-corrected spot location
   for num=1:length(targ_coords)
      tx_p = targ_coords(num,1); ty_p = targ_coords(num,2);
      [cx_n,cy_n]=g.notional_from_projected(tx_p,ty_p);
      [xs_n,ys_n] = meshgrid((cx_n-1):(cx_n+1),(cy_n-1):(cy_n+1));
      xs_n = xs_n(:); ys_n = ys_n(:); % notional coords near crude approx
      %calculating the projected coords from pixels around the notional pixel
      v_p = zeros(9,1); w_p = zeros(9,1);
      for i=1:9;
         [a_p,b_p] = g.projected_from_notional(xs_n(i),ys_n(i));
         v_p(i)=a_p; w_p(i)=b_p;
      end
      %creating a matrix of polynomial functions
      M = [ones(9,1) v_p w_p v_p.*v_p v_p.*w_p w_p.*w_p];
      %matrix inversion to evaluate polynomial coefficients
      coeffs_x_n_from_p = lscov(M,xs_n);
      coeffs_y_n_from_p = lscov(M,ys_n);
      ccx_n=[1 tx_p ty_p tx_p*tx_p tx_p*ty_p ty_p*ty_p]*coeffs_x_n_from_p;
```

```
      ccy_n=[1 tx_p ty_p tx_p*tx_p tx_p*ty_p ty_p*ty_p]*coeffs_y_n_from_p;
      cx(col,num)  = cx_n;  cy(col,num)  = cy_n;
      ccx(col,num) = ccx_n; ccy(col,num) = ccy_n;
   end
   disp(['time to calculate target coord mapping: ' num2str(cputime - T) 's']);

%%%%%%%%%%%%%%%%%%%%%%%%%%%%%%%%%%%%%%%%%%%%%%%%%%%%%%%%%%%%%%%%%%%%%%%
%%%%
end

%calculating the sinc function compensation
xs=1:N;
xs=repmat(xs,N,1);
%including the 90% linear fill factor)
xs=pi*(1)*(xs-(N/2)-1)/N;
ys=xs';
sincx=sin(xs)./xs;
sincy=sin(ys)./ys;
sinccomp=(1./sincx).*(1./sincy);
for iters=1:RGB_sets_per_video_frame
   for col=1:3
      T=cputime;
      % Calculate (x,y) coordinates from GenArray output
      nones=size(cx,2);

      outx=cx(col,:)'-N/2-1;
      outy=cy(col,:)'-N/2-1;
      zramp=zeros(N);
      for p=1:nones
         r = N*rand(1);
         zramp1=exp(2*pi*1j*(outx(p)*x+outy(p)*y+r)/N);
         ph = squeeze(abers(:,:,col));
         zramp = zramp + (sinccomp((outy(p)+(N/2)+1),(outx(p)+(N/2)+1))).*zramp1 .*ph;
         sinccomp((outy(p)+(N/2)+1),(outx(p)+(N/2)+1));
      end
%       figure(1); plot(outy,outx,'.'); axis([-640 640 -640 640]); hold on; plot(targ_coords(:,2)-N/2-
1,targ_coords(:,1)-N/2-1,'*')
      zramp = zramp/nones;
      arraym=fliplr(real(zramp));
      disp(['time to add holo phase ramps: ' num2str(cputime - T) 's']);

%%%%%%%%%%%%%%%%%%%%%%%%%%%%%%%%%%%%%%%%%%%%%%%%%%%%%%%%%%%%%%%%%%%%%%%
%%%
      %Converting continuous to binary phase hologram %%%%

      if ED==1
         T=cputime;
         %using error diffusion to calculate hologram.
         array_diff(:,:,(3*(iters-1)+col))=error_diffusion_quantizer_Garreths(arraym,(1*k2));
         disp(['time to calculate the error diffused binary hologram ' num2str(cputime - T) 's']);
      else
         T=cputime;
         %using a hard binarisation
         array_bin(:,:,(3*(iters-1)+col))=sign(real(arraym));
         disp(['time to calculate the hard-clipped binary hologram ' num2str(cputime - T) 's']);
      end

%%%%%%%%%%%%%%%%%%%%%%%%%%%%%%%%%%%%%%%%%%%%%%%%%%%%%%%%%%%%%%%%%%%%%%%
%%%
   end
end
```

```
if exist('array_diff','var')
    disp(['Size of matrix to convert to bin ', num2str(size(array_diff))]);
    bin_from_holos(array_diff,repmat([0 1
2],1,RGB_sets_per_video_frame),[outputfilepath,outputname,'.bin'],[outputfilepath,outputname,'.def
'],255)
    %hfs_from_holos(array_diff, repmat([0 1 2],1,RGB_sets_per_video_frame),
[outputfilepath,outputname,'.hfs'],[outputfilepath,outputname,'.bin'],[outputfilepath,outputname,'.def']
,[moduledatapath,'main2.xrn'], false, true, 255);
else
    disp(['Size of matrix to convert to bin ', num2str(size(array_bin))]);
    bin_from_holos(array_bin,repmat([0 1
2],1,RGB_sets_per_video_frame),[outputfilepath,outputname,'.bin'],[outputfilepath,outputname,'.def
'],255)
    %hfs_from_holos(array_bin, repmat([0 1 2],1,RGB_sets_per_video_frame),
[outputfilepath,outputname,'.hfs'],[outputfilepath,outputname,'.bin'],[outputfilepath,outputname,'.def']
,[moduledatapath,'main2.xrn'], false, true, 255);
end
end
```

Appendix 4 Summary of MUTED Measurements

	Parameter	Green		Blue	
		Upper	Lower	Upper	Lower
Spot power: Y44	Total power (mw)	491.9	497	180.4	189.3
	Mean power (µW)	10.04	10.14	3.68	3.86
	Standard deviation (µW)	0.38	0.41	0.35	0.29
	Fractional Variation (± %)	9.1	9.6	18.9	7.4
		Red	Green	Blue	White
	Mean Brightness (µW)	19.89	17.6	6.32	54.81
	Standard Deviation (µW)	1.09	1.56	0.32	3.77
	Fractional Variation (%)	5.46	8.85	5.09	6.87

Mirror reflectivity	Reflectivity at 45°	74.30%
	Reflectivity at 20°	80.50%

		Power	Polar-isation	Effic-iency
Power throughput	Projector Output total	2.42 mW	Linear horizontal	
	Projector output per spot	30.6 µW	Linear horizontal	
	Reflected from mirror	24.5 µW	Linear	80.1 %
	Array element (no 10° diff.)	5.4 µW	Linearl	22.4 %
	Array element (with 10° diff.)	3.68 µW	Linear	14.5 %
	LCD throughput	0.26 µW (est)-	Linear	**14.4** %

	X position (mm)	Eyes in positions marked (65 mm separation)		Spacing increased by 15 mm	
		Left	Right	Left	Right
Crosstalk	-200	3.5	8.7	2.2	7
	0	2.7	8.2	0.6	5.4
	200	2.2	6.4	2.2	6.4

Luminance & speckle	1.8 nits, speckle contrast = 60+/-4%

		Glass	Plexiglass
Relative array element throughput	Efficiency without horizontal diffuser	44.7 %	52.8 %
	Overall efficiency	29.2 %	34.7 %
	Soft aperture efficiency	66.9 %	65.7 %

Uniformity	Intra-element		± 19.0%
	Inter-element	White spot variation	± 6.9%
		Est. positional error	± 3.0% t o ± 13%

Projector stability	Y34	X = -3mm, Y = 6mm	Projectors not stable after warm-up
	Y43	= 4mm, Y = - 6 to 4 mm	
	Y44	X = 0mm, Y = -4 to -6	Proj. stable after warm-up

Table A.4.1: Summary of MUTED Measurements